Transactions of the ASME

TRANSACTIONS OF THE AMERICAN SOCIETY OF MECHANICAL ENGINEERS

VOLUME 76 OCTOBER 1954 NUMBER 7

Transactions

of The American Society of Mechanical Engineers

Published on the tenth of every month, except March, June, September, and December

Published monthly by The American Society of Mechanical Engineers. Publication office at 20th and Northampton Streets, Easton, Pa. The editorial department is located at the headquarters of the Society, 29 West Thirty-Ninth Street, New York 18, N. Y. Cable address, "Dynamic," New York. Price $1.50 a copy, $12.00 a year for Transactions and the *Journal of Applied Mechanics* to members and affiliates, $1.00 a copy, $6.00 a year. Changes of address must be received at Society headquarters seven weeks before they are to be effective on the mailing list. Please send old as well as new address.... By-Law: The Society shall not be responsible for statements or opinions advanced in papers or...printed in its publications (B13, Par. 4) ....Entered as second-class matter March 2, 1928, at the Post Office at Easton, Pa., under the Act of August 24, 1912....

Stability of Gas Flow in a Tube as Related to Vertical Annular Gas-Liquid Flow

By A. D. K. LAIRD,[1] BERKELEY, CALIF.

A model study of the pressure drop in the gas column of an upward annular gas-liquid flow system is described. The models were two rubber tubes with walls oscillating as axisymmetric standing waves. Pressure drops were shown to increase rapidly with increase of wave length, wave amplitude, and wave frequency. The mathematical analysis of the system was extended.

Introduction

UNDER certain conditions the simultaneous upward flow of gas and liquid in a vertical tube results in the phenomenon of annular flow; that is, the gas flows rapidly upward inside an annular layer of liquid which rises relatively slowly next to the wall. The drag of the gas on the liquid overcomes the force of gravity, so that the liquid is lifted up the tube and gains potential energy at the expense of the pressure energy of the gas.

When gas, at density ρ, is flowing at an average velocity V, in a tube of length L, and diameter d, the pressure drop Δp is related to the Weisbach pipe-friction factor f by the equation $\Delta p = fL\rho V^2 \div 2d$. For rigid walled tubes, f depends on the Reynolds number, $N_R = V\rho d \div \mu$, where μ is the dynamic viscosity. The values of f, based on the mean diameter of the air column in two-phase flow, have been found to be from 10 to 100 times those for rigid pipes with the same diameter as the air column and at equal Reynolds numbers less than 5000. In fact, it is necessary that f be of this magnitude to account for the energy transferred from the gas to the liquid. The mechanism by which the corresponding high axial force is developed at the interface was not known. Here, then, was an apparently simple flow system for which an adequate explanation of the lift force could not be given.

The only visible difference between the gas-liquid interface of annular upward flow and the gas-solid interface of a rigid tube was the capillary-wave system that always occurred at the former. It became the purpose of the present investigation to establish whether or not the wave system could cause this unexplained lift force, and if so, which of its features were the most important.

Method of Analysis

Previous experimentation on gas-liquid flow, carried out by many investigators (1, 2),[2] has resulted in a method of correlating data over a wide range of flow conditions. The particular conditions of annular upward flow have been investigated more recently (3, 4, 5) under the direction of J. A. Putnam.

Under the assumption that the velocity depends only on the radial position, the differential equations of motion were integrated by McElwee (4) and Pickrell (5) with the result that the pressure drop in the liquid phase, and hence in both phases, was found to be

$$\frac{\Delta p}{\Delta L} = \gamma_l + \frac{8\mu_l Q_l}{\pi b^4 R_l^2} - 2\,\frac{\gamma_l R_g}{R_l^2}\,[R_g \ln R_g + R_l] \quad \ldots\ldots [1]$$

where g, l are subscripts for gas and liquid, respectively

b = tube radius
R = saturation, or fraction of tube cross section occupied by particular phase
Q = volume flow rate
γ = specific weight

This equation is independent of the velocity distribution of the gas column. Measurements of pressure drop for a wide range of annular-flow conditions have shown that this equation predicts pressure drops that are from 10 to 20 per cent high. Thus a means of calculating the two-phase annular pressure drop has been found. This important result so far has not received proper recognition.

The corresponding equation for the gaseous phase predicted pressure drops that were too low by a factor of 10 to 100. Since steady laminar flow had been assumed in the derivation, it should be concluded that these conditions did not obtain in the gas core.

The effect of the unsteady flow caused by the waves at the gas-liquid interface, under the assumption of laminar flow in both phases, was investigated. The axially symmetric Navier-Stokes equations of motion were linearized by assuming the convective acceleration terms were negligible compared with the local acceleration terms. Thus

$$\left.\begin{aligned} \frac{\partial u}{\partial t} &= \frac{\partial \Omega}{\partial r} + \nu\left(\nabla^2 u - \frac{u}{r^2}\right) \\ \frac{\partial w}{\partial t} &= \frac{\partial \Omega}{\partial z} + \nu\nabla^2 w \end{aligned}\right\} \quad \ldots\ldots [2]$$

where

u, w = radial and axial velocity components, respectively
r, z, t = radial, axial, and time co-ordinates, respectively

$$\nabla^2 = \frac{\partial^2}{\partial z^2} + \frac{\partial^2}{\partial r^2} + \frac{1}{r}\frac{\partial}{\partial r}$$

$\Omega = gz - p/\rho$
g = acceleration of gravity
p = pressure
ρ = mass density
ν = kinematic viscosity

The departure of the interface from its mean position at $r = a$ is given by $\eta = \eta_0 \exp[i(kz + nt)]$, where $\lambda = 2\pi/k$ is the wave length. The frequency, $\mathfrak{F}$, of the wave is given by $\mathfrak{F} = n/2\pi$.

The resulting equations for the velocities were found to be

$$u_g = -ik \exp[i(kz + nt)][AI_1(kr) + BI_1(k'r)] \ldots [3]$$

---

[1] Assistant Professor of Mechanical Engineering, University of California.

[2] Numbers in parentheses refer to the Bibliography at the end of the paper.

Contributed by the Heat Transfer Division of The American Society of Mechanical Engineers and presented at the Heat Transfer and Fluid Mechanics Institute, Los Angeles, Calif., June 19, 1952.

Note: Statements and opinions advanced in papers are to be understood as individual expressions of their authors and not those of the Society. Manuscript received at ASME Headquarters, July 29, 1952. This paper was not preprinted.

$$u_l = -ik \exp[i(kz + nt)][CI_1(kr) + DK_1(kr) + EI_1(k'r) + FK_1(k'r)] \quad [4]$$

$$w_g = [1 + \exp[i(kz + nt)]][kAI_0(kr) + k'BI_0(k'r)] \quad [5]$$

$$w_l = [1 + \exp[i(kz + nt)]][kCI_0(kr) - kDK_0(kr) + k'EI_0(k'r) - k'FK_0(k'r)] \quad [6]$$

$$k'^2 = k^2 + \frac{in}{\nu} \quad [7]$$

where A, B, C, D, E, F are constants to be evaluated, and I_0, I_1, K_0, K_1 are modified Bessel functions.

Equations [5] and [6] representing axial velocities reduce to those found by Pickrell when expanded in power series of r up to second-order terms. These power series are rapidly convergent, so that the series represents the solution within 10 per cent. Hence the unsteady flow caused by the waves does not account for the pressure drop in the air column.

Another possible mechanism capable of producing the required lift force was a velocity distribution that produced a high wall shear. This distribution might be the result of turbulence at unusually small Reynolds numbers. Since the transition from laminar to turbulent flow as the Reynolds number is increased is preceded by unstable flow, the possibility of turbulence at Reynolds numbers less than the usual value of 2000 for a tube could be investigated by considering the stability of the gas flow. Reference to Equations [5] and [6] shows that the analytical determination of the stability conditions would be difficult. Consequently recourse was had to experiment.

It was noted that Equations [3], [5], and [7] are applicable to laminar flow of a gas through a tube with walls undergoing periodic deflections about a mean radius. The respective axial and radial velocities, w and u, are

$$w = [1 - \sin(kz + nt)][AkI_0(kr) + Bk'I_0(k'r)] \quad [8]$$

$$u = -k \cos(kz + nt)[AI_1(kr) + BI_1(k'r)] \quad [9]$$

where

$$A = n\eta_0 k'I_0(k'a) \div k[k'I_1(ka)I_0(k'a) - kI_0(ka)I_1(k'a)]$$

$$B = -n\eta_0 I_0(ka) \div [k'I_1(ka)I_0(k'a) - kI_0(ka)I_1(k'a)]$$

This system may be simulated by a rubber tube forced to deflect approximately sinusoidally with axial symmetry while gas is flowing inside. Two such models were built and pressure-drop data were taken.

To test the shape of the velocity-distribution curve for the air flow in the models, pitot-tube traverses were made. The corresponding pressure drops were measured.

Results

The numerical results of this investigation cover the range of Reynolds numbers from 300 to 4000, the range of frequencies from zero to 2000 cycles per minute (cpm), the amplitude-radius ratio range from 5 to 30 per cent, and the range of ka from 0.528 to 0.714. Figs. 1 to 6 display results from the model tests and give the effect of all the variables mentioned.

Velocity distributions for tube No. 1 at a Reynolds number of 1245 are shown in Fig. 7 for frequencies of zero and 590 cpm.

The principal result was the proof that the wave-boundary condition caused a high pressure drop in the air stream, and that this pressure drop was sensitive to the wave length, wave amplitude, and frequency.

Discussion

Several of the details of the rapid increase of friction factor with increase of frequency, amplitude, and wave length are of particular interest. The conventional friction factor, Reynolds number curves, shown in Figs. 1, 2, and 3 for model No. 1, have been cross-plotted in Figs. 4 and 5. At a given Reynolds number, the friction-factor ratio f/f_0 gives the ratio between the pressure drop

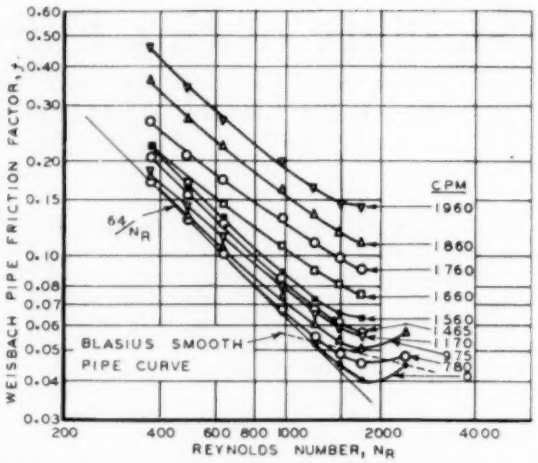

Fig. 1 Friction Factor as Function of Reynolds Number for Pulse Tube No. 1 With Frequency, Cpm, as Parameter (Amplitude-radius ratio = 0.046. Amplitude-wave length ratio = 0.0053 ka = 0.714.)

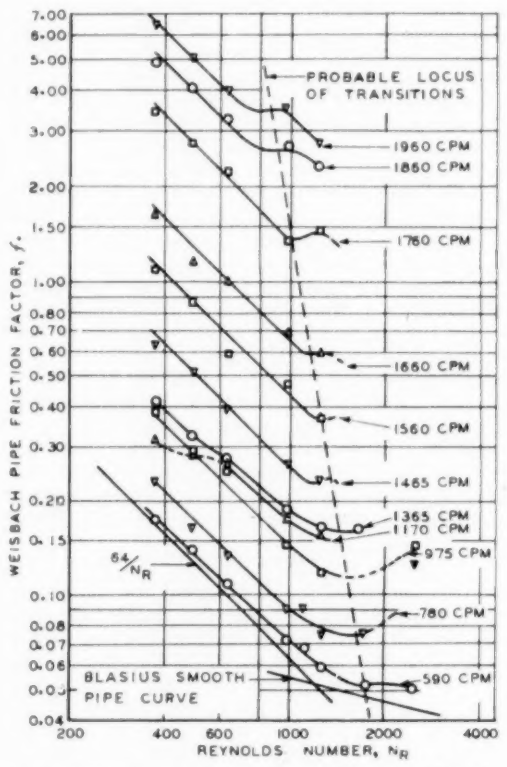

Fig. 2 Friction Factor as Function of Reynolds Number for Pulse Tube No. 1 With Frequency, Cpm, as Parameter (Amplitude-radius ratio = 0.093. Amplitude-wave length ratio = 0.011. ka = 0.714.)

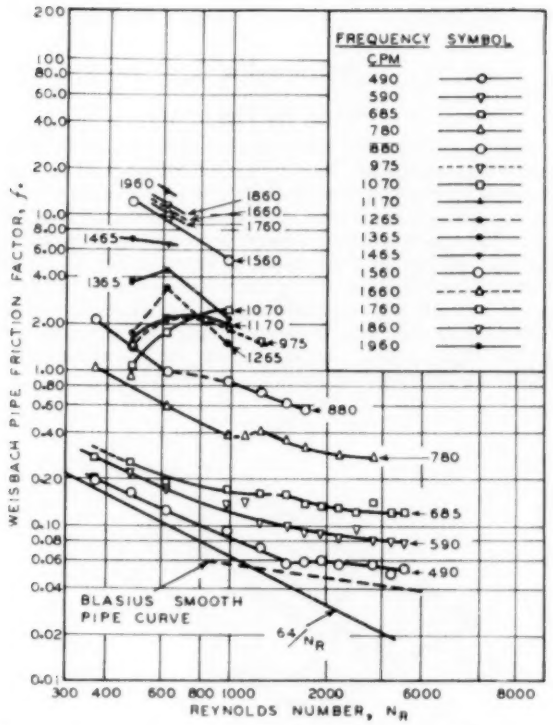

FIG. 3 FRICTION FACTOR AS FUNCTION OF REYNOLDS NUMBER FOR PULSE TUBE NO. 1 WITH FREQUENCY, CPM, AS PARAMETER
(Amplitude-radius ratio = 0.191. Amplitude-wave length ratio = 0.022. $ka = 0.714$.)

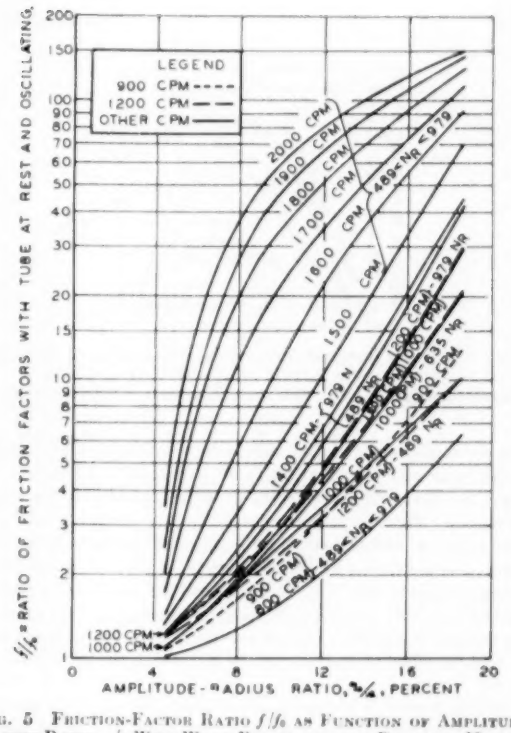

FIG. 5 FRICTION-FACTOR RATIO f/f_0 AS FUNCTION OF AMPLITUDE-RADIUS RATIO η_0/a WITH WAVE FREQUENCY AND REYNOLDS NUMBER AS PARAMETERS FOR PULSE TUBE NO. 1
(Cross plot from Fig. 4 using faired curves.)

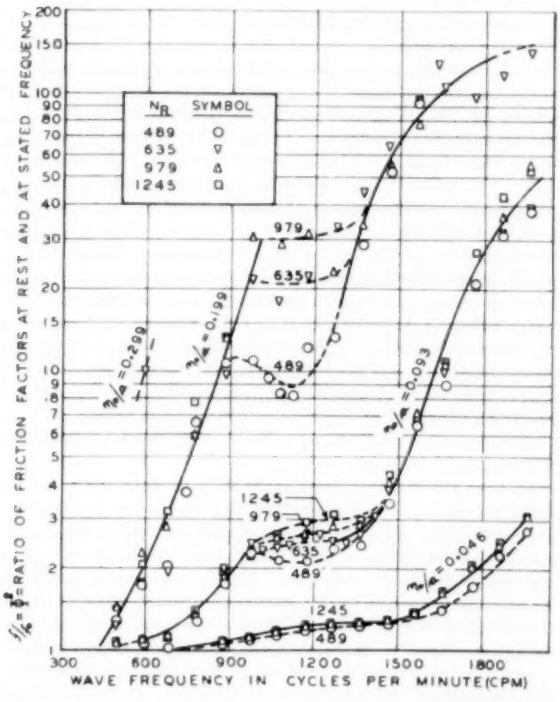

FIG. 4 FRICTION-FACTOR RATIO, $f/f_0 = \Phi^2$, AS FUNCTION OF WAVE FREQUENCY WITH REYNOLDS NUMBER, N_R, AND AMPLITUDE-RADIUS RATIO, η_0/a, AS PARAMETERS FOR PULSE TUBE NO. 1; $ka = 0.714$

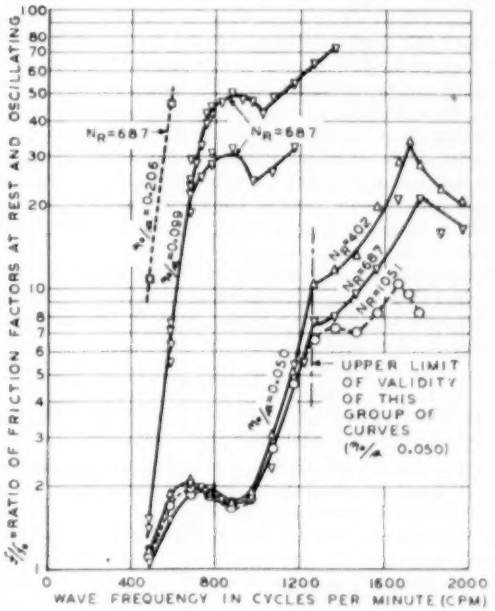

FIG. 6 FRICTION-FACTOR RATIO, f/f_0, AS FUNCTION OF WAVE FREQUENCY WITH REYNOLDS NUMBER, N_R, AND AMPLITUDE-RADIUS RATIO, η_0/a, AS PARAMETERS FOR PULSE TUBE NO. 2; $ka = 0.528$

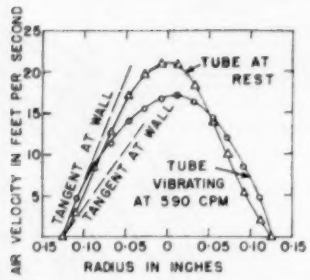

FIG. 7 VELOCITY DISTRIBUTION IN PULSE TUBE NO. 1 AT REST AND WHEN VIBRATING AT 590 CPM
(Reynolds number = 1245. Amplitude-radius ratio = 0.20. ka = 0.714.)

at a given frequency to the pressure drop for the tube at rest and is the same ratio as Martinelli's Φ^2 parameter. Remarks that apply to f/f_0 should apply also to Φ^2, for values of Φ^2 in the annular regime. Figs. 4 and 5 show there is some frequency and amplitude below which there is no increase of friction factor. The same facts are shown by Fig. 6 which is the plot for model No. 2 corresponding to Fig. 4. The increase of friction factor with frequency and with amplitude is roughly exponential over most of the range of variables. The wave-length change from 1.00 to 1.25 in. had the effect of multiplying the increase of the friction factor by 10.

In Fig. 1 there is no tendency for the transition from laminar to turbulent flow to occur at lower Reynolds number at higher frequencies. This tendency is shown, however, in Figs. 2 and 3 which indicate more tendency for higher amplitudes. Again, there is some amplitude below which this tendency does not occur.

The regions of Figs. 1, 2, and 3 in which the constant-frequency curves are parallel to the zero-frequency curve correspond to viscous-flow conditions. This is a significant fact suggesting the presence of eddies that in viscous flow produce velocity distribution of the same shape as found in turbulent flow. The existence of these eddies agrees with the general theory advanced by Munk (6). Such a flattened velocity distribution is shown in Fig. 7 where the flow conditions correspond to Fig. 3 at the same frequency and Reynolds number. The ratio of the velocity gradient at the wall of 590 cpm to the gradient at zero frequency was approximately 1.7. The corresponding ratio of pressure drops was 1.72. This agreement was closer than should be expected, but it does account for the axial force of the gas on the tube walls. Consequently, the lift force of the gas on the liquid in vertical two-phase annular flow must result primarily from viscous shear stresses at the interface.

The effect of Reynolds number is confined to isolated regions; over most of the range of variables the increase of friction factor is insensitive to Reynolds number. Further discussion may be found in the Appendix.

CONCLUSIONS

The following may be concluded for the case of annular upward flow of gas and liquid in a tube:

1 The model predicted the performance of the prototype.

2 A standing wave at the boundary of a gas column may cause high frictional resistance to flow.

3 The pressure drop can be calculated from the basic equations of fluid flow.

4 A new solution of the Navier-Stokes equations has been found.

5 The importance of the wave length, frequency, and amplitude of the interfacial waves has been established.

Appendix 1

APPARATUS AND PROCEDURE

Each of the models of the interfacial wave was a thin-walled rubber tube supported externally by stiff rubber rings at fixed distances apart. The rings, in turn, were supported by grooves on the inside of a lucite tube. The annular cells thus formed between the rings and the two tubes were connected alternately to the right and left-hand manifolds, as shown in Fig. 8. These manifolds were closed at one end and were connected at the other end to each side of a valveless pump. The pressure connections were made through lucite piezometric rings at the ends of the test section. The entrance, test, and delivery sections were approximately 40, 140, and 20 diameters, respectively.

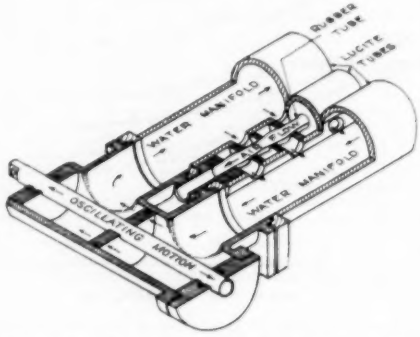

FIG. 8 SCHEMATIC SKETCH OF PUMP AND END OF PULSE-TUBE ILLUSTRATING CONSTRUCTION DETAILS AND ACTION

The wave length, which was twice the support ring spacing, was 1 in. for pulse tube No. 1, and 1.25 in. for pulse tube No. 2. The diameters of the pulse tubes were calculated by equating the measured pressure drops to the corresponding laminar-flow pressure drops; the effective diameter for tube No. 1 was 0.227 in., and for tube No. 2, 0.210 in. The amplitude of the rubber-tube waves was estimated by equating the volume of water required to deflect the walls in the shape of a sine curve between the supports, to the volume displaced by the pump plunger. These amplitudes were varied by changing the eccentric journal bearing on the shaft of the d-c motor that drove the plunger. The frequency was the motor speed which was controlled by rheostats. The airflow rate through the tube was controlled by a pressure regulator.

The action of the pulse tube is illustrated in Fig. 8. The course of the water during one stroke of the oscillating pump is shown by the small arrows; on the return stroke the water moved in the opposite direction. Since the displacement volume of the pump had to be accommodated during each stroke, the rubber wall was pushed in and pulled out alternately, thus causing a standing wave on the rubber tube.

To keep the mean pressure equal on both sides of the rubber tube, a connection was made from the air in the downstream pressure tap (B of Fig. 9) through a leveling bottle and into the manifold water. The air-water interface in the bottle was kept at the level of the tube center line. Manometers in the top of the manifold indicated the water pressure above the center line. A cock was provided in the air-outlet line to adjust the air pressure in the tube so that the manifold water pressure remained at a fixed value. During a run the manifold manometers were closed and the downstream water manometer (C in Fig. 9) indicated any changes in manifold pressure. At the upstream tap (A in. Fig. 9) the pressure in the air was higher than that in the water by the

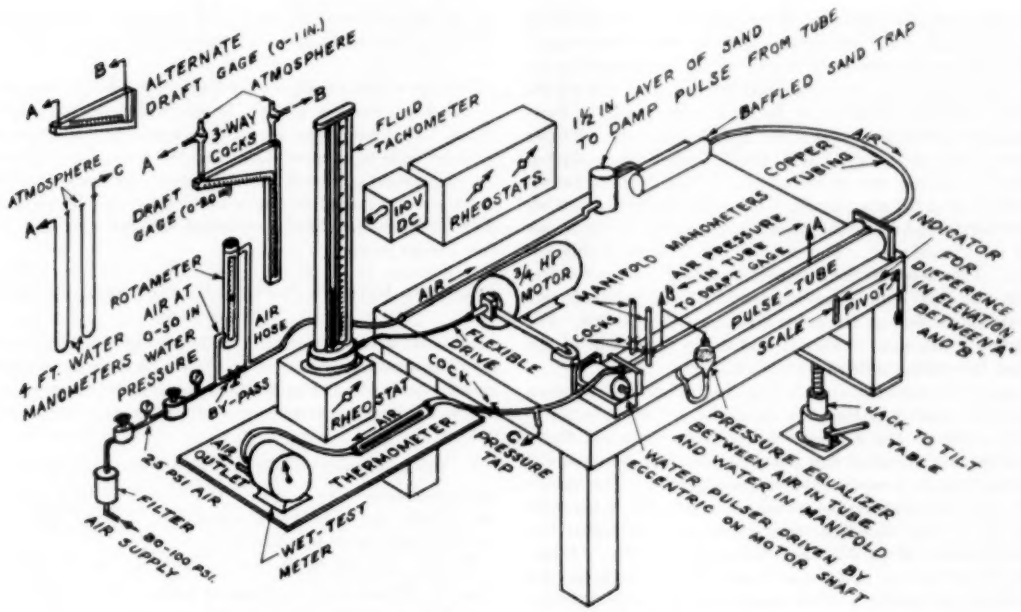

FIG. 9 SCHEMATIC DIAGRAM OF PULSE-TUBE TEST STATION

pressure drop of the test section. To compensate for this effect, the table on which the pulse tube was mounted was tilted so that the difference in elevation of the pressure taps was equal to the air pressure drop.

The general arrangement of the pulse-tube test station is shown in Fig. 9. All instruments were calibrated. The air-flow rate was kept constant by adjusting the pressure regulator to hold the Flowrator reading constant. The use of a sand pulsation damper made this control possible. The temperature of the flowing air was indicated by a thermometer in a glass section of the outlet pipe. The flow rate was measured by means of a wet test meter and stop watch. The motor speed was indicated by a fluid tachometer, driven by a flexible drive.

Velocity Distribution Measurement. Pulse tube No. 1 was used at rest, and when operating at 590 cpm with an amplitude-radius ratio of approximately 20 per cent. The air supply was connected to the normal downstream end. The manometer leads and table-tilt indicator were reversed. The pitot-impact tube was a No. 26 hypodermic needle ground square and tapered. Its outside diameter was 0.016 in. It was moved by a traversing gear with a 0.001-in. vernier. Axial and lateral positioning was done by eye. The traverse was made completely across the vertical diameter from wall to wall. The probe extended $^1/_2$ in. upstream from the open end of the lucite end pipe, which was 1.25 in. long.

RELIABILITY OF DATA

Throughout the experiment it was difficult and often impossible to make check runs on apparent anomalies. Because of the weakness of the 0.010-in. rubber tubing, the pulse tubes had a short life expectancy. Therefore it was necessary to explore as much as possible of the range of variables without undue repetition. The life of tube No. 1 was about 80 hr but tube No. 2 failed in less than 8 hr. Any holes that appeared had to be made airtight. The patching caused the loss of the cell and often the partial loss of the cell on each side. After a cell had been blanked off, the amplitude of the oscillation in the remaining cells was greater. Consequently, data taken after a repair showed higher pressure drops than before and reproduction of previous data was impossible. This inconvenience could be remedied to some extent by using Fig. 5 to find a correction to counteract the increase of f/f_0 with η_0/a. Slight real error should remain after such a correction when the repaired cells were well upstream, or were downstream from the test section. The tubes were considered ruined, however, after three cells had been inactivated in the test section.

During the pulse-tube tests, it was noted that not all the cells oscillated at the same amplitude. There was a region of comparatively small oscillations in the entrance section and in the middle of the test section. A region of large oscillations occurred in the delivery section. These regions did not change much with speed or amplitude and could not be shown to be related to any of the peculiarities of the pressure-drop measurements. There probably was some tendency toward a standing wave in the manifolds. This wave changed position slightly with varying frequency.

The effect of other complications may be pointed out in Fig. 6. The curves for $\eta_0 = 0.099a$ show an extreme example of lack of agreement between two runs under apparently the same conditions. Possibly the effective amplitude was reduced by the cushioning effect of a small volume of air in the pump, resulting in the lower curve. For $\eta_0 = 0.050a$ and frequencies above 1260, the data should be considered incorrect because of the failure of the differential manometer (AB in Fig. 9) to indicate the true pressure drop in the test section. The water manometers (A and C in Fig. 9) indicated that the f/f_0 curves actually increased at approximately the same rate as they did below 1260 cpm. The reason for the failure of the differential manometer is not known. These data were included in Fig. 6 because the apparent scatter in Fig. 4 at $\eta_0 = 0.199a$ for frequencies greater than 1600 cpm possibly may have had the same cause. Further experimentation would be needed to check this possibility.

ON STABILITY OF THE GAS FLOW

The stability of a fluid flow to an individual disturbance depends on whether or not the motion of the disturbed fluid will

cause energy from the main flow to be absorbed by the disturbed fluid. If energy is absorbed continuously the disturbance region will grow and turbulent flow will ensue. If the disturbance energy is dissipated faster than it is supplied laminar flow will result. The wave-boundary condition of the present investigation, however, imposes a periodic disturbance. If the disturbance disrupts the laminar flow and causes eddies the flow must be considered unstable (7) but may not be turbulent. Whether or not turbulence will occur in the gas column at Reynolds numbers much below 2000 will depend on the amplitude and frequency of the waves causing the disturbance. The data of Fig. 3 support this hypothesis. The slope of the constant-frequency curves for frequencies over 1500 cpm is approximately 1.3 and indicates turbulent transition flow at Reynolds numbers as low as 600. For the smaller amplitudes of Figs. 1 and 2 the depression of the transition Reynolds number is much less.

The apparent scatter of data in Fig. 3 at frequencies between 900 and 1500 appears on Fig. 4 as sensitivity of friction factor to Reynolds number. Fig. 2 shows that these regions do not represent transition to turbulent flow if it is assumed that lines parallel to the zero-frequency curve represent laminar flow. The regions possibly may be caused by the transition from stable to unstable viscous flow. That this transition should occur at higher frequencies for higher Reynolds numbers is a peculiar effect. Equation [8] shows that w, and hence A and B, must be larger for higher Reynolds numbers. This equation is the solution to the linearized Navier-Stokes equations and, as such, actually will not show instability but may give some indication of the roles played by the parameters as instability is approached. For a fixed value of the amplitude η_0, a larger value of the frequency, $\mathfrak{F} = n/2\pi$, is consistent with a larger A and Reynolds number, N_R. This trend is clearly shown in Fig. 4. Also, for a larger value of η_0, a smaller value of frequency may be consistent with stability; this trend also is shown in Fig. 4.

Lord Rayleigh has shown (8), by neglecting friction, that for infinitely small disturbances, instability results for $0 < ka < 1$, with maximum instability at $ka = 0.485$. Because of the nonlinearity of the vibrating system and the viscous damping, some small finite amplitude might be consistent with stability for ka slightly less than unity. The ka-value for tubes 1 and 2 were 0.714 and 0.528, respectively. The data show that for low frequencies the air flow was stable even at these small ka-values. For higher frequencies, however, Rayleigh's criterion for stability was supported. Further, the smaller ka-value gave the greater instability.

On the other hand, finite disturbances may cause instability for ka-values greater than unity. From measurements on the photographs of Pickrell's Fig. 212 b (5), a ka-value of 1.57 was estimated for an amplitude-radius ratio of 0.14. The corresponding f/f_0 value was 63.7, with a Reynolds number of 395. Consequently, the large amplitude-radius ratio was sufficient to cause instability for $ka > 1$.

As the gas-flow rate increases, so does the natural tendency toward instability, because of the increase of Reynolds number. Therefore the value of ka, which gives a maximum tendency toward instability at about $ka = 0.5$, increases with the Reynolds number until, as shown by Kawaratani's photographs (3), ka becomes 14 at $N_R = 10{,}000$. In other words, the increasing tendency toward turbulent flow with increasing N_R leaves a decreasing balance of the total instability requirement to be made up by the combined ka, η_0, $\mathfrak{F}$, and λ effects. Consequently, at higher gas-flow rates, Reynolds number is the important parameter.

The lower limit of annular flow is to be expected when the interfacial shear stresses are no longer sufficient to support the liquid. This condition must result when, as N_R decreases, the air flow tends to be more stable and the instability parameters of the waves must approach their maximum effectiveness. When the shear stress required becomes more than can be produced by the maximum instability consistent with annular flow, annular flow breaks down.

Relations Between Model and Prototype in Gas-Liquid Annular Flow

Previous investigators (3, 4, 5, 9) have established that R_l, the liquid saturation, is one of the most important parameters of annular upward gas-liquid flow. Its importance stems from its effects on the wave amplitude, on the frequency, and on length as follows:

1 The mean liquid depth $(b - a)$ is determined by R_l through the equation $(b - a) = b(1 - \sqrt{1 - R_l})$, where a and b are the air column and tube radii, respectively. This depth controls the maximum wave amplitude.

2 The air-column radius is fixed by the equation $a = b\sqrt{1 - R_l}$ and hence, for a given value of the parameter ka, the wave length is determined by the definition $\lambda = 2\pi a \div ka$.

3 The frequency of the interfacial capillary waves, $\mathfrak{F} = (2\pi\sigma \div \lambda^3\rho)^{1/2}$, is indirectly controlled by R_l through λ, where σ is the surface tension. The parameters η_0, λ, and $\mathfrak{F}$ were shown by the present investigation to be much more important than Reynolds number in the range tested. Consequently, the controlling influence of liquid saturation in the prototype can be inferred from the performance of the model.

The influence of the parameter ka is an essential part of the annular flow phenomenon. It may be considered as an instability promoter that makes possible the large lift forces needed at low gas-flow rates as discussed in the preceding section of the Appendix.

BIBLIOGRAPHY

1 "Proposed Correlation of Data for Isothermal Two-Phase, Two-Component Flow in Pipes," by R. W. Lockhart and R. C. Martinelli, *Chemical Engineering Progress*, vol. 45, January, 1949, pp. 39–45.

2 "Two-Phase Two-Component Flow in the Viscous Region," by R. C. Martinelli, J. A. Putnam, and R. W. Lockhart, Trans. American Institute of Chemical Engineers, vol. 42, 1946, pp. 681–702.

3 "Transition Behavior of Two-Phase Two-Component Fluid Flow in Tubes," by T. W. Kawaratani, MS thesis, University of California, Berkeley, Calif., 1950.

4 "Behavior of Two-Phase Two-Component Flow in Tubes," by F. D. McElwee, MS thesis, University of California, Berkeley, Calif., 1949.

5 "Behavior of Two-Phase Two-Component Fluid Flow in Tubes," by W. S. Pickrell, MS thesis, University of California, Berkeley, Calif., 1949.

6 "On Turbulent Fluid Motion," by M. M. Munk, Naval Ordinance Report 1572, 1950.

7 "The Theory of Sound," by Lord Rayleigh, Dover Publications, Inc., New York, N. Y., vol. 2, 1945, p. 76.

8 "On the Instability of Cylindrical Fluid Surfaces," by Lord Rayleigh, *Philosophical Magazine*, vol. 34, 1892, pp. 177–180.

9 Paper in preparation by J. A. Putnam and R. E. Buckland, data on file, Fluid Mechanics Laboratory, University of California, Berkeley, Calif.

Theoretical Calculation of the Equation of State and Transport Properties of Gases and Liquids[1]

By R. B. BIRD,[2] J. O. HIRSCHFELDER,[3] AND C. F. CURTISS,[3] MADISON, WIS.

Several years ago a summary article was written (1)[4] about the theoretical calculation of the viscosity and several other properties of gases and gas mixtures. Since that time further calculations of the equation of state and transport coefficients of dense gases and liquids have been made. Although the statistical mechanical theory is an involved and highly mathematical topic, and although some of the numerical computations are quite complex, the final results, nevertheless, may be presented in terms of tabulated functions, which are easy to use in practical calculations. The formulas and tables given in this paper should prove useful in engineering-design calculations and in chemical-process studies. Furthermore, the underlying statistical mechanical theory whenever possible should be used to give intelligent interpretation to the analysis and correlation of chemical and engineering data on the properties of matter.

Nomenclature

The following nomenclature is used in the paper:

R = gas constant
k = Boltzmann constant $= R/\bar{N}$
$\bar{N}$ = Avogadro number
h = Planck's constant
x_i, M_i = mole fraction and molecular weight of ith chemical species in a mixture
T = temperature
p = pressure
$\bar{V}$ = volume per mole
v = volume per molecule
ρ = density (mass per unit volume)
n = number density (number per unit volume)
φ = intermolecular potential-energy function
σ, ϵ = parameters ("force constants") in intermolecular potential-energy function (σ is in Ångström units, ϵ/k in °K)
μ = dipole moment of molecule
α = polarizability of molecule
B, C, D = second, third, fourth virial coefficients
$\mathfrak{D}$, η, λ = coefficients of diffusion, viscosity, thermal conductivity ("transport coefficients")
k_T = thermal-diffusion ratio
μ° = zero pressure Joule-Thomson coefficient
γ = ratio of specific heats
γ' = surface tension
$\Omega^{(l,s)*}$ = integrals in terms of which transport coefficients of dilute gases are expressed (Table 3)
A^*, B^*, C^* = special combinations of the $\Omega^{(l,s)*}$ which occur in formulas for transport coefficients of dilute gas mixtures (Table 3)
$f_\eta^{(3)}, f_\lambda^{(3)}, f_\mathfrak{D}^{(3)}$ = functions which give higher approximations to transport coefficients (Table 3)
° (superscript) = limiting value at zero pressure
∼ (above symbol) = quantity per mole
c (subscript) = quantity evaluated at critical point
r (subscript) = quantity made dimensionless by dividing by corresponding value of quantity at critical point
R (subscript) = quantity made dimensionless by dividing by appropriate combinations of p_c, V_c, T_c
* (superscript) = quantity made dimensionless by dividing by proper combination of σ and ϵ
★ (superscript) = quantity made dimensionless by dividing by combinations of σ and ϵ in such a way as to make use of rigid sphere quantities

$$T^* = kT/\epsilon \qquad t^* = \mu^{*2}/\sqrt{8}$$
$$v^* = v/\sigma^3 \qquad \alpha^* = \alpha/\sigma^3$$
$$p^* = p\sigma^3/\epsilon \qquad B^\star = B/b_0$$
$$\mu^* = \mu/\sqrt{\epsilon\sigma^3} \qquad C^\star = C/b_0^2$$

1 Potential Energy of Interaction Between Two Molecules[5]

In statistical mechanical theory one does not usually work in terms of the force of interaction between two molecules, but rather in terms of the potential energy of interaction φ. If φ depends only upon the intermolecular distance r, then $-d\varphi/dr$ is the force acting between the two molecules.

[5] The theory of intermolecular forces has been discussed in review articles by London (2) and Margenau (3). An elementary discussion of the subject may be found in MTGL §1.3, and a complete survey is given in MTGL chapters 12, 13, 14.

---

[1] Part of this work was carried out under Contract NOrd 9938, Navy Bureau of Ordnance.

[2] Department of Chemical Engineering, University of Wisconsin.
[3] University of Wisconsin, Naval Research Laboratory, Department of Chemistry.

[4] Numbers in parentheses refer to the Bibliography at the end of the paper.

Contributed by the Heat Transfer Division and presented at the Annual Meeting, New York, N. Y., November 29–December 4, 1953, of The American Society of Mechanical Engineers.

Note: This paper is very similar to chapter 5.5, prepared by the authors for the "Handbook of Physics," edited by E. U. Condon, McGraw-Hill Book Company, New York, N. Y., 1954. A detailed discussion of the material contained in this survey may be found in "The Molecular Theory of Gases and Liquids," by J. O. Hirschfelder, C. F. Curtiss, and R. B. Bird (to be published in 1954 by John Wiley & Sons, Inc., New York, N. Y.). In this book (hereinafter referred to as MTGL) there is given a discussion of the theoretical basis for the formulas presented in this paper, and many numerical examples are given in order to illustrate the use of the formulas and the accompanying tabulated functions. The material discussed in this paper is given in chapters 3, 4, 8, and 9 of MTGL. The nomenclature used here is the same as that in the book.

 Manuscript received at ASME Headquarters, August 13, 1953. Paper No. 53—A-87.

In principle the dependence of φ on the separation between two interacting molecules and their mutual orientation can be obtained by a priori quantum mechanical calculation. In practice, however, attempts along this line have yielded results for only the simplest of atoms and molecules. Accordingly, it is customary to use empirical potential-energy functions (sometimes referred to as "molecular models") with several adjustable parameters and to determine these parameters from experimental measurements of bulk properties in conjunction with the statistical mechanical calculations of the same properties.

(a) Empirical Potential Energy Functions for Nonpolar and Polar Molecules. At the present time the most used potential energy function for nonpolar molecules is the Lennard-Jones (6–12) potential and for polar molecules the Stockmayer potential. These empirical functions are as follows:

Lennard-Jones (nonpolar)

$$\varphi(r) = 4\epsilon\left[\left(\frac{\sigma}{r}\right)^{12} - \left(\frac{\sigma}{r}\right)^{6}\right] \quad \ldots\ldots\ldots [1.1]$$

Stockmayer (polar)

$$\varphi(r, \theta_1, \theta_2, \phi_2 - \phi_1) = 4\epsilon\left[\left(\frac{\sigma}{r}\right)^{12} - \left(\frac{\sigma}{r}\right)^{6}\right] - \frac{\mu^2}{r^3} f(\theta_1, \theta_2, \phi_2 - \phi_1) \quad \ldots\ldots [1.2]$$

in which σ and ϵ are adjustable parameters (or "force constants"), characteristic of the chemical species of the colliding molecules.

In the Lennard-Jones potential the r^{-6} term is a very good first approximation to the long-range attractive forces, and the r^{-12} term is a fair approximation to the short-range repulsive forces. The parameter ϵ is the maximum energy of attraction, and σ is that value of r for which φ is zero (see Fig. 1). The Lennard-Jones potential has been shown to be reasonably good for representing the interaction between spherical (and almost spherical) nonpolar molecules.

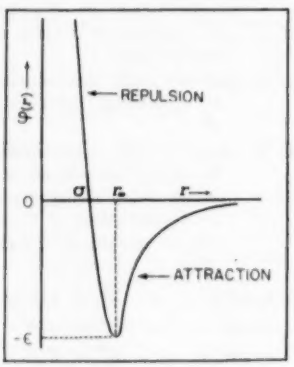

FIG. 1 LENNARD-JONES POTENTIAL ENERGY OF MOLECULAR INTERACTION AS A FUNCTION OF DISTANCE r BETWEEN THE TWO MOLECULES

(Distance r_m, which corresponds to minimum in $\varphi(r)$ is $\sqrt[6]{2}\,\sigma$. When $r > r_m$ molecules are attracted to one another; when $r < r_m$ molecules repel one another.)

In the Stockmayer potential the r^{-6} and r^{-12} terms have the same significance as in the Lennard-Jones potential, but the parameters σ and ϵ have to be interpreted somewhat differently. The r^{-3} term represents the long-range attraction between two point dipoles, the mutual orientation of which is described by the angles θ_1, θ_2, and $\phi_2 - \phi_1$. The function $f(\theta_1, \theta_2, \phi_2 - \phi_1)$ is equal to $[2\cos\theta_1\cos\theta_2 - \sin\theta_1\sin\theta_2\cos(\phi_2 - \phi_1)]$, and μ is the dipole moment of a single molecule. The Stockmayer potential is reasonably good for simple polar molecules. For complex polar molecules, however, it is less appropriate, inasmuch as the angle dependence of the short-range repulsive forces and the dipole-quadrupole interaction are not taken into account.

(b) Determination of Parameters in Empirical Potential-Energy Functions. The parameters σ and ϵ in the Lennard-Jones potential are most satisfactorily determined from experimental second virial coefficients or viscosity coefficients in conjunction with the statistical mechanical formulas for these properties which are given in sections 2 and 4. In Table 1 is given the most complete tabulation available for these parameters. Also given is the value of $b_0 = (2/3)\pi\mathcal{N}\sigma^3$, which is used in equation-of-state calculations. If b_0 is in cm³ mol⁻¹ and σ is in Ångström units, then $b_0 = 1.2615\sigma^3$.

Frequently viscosity and second virial-coefficient data are not available for obtaining these potential parameters. Then use must be made of empirical relationships to estimate the σ and ϵ of the Lennard-Jones potential from the properties of the substance at its critical point (c),[6] its melting point (m), its boiling point (b), and its Boyle point (B), or the absolute zero (z). These relations are given in terms of ϵ/k (in °K) and b_0 (in cm³ mole⁻¹).

$$\left.\begin{array}{ll} \epsilon/k = 0.77T_c & b_0 = 0.75\mathcal{V}_c = 18.47T_c/p_c \\ \epsilon/k = 1.15T_b & b_0 = 2.0\mathcal{V}_b^{(\text{liq})} \\ \epsilon/k = 1.92T_m & b_0 = 2.3\mathcal{V}_m^{(\text{sol})} \\ \epsilon/k = 0.292T_B & \ldots \\ \ldots & b_0 = 2.293\mathcal{V}_z^{(\text{sol})} \end{array}\right\} \quad [1.3]$$

These formulas may be used to estimate potential parameters for the Lennard-Jones potential, and the parameters in turn may be used to calculate the equation of state and the transport coefficients with the aid of the formulas and tables given in subsequent sections.

In Table 2 is given the most complete tabulation available of the parameters σ and ϵ for the Stockmayer potential as determined from experimental second virial coefficients. In addition, the parameter $t^* = \mu^{*2}/\sqrt{8} = \mu^2/\epsilon\sigma^3\sqrt{8}$ is given. This quantity is a measure of the deviation of the properties of polar substances from nonpolar behavior.

(c) Empirical Combining Laws for Interactions Between Two Dissimilar Molecules. The potential parameters given in Tables 1 and 2 are for interactions between molecules of the same chemical species. In the calculation of the bulk properties of mixtures it is necessary to know the potential-energy function describing the interaction between pairs of molecules of different species. The best way to obtain this information is from the temperature dependence of gaseous binary diffusion coefficients. In view of the fact that only meager diffusion data exist, it is necessary to employ empirical combining laws, which have been demonstrated to be reasonably adequate (1). These laws are as follows:

(i) *Nonpolar-nonpolar interaction:* The interaction of two nonpolar molecules of species 1 and 2 is described by the Lennard-Jones potential, where the parameters σ and ϵ are given by

$$\sigma_{12} = \frac{1}{2}(\sigma_1 + \sigma_2); \quad \epsilon_{12} = \sqrt{\epsilon_1\epsilon_2} \quad \ldots\ldots\ldots [1.4]$$

where σ_i and ϵ_i are the parameters appropriate for molecules of the ith species as given in Table 1.

[6] A complete summary of values of the critical constants has been compiled recently by Kobe and Lynn (4).

(ii) *Polar-polar interaction:* The interaction of two polar molecules of species 1 and 2 is described by the Stockmayer potential, in which the parameters σ and ϵ are given by Equation [1.4], were σ_i and ϵ_i are the parameters given in Table 2. Also, the parameter t^* characteristic of the unlike interaction is given by

$$t_{12}^* = \frac{\mu_1\mu_2}{\sqrt{8}\,\epsilon_{12}\sigma_{12}^3} \doteq \sqrt{t_1^* t_2^*} \quad \ldots\ldots\ldots\ldots [1.5]$$

where μ_i is the dipole moment of the ith type of molecule and t_i^* is the quantity defined previously and tabulated in Table 2.

(iii) *Nonpolar-polar interaction:* The interaction between a polar molecule p and a nonpolar molecule n is described approximately by the Lennard-Jones potential (1) in which the parameters σ and ϵ are given by

$$\sigma_{pn} = \frac{1}{2}(\sigma_p + \sigma_n)\xi^{-1/6}; \quad \epsilon_{pn} = \sqrt{\epsilon_p\epsilon_n}\,\xi^2 \ldots\ldots [1.6]$$

in which the factor ξ is given by

$$\xi = \left[1 + \frac{1}{2}\sqrt{2}\,\alpha_n^* t_p^* \sqrt{\epsilon_p/\epsilon_n}\right] \ldots\ldots\ldots [1.7]$$

The parameters σ_n and ϵ_n are obtained from Table 1, and σ_p, ϵ_p, t_p^* are obtained from Table 2. The quantity α_n^* is the polarizability of the nonpolar molecule α_n divided by σ^3.

(*d*) *Present Status of Theory of Intermolecular Forces.* Quantum mechanical calculations have given us a considerable amount of information about the theory of the forces between spherical molecules at distances from one another which are large with respect to molecular dimensions (2, 3, 61). The theory of these long-range forces has also been worked out for asymmetric molecules by London (5) and for long conjugated double-bond molecules by Coulson and Davies (6). The a priori calculation of the potential energy of interaction for all values of the separation has progressed very little beyond the interaction of two noble gas atoms (7) and of two hydrogen molecules (8). The inherent numerical difficulties in calculating the forces between more complicated molecules are exceedingly great. Advances along this line are to be expected, however, along with the development of larger electronic computers.

Another approach to the study of intermolecular forces is to determine the adjustable parameters in empirical potential-energy functions which are more realistic and hence more elaborate than the Lennard-Jones and Stockmayer potentials. For spherical nonpolar molecules Buckingham and Corner (9) have proposed a potential-energy function which contains an additional attractive term proportional to r^{-6} to account for the induced dipole-induced quadrupole interaction, and the repulsive part of which is of an exponential form. For nonspherical molecules several models (which are extensions of the Lennard-Jones potential) have been proposed—one by Corner (10) and a somewhat simpler one by Kihara (11).

For polar molecules Rowlinson (12) has suggested that the Stockmayer potential be modified by the inclusion of a term proportional to r^{-4}, which represents the dipole-quadrupole interaction. The success of this semiempirical sort of an approach is definitely limited by the lack of very accurate experimental measurements of the bulk properties which are needed for the unique determination of the adjustable parameters in the potential functions. Furthermore, a considerable amount of information needs yet to be compiled about the quadrupole and higher multipole moments of molecules; it is hoped that such information eventually will be obtained from the analysis of the pressure-broadening of microwave spectra (13, 14).

2 Equation of State of Dilute and Moderately Dense Gases

At very low pressures and high temperatures the pressure of a gas is given by the ideal gas law, $pV = NkT$. The thermodynamic properties of a gas under such conditions (that is, the so-called "zero-pressure" properties) can be calculated by means of statistical mechanics for substances consisting of polyatomic molecules. The complete details of the theory are given in the textbook of Mayer and Mayer (15) and are summarized from the point of view of practical computations in the chemical-engineering text of Hougen and Watson (16).

Two approaches have been used in the study of the deviations of the equation of state of gases from the ideal gas law. One method leads to an expression for the pressure in terms of the "configurational integral" Q_N, which (for angle-independent potential functions) is

$$\int\int \cdots \int \exp\left(-\frac{1}{2}\sum_{i=1}^{N}\sum_{j=1}^{N} \varphi(r_{ij})/kT\right) dr_1 dr_2 \ldots dr_N$$

The quantity $(1/2)\Sigma\Sigma\varphi(r_{ij})$ is just the total potential energy of the molecules in the gas in a given configuration, and N is total number of molecules in the gas. The second method leads to an expression for the pressure in terms of the "radial distribution function" $g(r)$. The latter is so defined that $(N^2/2V)\,g(r)\,4\pi r^2 dr$ is the number of molecules for which the separation lies between r and $r + dr$. In terms of these quantities the equation of state is written as

$$pV = kT(\partial \ln Q_N/\partial \ln V)_T \ldots\ldots\ldots\ldots [2.1]$$

$$pV = NkT - \frac{N^2}{6V}\int g(r) r \frac{d\varphi}{dr} 4\pi r^2 dr \ldots\ldots [2.2]$$

It has been established that these two expressions for the equation of state are equivalent (17). These two equations form the starting point for the theoretical and computational results discussed in this and the following section. It should be noted that if $\varphi(r) = 0$ (i.e., no intermolecular forces), then Equations [2.1] and [2.2] both reduce to the ideal gas law.

(*a*) *Virial Form of Equation of State.* It is possible to develop both $\ln Q_N$ and $g(r)$ as power series in the number density N/V. This allows the equation of state to be written in the "virial expansion" form

$$\frac{p\bar{V}}{RT} = 1 + \frac{B(T)}{\bar{V}} + \frac{C(T)}{\bar{V}^2} + \frac{D(T)}{\bar{V}^3} + \ldots\ldots [2.3]$$

in which B, C, D, ... are the second, third, fourth, ... virial coefficients. For some purposes it is more convenient to write this expansion in terms of powers of the pressure

$$\frac{p\bar{V}}{RT} = 1 + B'(T)p + C'(T)p^2 + D'(T)p^3 + \ldots\ldots\ldots [2.4]$$

in which $B' = B/RT$ and $C' = (C - B^2)/(RT)^2$. The virial coefficients are functions of the temperature only and are given as integrals which contain the intermolecular potential function φ. For angle-independent potentials (such as the Lennard-Jones potential) the second and third virial coefficients are given by

$$B(T) = -2\pi N \int_0^\infty f_{12} r_{12}^2 dr_{12} \ldots\ldots\ldots [2.5]$$

$$C(T) = -\frac{8\pi^2 N^2}{3}\int\int\int f_{12} f_{13} f_{23}\, r_{12} r_{13} r_{23}\, dr_{12} dr_{13} dr_{23} \ldots [2.6]$$

(integral over all r_{12}, r_{13}, r_{23} which form a triangle)

TABLE 1 FORCE CONSTANTS FOR LENNARD-JONES (6-12) POTENTIAL[a]

Notes: 1) Whenever possible the parameters obtained from viscosity data should be used for making transport property calculations, and parameters from experimental second virial coefficients should be used for calculations of equation of state and thermodynamic properties.

2) For the lighter gases two sets of force constants are given: those labeled "Cl", which were determined using classical formulae, (which are not strictly applicable), and those labeled "Qu", which were obtained from quantum mechanical formulae. The latter are the true force constants while the former are only "effective" force constants. For accurate calculations and for extrapolations to high temperature the "Qu" parameters must be used -- in conjunction with the quantum mechanical formulae and tabulated functions. The "Cl" parameters are useful for rough calculations -- in conjunction with the classical formulae and tabulated functions.

3) Force constants are given here for a number of substances which are polar and/or non-spherical and hence are not described by the Lennard-Jones potential. These constants along with the tabulated functions based on the Lennard-Jones potential may, however, be useful for purposes of calculations until the theory needed for describing complex molecules has been developed.

4) Where two sets of force constants obtained from viscosity data are shown the temperature range of the data from references a, c is from 80° K to 300°K, and for the data in reference e is generally in the range from 300°K to 1000°K.

GAS	Force Constants from Viscosity			Force Constants from Second Virial Coefficients			
	ϵ/k (°K)	σ (Å)	Refs. for Data	ϵ/k (°K)	σ (Å)	$b_o = \frac{2}{3}\pi \tilde{N} \sigma^3$ (cc/mol)	Refs. for Data
Light Gases							
He(Qu)	-	-	-	10.22	2.556	21.07	A
He(Cl)	10.22	2.576	a, b	6.03	2.63	18.10	A
H_2(Qu)	-	-	-	37.00	2.928	31.67	B
H_2(Cl)	33.3 38.0	2.968 2.915	c, b e	29.2	2.87	29.76	B
D_2(Qu)	-	-	-	37.00	2.928	31.67	C
D_2(Cl)	39.3	2.948	d	31.1	2.87	29.77	C

[a] This table is an augmentation of a table given in J. O. Hirschfelder, R. B. Bird, E. L. Spotz, *Chemical Reviews*, vol. 44, 1949, pp. 205–231.

TABLE 1 (*Continued*)

GAS	Force Constants from Viscosity			Force Constants from Second Virial Coefficients			
	ϵ/k (°K)	σ (Å)	Refs. for Data	ϵ/k (°K)	σ (Å)	$b_o = \frac{2}{3}\pi N \sigma^3$ (cc/mol)	Refs for Data
Noble Gases							
Ne	35.7	2.789	a	35.60	2.749	26.21	D
	27.5	2.858	e, f, g	34.9	2.78	27.10	E
A	124	3.418	a	119.8	3.405	49.80	F
	116	3.465	e	122.	3.40	49.58	E
Kr	190	3.61	b	171.	3.60	58.86	G
				158	3.597	58.7	H
Xe	229	4.055	l	221	4.100	86.94	J
				217	3.963	78.5	H
Simple Poly-atomic Gases:							
Air	97.0	3.617	c	99.2	3.522	55.11	K
	84.0	3.689	e, f, j	102.	3.62	60.34	L
N_2	91.5	3.681	c	95.05	3.690	63.78	M
	79.8	3.749	e, h	95.9	3.71	64.42	E
O_2	113.	3.433	c	117.5	3.58	57.75	H
	88.0	3.541	e	118	3.46	52.26	L
CO	110.	3.590	c	100.2	3.763	67.22	N
	88.0	3.706	e, h				
CO_2	190.	3.996	c	189	4.486	113.9	P
	213	3.897	e, i	205	4.07	85.05	Q
NO	119	3.470	c	131	3.17	40.	R
	91.0	3.599	l				
N_2O	220	3.879	c	189	4.59	122.	R
	237.	3.816	i				
CH_4	137.	3.882	c	148.2	3.817	70.16	S
	144.	3.796	k				
CF_4	-	-	-	152.5	4.70	131.0	T
CCl_4	327	5.881	b	-	-	-	-
SO_2	252	4.290	e	-	-	-	-
SF_6	-	-	-	200.9	5.51	211.1	T
F_2	112	3.653	n	-	-	-	-
Cl_2	357	4.115	p	-	-	-	-
	257	4.400	l	-	-	-	-
Br_2	520	4.268	q, r	-	-	-	-
I_2	550	4.982	p	-	-	-	-

TABLE 1 (*Continued*)

GAS	Force Constants from Viscosity			Force Constants for Second Virial Coefficients			
	ϵ/k (°K)	σ (Å)	Refs. for Data	ϵ/k (°K)	σ (Å)	$b_o = \frac{2}{3}\pi \tilde{N} \sigma^3$ (cc/mol)	Refs. for Data
Other inorganic Vapors:							
HCl	360	3.305	m	-	-	-	-
HI	324	4.123	l	-	-	-	-
AsH_3	281	4.06	b	-	-	-	-
HgI_2	698	5.625	g	-	-	-	-
$HgBr_2$	530	5.414	p	-	-	-	-
$SnBr_4$	465	6.666	p	-	-	-	-
$SnCl_4$	1550	4.540	p	-	-	-	-
Hg	851	2.898	u	-	-	-	-
Hydrocarbons:							
$CH \equiv CH$	185	4.221	s	-	-	-	-
$CH_2 = CH_2$	205	4.232	b	199.2	4.523	116 7	U
C_2H_6	230	4.418	b	243	3.954	78.	H
C_3H_8	254	5.061	b	242	5.637	226.	H
$n\text{-}C_4H_{10}$	410	4.997	s	297	4.971	155.	H
$i\text{-}C_4H_{10}$	313	5.341	s	-	-	-	-
$n\text{-}C_5H_{12}$	345	5.769	t	-	-	-	-
$n\text{-}C_6H_{14}$	413	5.909	t	-	-	-	-
$n\text{-}C_7H_{16}$		-	-	282	8.88	884.	H
$n\text{-}C_8H_{18}$	320	7.451	b				
$n\text{-}C_9H_{20}$	240	8.448	b				
Cyclo-hexane	324	6.093	t				
C_6H_6	440	5.270	b				
Other Organic Vapors:							
CH_3OH	507	3.585	t				
C_2H_5OH	391	4.455	t				
CH_3Cl	855	3.375	p				
CH_2Cl_2	406	4.759	p				
$CHCl_3$	327	5.430	b				
C_2N_2	339	4.38	b				
COS	335	4.13	b				
CS_2	488	4.438	t				

TABLE 1 (*Continued*)

A—A. Michels and H. Wouters, Physica, 8, 923 (1941)
B—A. Michels and M. Goudeket, Physica, 8, 347 (1941)
C—A. Michels and M. Goudeket, Physica, 8, 353 (1941)
D—R. A. Buckingham, Proc. Roy. Soc., A168, 264 (1938)
E—L. Holborn and J. Otto, Zeits. für Phys., 33, 1 (1925)
F—A. Michels, Hub. Wijker, and Hk. Wijker, Physica (1949)
G—J. A. Beattie, R. J. Barriault, and J. S. Brierley, J. Chem. Phys., 20, 163, (1953)
H—D. M. Newitt, "Design of High Pressure Plant and the Properties of Fluids at High Pressures," Oxford (1940)
J—J. A. Beattie, R. J. Barriault, and J. S. Brierley, J. Chem. Phys., 19, 1222 (1951)
K—L. Holborn and H. Schultze, Ann. der Physik, 47, 1089 (1915)
L—L. Holborn and J. Otto, Zeits. für Physik, 10, 367 (1922)
M—A. Michels, H. Wouters, and J. de Boer, Physica, 1, 587 (1934)
N—J. Corner, Proc. Roy. Soc., 58, 737 (1946)
P—A. Michels and C. Michels, Proc. Roy. Soc., A153, 201 (1936)
Q—K. E. MacCormack and W. G. Schneider, J. Chem. Phys., 18, 1269, (1950)
R—J. O. Hirschfelder, F. T. McClure, C. F. Curtiss, and D. W. Osborne, NDRC Report A116 (November, 1946)
S—A. Michels and G. W. Nederbragt, Physica, 2, 1000 (1935).
T—K. E. MacCormack and W. G. Schneider, J. Chem. Phys., 19, 849, (1951)
U—A. Michels and M. Geldermans, Physica, 9, 967 (1942)
a—H. L. Johnston and E. R. Grilly, J. Phys. Chem., 46, 938 (1942)
b—Landolt-Bornstein, "Physikalisch-Chemische Tabellen"
c—H. L. Johnston and K. E. McCloskey, J. Phys. Chem., 44, 1038 (1940)
d—A. van Itterbeek and A. Claes, Physica, 5, 938 (1938)
e—M. Trautz, A. Melster and R. Zinc, Ann. de Physik (5), 7, 409–452 (1930) (H_2, Ne, A, Air, N_2, O_2, CO, CO_2, CH_4, SO_2)
f—M. Trautz and H. E. Binkele, Ann. de Physik (5), 5, 461 (1930) (H_2, Ne, A, Air)
g—M. Trautz and H. Zimmerman, Ann. d. Physik (5), 22, 189 (1935) (H_2, Ne)
h—M. Trautz and P. B. Baumann, Ann. d. Physik (5), 2, 733 (1929). (H_2, Air, N_2, CO)
i—M. Trautz and F. Kurz, Ann. d. Physik (5), 9, 981 (1931) (H_2, CO_2, N_2O)
j—M. Trautz and W. Weisel, Ann. d. Physik (4), 78, 305 (1925) (Air)
k—M. Trautz and K. G. Sorg, Ann. d. Physik (5), 10, 81 (1931) (CH_4)
l—M. Trautz, R. Heberling, I. Husseini, F. Ruf, and A. Freytag, Ann. d. Physik (5), 20, 118–114 (1934) (Xe, NO, Cl_2, HI)
m—M. Trautz and A. Narath, Ann. d. Physik (5), 7, 427 (1930) (HCl)
n—E. Kanda, Bull. Chem. Soc., Japan, 12, 465 (1937)
p—H. Braune, R. Linke, Z. Physik. Chem., A148, 195 (1930)
q—A. O. Rankine, Proc. Roy. Soc., 88, 582 (1913)
r—H. Braune, R. Basch and W. Wentzel, Z. Phys. Chem., A137, 176, 447 (1928)
s—T. Titani, Bull Chem. Soc. Japan, 5, 98 (1930)
t—T. Titani, Bull. Chem. Soc. Japan, 8, 255 (1933)
u—L. F. Epstein and M. D. Powers, J. Phys. Chem. (to be published)

where $f_{12} = [\exp[-\varphi(r_{12})/kT] - 1]$. For angle-dependent potentials (such as the Stockmayer potential) $B(T)$ is given by a 4-fold integral and $C(T)$ by a 9-fold integral, since φ and the f_{ij} are both angle-dependent. The second virial coefficient basically describes the deviations from the ideal gas law $p\bar{V} = RT$ due to binary collisions. The third virial coefficient describes the deviations due to ternary collisions. Thus, as the density of a gas is increased, more virial coefficients are needed to explain the p-V-T behavior.

(*b*) *Virial Coefficients for Nonpolar Gases.* The second and third virial coefficients have been evaluated for nonpolar molecules (Lennard-Jones potential) and the results may be expressed in the very simple form

$$B(T) = b_0 B^*(T^*) \quad [2.7]$$

$$C(T) = b_0^2 C^*(T^*) \quad [2.8]$$

The functions $B^*(T^*)$ and $C^*(T^*)$ are given in Table 3(*a*). The parameters σ and ϵ in the Lennard-Jones potential enter into the expression through the unit of volume $b_0 = (2/3)\pi\bar{N}\sigma^3$ and the reduced temperature $T^* = kT/\epsilon$. Thus the potential parameters in Table 1 can be used to calculate $B(T)$ and $C(T)$ for nonpolar molecules from Table 2. It has been found that the agreement between the experimental and calculated $B(T)$ is excellent, and that for $C(T)$ it is moderately good (18). Also given in Table 3(*a*) is the function $[T^*(dB^*/dT^*) - B^*]$ which is simply related to the zero-pressure Joule-Thomson coefficient μ°

$$\mu^\circ \bar{C}_p^\circ = b_0 \left[T^* \frac{dB^*}{dT^*} - B^* \right] \quad [2.9]$$

in which $\bar{C}_p^\circ$ is the zero-pressure heat capacity per mole at constant pressure. Agreement between experimental and calculated values of $\mu^\circ \bar{C}_p^\circ$ has been found to be extremely good (60).

(*c*) *Virial Coefficients for Polar Gases.* The second and third virial coefficients also have been evaluated for polar molecules (Stockmayer potential) and the results are given simply as

$$B(T) = b_0 B^*(T^*, t^*) \quad [2.10]$$

$$C(T) = b_0^2 C^*(T^*, t^*) \quad [2.11]$$

The functions $B^*(T^*, t^*)$ and $C^*(T^*, t^*)$ are given in Tables 4(*a*) and 4(*b*). (These functions for $t^* = 0$ are the same as those for the Lennard-Jones potential.) Here the σ and ϵ of the Stockmayer potential enter into the expressions through $b_0 = (2/3)\pi\bar{N}\sigma^3$ and $T^* = kT/\epsilon$ and, in addition, in the quantity t^*, which is a measure of the deviation from nonpolar behavior. Hence the potential parameters in Table 2 may be used to calculate $B(T)$ from Table 4(*a*) and $C(T)$ from Table 4(*b*) for polar molecules. What few good experimental measurements are available indicate that the use of these tables gives reasonably good agreement with experiment. See Ref. (*a*), Table 4(*b*). Tables also have been prepared for calculating Joule-Thomson coefficients of polar gases (see MTGL, Table IIB).

(*d*) *Virial Coefficients for Mixtures of Gases.* Thus far the discussion has been restricted to the calculation of the equation of state for pure substances. The virial equation of state, Equation [2.3] also may be used for multicomponent mixtures containing both nonpolar and polar components. For a mixture made up of ν-components the second virial coefficient is given by

$$B_{mix} = \sum_{i=1}^{\nu} \sum_{j=1}^{\nu} x_i x_j B_{ij} \quad [2.12]$$

The quantity B_{jj} is the second virial coefficient for the pure j^{th} substance, calculated according to Equation [2.7] if that substance is nonpolar or according to Equation [2.10] if that substance is polar. The quantity B_{ij} is the second virial coefficient calculated for a hypothetical substance, characterized by intermolecular potential parameters σ_{ij} and ϵ_{ij}, appropriate for the various interactions between pairs of dissimilar molecules in the gas. The following table indicates how the B_{ij} are to be calculated:

Nature of molecule i	Nature of molecule j	σ_{ij} and ϵ_{ij} to be computed from Equation	Table	B_{ij} given by formula	B^* is tabulated in table
Nonpolar	Nonpolar	[1.4]	1	$\left(\frac{2}{3}\pi\bar{N}\sigma_{ij}^3\right) B^*(kT/\epsilon_{ij})$	3
Nonpolar	Polar	[1.6], [1.7]	1, 2	$\left(\frac{2}{3}\pi\bar{N}\sigma_{ij}^3\right) B^*(kT/\epsilon_{ij})$	3
Polar	Polar	[1.5]	2	$\left(\frac{2}{3}\pi\bar{N}\sigma_{ij}^3\right) B^*(kT/\epsilon_{ij};\ t_{ij}^*)$	4

It is not possible to calculate the third virial coefficient of gaseous mixtures exactly by use of the tables given here, inasmuch as the C_{ijk} have not been evaluated for the Lennard-Jones and the Stockmayer potentials. A method for estimating these quantities, nevertheless, has been proposed (18).

(*e*) *Present Status of Theory, Calculations, and Experimental Data.* The status of the theoretical development of the equation of state at moderate densities is quite satisfactory. In fact, the virial expansion is one of the cleanest-cut developments in the subject of statistical mechanics. The quantum mechanical theory has been developed as well as the classical theory (17). The only assumption which goes into calculations based upon the theory is that of the potential-energy function describing the molecular

TABLE 2 FORCE CONSTANTS FOR STOCKMAYER POTENTIAL[?]

$b_o\,(cc/mol) = 2\pi\tilde{N}\sigma^3/3 = 1.2615\left[\sigma\,(\text{Å})\right]^3$

$t^* = (8)^{-1/2}\mu^{*2}$ $\qquad \mu^* = \mu/\sqrt{\epsilon\sigma^3}$

Substance	μ (debyes‡)	t^*	ϵ/k (°K)	σ (Å)	b_o (cc/mol)	Ref. for B(T) data
$CHCl_3$	1.05	0.1	1060	2.98	33.45	a
$CHCl_2F$(*)	1.29	0.1	381	4.82	141.	b
C_2H_5Cl	2.02	0.2	320	5.41	199.7	a
CH_3Cl	1.89	0.6	380	3.43	50.73	c
CH_3COCH_3	2.74	0.7	520	3.76	66.87	a
CH_3OH	1.66	0.8	630	2.40	17.48	a
NH_3	1.47	1.0	320	2.60	22.12	d
CH_3F	1.82	1.07	207	3.36	47.85	e
H_2O	1.83	1.2	380	2.65	23.42	f
CH_3CN	3.5	1.2	400	4.02	82.04	a
CH_3CHO	2.7	1.4	270	3.68	62.75	g

a. Lambert, Roberts, Rowlinson and Wilkinson, Proc. Roy. Soc., A196, 113 (1949)
b. "Thermodynamic Properties of Dichloromonofluoromethane", Kinetic Chemicals Inc. (1939)
c. "Methyl Chloride", E. I. du Pont de Nemours & Co., The R & H Chemicals Department; 5th Ed., (1940)
d. F. G. Keyes, J.A.C.S., 60, 1761 (1938) has correlated the experimental data of C. H. Meyers and R. S. Jessup, Refrig. Eng., 11, 345(1925); J. A. Beattie and C. K. Lawrence, J.A.C.S., 52, 6 (1930)
e. A. Michels and A. Visser, (in preparation)
f. F. G. Keyes, L. B. Smith, & H. T. Gerry, Proc. Am. Acad. Arts Sci. 70, 319 (1936); S.C. Collins & F. G. Keyes, ibid., 72, 283 (1938)
g. Alexander and Lamber, Trans. Faraday Soc., 37, 421 (1941)

(*) The force constants for $CHCl_2F$ are those calculated in the illustrative example in Section 10c of MTGL.
‡ From a table given by J. S. Rowlinson, Trans. Far. Soc., 45, 980 (1949)
⊛ The values given for CH_3F were calculated by R. J. Lunbeck and C. A. ten Seldam, Physica 27, 788 (1951)
‡ 1 debye = 1×10^{-18} e.s.u.

TABLES 3(a) FUNCTIONS USED IN CALCULATION OF PROPERTIES OF DILUTE AND MODERATELY DENSE NONPOLAR GASES (LENNARD-JONES POTENTIAL)[a]

T^*	B^*	$T^* \frac{dB^*}{dT^*} - B^*$	C^*	$\Omega^{(1,1)*}$	$\Omega^{(2,2)*}$	k_T^* Heavy isotopes
0.30	-27.880581	104.488		2.662	2.785	0.086
0.35	-18.754895	64.003		2.476	2.628	0.035
0.40	-13.798835	44.066		2.318	2.492	- 0.002
0.45	-10.754975	32.744		2.184	2.368	- 0.032
0.50	- 8.720205	25.644		2.066	2.257	- 0.048
0.55	- 7.2740858	20.8563		1.966	2.156	- 0.059
0.60	- 6.1979708	17.4468		1.877	2.065	- 0.063
0.65	- 5.3681918	14.9137		1.798	1.982	- 0.063
0.70	- 4.7100370	12.9672	- 3.37664	1.729	1.908	- 0.057
0.75	- 4.1759283	11.4299	- 1.79197	1.667	1.841	- 0.049
0.80	- 3.7342254	10.1884	- 0.84953	1.612	1.780	- 0.039
0.85	- 3.3631193	9.1665	- 0.27657	1.562	1.725	- 0.025
0.90	- 3.0471143	8.3120	+ 0.07650	1.517	1.675	- 0.010
0.95	- 2.7749102	7.5877	0.29509	1.476	1.629	+ 0.005
1.00	- 2.5380814	6.9663	0.42966	1.439	1.587	0.019
1.05	- 2.3302208	6.4279	0.51080	1.406	1.549	0.033
1.10	- 2.1463742	5.9570	0.55762	1.375	1.514	0.047
1.15	- 1.9826492	5.5419	0.58223	1.346	1.482	0.066
1.20	- 1.8359492	5.1734	0.59240	1.320	1.452	0.080
1.25	- 1.7037784	4.8442	0.59326	1.296	1.424	0.099
1.30	- 1.5841047	4.5483	0.58815	1.273	1.399	0.108
1.35	- 1.4752571	4.2810	0.57933	1.253	1.375	0.127
1.40	- 1.3758479	4.0385	0.56831	1.233	1.353	0.141
1.45	- 1.2847160	3.8174	0.55611	1.215	1.333	0.155
1.50	- 1.2008832	3.6150	0.54339	1.198	1.314	0.169
1.55	- 1.1235183	3.4292	0.53059	1.182	1.296	0.183
1.66	- 1.0519115	3.2579	0.51803	1.167	1.279	0.197
1.65	- 0.98545337	3.0996	0.50587	1.153	1.264	0.211
1.70	- 0.92361639	2.9529	0.49425	1.140	1.248	0.221

[a] The quantities tabulated in the first three columns are taken from R. B. Bird, Doctoral Dissertation, University of Wisconsin (1950). The quantities tabulated in the last three columns are taken from J. O. Hirschfelder, R. B. Bird, and E. L. Spotz, *Journal of Chemical Physics*, vol. 16, 1948, p. 968.

TABLE 3(a) (*Continued*)

T^*	B^*	$T^* \frac{dB^*}{dT^*} - B^*$	C^*	$\Omega^{(1,1)*}$	$\Omega^{(2,2)*}$	k_T^* Heavy Isotopes
1.75	-0.86594279	2.8165	0.48320	1.128	1.234	0.230
1.80	-0.81203328	2.6894	0.47277	1.116	1.221	0.244
1.85	-0.76153734	2.5706	0.46296	1.105	1.209	0.253
1.90	-0.71414733	2.4595	0.45376	1.094	1.197	0.263
1.95	-0.66959030	2.3553	0.44515	1.084	1.186	0.277
2.00	-0.62762535	2.2573	0.43710	1.075	1.175	0.286
2.10	-0.55063308	2.0782	0.42260	1.057	1.156	0.305
2.20	-0.48170997	1.9183	0.40999	1.041	1.138	0.323
2.30	-0.41967761	1.7749	0.39900	1.026	1.122	0.337
2.40	-0.36357566	1.6455	0.38943	1.012	1.107	0.356
2.50	-0.31261340	1.5281	0.38108	0.9996	1.093	0.370
2.60	-0.26613345	1.4213	0.37378	0.9878	1.081	0.383
2.70	-0.22358626	1.3236	0.36737	0.9770	1.069	0.397
2.80	-0.18450728	1.2340	0.36173	0.9672	1.058	0.411
2.90	-0.14850215	1.1515	0.35675	0.9576	1.048	0.420
3.00	-0.11523390	1.0752	0.35234	0.9490	1.039	0.434
3.10	-0.08441245	1.0046	0.34842	0.9406	1.030	0.443
3.20	-0.05578696	0.93906	0.34491	0.9328	1.022	0.447
3.30	-0.02913997	0.87802	0.34177	0.9256	1.014	0.461
3.40	-0.00428086	0.82104	0.33894	0.9186	1.007	0.466
3.50	0.01895684	0.76776	0.33638	0.9120	0.9999	0.475
3.60	0.04072012	0.71782	0.33407	0.9058	0.9932	0.479
3.70	0.06113882	0.67094	0.33196	0.8998	0.9870	0.489
3.80	0.08032793	0.62684	0.33002	0.8942	0.9811	0.493
3.90	0.09839014	0.58528	0.32825	0.8888	0.9755	0.497
4.00	0.11541691	0.54607	0.32662	0.8836	0.9700	0.507
4.10	0.13149021	0.50900	0.32510	0.8788	0.9649	0.511
4.20	0.14668372	0.47392	0.32369	0.8740	0.9600	0.516
4.30	0.16106381	0.44067	0.32238	0.8694	0.9553	0.520
4.40	0.17469039	0.40912	0.32115	0.8652	0.9507	0.525

TABLE 3(a) (*Continued*)

T^*	B^*	$T^* \frac{dB^*}{dT^*} - B^*$	C^*	$\Omega^{(1,1)*}$	$\Omega^{(2,2)*}$	k_T^* Heavy Isotopes
4.50	0.18761774	0.37914	0.32000	0.8610	0.9464	0.529
4.60	0.19989511	0.35062	0.31891	0.8568	0.9422	0.533
4.70	0.21156728	0.32346	0.31788	0.8530	0.9382	0.538
4.80	0.2267507	0.29756	0.31690	0.8492	0.9343	0.543
4.90	0.23325577	0.27285	0.31596	0.8456	0.9305	0.542
5.0	0.24334351	0.24925	0.31508	0.8422	0.9269	0.547
6.0	0.32290437	0.06107	0.30771	0.8124	0.8963	0.578
7.0	0.37608846	-0.06783	0.30166	0.7896	0.8727	0.591
8.0	0.41343396	-0.16095	0.29618	0.7712	0.8538	0.604
9.0	0.44059784	-0.23090	0.29103	0.7556	0.8379	0.607
10.0	0.46087529	-0.28501	0.28610	0.7424	0.8242	0.616
20.0	0.52537420	-0.49671	0.24643	0.6640	0.7432	0.625
30.0	0.52692546	-0.54442	0.21954	0.6232	0.7005	0.627
40.0	0.51857502	-0.55789	0.20012	0.5960	0.6718	0.625
50.0	0.50836143	-0.56001	0.18529	0.5756	0.6504	0.623
60.0	0.49821261	-0.55758	0.17347	0.5596	0.6335	0.622
70.0	0.48865069	-0.55316	0.16376	0.5464	0.6194	0.621
80.0	0.47979009	-0.54787	0.15560	0.5352	0.6076	0.621
90.0	0.47161504	-0.54226	0.14860	0.5256	0.5973	0.620
100.0	0.46406948	-0.53659	0.14251	0.5170	0.5882	0.619
200.0	0.41143168	-0.48897	0.10679	0.4644	0.5320	0.615
300.0	0.38012787	-0.45665	0.08943	0.4360	0.5016	0.612
400.0	0.35835117	-0.43310	0.07862	0.4170	0.4811	0.611

interaction. A good survey of the equation of state and intermolecular forces has recently been given by de Boer (61).

Practically no calculations of virial coefficients higher than the third have been made. The higher coefficients are exceedingly sensitive to the exact shape of the potential-energy function, and hence little would seem to be gained by their calculation until more information is obtained about the nature of the intermolecular interaction. Some calculations of the second virial coefficient have been made for potentials more complex than the Lennard-Jones and the Stockmayer potentials.

For spherical nonpolar molecules Rice and Hirschfelder (19) have evaluated $B(T)$ for a three-parameter Buckingham potential, which includes an r^{-6} attraction term and an exponential repulsion term. For elongated molecules calculations of $B(T)$ have been made by both Corner (10) and Kihara (11). Kihara also has shown how the second virial coefficient can be calculated for flat, disk-shaped molecules (11), such as benzene and cyclohexane, and recently has shown how his work can be extended to still other shapes (20). Neither the work of Kihara nor that of Corner has been extended to higher virial coefficients or to gaseous mixtures. There remains, therefore, a tremendous amount of work to be done in the field—particularly as regards nonspherical molecules. As high-speed computing devices are improved it will be possible to evaluate the virial coefficients for much more complex potential-energy functions and also to extend the calculations to the fourth and higher virial coefficients.

Experimental data for the noble gases and about a dozen simple molecular gases are available over limited ranges of pressure and temperature. The primary contributors to this work have been Holborn and Otto (Germany), Michels (Holland), and Beattie (U. S.). There are, however, only very meager data on gaseous mixtures and almost no data on polar gases and gases consisting of long molecules.

3 Equation of State of Dense Gases and Liquids

It would be possible to describe the equation of state of dense gases and liquids by means of the virial equation of state, Equation [2.3], but the numerical evaluation of many virial coefficients would be necessary. Furthermore, there is some question as to the convergence of the virial expansion in the neighborhood of the critical point. This approach has been used in the theoretical study of condensation, but no quantitative results are obtained (15). The most significant theoretical and computational advances have been made by substituting into Equation [2.1] an approximate expression for the configurational integral, or by substituting into Equation [2.2] an approximate expression for the radial distribution function. We now summarize and compare the results obtained by these two methods.

(*a*) *Calculations Based on an Approximate Expression for Configurational Integral.* In this development one begins by supposing that the molecules of the dense gas or liquid are frozen at the lattice points of some sort of regular network, just as though the substance were a perfect crystal. Then one molecule, called the "wanderer," is allowed to stray from its lattice point, all other

TABLE 3(*b*) FUNCTIONS USED IN CALCULATION OF PROPERTIES OF DILUTE AND MODERATELY DENSE NONPOLAR GASES (LENNARD-JONES POTENTIAL)[a]

T^*	A^*	B^*	C^*	$f_\eta^{(3)}$	$f_\lambda^{(3)}$	$f_B^{(3)}$
0.30	1.046	1.289	0.848	1.0014	1.0022	1.0001
0.50	1.093	1.284	0.825	1.0002	1.0003	1.0000
0.75	1.105	1.233	0.825	1.0000	1.0000	1.0000
1.00	1.103	1.192	0.837	1.0000	1.0001	1.0000
1.25	1.099	1.165	0.851	1:0001	1.0002	1.0002
1.50	1.097	1.143	0.863	1.0004	1.0006	1.0006
2.00	1.094	1.119	0.884	1.0014	1.0021	1.0016
2.50	1.094	1.106	0.899	1.0025	1.0038	1.0026
3.00	1.095	1.101	0.911	1.0034	1.0052	1.0037
4.00	1.098	1.095	0.924	1.0049	1.0076	1.0050
5.00	1.101	1.092	0.932	1.0058	1.0090	1.0059
10.0	1.110	1.094	0.945	1.0075	1.0116	1.0076
50.0	1.130	1.095	0.948	1.0079	1.0124	1.0080
100.0	1.138	1.095	0.948	1.0080	1.0125	1.0080
400.0	1.154	1.095	0.948	1.0080	1.0125	1.0080

[a] From J. O. Hirschfelder, R. B. Bird, and E. L. Spotz, *Journal of Chemical Physics*, vol. 16, 1948, p. 968.

TABLE E(a) SECOND VIRIAL COEFFICIENT FOR POLAR MOLECULES (THE STOCKMAYER POTENTIAL)[a]

$B(T) = b_0 B^*(T^*;t^*)$ $\quad b_0 = \frac{2}{3}\pi \tilde{N}\sigma^3$ $\quad T^* = kT/\epsilon$ $\quad t^* = 8^{-\frac{1}{2}}\mu^{*2} = 8^{-\frac{1}{2}}\mu^2/\epsilon\sigma^3$

	$B^*(T^*;t^*)$						
T^*	$t^* = 0.1$	0.2	0.3	0.4	0.5	0.6	0.7
.30	-31.129	-42.968	-72.01				
.35	-20.355	-25.879	-38.07	-64.11			
.40	-14.717	-17.777	-24.090	-36.28	-60.4		
.45	-11.339	-13.241	-16.985	-23.733	-35.92	-58.8	
.50	- 9.1199	-10.401	-12.841	-17.026	-24.11	-36.36	-59.
.55	- 7.5631	- 8.4786	-10.181	-12.996	-17.53	-24.91	-37.3
.60	- 6.4159	- 7.1001	- 8.3495	-10.360	-13.477	-18.33	-26.0
.65	- 5.5381	- 6.0677	- 7.0213	- 8.5234	-10.789	-14.185	-19.34
.70	- 4.8460	- 5.2675	- 6.0183	- 7.1813	- 8.8965	-11.394	-15.05
.75	- 4.2871	- 4.6304	- 5.2364	- 6.1627	- 7.5043	- 9.413	-12.13
.80	- 3.8268	- 4.1116	- 4.6110	- 5.3659	- 6.4433	- 7.9476	-10.040
.85	- 3.4414	- 3.6815	- 4.1000	- 4.7271	- 5.6113	- 6.8267	- 8.486
.90	- 3.1142	- 3.3193	- 3.6758	- 4.2045	- 4.9432	- 5.9457	- 7.292
.95	- 2.8330	- 3.0103	- 3.3166	- 3.7695	- 4.3961	- 5.2373	- 6.3523
1.00	- 2.5889	- 2.7437	- 3.0102	- 3.4021	- 3.9406	- 4.6567	- 5.5953
1.05	- 2.3750	- 2.5114	- 2.7455	- 3.0881	- 3.5559	- 4.1732	- 4.9744
1.10	- 2.1862	- 2.3072	- 2.5145	- 2.8167	- 3.2271	- 3.7649	- 4.4572
1.15	- 2.0183	- 2.1265	- 2.3113	- 2.5799	- 2.9430	- 3.4160	- 4.0203
1.20	- 1.8680	- 1.9653	- 2.1312	- 2.3716	- 2.6952	- 3.1146	- 3.6471
1.25	- 1.7328	- 1.8208	- 1.9706	- 2.1870	- 2.4773	- 2.8519	- 3.3249
1.30	- 1.6105	- 1.6905	- 1.8264	- 2.0223	- 2.2844	- 2.6211	- 3.0442
1.35	- 1.4994	- 1.5724	- 1.6963	- 1.8746	- 2.1124	- 2.4168	- 2.7976
1.40	- 1.3980	- 1.4649	- 1.5784	- 1.7413	- 1.9581	- 2.2348	- 2.5795
1.45	- 1.3051	- 1.3667	- 1.4710	- 1.6205	- 1.8190	- 2.0717	- 2.3854
1.50	- 1.2197	- 1.2766	- 1.3728	- 1.5106	- 1.6931	- 1.9247	- 2.2115
1.55	- 1.1410	- 1.1937	- 1.2827	- 1.4101	- 1.5785	- 1.7917	- 2.0549
1.60	- 1.0681	- 1.1171	- 1.1998	- 1.3179	- 1.4738	- 1.6708	- 1.9133
1.65	- 1.0006	- 1.0462	- 1.1232	- 1.2330	- 1.3778	- 1.5604	- 1.7846
1.70	- 0.93775	- 0.98038	- 1.0523	- 1.1547	- 1.2896	- 1.4594	- 1.6674
1.75	- 0.87917	- 0.91908	- 0.98633	- 1.0821	- 1.2079	- 1.3662	- 1.5597
1.80	- 0.82445	- 0.86190	- 0.92498	- 1.0147	- 1.1325	- 1.2804	- 1.4610
1.85	- 0.77322	- 0.80844	- 0.86772	- 0.95197	- 1.0625	- 1.2011	- 1.3699
1.90	- 0.72516	- 0.75834	- 0.81417	- 0.89345	- 0.99736	- 1.1275	- 1.2858
1.95	- 0.67998	- 0.71130	- 0.76398	- 0.83873	- 0.93662	- 1.0590	- 1.2078
2.00	- 0.63745	- 0.66707	- 0.71686	- 0.78747	- 0.87985	- 0.99526	- 1.1353
2.1	- 0.55947	- 0.58607	- 0.63076	- 0.69408	- 0.77679	- 0.87993	- 1.0048
2.2	- 0.48969	- 0.51373	- 0.55409	- 0.61121	- 0.68573	- 0.77850	- 0.89060
2.3	- 0.42693	- 0.44877	- 0.48540	- 0.53721	- 0.60472	- 0.68865	- 0.78989
2.4	- 0.37020	- 0.39012	- 0.42354	- 0.47076	- 0.53224	- 0.60856	- 0.70049
2.5	- 0.31868	- 0.33695	- 0.36576	- 0.41079	- 0.46702	- 0.53676	- 0.62063
2.6	- 0.27172	- 0.28852	- 0.31668	- 0.35642	- 0.40807	- 0.47205	- 0.54292
2.7	- 0.22875	- 0.24426	- 0.27025	- 0.30692	- 0.35453	- 0.41347	- 0.48420
2.8	- 0.18929	- 0.20366	- 0.22774	- 0.26167	- 0.30572	- 0.36020	- 0.42552
2.9	- 0.15295	- 0.16630	- 0.18867	- 0.22018	- 0.26106	- 0.31159	- 0.37210
3.0	- 0.11937	- 0.13182	- 0.15266	- 0.18200	- 0.22005	- 0.26705	- 0.32330
3.1	- 0.08828	- 0.09991	- 0.11937	- 0.14677	- 0.18229	- 0.22612	- 0.27854
3.2	- 0.05941	- 0.07030	- 0.08852	- 0.11417	- 0.14740	- 0.18839	- 0.23738
3.3	- 0.03254	- 0.04277	- 0.05986	- 0.08393	- 0.11509	- 0.15351	- 0.19940

[a] This table was prepared by J. S. Rowlinson from tabulated functions given by R. B. Bird, Doctoral Dissertation, University of Wisconsin, 1950. A similar table has been prepared by R. J. Lunbeck and C. A. ten Seldam, *Physica*, vol. 27, 1951, p. 788.

TABLE 4(a) (*Continued*)

T^*	$t^* = 0.1$	0.2	0.3	0.4	0.5	0.6	0.7
3.4	- 0.00748	- 0.01710	- 0.03318	- 0.05580	- 0.08509	- 0.12118	- 0.16427
3.5	+ 0.01594	+ 0.00688	- 0.00828	- 0.02959	- 0.05717	- 0.09115	- 0.13169
3.6	0.03787	0.02931	+ 0.01501	- 0.00511	- 0.03113	- 0.06318	- 0.10140
3.7	0.05844	0.05035	0.03682	+ 0.01780	- 0.00680	- 0.03708	- 0.07318
3.8	0.07778	0.07011	0.05729	0.03928	+ 0.01598	- 0.01268	- 0.04684
3.9	0.09597	0.08869	0.07653	0.05944	0.03736	+ 0.01018	- 0.02219
4.0	0.11312	0.10620	0.09465	0.07841	0.05744	0.03163	+ 0.00091
4.1	0.12930	0.12272	0.11173	0.09628	0.07633	0.05180	0.02259
4.2	0.14460	0.13833	0.12786	0.11314	0.09414	0.07078	0.04298
4.3	0.15907	0.15309	0.14310	0.12907	0.11095	0.08868	0.06218
4.4	0.17279	0.16708	0.15754	0.14414	0.12684	0.10558	0.08029
4.5	0.18580	0.18034	0.17122	0.15841	0.14187	0.12155	0.09740
4.6	0.19815	0.19293	0.18420	0.17194	0.15611	0.13668	0.11357
4.7	0.20990	0.20489	0.19652	0.18478	0.16962	0.15101	0.12888
4.8	0.22107	0.21627	0.20825	0.19699	0.18245	0.16461	0.14340
4.9	0.23172	0.22711	0.21941	0.20860	0.19465	0.17752	0.15718
5.0	0.24187	0.23744	0.23004	0.21965	0.20625	0.18980	0.17026
6	0.32187	0.31877	0.31360	0.30634	0.29699	0.28552	0.27191
7	0.37532	0.37302	0.36918	0.36380	0.35687	0.34838	0.33832
8	0.41284	0.41106	0.40809	0.40393	0.39857	0.39201	0.38424
9	0.44012	0.43870	0.43633	0.43301	0.42873	0.42349	0.41729
10	0.46049	0.45932	0.45738	0.45466	0.45116	0.44687	0.44179
20	0.52527	0.52495	0.52441	0.52367	0.52271	0.52153	0.52014
30	0.52687	0.52672	0.52647	0.52611	0.52566	0.52510	0.52444
40	0.51854	0.51845	0.51830	0.51809	0.51782	0.51749	0.51710
50	0.50834	0.50828	0.50818	0.50804	0.50876	0.50764	0.50738
60	0.49820	0.49815	0.49808	0.49798	0.49785	0.49769	0.49750
70	0.48864	0.48861	0.48855	0.48847	0.48838	0.48826	0.48811
80	0.47978	0.47976	0.47971	0.47965	0.47957	0.47948	0.47937
90	0.47161	0.47159	0.47155	0.47150	0.47144	0.47136	0.47127
100	0.46406	0.46405	0.46402	0.46398	0.46392	0.46386	0.46379
200	0.41143	0.41142	0.41142	0.41140	0.41139	0.41137	0.41135
300	0.38013	0.38012	0.38012	0.38011	0.38011	0.38010	0.38009
400	0.35835	0.35835	0.35835	0.35834	0.35834	0.35833	0.35833

molecules being held fixed at their lattice points. The wanderer can move in a "cage" formed by its nearest neighbors; the volume of this cage is referred to as the "free volume." The configurational integral for the wanderer may be calculated by taking into account the intermolecular forces between the wanderer and its nearest neighbors. The calculations may be refined by considering also the interactions with the next nearest neighbors, and so forth. Now each molecule in the dense gas or liquid may be assumed to behave in very nearly the same manner as the wanderer. Hence it is assumed that the total configurational integral Q_N in Equation [2.1] is just the configurational integral for the one wanderer raised to the Nth power. This type of approach is due originally to Lennard-Jones and Devonshire (21).

Extensive punched-card calculations have been made (22) for such a model, in which the Lennard-Jones potential energy of interaction is used, and in which interactions between the wanderer and the first three shells of neighbors are included. The results are presented in a simple tabular form in Table 5(*a*). The compressibility factor $p\bar{v}/RT$ is there given in terms of the reduced volume, $v^* = v/\sigma^3$, and the reduced temperature $T^* = kT/\epsilon$. Hence for a given value of the specific volume v and the temperature T one may compute the reduced variables v^* and T^* by means of the parameters σ and ϵ given in Table 1, and then obtain the compressibility factor from Table 5(*a*). Similar tables for the various thermodynamic functions also have been prepared (22). These tables have been shown to give good results at very high densities, but the agreement with experiment becomes less satisfactory as the density is decreased. This is easily understood, since at high densities the molecules are, in fact, restrained to move in a sort of free volume in a manner similar to that described by the model used in the calculations. At lower density, however, the molecules are free to roam out of their cages, and hence the model no longer describes the physical reality.

(*b*) *Calculations Based on an Approximate Expression for Radial Distribution Function.* It is possible to obtain an integral equation for the radial distribution function $g(r)$ [or the distribution function for "pairs," which is closely related to $g(r)$] in terms of the next higher distribution function—that is, the distribution function for "triples." Since the latter is not known, it is impossible to solve the equation for $g(r)$. It is customary to obviate this difficulty by writing the distribution function for triples as the product of three distribution functions for pairs. This is known as the "superposition approximation" (23), the validity of which has not yet been assessed fully. When this approximation has been introduced, the integral equation then may be solved to give an approximation to the function $g(r)$. This can in turn be used in Equation [2.2] to obtain the equation of state.

By means of high-speed computing devices the radial distribution function has been evaluated for a (slightly modified) Lennard-Jones potential (24). The curves of $g(r)$ obtained for various temperatures were used to obtain the compressibility factors given in Table 5(*b*). The symbols v^* and T^* have the same significance

TABLE 4(a) (*Continued*)

T^*	$t^* = 0.8$	0.9	1.0	1.1	1.2	1.3	1.4	1.5
0.55	-58.8							
0.60	-38.5	-59.7						
0.65	-27.3	-40.0						
0.70	-20.50	-28.8	-41.8					
0.75	-16.05	-21.78	-30.4	-43.5				
0.80	-12.973	-17.14	-23.2	-32.0	-45.8			
0.85	-10.759	-13.90	-18.4	-24.7	-34.4	-47.		
0.90	- 9.103	-11.612	-14.92	-19.61	-26.3	-35.7	-50.3	
0.95	- 7.828	- 9.790	-12.42	-16.00	-21.0	-27.9	-37.8	-52.
1.00	- 6.820	- 8.440	-10.54	-13.36	-17.2	-22.3	-29.8	-40.
1.05	- 6.008	- 7.342	- 9.08	-11.35	-14.3	-18.4	-24.3	-31.
1.10	- 5.3413	- 6.4696	- 7.915	- 9.780	-12.21	-15.42	-19.6	-25.4
1.15	- 4.7855	- 5.7520	- 6.976	- 8.534	-10.53	-13.13	-16.5	-21.1
1.20	- 4.3161	- 5.1537	- 6.203	- 7.524	- 9.20	-11.34	-14.1	-17.7
1.25	- 3.9152	- 4.6483	- 5.559	- 6.693	- 8.11	- 9.90	-12.2	-15.1
1.30	- 3.5690	- 4.2164	- 5.014	- 5.998	- 7.21	- 8.74	-10.7	-13.1
1.35	- 3.2676	- 3.8438	- 4.5484	- 5.4111	- 6.471	- 7.780	- 9.41	-11.46
1.40	- 3.0030	- 3.5193	- 4.1466	- 4.9092	- 5.839	- 6.976	- 8.38	-10.12
1.45	- 2.7691	- 3.2345	- 3.7970	- 4.4762	- 5.298	- 6.296	- 7.51	- 9.00
1.50	- 2.5609	- 2.9829	- 3.4903	- 4.0994	- 4.831	- 5.714	- 6.78	- 8.08
1.55	- 2.3745	- 2.7591	- 3.2192	- 3.7688	- 4.426	- 5.212	- 6.15	- 7.29
1.60	- 2.2069	- 2.5589	- 2.9783	- 3.4768	- 4.069	- 4.774	- 5.612	- 6.62
1.65	- 2.0554	- 2.3788	- 2.7629	- 3.2173	- 3.7548	- 4.3909	- 5.145	- 6.045
1.70	- 1.9180	- 2.2165	- 2.5697	- 2.9860	- 3.4760	- 4.0532	- 4.735	- 5.541
1.75	- 1.7923	- 2.0685	- 2.3943	- 2.7770	- 3.2256	- 3.7517	- 4.370	- 5.097
1.80	- 1.6775	- 1.9340	- 2.2357	- 2.5889	- 3.0014	- 3.4831	- 4.046	- 4.706
1.85	- 1.5720	- 1.8110	- 2.0912	- 2.4183	- 2.7990	- 3.2419	- 3.758	- 4.359
1.90	- 1.4749	- 1.6981	- 1.9591	- 2.2630	- 2.6156	- 3.0244	- 3.498	- 4.049
1.95	- 1.3852	- 1.5941	- 1.8380	- 2.1211	- 2.4487	- 2.8273	- 3.265	- 3.771
2.00	- 1.3021	- 1.4982	- 1.7265	- 1.9910	- 2.2963	- 2.6479	- 3.053	- 3.520
2.1	- 1.1531	- 1.3268	- 1.5285	- 1.7610	- 2.0282	- 2.3342	- 2.6846	- 3.0857
2.2	- 1.0234	- 1.1785	- 1.3580	- 1.5643	- 1.8002	- 2.0693	- 2.3758	- 2.7248
2.3	- 0.90957	- 1.0490	- 1.2100	- 1.3943	- 1.6044	- 1.8431	- 2.1138	- 2.4204
2.4	- 0.80895	- 0.93509	- 1.0803	- 1.2461	- 1.4345	- 1.6479	- 1.8889	- 2.1606
2.5	- 0.71944	- 0.83413	- 0.96584	- 1.1159	- 1.2860	- 1.4780	- 1.6940	- 1.9368
2.6	- 0.63934	- 0.74412	- 0.86421	- 1.0008	- 1.1551	- 1.3289	- 1.5239	- 1.7423
2.7	- 0.56729	- 0.66342	- 0.77343	- 0.89828	- 1.0391	- 1.1972	- 1.3742	- 1.5719
2.8	- 0.50216	- 0.59072	- 0.69191	- 0.80654	- 0.93559	- 1.0802	- 1.2416	- 1.4215
2.9	- 0.44304	- 0.52492	- 0.61833	- 0.72400	- 0.84275	- 0.97554	- 1.1235	- 1.2879
3.0	- 0.38917	- 0.46511	- 0.55165	- 0.64940	- 0.75908	- 0.88152	- 1.0177	- 1.1687
3.1	- 0.33989	- 0.41054	- 0.49096	- 0.58168	- 0.68333	- 0.79663	- 0.92240	- 1.0616
3.2	- 0.29466	- 0.36057	- 0.43552	- 0.51998	- 0.61449	- 0.71967	- 0.83625	- 0.96505
3.3	- 0.25302	- 0.31468	- 0.38472	- 0.46355	- 0.55167	- 0.64962	- 0.75801	- 0.87758
3.4	- 0.21459	- 0.27239	- 0.33800	- 0.41179	- 0.49417	- 0.58562	- 0.68671	- 0.79805
3.5	- 0.17900	- 0.23332	- 0.29493	- 0.36415	- 0.44135	- 0.52697	- 0.62149	- 0.72546
3.6	- 0.14598	- 0.19713	- 0.25510	- 0.32018	- 0.39270	- 0.47305	- 0.56164	- 0.65899
3.7	- 0.11527	- 0.16352	- 0.21818	- 0.27949	- 0.34776	- 0.42333	- 0.50657	- 0.59792

TABLE 4(a) (*Continued*)

T*	t* = 0.8	0.9	1.0	1.1	1.2	1.3	1.4	1.5
3.8	-0.08664	-0.13225	-0.18388	-0.24176	-0.30615	-0.37736	-0.45574	-0.54166
3.9	-0.05989	-0.10308	-0.15193	-0.20667	-0.26752	-0.33476	-0.40870	-0.48968
4.0	-0.03486	-0.07582	-0.12213	-0.17397	-0.23158	-0.29519	-0.36507	-0.44155
4.1	-0.01140	-0.05030	-0.09426	-0.14345	-0.19807	-0.25834	-0.32451	-0.39687
4.2	+0.01064	-0.02636	-0.06815	-0.11490	-0.16677	-0.22397	-0.28673	-0.35530
4.3	0.03137	-0.00387	-0.043659	-0.08814	-0.13747	-0.19184	-0.25145	-0.31654
4.4	0.05089	+0.01729	-0.020639	-0.06302	-0.11000	-0.16175	-0.21846	-0.28033
4.5	0.06932	0.03723	+0.00103	-0.03941	-0.08421	-0.13353	-0.18755	-0.24645
4.6	0.08672	0.05605	0.02145	-0.01717	-0.05995	-0.10702	-0.15854	-0.21469
4.7	0.10318	0.07383	0.040732	+0.00380	-0.03709	-0.08207	-0.13127	-0.18486
4.8	0.11877	0.09065	0.05896	0.02360	-0.01554	-0.05856	-0.10560	-0.156812
4.9	0.13355	0.10659	0.076204	0.04232	+0.00483	-0.03637	-0.08140	-0.13039
5.0	0.14758	0.12170	0.09255	0.06004	0.02409	-0.01540	-0.05855	-0.10548
6.	0.25614	0.23818	0.21799	0.19554	0.17077	+0.14364	+0.11409	+0.08206
7.	0.32667	0.31341	0.29853	0.28199	0.26379	0.24389	0.22225	0.19885
8.	0.37524	0.36502	0.35355	0.34082	0.32682	0.31154	0.29494	0.27702
9.	0.41012	0.40197	0.39283	0.38270	0.37157	0.35942	0.34625	0.33203
10.	0.43593	0.42927	0.42180	0.41353	0.40444	0.39453	0.38379	0.37221
20.	0.51854	0.51672	0.51468	0.51243	0.50996	0.50728	0.50438	0.50125
30.	0.52367	0.52281	0.52184	0.52077	0.51960	0.51833	0.51695	0.51547
40.	0.51665	0.51613	0.51556	0.51493	0.51423	0.51348	0.51266	0.51179
50.	0.50707	0.50673	0.50635	0.50593	0.50546	0.50496	0.50441	0.50383
60.	0.49729	0.49704	0.49676	0.49646	0.49613	0.49576	0.49537	0.49495
70.	0.48795	0.48776	0.48755	0.48732	0.48707	0.48679	0.48650	0.48618
80.	0.47924	0.47909	0.47893	0.47874	0.47854	0.47833	0.47810	0.47784
90.	0.47117	0.47105	0.47091	0.47077	0.47061	0.47043	0.47024	0.47004
100.	0.46370	0.46360	0.46349	0.46337	0.46323	0.46309	0.46293	0.46276
200.	0.41132	0.41129	0.41126	0.41123	0.41119	0.41115	0.41110	0.41105
300.	0.38008	0.38006	0.38005	0.38003	0.38001	0.37999	0.37997	0.37994
400.	0.35832	0.35831	0.35830	0.35829	0.35828	0.35827	0.35825	0.35824

as in Table 5(*a*). Similar tables for the various thermodynamic functions also have been prepared (24).

In Fig. 2 we show a comparison of the results of the two methods (approximate configurational integral and approximate radial distribution function) with each other and with the experimental

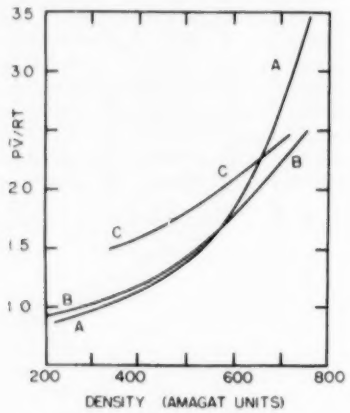

FIG. 2 0° C ISOTHERM FOR ARGON

(According to [A] experimental measurements of Michels, Wijker, and Wijker, *Physica*, vol. 15, 1949, p. 627; [B] calculations based on an approximate radial distribution function, reference 22; and [C] calculations based on approximate configuration integral, reference (24). This figure is taken from Kirkwood, Lewinson, and Alder, reference 24.)

measurements for argon (24). The discrepancy between the two calculated curves is a measure of the reasonableness of the approximations introduced in the two methods. Both theoretical approaches give good qualitative predictions but leave a great deal to be desired for quantitative work.

(*c*) *Present Status of Theory, Calculations, and Experimental Data.* The original theory of Lennard-Jones and Devonshire has been modified by a number of people in order to obtain better agreement with the experimental data. These modifications have resulted in a host of different theories of the liquid state, which are usually referred to as "cell theories," "lattice theories," or "free-volume theories." One type of modification permits double occupancy of a unit cell (25, 26). Another approach assumes that there are vacant lattice sites or "holes," and that the number of holes increases with decreasing density. Unfortunately, these various modifications have not resulted in much improvement of the results. The present status of the lattice theories has been summarized by Rowlinson and Curtiss (27). Some work has been done on the extension of the Lennard-Jones-Devonshire theory to the theory of solutions by Prigogine, Kirkwood, and others (28, 29, 30, 31). Up to now nothing has been done about extending the theory to the study of compressed gases and liquids composed of nonspherical molecules and polar molecules. A nice summary of the present knowledge about the liquid state has been given recently by de Boer (32).

No calculations have been made for the Lennard-Jones-Devonshire theory for a potential function containing more than two adjustable parameters. The calculations which have been made

TABLE 4(b) THIRD VIRIAL COEFFICIENT FOR POLAR MOLECULES (STOCKMAYER POTENTIAL FUNCTION)[a]

$C(T) = b_0 C^*(T^*, t^*)$ $\quad b_0 = \frac{2}{3}\pi N\sigma^3$ $\quad T^* = kT/\epsilon$ $\quad t^* = 8^{-\frac{1}{2}}\mu^{*2} = 8^{-\frac{1}{2}}(\mu^2/\epsilon\sigma^3)$

$C^*(T^*, t^*)$

t^*	0.0	0.1	0.2	0.3	0.4	0.5	0.6	0.7	0.8	1.0	1.2
T^*											
1.0	0.4297	0.4440	0.5304	0.740							
1.2	0.5924	0.6177	0.7162	0.9216	1.268	1.78	2.5	3.4	4.6	7.	
1.4	0.5683	0.5900	0.6679	0.8221	1.075	1.451	2.0	2.7	3.7	6.3	9.
1.6	0.5180	0.5351	0.5940	0.7075	0.8899	1.158	1.53	2.03	2.69	4.72	7.0
1.8	0.4728	0.4861	0.5311	0.6161	0.7507	0.9455	1.214	1.572	2.03	3.36	5.2
2.0	0.4371	0.4476	0.4826	0.5478	0.6496	0.7957	0.995	1.257	1.595	2.46	4.0
2.5	0.3811	0.3873	0.4076	0.4445	0.5195	0.5807	0.6871	0.825	0.999	1.482	2.19
3.0	0.3523	0.3563	0.3692	0.3924	0.4275	0 4761	0.5403	0.6223	0.7248	1.002	1.401
4.0	0.3266	0.3286	0.3350	0.3463	0.3630	0.3859	0.4156	0.4529	0.4986	0.6194	0.7857
6.0	0.3077	0.3085	0.3109	0.3151	0.3213	0.3296	0.3401	0.3532	0.3690	0.4095	0.4640
8.0	0.2962	0.2966	0.2978	0.3000	0.3031	0.3072	0.3124	0.3188	0.3265	0.3459	0.3715
10.0	0.2861	0.2863	0.2871	0.2884	0.2902	0.2926	0.2957	0.2995	0.3039	0.3151	0.3297

[a] J. S. Rowlinson, *Journal of Chemical Physics*, vol. 19, 1951, p. 827.

TABLE 5(a) COMPRESSIBILITY FACTOR pV/NkT BASED ON LENNARD-JONES DEVONSHIRE (3-SHELL) MODELS[a]

$T^* = kT/\epsilon$ \ $V^* = V/\sigma^3 = (a/\sigma)^3/\sqrt{2} = a^{*3}/\sqrt{2}$	0.8	0.9	1.0	1.2	1.4	1.5	1.6	1.8	2.0	2.2	2.4
0.70	215.9	117.27	64.01	17.650	2.358	-0.8136	-2.642	-3.738	-3.566	-3.066	-2.535
0.75	202.2	109.97	60.26	17.142	2.695	-0.3818	-1.999	-3.059	-2.948	-2.528	-2.070
0.80	190.2	103.57	56.97	16.528	2.987	+0.0812	-1.442	-2.472	-2.413	-2.062	-1.667
0.85	179.6	97.92	54.07	15.984	3.240	0.4862	-0.955	-1.960	-1.947	-1.654	-1.315
0.90	170.13	92.92	51.49	15.500	3.462	0.8429	-0.5276	-1.511	-1.537	-1.296	-1.004
0.95	161.66	88.40	49.18	15.065	3.657	1.1593	-0.1491	-1.113	-1.1743	-0.9789	-0.729
1.00	154.02	84.35	47.10	14.672	3.830	1.4411	+0.1881	-0.759	-0.8515	-0.6961	-0.483
1.05	147.10	80.66	45.21	14.316	3.886	1.6935	0.4897	-0.443	-0.5627	-0.4427	-0.2624
1.1	140.80	77.355	43.50	13.991	4.018	1.9205	0.7608	-0.1585	-0.3030	-0.191	-0.0634
1.2	129.74	71.525	40.50	13.419	4.245	2.311	1.2272	+0.3309	+0.1444	+0.203	+0.2803
1.3	120.38	66 593	37.953	12.932	4.432	2.634	1.6128	0.7357	0.5151	0.528	0.5663
1.4	111.33	62.365	35.768	12.510	4.587	2.904	1.9355	1.0750	0.8262	0.803	0.8067
1.6	99.23	55.492	32.205	11.816	4.826	3.326	2.4417	1.6086	1.3168	1.234	1.1887
1.8	89.03	50.142	28.521	11.266	4.998	3.636	2.8163	2.0054	1.7135	1.557	1.476
2.0	80.866	45.856	27.258	10.817	5.123	3.870	3.1010	2.3090	1.9919	1.807	1.698
2.5	66.149	38.120	22.172	9.885	5.310	4.248	3.570	2.816	2.460	2.230	2.077
3.0	56.330	33.020	20.435	9.284	5.395	4.458	3.841	3.149	2.741	2.486	2.310
3.5	49.300	29.262	18.466	8.838	5.427	4.579	4.006	3.336	2.922	2.653	2.461
4	44.015	26.436	16.982	8.488	5.430	4.648	4.110	3.457	3.043	2.766	2.565
5	36.676	22.471	14.809	7.963	5.393	4.705	4.253	3.595	3.185	2.901	2.691
7	28.074	17.897	12.312	7.281	5.259	4.720	4.283	3.684	3.290	3.009	2.797
10	21.584	14.307	10.373	6.659	5.067	4.591	4.212	3.673	3.305	3.035	2.829
20	13.735	9.998	7.666	5.668	4.576	4.211	3.920	3.486	3.175	2.942	2.760
50	8.717	6.969	5.910	4.624	3.905	3.652	3.444	3.122	2.885	2.702	2.556
100	6.733	5.630	4.902	4.000	3.462	3.267	3.104	2.849	2.657	2.493	2.348
400	4.476	3.962	3.592	3.096	2.777	2.655	2.543	2.319	2.082	1.856	1.661

[a] R. H. Wentorf, R. J. Buehler, J. O. Hirschfelder, and C. F. Curtiss, *Journal of Chemical Physics*, vol. 18, 1950, p. 1484.

TABLE 5(a) (*Continued*)

T^* \ a^{*3}	2.5	2.6	2.8	3.0	3.5	4.0	5.0	6.0
0.70	-2.310	-2.107	-1.760	-1.486	-1.0215	-0.7382	-0.399	-0.1841
0.75	-1.877	-1.701	-1.402	-1.165	-0.7626	-0.5168	-0.221	-0.0329
0.80	-1.501	-1.349	-1.091	-0.885	-0.5366	-0.3234	-0.0661	+0.0990
0.85	-1.172	-1.0407	-0.817	-0.6395	-0.3376	-0.1531	+0.0708	0.2149
0.90	-0.8808	-0.7681	-0.575	-0.4219	-0.1613	-0.0021	0.1924	0.3173
0.95	-0.6232	-0.5265	-0.360	-0.2282	-0.0040	+0.1329	0.3009	0.4084
1.00	-0.3932	-0.3105	-0.168	-0.0547	+0.1371	0.2541	0.3985	0.4897
1.05	-0.1865	-0.1162	+0.005	+0.1015	0.2645	0.3634	0.4865	0.5676
1.1	+0.0002	+0.0590	0.161	0.2427	0.3798	0.4626	0.5664	0.6282
1.2	0.3222	0.3623	0.432	0.4880	0.5804	0.6353	0.7057	0.7411
1.3	0.5908	0.6151	0.659	0.6933	0.7489	0.7806	0.8230	0.8340
1.4	0.8173	0.8287	0.850	0.8673	0.8922	0.9044	0.9230	0.9113
1.6	1.177	1.1684	1.156	1.1453	1.122	1.1035	1.084	1.030
1.8	1.448	1.425	1.387	1.357	1.297	1.256	1.207	1.115
2.0	1.658	1.624	1.568	1.522	1.435	1.376	1.304	1.761
2.5	2.017	1.965	1.878	1.806	1.675	1.586	1.471	1.266
3.0	2.238	2.176	2.070	1.985	1.826	1.719	1.571	1.305
3.5	2.383	2.314	2.198	2.104	1.928	1.810	1.633	1.321
4	2.483	2.410	2.287	2.187	2.001	1.874	1.670	1.323
5	2.605	2.529	2.398	2.291	2.093	1.957	1.700	1.311
7	2.708	2.630	2.495	2.385	2.178	2.031	1.682	1.271
10	2.743	2.666	2.534	2.424	2.217	2.048	1.606	1.219
20	2.683	2.614	2.494	2.394	2.166	1.901	1.402	1.128
50	2.492	2.431	2.308	2.178	1.829	1.531	1.191	1.056
100	2.270	2.188	2.020	1.856	1.520	1.305	1.101	1.029
400	1.579	1.506	1.387	1.296	1.156	1.085	1.026	1.007

TABLE 5(b) COMPRESSIBILITY FACTOR AS OBTAINED FROM RADIAL DISTRIBUTION FUNCTION*

v* \ T*	0.833	1.000	1.250	1.677	2.500	5.000	∞
13.82		0.629	0.768	0.883			1.167
3.632	-0.594	-0.156	0.264	0.670	1.064	1.456	1.833
2.260	-1.445	-0.734	-0.038	0.649	1.326	1.998	2.667
1.483	-2.433	-1.268	-0.115	1.018	2.139	3.242	4.333
1.222	-2.829	-1.382	0.052	1.467	2.856	4.223	5.567

* J. G. Kirkwood, V. A. Lewinson, and B. J. Alder, *Journal of Chemical Physics*, vol. 20, 1952, p. 929.

for the various modified lattice theories and hole theories are not very extensive in scope, and hence the best statistical mechanical calculations for practical purposes are those given in Table 5(*a*).

Accurate experimental measurements of the equation of state of dense gases and liquids have been limited to simple gases. A considerable amount of work needs to be done toward extending the measurements to more complex substances and to multicomponent mixtures. A survey of recent experimental equation-of-state-measurements and engineering applications has been given by Smith (33).

4 Transport Coefficients of Dilute Gases

Diffusion, viscosity, and thermal conductivity are referred to as "transport phenomena" inasmuch as diffusion is the transport of mass, viscosity is the transport of momentum, and thermal conductivity is the transport of energy by means of molecular motion and molecular collisions. (In the early development of kinetic theory these phenomena were described in terms of the "mean free path" between collisions; hence they are also sometimes called "mean free-path phenomena.")

Rigorous expressions for the transport coefficients of dilute gases were first obtained by Chapman and by Enskog, whose investigations were performed independently. The rigorous development also predicted the transport of mass by thermal gradients (called "thermal diffusion" or the "Soret effect") and the transport of energy resulting from concentration gradients (the "diffusion-thermo effect" or "Dufour effect"). A full account of their theory and the results for pure gases and binary mixtures may be found in the treatise of Chapman and Cowling (34). The theory also has been extended to include multicomponent mixtures (35).

(*a*) *Brief Summary of Theoretical and Computational Development.* The Chapman-Enskog development differs from the earlier mean-free-path theories in that it attacks the fundamental problem of solving the Boltzmann integrodifferential equation for the molecular distribution function. The use of this equation as the starting point in the development has been justified by means of nonequilibrium statistical mechanical arguments (36). The solution of Boltzmann equation enables one to express the transport coefficients in terms of a set of double integrals $\Omega^{(l,s)}$, which involve explicitly the dynamics of a binary collision and hence the intermolecular force law. The theoretical development is quite intricate, and the mathematical calculations involved are very lengthy.

The results apply at low densities (where intermolecular collisions can be considered unimportant) but not at such low densities that the dimensions of the vessel are large compared with the mean free path of the molecules (i.e., "Knudsen gases"). Strictly speaking, the results apply to monoatomic gases only. Practically, however, it is found that the internal motions of the molecules are relatively unimportant in mass and momentum transfer, and hence the results of the Chapman-Enskog theory may be applied freely to the calculation of diffusion and viscosity coefficients of polyatomic molecules. The same is not true for thermal conductivity where the internal modes of motion contribute substantially to the energy transport in the gas. This effect can be corrected for approximately, however, by the "Eucken correction" which is discussed in section 4(*c*). The Chapman-Enskog theory can be used only for angle-independent potential functions (such as the Lennard-Jones potential) and hence can not be used to calculate the transport coefficients for polar molecules.

The evaluation of the $\Omega^{(l,s)}$ for the Lennard-Jones potential has been performed independently by several groups of investigators (37, 38, 39, 40) and the excellent agreement between the results indicates that no computational errors have been made. The results are tabulated in terms of the functions $\Omega^{(l,s)*}(T^*)$, which are just the values of the $\Omega^{(l,s)}$ for the Lennard-Jones potential divided by the corresponding values for rigid spheres. These results are given in Table 3. The function $\Omega^{(1,1)*}$ is used for calculating the first approximation to the coefficient of diffusion; the function $\Omega^{(2,2)*}$ is used for calculating the first approximation to the coefficients of viscosity and thermal conductivity of pure gases. In addition, we also give several other very slowly varying functions[7] which are special combinations of the $\Omega^{(l,s)*}$: the functions A^*, B^*, and C^* which are used in calculating the transport coefficients of mixtures, and the functions $f_\eta^{(3)}$, $f_\lambda^{(3)}$ and $f_\mathfrak{D}^{(2)}$ which give the higher approximations to η, λ, and $\mathfrak{D}$.

We now summarize the formulas to be used in conjunction with these tables. These formulas are written in the forms most convenient for practical calculations. The following units are used: η(gm cm^{-1} sec^{-1}), $\mathfrak{D}$(cm^2 sec^{-1}), λ(cal cm^{-1} sec^{-1} deg^{-1}), T(° K), p(atm), ϵ/k(°K), σ(Å). [Note: 1 Ångström unit = 10^{-8} cm.] When no subscripts are attached to the quantities $\Omega^{(l,s)*}$, A^*, B^*, C^*, they are to be calculated as a function of $T^* = kT/\epsilon$, where ϵ/k is the parameter given in Table 1 for interactions between pairs of similar molecules. When the subscripts ij are attached,

[7] Formulas for these quantities in terms of the $\Omega^{(l,s)*}$ are given in MTGL, ch. 8, appendix A.

these quantities are to be computed as functions of $T_{ij}^* = kT/\epsilon_{ij}$, where the ϵ_{ij}/k are the parameters characteristic of interactions between pairs of dissimilar molecules as given by the combining law in Equation [1.4]. No comparison is given here between the experimental results and the values calculated according to these tables and formulas, since extensive tables have been presented elsewhere for this purpose (1, 40). Generally the coefficients of viscosity and diffusion can be calculated to within 1 or 2 per cent over a range of temperature of about 400 deg K. The agreement for thermal conductivity is not quite so good since the theory for polyatomic molecules (the Eucken correction) is rough. The thermal diffusion ratio may be in error by as much as 10 per cent, for this property is highly sensitive to the exact form of the potential function which is used.

(b) The Coefficient of Viscosity. For a pure nonpolar gas the first approximation[8] to the coefficient of viscosity is given by

$$[\eta]_1 \times 10^7 = 266.93 \frac{\sqrt{MT}}{\sigma^2 \Omega^{(2,2)^*}} \quad \ldots\ldots [4.1]$$

Higher approximations may be written as

$$[\eta]_k = [\eta]_1 f_\eta^{(k)} \quad \ldots\ldots [4.2]$$

where the function $f_\eta^{(k)}$ is a very slowly varying function of T^*. The function $f_\eta^{(2)}$ is given in Table 3 and is very nearly unity.

In order to discuss the viscosity of a binary mixture it is convenient to define a quantity $[\eta_{12}]_1$ thus

$$[\eta_{12}]_1 \times 10^7 = \frac{266.93 \sqrt{2M_1M_2T/(M_1 + M_2)}}{\sigma_{12}^2 \Omega_{12}^{(2,2)^*}} \quad \ldots\ldots [4.3]$$

This quantity may be regarded as the coefficient of viscosity of a hypothetical pure substance, the molecules of which have a molecular weight $2M_1M_2/(M_1 + M_2)$ and interact according to a potential curve specified by the interaction parameters σ_{12} and ϵ_{12}. (This is similar to the quantity B_{12} defined in Equation [2.12].) If in Equation [4.3] the subscript 2 is replaced by 1, then the resulting expression is identical with the formula given in Equation [4.1] for the pure substance 1.

We may now write the viscosity of a nonpolar binary mixture in terms of $[\eta_1]_1$, $[\eta_2]_1$, and $[\eta_{12}]_1$

$$\frac{1}{[\eta_{mix}]_1} = \frac{X_\eta + Y_\eta}{1 + Z_\eta}$$

$$X_\eta = \frac{x_1^2}{[\eta_1]_1} + \frac{2x_1x_2}{[\eta_{12}]_1} + \frac{x_2^2}{[\eta_2]_1}$$

$$Y_\eta = \frac{3}{5} A_{12}^* \left\{ \frac{x_1^2}{[\eta_1]_1} \left(\frac{M_1}{M_2}\right) + \frac{2x_1x_2}{[\eta_{12}]_1} \left(\frac{(M_1 + M_2)^2}{4M_1M_2}\right) \times \left(\frac{[\eta_{12}]_1^2}{[\eta_1]_1[\eta_2]_1}\right) + \frac{x_2^2}{[\eta_2]_1} \left(\frac{M_2}{M_1}\right) \right\}$$

$$Z_\eta = \frac{3}{5} A_{12}^* \left\{ x_1^2 \left(\frac{M_1}{M_2}\right) + 2x_1x_2 \left[\left(\frac{(M_1 + M_2)^2}{4M_1M_2}\right) \times \left(\frac{[\eta_{12}]_1}{[\eta_1]_1} + \frac{[\eta_{12}]_1}{[\eta_2]_1}\right) - 1 \right] + x_2^2 \left(\frac{M_2}{M_1}\right) \right\} \quad \ldots\ldots [4.4]$$

For binary mixtures of heavy isotopes the viscosity is given to a good approximation by

$$\frac{1}{\sqrt{[\eta_{mix}]_1}} = \frac{x_1}{\sqrt{[\eta_1]_1}} + \frac{x_2}{\sqrt{[\eta_2]_1}} \quad \ldots\ldots [4.5]$$

[8] The degree of approximation is indicated by the subscript on the square bracket about the symbol.

It should be pointed out that the quantity $[\eta_{12}]_1$ is closely related to the coefficient of diffusion

$$[\eta_{12}]_1 = \frac{5}{3} \frac{M_1M_2}{(M_1 + M_2)} \frac{p[\mathfrak{D}_{12}]_1}{A_{12}^* RT} \quad \ldots\ldots [4.6]$$

If diffusion data were available it would be better to make use of them to obtain the quantity $[\eta_{12}]_1$ than to use Equation [4.3]. In view of the lack of such information we write Equation [4.4] in terms of $[\eta_{12}]_1$.

For nonpolar gas mixtures containing ν-components the coefficient of viscosity is as follows[9]

$$[\eta_{mix}]_1 = - \frac{\begin{vmatrix} H_{11} & H_{12} \ldots H_{1\nu} & x_1 \\ H_{12} & H_{22} \ldots H_{2\nu} & x_2 \\ \vdots & \vdots \quad \vdots & \vdots \\ H_{1\nu} & H_{2\nu} \ldots H_{\nu\nu} & x_\nu \\ x_1 & x_2 \quad \ldots x_\nu & 0 \end{vmatrix}}{|H_{ij}|} \quad \ldots\ldots [4.7]$$

in which $|H_{ij}|$ is the determinant of the H_{ij}, which are defined by

$$H_{ii} = \frac{x_i^2}{[\eta_i]_1} + \sum_{k \neq i}^{\nu} \frac{2x_ix_k}{[\eta_{ik}]_1} \frac{M_iM_k}{(M_i + M_k)^2} \left[\frac{5}{3A_{ik}^*} + \frac{M_k}{M_i} \right]$$

$$H_{\substack{i \\ i \neq j}} = - \frac{2x_ix_j}{[\eta_{ij}]_1} \frac{M_iM_j}{(M_i + M_j)^2} \left[\frac{5}{3A_{ij}^*} - 1 \right] \quad \ldots\ldots [4.8]$$

Because of the complexity of this formula it is sometimes convenient to use an empirical simplification of this expression. The ratio of determinants in Equation (4.7) may be expanded thus

$$[\eta_{mix}]_1 = \sum_{i=1}^{\nu} \frac{x_i^2}{H_{ii}} - \sum_{i=1}^{\nu} \sum_{j \neq i}^{\nu} \frac{x_ix_jH_{ij}}{H_{ii}H_{jj}} + \sum_{i=1}^{\nu} \sum_{j \neq i}^{\nu} \sum_{k \neq i}^{\nu} \frac{x_jx_kH_{ij}H_{ik}}{H_{ii}H_{jj}H_{kk}} \quad \ldots\ldots [4.9]$$

Since the off-diagonal elements H_{ij} are small in comparison with the diagonal elements H_{ii}, the primary contribution is given by the first term. To make the off-diagonal elements vanish exactly it is necessary to assume that $A^* = 5/3$. When the same assumption is made in the diagonal elements, Equation [4.9] becomes

$$[\eta_{mix}]_1 \doteq \sum_{i=1}^{\nu} \frac{x_i^2}{H_{ii}} \doteq \sum_{i=1}^{\nu} \frac{x_i^2}{\frac{x_i^2}{[\eta_i]_1} + \sum_{\substack{k=1 \\ k \neq i}}^{\nu} 2x_ix_k \frac{RT}{pM_k[\mathfrak{D}_{ik}]_1}} \quad \ldots\ldots [4.10]$$

where use has been made of Equation [4.6] to introduce the diffusion coefficients. This expression is not satisfactory because of the unrealistic value assumed for A^*. Buddenberg and Wilke (41) have recently shown by an extensive analysis of experimental data that Equation [4.10] describes the coefficient of viscosity of multicomponent systems if the numerical constant 2 is replaced by the empirical value 1.385. Hence a very good approximation to Equation [4.7] is[10]

[9] This formula lends itself well to systematized calculations as is shown in an illustrative example in MTGL, ch. 8. The use of equation [4.11] also is illustrated.

[10] Buddenberg and Wilke (41) did not derive Equation [4.11] from the rigorous kinetic theory of multicomponent gas mixtures (35) as is done here. Their work was based on some earlier approximate treatments of kinetic theory given by Sutherland and others.

$$[\eta_{mix}]_l = \sum_{i=1}^{r} \frac{x_i^2}{\frac{x_i^2}{[\eta_i]_l} + 1.385 \sum_{\substack{k=1 \\ k \neq i}}^{r} x_i x_k \frac{RT}{pM_i[\mathfrak{D}_{ik}]_l}} \quad [4.11]$$

This relation enables one to calculate $[\eta_{mix}]_l$ quite simply from calculated or experimental values of the viscosities of the pure components and the coefficients of diffusion.

(*c*) ***Coefficient of Thermal Conductivity.*** For a pure monatomic gas the coefficient of thermal conductivity is given by

$$[\lambda]_l \times 10^7 = 1989.1 \frac{\sqrt{T/M}}{\sigma^2 \Omega^{(2,2)*}} = \frac{15}{4} \frac{R}{M} [\eta]_l \times 10^7 \quad [4.12]$$

The proportionality to the coefficient of viscosity is well known from earlier simple kinetic-theory treatments. Higher approximations are given by

$$[\lambda]_k = [\lambda]_l f_\lambda^{(k)} \quad [4.13]$$

The correction factor $f_\lambda^{(2)}$, which is very close to unity, is given in Table 3 along with $f_\eta^{(2)}$. For a pure polyatomic gas the following approximate relation may be used

$$[\lambda]_l^{\text{Eucken}} = \frac{15}{4} \frac{R}{M} [\eta]_l \left\{ \frac{4}{15} \frac{\bar{C}_v}{R} + \frac{3}{5} \right\} \quad [4.14]$$

The factor within braces (the "Eucken correction") takes into account approximately the transfer of energy between the translational and internal degrees of freedom when polyatomic molecules collide.

To describe the thermal conductivity of mixtures it is convenient to introduce the quantity $[\lambda_{12}]_l$ (analogous to $[\eta_{12}]_l$) defined as

$$[\lambda_{12}]_l \times 10^7 = 1989.1 \frac{\sqrt{T(M_1 + M_2)/2M_1M_2}}{\sigma_{12}^2 \Omega_{12}^{(2,2)*}} \quad [4.15]$$

In terms of this quantity and the thermal conductivities of the pure components, the coefficient of thermal conductivity of a binary monatomic gas mixture may be written as

$$\frac{1}{[\lambda_{mix}]_l} = \frac{X_\lambda + Y_\lambda}{1 + Z_\lambda}$$

$$X_\lambda = \frac{x_1^2}{[\lambda_1]_l} + \frac{2x_1x_2}{[\lambda_{12}]_l} + \frac{x_2^2}{[\lambda_2]_l}$$

$$Y_\lambda = \frac{x_1^2}{[\lambda_1]_l} U^{(1)} + \frac{2x_1x_2}{[\lambda_{12}]_l} U^{(V)} + \frac{x_2^2}{[\lambda_2]_l} U^{(2)}$$

$$Z_\lambda = x_1^2 U^{(1)} + 2x_1x_2U^{(Z)} + x_2^2U^{(2)}$$

$$U^{(1)} = \frac{4}{15} A_{12}^* - \frac{1}{12}\left(\frac{12}{5} B_{12}^* + 1\right) \frac{M_1}{M_2} + \frac{1}{2} \frac{(M_1 - M_2)^2}{M_1M_2}$$

$$U^{(2)} = \frac{4}{15} A_{12}^* - \frac{1}{12}\left(\frac{12}{5} B_{12}^* + 1\right) \frac{M_2}{M_1} + \frac{1}{2} \frac{(M_2 - M_1)^2}{M_1M_2}$$

$$U^{(V)} = \frac{4}{15} A_{12}^* \left(\frac{(M_1 + M_2)^2}{4M_1M_2}\right) \frac{[\lambda_{12}]_l^2}{[\lambda_1]_l[\lambda_2]_l} - \frac{1}{12}\left(\frac{12}{5} B_{12}^* + 1\right) - \frac{5}{32 A_{12}^*}\left(\frac{12}{5} B_{12}^* - 5\right) \frac{(M_1 - M_2)^2}{M_1M_2}$$

$$U^{(Z)} = \frac{4}{15} A_{12}^* \left[\left(\frac{(M_1 + M_2)^2}{4M_1M_2}\right)\left(\frac{[\lambda_{12}]_l}{[\lambda_1]_l} + \frac{[\lambda_{12}]_l}{[\lambda_2]_l}\right) - 1\right] - \frac{1}{12}\left(\frac{12}{5} B_{12}^* + 1\right) \quad [4.16]$$

For binary mixtures of heavy isotopes this may be approximated closely by

$$\frac{1}{\sqrt{[\lambda_{mix}]_l}} = \frac{x_1}{\sqrt{[\lambda_1]_l}} + \frac{x_2}{\sqrt{[\lambda_2]_l}} \quad [4.17]$$

The quantity $[\lambda_{12}]_l$ is closely related to the coefficient of diffusion

$$[\lambda_{12}]_l = \frac{25}{8} \frac{p[\mathfrak{D}_{12}]_l}{A_{12}^* T} \quad [4.18]$$

When diffusion-coefficient data become available, they should be used to replace the calculated quantities $[\lambda_{12}]_l$. The rigorous kinetic theory for multicomponent gas mixtures also gives formulas for the coefficient of thermal conductivity of mixtures containing three or more monatomic components (35).

There is at present no rigorous method for calculating the thermal conductivity of mixtures of polyatomic gases. However, the coefficient of thermal conductivity for binary mixtures may be estimated if the thermal conductivities of the pure components are known experimentally. First, one calculates the thermal conductivity of the pure components as if they were monatomic, i.e., by means of Equation [4.12], and these quantities are designated as $[\lambda_1]_l^{mon}$ and $[\lambda_2]_l^{mon}$. Then similarly, one calculates the thermal conductivity of the mixture according to Equation [4.16] and this is called $[\lambda_{mix}]_l^{mon}$. An empirical expression for the coefficient of thermal conductivity for the polyatomic gas mixture is then

$$[\lambda_{mix}]_l^{poly} = [\lambda_{mix}]_l^{mon} \{x_1E_1 + x_2E_2\} \quad [4.19]$$

in which $E_i = (\lambda_i)_{expt}/[\lambda_i]_l^{mon}$ may be regarded as "experimental Eucken corrections" for the pure components.

(*d*) ***Coefficient of Diffusion.*** In the first approximation the coefficient of binary diffusion for nonpolar gases is given by

$$[\mathfrak{D}_{12}]_l = 0.0026280 \frac{\sqrt{T^3(M_1 + M_2)/2M_1M_2}}{p\sigma_{12}^2 \Omega_{12}^{(1,1)*}} \quad [4.20]$$

The second approximation to $\mathfrak{D}_{12}$ may be written as

$$[\mathfrak{D}_{12}]_2 = [\mathfrak{D}_{12}]_l f_{\mathfrak{D}_{12}}^{(2)} \quad [4.21]$$

The function $f_{\mathfrak{D}_{12}}^{(2)}$ is a complicated function of the molecular weights and mole fractions of the two species and also depends slightly on the forces between similar pairs of molecules. It differs from unity by at most several per cent. The fact that $[\mathfrak{D}_{12}]_l$ depends solely on the forces between dissimilar molecules means that the temperature dependence of the diffusion coefficient provides an excellent method for evaluating the parameters σ_{12} and ϵ_{12} between unlike pairs of molecules. It is unfortunate that there are so few diffusion measurements recorded in the literature.

It should be noticed that Equation [4.20] can be used to describe the interdiffusion of a polar gas and a nonpolar gas. It is pointed out in section 1 that the potential energy of interaction between a polar and a nonpolar molecule is very nearly of the same form as that between two nonpolar molecules. Hence the function $\Omega^{(1,1)*}$ may be used in conjunction with the combining laws in Equations [1.6] and [1.7].

When Equation [4.20] is written for a single component that first approximation to the formula for "self-diffusion" is obtained

$$[\mathfrak{D}]_l = 0.0026280 \frac{\sqrt{T^3/M}}{p\sigma^2 \Omega^{(1,1)*}} \quad [4.22]$$

The second approximation to the coefficient of self-diffusion is given by

$$[\mathfrak{D}]_2 = [\mathfrak{D}]_l f_\mathfrak{D}^{(2)} \quad [4.23]$$

The function $f_{\mathfrak{D}}^{(2)}$ depends only on the reduced temperature and is given in Table 3. It does not differ from unity by more than 1 per cent.

Let us now inquire as to the meaning of the coefficient of self-diffusion. Clearly if the molecules are all physically identical it is impossible to measure their interdiffusion. It is, however, possible to measure quantities experimentally which were very nearly coefficients of self-diffusion

(i) *Interdiffusion of heavy isotopes* for which $\sigma_{12} = \sigma_1 = \sigma_2$, $\epsilon_{12} = \epsilon_1 = \epsilon_2$, and $2M_1M_2/(M_1 + M_2) \cong M_1$ or M_2.

(ii) *Interdiffusion of ortho and para forms* for which

$2M_1M_2/(M_1 + M_2) = M_1 = M_2$ and $\sigma_{12} \cong \sigma_1$ or σ_2, $\epsilon_{12} \cong \epsilon_1$ or ϵ_2,

slight differences in the interaction potential resulting from the effects of the different rotational states.

It is apparent that the coefficient of self-diffusion must be regarded as somewhat artificial. It is more correct simply to consider it as a limiting form of the coefficient of binary diffusion. It is interesting to note that in this limit of equal masses and equal intermolecular forces Equation [4.6] simplifies to

$$\frac{\rho[\mathfrak{D}]_1}{[\eta]_1} = \frac{6}{5} A^* \qquad [4.24]$$

The function A^* is very slowly varying in T^* approximately equal to 1.1 (see Table 3), and hence $\rho[\mathfrak{D}]_1/[\eta]_1$ has very nearly the constant value 4/3 (the theoretical basis for the Schmidt number).

The rigorous theory of multicomponent mixtures (35) also gives expressions for the coefficients of diffusion in gases containing more than two components. An empirical approach to the problem of multicomponent diffusion has been proposed by Wilke (42).

(*e*) *Thermal-Diffusion Ratio.* The first approximation to the thermal-diffusion ratio in binary nonpolar gas mixtures is given by the following expression

$$\left.\begin{aligned} [k_T]_1 &= \frac{x_1x_2}{6[\lambda_{12}]_1}\,\frac{S^{(1)}x_1 - S^{(2)}x_2}{X_\lambda + Y_\lambda}\,(6C_{12}^* - 5) \\ S^{(1)} &= \frac{M_1 + M_2}{2M_2}\,\frac{[\lambda_{12}]_1}{[\lambda_1]_1} - \frac{15}{4A_{12}^*}\left(\frac{M_2 - M_1}{2M_1}\right) - 1 \\ S^{(2)} &= \frac{M_2 + M_1}{2M_1}\,\frac{[\lambda_{12}]_1}{[\lambda_2]_1} - \frac{15}{4A_{12}^*}\left(\frac{M_1 - M_2}{2M_2}\right) - 1 \end{aligned}\right\} \qquad [4.25]$$

in which X_λ, Y_λ, $[\lambda_1]_1$, $[\lambda_2]_1$ and $[\lambda_{12}]_1$ are quantities defined in the discussion of thermal conductivity. The primary concentration dependence is given by x_1x_2, the dependence on the molecular weights is given mainly by $S^{(1)}$ and $S^{(2)}$, and the principal temperature dependence is given by $(6C_{12}^* - 5)$. A positive value of k_T signifies that component 1 tends to move into the cooler region and 2 toward the warmer region. The temperature at which k_T undergoes a change of sign is referred to as the "inversion temperature."

For the thermal diffusion of heavy isotopes Equation [4.25] may be simplified considerably, by expanding it in powers of $(M_1 - M_2)/(M_1 + M_2)$ and taking the first term. When this in turn is divided by the corresponding rigid sphere value we get

$$[k_T^*]_1 = \frac{[k_T]_1}{[k_T]_1^{\text{rig. sph.}}} = \frac{59}{7}\,\frac{(2A^* + 5)(6C^* - 5)}{A^*(16A^* - 12B^* + 55)} \qquad [4.26]$$

which is a function of T^* alone. This function, which is tabulated in Table 3, has been shown (43) to be valid for values of $(M_1 - M_2)/(M_1 + M_2)$ up to 0.15

Formulas for the thermal-diffusion coefficients in multicomponent gas systems have been derived from the rigorous kinetic-theory treatment (35).

(*f*) *Present Status of Theory, Calculations, and Experimental Data.* The foregoing formulas and the accompanying tables are strictly applicable only to gases and gaseous mixtures made up of molecules whose interaction can be described by a spherically symmetric potential-energy function. Quite recently the theory of transport phenomena in gases has been generalized by Wang-Chang and Uhlenbeck (44) and independently by de Boer (45) to include rigorously the internal motion of polyatomic molecules. These theoretical advances ultimately will provide us with a means for calculating the transport coefficients of long molecules and of polar molecules. In particular, it will enable us to understand the effects of the internal molecular motions on the coefficient of thermal conductivity. Up to the present only very limited calculations have been made by means of these generalized theories.

Quite recently the $\Omega^{(l,s)}$ integrals have been evaluated for the three-parameter Buckingham interaction potential (46). These calculations along with the analogous calculations of the second virial coefficients (19) should provide some new information concerning the interaction of spherical nonpolar molecules.

There are quite extensive experimental data for the viscosity of a number of simple gases, the primary contributors to this field being Trautz and coworkers (Germany) and H. L. Johnston and collaborators (U. S.). In the temperature range where the data of these two groups overlap, there seems to be some disagreement for several gases. For binary mixtures a considerable amount of data have been obtained by Trautz and his colleagues. There are practically no data available on the viscosity of mixtures of gases containing more than two chemical species. The situation with respect to the coefficient of thermal conductivity seems to be about the same as for viscosity. In recent years there have been quite a few measurements of thermal diffusion in connection with the study of separation processes. The transport coefficient which has been quite seriously neglected is the coefficient of diffusion, for which there are but a few measurements. As mentioned earlier, one can gain valuable information about the forces between dissimilar molecules from the temperature dependence of this quantity.

An extensive summary of recent experimental transport property data has been given by E. F. Johnson (47). The present status of the engineering applications to fluid dynamics, heat transfer, and mass transfer has been summarized in review articles by Baron and Oppenheim (48), Eckert (49), and Pigford (50).

5 Transport Coefficients of Dense Gases and Liquids

There are three main theories of transport phenomena of dense gases and liquids which will be discussed briefly in increasing order of the mathematical complexity of the theory. First, we discuss the Eyring theory (for liquids), which is a special application of the theory of absolute reaction rates. Then we summarize the Enskog theory (of dense gases) which is a simple extension of the Chapman-Enskog theory for dilute gases. Finally, we indicate what progress has been made by Kirkwood and coworkers and by Born and Green in an attempt to describe transport phenomena by means of a rigorous nonequilibrium statistical mechanical development.

(*a*) *Eyring Theory (Liquids).* The theory developed by Eyring and coworkers (51, 52, 53) has been moderately successful in predicting the transport coefficients in the liquid phase and explaining them on a simple pictorial basis. It is not possible by means of this approach to obtain expressions for the transport coefficients in terms of the intermolecular forces. Rather, one obtains relationships among various macroscopic quantities.

It is found that the viscosity depends exponentially on the temperature in the following way

$$\eta = nh \exp(0.408\ \Delta U_{vap}/RT) \quad [5.1]$$

in which h is Planck's constant and n is the number density, i.e., the number of molecules per unit volume. The general form of this relation is found from the theory and the numerical constant 0.408 is obtained from the experimental data. According to Trouton's rule, ΔU_{vap} is approximately equal to $9.4RT_b$, where T_b is the boiling temperature at 1 atm pressure. Substitution of this into Equation [5.1] gives the relation

$$\eta = nh \exp(3.8T_b/T) \quad [5.2]$$

which is useful for rough estimates. The theory also predicts the following relation between the coefficients of viscosity and self-diffusion

$$\eta\mathfrak{D} = n^{1/3}kT \quad [5.3]$$

The best empirical relationship which Eyring and his coworkers were able to find for the variation of the viscosity of a binary mixture with composition is

$$\log \eta_{mix} = x_1 \log \eta_1 + x_2 \log \eta_2 \quad [5.4]$$

where η_1 and η_2 are the viscosities of the two pure components.

For a monatomic liquid the thermal conductivity of a liquid may be related to the speed of sound in the liquid, c, by

$$\lambda = \sqrt{\frac{8}{\pi}}\, kn^{2/3}\gamma^{-1/2}c \quad [5.5]$$

in which $\gamma = C_p/C_v$. For polyatomic molecules this has to be multiplied by the Eucken correction $(9\gamma-5)/4$ to take into account the internal degrees of freedom of the molecules. In order to make the resulting equation agree with a very satisfactory empirical relation of Bridgman (54), Eyring supposed that only the rotational and translational degrees of freedom are effective in transferring energy so that the proper value to use for γ in the Eucken correction is usually 4/3. Hence we write for polyatomic liquids

$$\lambda = 2.80kn^{2/3}\gamma^{-1/2}c \quad [5.6]$$

Here $\gamma = C_p/C_v$ should be taken to be those values which are found in speed of sound measurements (presumably it is different from the factor 4/3 used in the Eucken correction). This formula has been found satisfactory for a large number of liquids (a mean deviation of around 10 per cent). Bridgman has pointed out that Equation [5.6] gives the correct temperature dependence of the thermal conductivity of liquids at 1 atm. However, for most liquids the thermal conductivity increases by a factor of 2 when the pressure is raised to 12,000 atm whereas Equation [5.6] indicates that the thermal conductivity should increase by a factor of 4.

The Eyring theory of transport properties predicts the variation of the coefficient of viscosity with force. Let us define a parameter $z = F/2nkT$, where F is the shearing force applied to a square centimeter of liquid. Then, if F is sufficiently small that z is somewhat less than unity, the flow is "Newtonian" in the sense that the coefficient of viscosity η_0 is a constant independent of F. However, if z is large compared to unity, the flow is "non-Newtonian" and the coefficient of viscosity as a function of the applied force is given by the relation[11]

$$\eta/\eta_0 = z/\sinh z \quad [5.7]$$

At the present time there is no other molecular theory for non-Newtonian flow.

The Eyring theory has been used to study the viscosities of the liquids composed of molecules which are nonspherical such as long-chain hydrocarbons and long-chain polymers. The influence of pressure on the viscosity of liquids has also been examined.

(*b*) *Enskog Theory (Dense Gases).* The rigorous kinetic theory of dilute gases which was described in section 4 is based on the Boltzmann equation. In its derivation it is assumed that there are two-body collisions only and that the molecules have no finite extension in place (or, more correctly, that the molecular diameter is negligibly small in comparison with the average distance between the molecules). Both of these assumptions are certainly valid in dilute gases. In dense gases, however, these two assumptions have to be reconsidered.

Enskog (55) was the first to make an advance in this direction by developing a kinetic theory of dense gases made up of rigid spherical molecules of diameter σ. For this special molecular model there are no three-body and higher-order collisions. By thus considering only two-body collisions and by taking into account the finite size of the molecules he succeeded in grafting a theory of dense gases onto his earlier theory of dilute gases. As a gas is compressed there are two effects which become important owing to the fact that molecules have volume: (*a*) the "collisional transfer" of momentum and energy—when two rigid sphere molecules undergo a collision, there is an instantaneous transport of energy and momentum from the center of one molecule to the center of the other;[12] and (*b*) the change in the rate of collisions—the frequency of collisions tends to become greater because σ is not negligibly small compared with the average distance between the molecules, and on the other hand, the frequency of collisions tends to be smaller because the molecules are close enough to shield one another from oncoming molecules. The net increase in frequency of collisions may be related to the equation of state of the gas.

The results of the Enskog theory for the transport coefficients divided by their limiting values at zero pressure (and multiplied by a reduced volume) may be written in the form:

Shear Viscosity

$$\left(\frac{\eta}{\eta^\circ}\right)\left(\frac{\tilde{V}}{b_0}\right) = \frac{1}{y} + 0.8 + 0.761y \quad [5.8]$$

Bulk Viscosity

$$\left(\frac{\kappa}{\eta^\circ}\right)\left(\frac{\tilde{V}}{b_0}\right) = 1.002y \quad [5.9]$$

Thermal Conductivity[13]

$$\left(\frac{\lambda}{\lambda^\circ}\right)\left(\frac{\tilde{V}}{b_0}\right) = \frac{1}{y} + 1.2 + 0.755y \quad [5.10]$$

Self-Diffusion[14]

$$\left(\frac{\mathfrak{D}}{\mathfrak{D}^\circ}\right)\left(\frac{\tilde{V}}{b_0}\right) = \frac{1}{y} \quad [5.11]$$

[11] Here we have assumed that the distance between lattice sites in the liquid is equal to the distance between neighboring molecular planes. This represents an additional approximation to the Eyring theory.

[12] In liquids collisional transfer is the primary mechanism for the transport of momentum, while in gases the momentum transport is due primarily to molecular motion. This explains the fact that the viscosity of gases increases with temperature while that of liquids decreases with temperature.

[13] This applies to monatomic substances only.

[14] $\mathfrak{D}^\circ$ may be calculated as $\mathfrak{D}^\circ = M\mathfrak{D}^1/\rho RT$, where $\mathfrak{D}^1$ is the coefficient of self-diffusion calculated at 1 atm pressure according to equation (4.22).

In these relations $b_0 = \frac{2}{3}\pi N\sigma^3$ and

$$y = \frac{p\bar{V}}{RT} - 1 \quad \ldots\ldots\ldots\ldots\ldots\ldots [5.12]$$

The curves for η and λ both exhibit minima which are

$$\left[\frac{\eta}{\eta^\circ}\frac{\bar{V}}{b_0}\right]_{\min} = 2.545 \quad \text{at} \quad y = 1.146 \ldots\ldots [5.13]$$

$$\left[\frac{\lambda}{\lambda^\circ}\frac{\bar{V}}{b_0}\right]_{\min} = 2.938 \quad \text{at} \quad y = 1.151 \ldots\ldots [5.14]$$

To complete the statement of the results for rigid spherical molecules we need but to add that y is given exactly at low and moderate densities by the virial equation $[y = (b_0/\bar{V}) + 0.6250(b_0/\bar{V})^2 + 0.2869(b_0/\bar{V})^3 + \ldots]$ and approximately at high densities from the distribution-function method described in section 3 (51, 52).

Although the formulas for the transport coefficients given in the foregoing text were obtained for gases composed of rigid spherical molecules, Enskog showed that these results can be applied to real gases with reasonable success. In order to use the foregoing formulas it is necessary to specify b_0 and y. Enskog suggested that the pressure p in Equation [5.12] be replaced by the "thermal pressure" $T(\partial p/\partial T)_v$ so that y may be determined from the experimental p-V-T data from the relation

$$y = \frac{\bar{V}}{RT}\left[T\left(\frac{\partial p}{\partial T}\right)_{\bar{V}}\right] - 1 \quad \ldots\ldots\ldots\ldots [5.15]$$

(For rigid spheres Equations [5.12] and [5.15] are identical but such is not the case for real gases.) Enskog also suggested that b_0 be evaluated by fitting the minimum in the curve of $(\eta/\eta^\circ)\bar{V}$ as a function of y. The usefulness of this method of Enskog has been demonstrated by numerical comparisons for N_2 and CO_2, the only two gases for which high-density viscosity and equation-of-state data are both available. The pressure dependence of the viscosity of N_2 is described quite accurately over a pressure range of 1000 atm, and that of CO_2 over a 100-atm range. The Enskog theory has been extended to binary mixtures by Thorne,[15] but no numerical comparisons with experiment have been made.

(*c*) ***Kirkwood-Born-Green Theory.*** The theory of transport phenomena in dense gases and liquids has been developed by means of nonequilibrium statistical mechanics (36, 56). The final results are given in terms of the nonequilibrium radial-distribution function just as the equation of state of dense gases and liquids is given in terms of the equilibrium radial-distribution function. The nonequilibrium radial-distribution function is given as the solution of an integral equation, which involves the next higher-order distribution function. Here, just as in the equilibrium case, some sort of superposition approximation is introduced in order to get rid of the higher-order function. At the present time only some rough calculations have been made, and accordingly, the method does not yet provide a means for practical computations. It is hoped that this approach ultimately will lead to the calculation of the properties of dense gases and liquids with accuracy comparable to that for dilute gases described in section 4. Considerable theoretical and computational work needs to be done, however.

(*d*) ***Present Status of the Theory, Calculations, and Experimental Data.*** Until the rigorous statistical mechanical treatment is developed further, the Eyring and Enskog theories will provide the best means for interpreting the high-pressure transport phenomena. The Enskog theory has been studied recently, with the idea of extending it to any type of molecular interaction (57).

[15] See reference (33), p. 292.

There are good high-density transport-coefficient data available for only a few gases—by no means enough to make satisfactory empirical correlations in the absence of the theory. Drickamer and his coworkers at the University of Illinois have done a considerable amount of experimental research during the past five years on the diffusion and thermal diffusion in the critical region. The particular appropriateness of thermal diffusion as a means for separating complex liquid mixtures has been discussed by Jones and Milberger (62). Recently two surveys have been made on the available thermal conductivity data of dense gases and liquids (63, 64).

6 Some Applications of the Principle of Corresponding States

As we have seen in the preceding sections there are numerous gaps in the theory, the calculations, and the experimental data. In engineering problems for which all of these are absent, it becomes necessary to fall back upon a more general method of predicting the properties of matter. Hence we summarize here the basic ideas connected with the principle of corresponding states.

(*a*) ***Reduction in Terms of Critical Parameters.*** In the early studies of the behavior of matter it was recognized that all substances behave in approximately the same manner. For example, the p-V isotherms of all substances were found to be of hyperbolic form at high temperatures, to exhibit a critical point (that is, a point at which $(\partial p/\partial V)_T = (\partial^2 p/\partial V^2)_T = 0$), and to show condensation phenomena at low temperatures. The critical point occupies a unique place on the p-V isotherms and represents a certain specific state of aggregation of the substance. It was suggested by van der Waals that the critical point is therefore a "point of corresponding states" and that the properties of various substances should be compared under conditions where the variables are the same multiples of the variables at the critical point. Accordingly, the compressibility factor may be written as a universal function of the reduced pressure $p_r = p/p_c$ and the reduced temperature $T_r = T/T_c$

$$p\bar{V}/RT = Z(p_r, T_r) \quad \ldots\ldots\ldots\ldots [6.1]$$

in which $Z(p_r, T_r)$ is the same function for all substances. This is the basis for the widely used "generalized compressibility charts" and the "generalized charts of thermodynamic functions" of Hougen and Watson (16). These charts provide an excellent means for industrial calculations because they are quick and easy to use.

In a similar fashion the principle of corresponding states may be used in the correlation of transport-coefficient data. These quantities also may be expressed as universal functions of p_r and T_r

$$\mathfrak{D}_r = \mathfrak{D}/\mathfrak{D}_c = \mathfrak{D}_r(p_r, T_r) \quad \ldots\ldots\ldots\ldots [6.2]$$

$$\eta_r = \eta/\eta_c = \eta_r(p_r, T_r) \quad \ldots\ldots\ldots\ldots [6.3]$$

$$\lambda_r = \lambda/\lambda_c = \lambda_r(p_r, T_r) \quad \ldots\ldots\ldots\ldots [6.4]$$

Equation [6.3] provides the basis for Hougen and Watson's "generalized viscosity chart" (16). Such extensive charts have not been prepared for the other transport coefficients because of lack of experimental data. Other methods of reducing the variables have been suggested. One method consists of reducing the transport coefficients by dividing by the appropriate combinations of critical constants; for example

$$\eta_R = M^{-1/6}p_c^{-2/3}T_c^{1/6}\,\eta = \eta_R(p_r, T_r)$$

In another method one divides the transport coefficient by its limiting value at zero-pressure, thus

$$\eta^\phi = \eta/\eta^\circ = \eta^\phi(p_r, T_r)$$

The use of the principle of corresponding states is not confined to the correlation of compressibility data and transport-coefficient data. Other properties such as surface tension, vapor pressure, melting lines, and Joule-Thomson coefficients can be predicted by means of the corresponding states arguments. For example, the reduced surface tension $\gamma'_R = \gamma' \mathcal{V}_c^{2/3} T_c^{-1}$ should be a universal function of $T_r = T/T_c$. And indeed it has been found that the surface tension of many substances is described by a relation of the form $\gamma'_R \sim (1 - T_r)^{11/9}$.

In the early development it was recognized that all substances did not truly obey the principle of corresponding states. It was noted, however, that those substances containing molecules which are similar in structure tend to exhibit closely similar behavior; that is, the halogens would be expected to obey one principle of corresponding states, while the saturated hydrocarbons would be expected to obey another. This correlation of the bulk behavior of substances with the molecular structure was first suggested by Kamerlingh Onnes and was called by him the "principle of mechanical equivalence." Its usefulness lies in the fact that if data are available for the physical properties of several chemically related substances, then the properties of other substances of the same general structure may be estimated by the application of the principle of corresponding states.

(*b*) *Reduction in Terms of Molecular Parameters.* Recently the principle of corresponding states has been studied extensively from a different point of view (17, 58), which has been made possible because of recent advances in the statistical mechanical theory of matter. If the molecules in a substance obey a two-constant potential function of the form $\varphi(r) = \epsilon f(r/\sigma)$ (the Lennard-Jones potential is of this form), then the various variables describing the properties of the substance and the state of the system may be expressed in reduced units by means of the appropriate combinations of the parameters ϵ and σ: $p^* = p\sigma^3/\epsilon$, $T^* = kT/\epsilon$, and $v^* = v/\sigma^3$. Hence the equation of state assumes the reduced form

$$p^* = p^*(v^*, T^*) \quad [6.5]$$

That is, the reduced pressure is a function of the reduced volume and the reduced temperature and is the same for all substances. The parameters σ and ϵ may be expressed in terms of critical properties for many nonpolar substances, Equation [1.3]. If these relations are used in Equation [6.5], we can obtain the fact that $p_r = p_r(V_r, T_r)$ which is a justification for the older statement of the principle of corresponding state based on critical properties.

Similarly, the transport coefficients may be expressed in terms of corresponding states relationships, based on reduction of quantities with the σ and ϵ of the potential function

$$\mathfrak{D}^* = \frac{\mathfrak{D}\sigma^2}{\sqrt{m\epsilon}} \frac{m}{\sigma^3} = \mathfrak{D}^*(v^*, T^*) \quad [6.6]$$

$$\eta^* = \frac{\eta\sigma^2}{\sqrt{m\epsilon}} = \eta^*(v^*, T^*) \quad [6.7]$$

$$\lambda^* = \frac{\lambda\sigma^2}{\sqrt{m\epsilon}} \frac{m}{k} = \lambda^*(v^*, T^*) \quad [6.8]$$

Thus the reduced transport coefficients are universal functions of the reduced volume and the reduced temperature. Other properties, such as vapor pressure and surface tension, may also be expressed in this fashion.

For molecules which do not have spherically symmetric potential functions the use of reduced variables leads to a different sort of result. As an example, we consider those polar molecules which obey the Stockmayer potential. It is easy to show that the equation of state in reduced units for a substance containing molecules with dipole moment μ assumes the form

$$p^* = p^*(v^*, T^*; \mu^*) \quad [6.9]$$

where $\mu^* = \mu/\sqrt{\epsilon\sigma^3}$ is the dipole moment of the molecule in reduced units. Thus molecules which have the same value of μ^* obey the same principle of corresponding states. Similar results are found for elongated molecules of length l and "width" σ

$$p^* = p^*(v^*, T^*; l^*) \quad [6.10]$$

where $l^* = l/\sigma$ is the length-to-width ratio of the molecules. Equations [6.9] and [6.10] are examples of the principle of mechanical equivalence of Kamerlingh Onnes.

The quantum effects in the noble-gas series have been studied extensively by means of the quantum mechanical principle of corresponding states (58, 61). According to this principle the equation of state is given by the reduced equation

$$p^* = p^*(v^*, T^*; \Lambda^*) \quad [6.11]$$

in which Λ^* is the quantum mechanical parameter $h/\sigma\sqrt{m\epsilon}$. The value of Λ^* is a measure of the importance of quantum effects for various substances. The larger the value of Λ^* the more a substance is expected to deviate from classical behavior at a given temperature. For the noble gases the values of Λ^* are: He^3—3.08, He^4—2.67, Ne—0.59, A—0.19, Kr—0.10, and Xe—0.06. $\Lambda^* = 0$ corresponds to classical behavior. For most substances Λ^* is small compared to unity, and quantum effects are negligible except at extremely low temperatures. For the isotopes of helium and hydrogen, however, quantum effects are observable (though small) at room temperature and become quite large at very low temperatures. The quantum mechanical principle of corresponding states was used to predict the properties of the light helium isotope (59) and the hydrogen isotopes (60).

BIBLIOGRAPHY

1 "Viscosity and Other Physical Properties of Gases and Gas Mixtures," by J. O. Hirschfelder, R. B. Bird, and E. L. Spotz, Trans. ASME, vol. 72, 1949, pp. 921–937.

2 "The General Theory of Molecular Forces," by F. London, Trans. Faraday Society, vol. 33, part 1, 1937, pp. 8–26.

3 "Van der Waals Forces," by H. Margenau, *Reviews of Modern Physics*, vol. 11, 1939, pp. 1–35.

4 "The Critical Properties of Elements and Compounds," by K. A. Kobe and R. E. Lynn, Jr., *Chemical Reviews*, vol. 52, 1953, pp. 121–236.

5 "On Centers of van der Waals Attraction," by F. London, *Journal of Physical Chemistry*, vol. 46, 1942, pp. 305–316.

6 "Long Range Forces Between Large Chain Molecules," by C. A. Coulson and P. L. Davies, Trans. Faraday Society, vol. 48, part 9, 1952, pp. 777–788.

7 "The Mutual Repulsive Potential of Closed Shells," by W. E. Bleick and J. E. Mayer, *Journal of Chemical Physics*, vol. 2, 1934, pp.252–259.

8 "The Non-Spherical Potential Field Between Two Hydrogen Molecules," by J. de Boer, *Physica*, vol. 9, 1942, pp. 363–382.

9 "Tables of Second Virial and Low-Pressure Joule-Thomson Coefficients for Intermolecular Potentials With Exponential Repulsion," by R. A. Buckingham and J. Corner, Proceedings of the Royal Society, London, England, series A, vol. 189, no. A1016, 1947, pp. 118–129.

10 "The Second Virial Coefficient of a Gas of Non-Spherical Molecules," by J. Corner, Proceedings of the Royal Society, London, England, series A, vol. 192, no. A1029, 1948, pp. 275–291.

11 "The Second Virial Coefficient of Non-Spherical Molecules," by T. Kihara, *Journal of the Physical Society of Japan*, vol. 6, 1941, pp. 289–296.

12 "The Lattice Energy of Ice and the Second Virial Coefficient of Water Vapor," by J. S. Rowlinson, Trans. Faraday Society, vol. 47, part 2, 1951, pp. 120–129.

13 "Pressure Broadening in the Microwave and Infra-Red Regions," by P. W. Anderson, *Physical Review*, vol. 76, 1949, pp. 647–661.

14 "Microwave Collision Diameters II. Theory and Correlation With Molecular Quadrupole Moments," by W. V. Smith and R. Howard, *Physical Review*, vol. 79, 1950, pp. 132–136.

15 "Statistical Mechanics," by J. E. Mayer and M. G. Mayer, John Wiley and Sons, Inc., New York, N. Y., 1940.

16 "Chemical Process Principles," by O. A. Hougen and K. M. Watson, John Wiley and Sons, Inc., New York, N. Y., 1947.

17 "Molecular Distribution and Equation of State of Gases," by J. de Boer, Reports on Progress in Physics, vol. 12, 1949, pp. 305–374.

18 "The Third Virial Coefficient of Non-Polar Gases," by R. B. Bird, E. L. Spotz, and J. O. Hirschfelder, *Journal of Chemical Physics*, vol. 18, 1950, pp. 1392–1402.

19 "Second Virial Coefficients of Gases Obeying a Modified Buckingham (6-exp) Potential," by W. E. Rice and J. O. Hirschfelder, *Journal of Chemical Physics*, vol. 22, 1954, pp. 187–192.

20 "Virial Coefficients and Models of Molecules in Gases," by T. Kihara, *Reviews of Modern Physics*, vol. 25, no. 4, 1953, pp. 831–843. Also released as University of Wisconsin Report OOR-7, June 5, 1953.

21 "Critical Phenomena in Gases," by J. E. Lennard-Jones and A. F. Devonshire, Proceedings of the Royal Society, London, England, series A, vol. 163, no. 912, 1937, pp. 53–70.

22 "Lennard-Jones and Devonshire Equation of State for Compressed Gases and Liquids," by R. H. Wentorf, R. J. Buehler, J. O. Hirschfelder, and C. F. Curtiss, *Journal of Chemical Physics*, vol. 18, 1950, pp. 1484–1500.

23 "Statistical Mechanics of Fluid Mixtures," by J. G. Kirkwood, *Journal of Chemical Physics*, vol. 3, 1935, pp. 300–313.

24 "Radial Distribution Function and the Equation of State of Fluids Composed of Molecules Interacting According to the Lennard-Jones Potential," by J. G. Kirkwood, V. A. Lewinson, and B. J. Alder, *Journal of Chemical Physics*, vol. 20, 1952, pp. 929–938.

25 "Une généralisation de la méthode de Lennard-Jones et Devonshire pour le calcul de l'intégrale de configuration," by P. Janssens and I. Prigogine, *Physica*, vol. 16, nos. 11–12, 1950, pp. 895–906.

26 "The Communal Entropy of Dense Systems," by J. Pople, *Philosophical Magazine*, vol. 42, 1951, pp. 459, 467.

27 "Lattice Theories of the Liquid State," by J. S. Rowlinson and C. F. Curtiss, *Journal of Chemical Physics*, vol. 19, 1951, pp. 1519–1529.

28 "Application of the Cell Method to the Statistical Thermodynamics of Solutions," by I. Prigogine and V. Mathot, *Journal of Chemical Physics*, vol. 20, 1952, pp. 49–57.

29 "On the Influence of Nonrandomness of Mixing in the Cell Model of Solutions," by I. Sarolea, *Journal of Chemical Physics*, vol. 21, 1953, pp. 182–183.

30 "On the Specific Molar Quantities in the Cell Model of Solutions," by J. Nasielski, *Journal of Chemical Physics*, vol. 21, 1953, pp. 184–185.

31 "Free Volume Theory of Multicomponent Fluid Mixtures," by Z. W. Salsburg and J. G. Kirkwood, *Journal of Chemical Physics*, vol. 20, 1952, pp. 1538–1543.

32 "Theories of the Liquid State," J. de Boer, Proceedings of the Royal Society, London, England, series A, vol. 215, 1952, pp. 4–29.

33 "Thermodynamics," by J. M. Smith, *Industrial and Engineering Chemistry*, vol. 45, 1953, pp. 963–968.

34 "The Mathematical Theory of Non-Uniform Gases," by S. Chapman and T. G. Cowling, Cambridge University Press, Cambridge, England, second edition, 1951.

35 "Transport Properties of Multicomponent Gas Mixtures," by C. F. Curtiss and J. O. Hirschfelder, *Journal of Chemical Physics*, vol. 17, 1949, pp. 550–555.

36 "The Statistical Mechanical Theory of Transport Phenomena:"

(*a*) "General Theory," by J. G. Kirkwood, *Journal of Chemical Physics*, vol. 14, 1946, pp. 180–201. Errata: vol. 14, 1946, p. 347.

(*b*) "Transport in Gases," by J. G. Kirkwood, *Journal of Chemical Physics*, vol. 15, 1947, pp. 72–76. Erratum: vol. 15, 1947, p. 155.

(*c*) "The Coefficients of Shear and Bulk Viscosity in Liquids," by J. G. Kirkwood, F. P. Buff, and M. S. Green, *Journal of Chemical Physics*, vol. 17, 1949, pp. 988–994. Errata: vol. 18, 1950, pp. 901–902.

(*d*) "The Equations of Hydrodynamics," by J. H. Irving and J. G. Kirkwood, *Journal of Chemical Physics*, vol. 18, 1950, pp. 817–829.

(*e*) "Quantum Hydrodynamics," by J. H. Irving and R. W. Zwanzig, *Journal of Chemical Physics*, vol. 19, 1951, pp. 1173–1180.

(*f*) "A Calculation of the Coefficients of Shear and Bulk Viscosity of Liquids," by R. W. Zwanzig, J. G. Kirkwood, K. F. Strupp, and I. Oppenheim, *Journal of Chemical Physics*, vol. 21, no. 11, 1953, pp. 2050–2055.

37 "Determination of Intermolecular Forces from Transport Phenomena in Gases:"

(*a*) By M. Kotani, Proceedings of the Physico-Mathematical Society of Japan, vol. 24, 1942, pp. 76–95.

(*b*) By T. Kihara and M. Kotani, Proceedings of the Physico-Mathematical Society of Japan, vol. 24, 1943, pp. 602–614.

38 "The Viscosity and Heat Conductivity of Gases With Central Intermolecular Forces," by J. de Boer and J. van Kranendonk, *Physica*, vol. 14, 1948, pp. 442–452.

39 "The Transport Properties of Non-Polar Gases," by J. S. Rowlinson, *Journal of Chemical Physics*, vol. 17, 1949, p. 101.

40 "The Transport Properties for Nonpolar Gases," by J. O. Hirschfelder, R. B. Bird, and E. L. Spotz:

(*a*) *Journal of Chemical Physics*, vol. 16, 1948, pp. 968–981.

(*b*) *Chemical Reviews*, vol. 44, 1949, pp. 205–231.

41 "Calculation of Gas Mixture Viscosities," by J. W. Buddenberg and C. R. Wilke, *Industrial and Engineering Chemistry*, vol. 41, 1949, pp. 1345–1347.

42 "Diffusion Coefficients in Multicomponent Gas Mixtures," by D. F. Fairbanks and C. R. Wilke, *Industrial and Engineering Chemistry*, vol. 42, 1950, pp. 471–475.

43 "Diffusion Properties of Gases. Part 3: The Diffusion and Thermal Diffusion Coefficients for Isotopic Gases and Gas Mixtures," by E. R. S. Winter, Trans. Faraday Society, vol. 46, Part 2, 1950, pp. 81–92.

44 "Transport Properties of Polyatomic Gases," by C. S. Wang-Chang and G. E. Uhlenbeck, University of Michigan, CM-681, Project NOrd 7924, 1951.

45 "Viscositeit en Warmtegeleiding van Roterende Moleculen," by J. de Boer; manuscript loaned to one of the authors.

46 "Transport Properties of Gases Obeying a Modified Buckingham (6-exp) Potential," by E. A. Mason, *Journal of Chemical Physics*, vol. 22, 1954, pp. 169–186.

47 "Molecular Transport Properties of Fluids," by E. F. Johnson, *Industrial and Engineering Chemistry*, vol. 45, 1953, pp. 902–906.

48 "Fluid Dynamics," by T. Baron and A. K. Oppenheim, *Industrial and Engineering Chemistry*, vol. 45, 1953, pp. 941–951.

49 "Heat Transfer," by E. R. G. Eckert, *Industrial and Engineering Chemistry*, vol. 45, 1953, pp. 951–956.

50 "Mass Transfer," by R. L. Pigford, *Industrial and Engineering Chemistry*, vol. 45, 1953, pp. 956–962.

51 "The Theory of Rate Processes," by S. Glasstone, K. J. Laidler, and H. Eyring, McGraw-Hill Book Co., Inc., New York, N. Y., 1941. chapter 9: "Viscosity and Diffusion," pp. 477–551.

52 "Diffusion, Thermal Conductivity and Viscous Flow in Liquids," by R. E. Powell, W. E. Roseveare, and H. Eyring, *Industrial and Engineering Chemistry*, vol. 33, 1941, pp. 430–435.

53 "The Theory of Absolute Reaction Rates and Its Application to Viscosity and Diffusion in the Liquid State," by J. F. Kincaid, H. Eyring, and A. E. Stearn, *Chemical Reviews*, vol. 28, 1941, pp. 301–366.

54 "The Thermal Conductivity of Liquids Under Pressure," by P. W. Bridgman, Proceedings of the American Academy of Arts and Sciences, vol. 59, 1923, pp. 139–169.

55 "Kinetische Theorie der Wärmeleitung, Reibung und Selbstdiffusion in Gewissen Verdichteten Gasen und Flüssigkeiten," by D. Enskog, Kungliga Svenska Vetenskapsakademiens Handlingar, vol. 63, 1922; see also chapter 16 of ref. 34.

56 "A General Kinetic Theory of Liquids," by M. Born and H. S. Green, Cambridge University Press, Cambridge, England, 1949.

57 "The Kinetic Theory of Dense Gases," by C. F. Curtiss, University of Wisconsin Report OOR-3, January 28, 1953, Madison, Wis.

58 "Quantum Theory of Condensed Permanent Gases:"

(*a*) "The Law of Corresponding States," by J. de Boer, *Physica*, vol. 14, no. 2–3, 1948, pp. 139–148.

(*b*) "The Solid State and the Melting Line," by J. de Boer and B. S. Blaisse, *Physica*, vol. 14 no. 2–3, 1948, pp. 149–164.

(*c*) "The Equation of State of Liquids," by J. de Boer and R. J. Lunbeck, *Physica*, vol. 14, no. 8, 1948, pp. 520–529.

59 "The Properties of the Condensed Phase of the Light Helium Isotope," by J. de Boer and R. J. Lunbeck, *Physica*, vol. 14, no. 8, 1948, pp. 510–519.

60 "Het Principe van Overeenstemmende Toestanden in de Quantummechanica," Doctoral Dissertation by R. J. Lunbeck, University of Amsterdam, 1950 (in Dutch).

61 "Toestandsvergelijking en Intermoleculaire Krachten," by J. de Boer, Nederlands Tijdschrift voor Natuurkunde, vol. 19, no. 10, 1953, pp. 231–250.

62 "Separation of Organic Liquid Mixtures by Thermal Diffu-

sion," by A. L. Jones and E. C. Milberger, *Industrial and Engineering Chemistry*, vol. 45, no. 12, 1953, pp. 2689–2696.

63 "A Literature Survey of the Thermal Conductivity of Liquids," by B. C. Sakiadis and J. Coates, Engineering Experiment Station Bulletin No. 34, Louisiana State University and Agricultural and Mechanical College, Baton Rouge, La.

64 "Wärmeleiting in hochverdichteten Gasen," by E. U. Franck, *Chemie Ingenieur Technik*, vol. 25, no. 5, 1953, pp. 238–248.

Discussion

H. G. Drickamer.[16] The authors have done a remarkable job of condensation and organization in presenting a reasonably complete summary of a very broad and very important field. It would appear that the next development to be hoped for in the field of nonequilibrium processes is a perturbation treatment for moderately dense gases somewhat analogous to virial treatment for the thermodynamic properties. It is to be hoped that such a treatment will include diffusion and thermal diffusion as soon as possible. Viscosity is hardly sensitive enough to provide an adequate test of the theory, as even Enskog's dense-gas theory predicts the viscosity of nitrogen accurately to 1000 atm, while the thermal conductivity of other than monatomic gases offers many theoretical problems even at low pressure.

The authors mention the lack of accurate experimental data, and it is true that there is an appalling scarcity of such information. On the other hand, the experiments, even at the present level of accuracy, are difficult, and the problems in increasing the accuracy are formidable. It seems that in the presently available data on diffusion and thermal diffusion in moderately dense gases, there is a sufficient initial test of any new theory. If the theoretical groups could develop a reasonably sophisticated theory or theories, such that a particular set of experiments would be definitive, there would be an incentive for further, more accurate experimental work in the field.

W. E. Ranz.[17] An engineer willing to plow his way through this formidable review paper will be rewarded by finding among the bewildering array of symbols several good recipes for estimating physical properties. At the same time he will be brought up to date on the state of applied statistical mechanics, an abstract subject which, to the surprise of some of us, now appears useful for attacking engineering problems other than those involving thermodynamics.

Here elaborate and elegant analysis has been reduced to useful approximations. In some respects, it is the most desirable engineering approach. We are able to use the best of much information instead of making much out of nearly nothing. It is regrettable that the authors have not been able to carry the process to a logical conclusion. Instead of statements of "extremely good agreement," "reasonable good agreement," and "good agreement," actual odds on the expected accuracy of each equation would have pin-pointed its significance. Certainly the relative merit of this approach over more empirical methods, e.g., corresponding states, should be investigated. Perhaps the task of evaluation is properly the duty of engineers who have need of these equations.

Of considerable novelty are the combining laws suggested for mixtures. One is led to inquire whether this method of averaging intermolecular force constants yields any better results than volume and mass averages, or such empirical sorcery as corresponding states based on a pseudocritical point.

Although it is not stated in so many words, this paper contains an implied warning to practical scientists and engineers that a theoretician may be able to calculate physical properties more accurately than our defective experimental methods can measure them. The pleas for more and better experimental measurements of properties such as the diffusion coefficient should not go unheeded.

Here we have an excellent example of the co-operation of pure scientists and engineers. The authors are to be commended for reducing their work to useful form.

[16] University of Illinois, Urbana, Ill.

[17] Associate Professor of Engineering Research, Pennsylvania State Univ., State College, Pa.

Authors' Closure

In answer to Professor Ranz's question, the best way to present an assessment of these theoretical formulas is to give extensive tables comparing calculated values with experimental quantities for a large number of substances over wide ranges of temperature, pressure, and composition. Such comparisons are given in MTGL, and more detailed discussions can be found in the original references:

	References
Virial coefficients for nonpolar gases	18, 20
Virial coefficients for polar gases	Ref. a, Table 4(b)
Compressibility of dense gases	22
Transport coefficients of dilute	1, 40, 43
Transport coefficients of dense gases	55
Transport coefficients of liquids	51, 52
Quantum effects in physical properties	58, 60

In studying the comparisons between experimental and theoretical results, several important factors should be kept in mind: All of the calculations just discussed (with the exception of virial coefficients) are based on theories which assume that the intermolecular potential-energy functions are spherically symmetrical. A further restriction is in the choice of the Lennard-Jones (6–12) potential to represent this spherically symmetric interaction. In spite of this the pressure, temperature, and composition dependence of many properties can be predicted quite satisfactorily when the foregoing tables and formulas are used. At the present time there is a great deal of research under way designed to improve our knowledge of intermolecular forces and to extend the statistical mechanical theories.

The Tabulation of Imperfect-Gas Properties for Air, Nitrogen, and Oxygen

By NEWMAN A. HALL[1] AND WARREN E. IBELE,[2] MINNEAPOLIS, MINN.

Recent theoretical developments of intermolecular forces have established a basis upon which a valid extension of gas-property data may be prepared. This paper establishes the fact that deviation from perfect-gas behavior may be expressed fundamentally by the compressibility factor. Tables of virial coefficients and temperature derivatives for air, nitrogen, and oxygen are given, as well as tables of compressibility factors for these three gases.

Nomenclature

The following nomenclature is used in the paper:

B = second virial coefficient, $ft^3\,lb^{-1}$
B' = first temperature derivative, second virial coefficient, $ft^3\,lb^{-1}\,deg\,F^{-1}$
B'' = second temperature derivative, second virial coefficient, $ft^3\,lb^{-1}\,deg\,F^{-2}$
C = third virial coefficient, $(ft^3\,lb^{-1})^2$
C' = first temperature derivative, third virial coefficient, $(ft^3\,lb^{-1})^2\,deg\,F^{-1}$
C'' = second temperature derivative, third virial coefficient, $(ft^3\,lb^{-1})^2\,deg\,F^{-2}$
C_v^0 = constant-volume heat capacity at zero pressure, Btu $lb^{-1}\,deg\,F^{-1}$
C_v = constant-volume heat capacity, Btu $lb^{-1}\,deg\,F^{-1}$
C_p^0 = constant-pressure heat capacity at zero pressure, Btu $lb^{-1}\,deg\,F^{-1}$
C_p = constant-pressure heat capacity Btu $lb^{-1}\,deg\,F^{-1}$
h = enthalpy, Btu lb^{-1}
p = pressure, atm
$°R$ = gas constant, Btu $lb^{-1}\,deg\,R^{-1}$ or $ft^3\,atm\,lb^{-1}\,deg\,R^{-1}$
S = entropy, Btu $lb^{-1}\,deg\,R^{-1}$
S^* = entropy of ideal gas at pressures of 1 atm, Btu $lb^{-1}\,deg\,R^{-1}$
T = temperature deg F, absolute
V = volume $ft^3\,lb^{-1}$
Z = compressibility factor
ρ = density, lb ft^{-3}

Introduction

Problems in design involving the use of any gas as a working medium require accurate data for the thermodynamic properties of the gas. One of the continuing tasks of thermodynamic investigations is the extension of such data to greater ranges of temperature and pressure. This develops progressively by the gradual accumulation of experimental measurements of high accuracy and consistency and in due course sufficiently significant theoretical means become available to correlate these data to provide charts or tabulations of comparable accuracy.

In general, such tabulations may provide extrapolations to properties not directly measured and within limits to pressure and temperature domains not originally bracketed. Much progress has been made in this area and it has been possible for some time to extend, in many respects, beyond the perfect-gas domain, the region where systematic presentation of thermodynamic properties is possible. The availability of such empirical equations as the Beattie-Bridgman and the Benedict-Webb-Rubin has taken care of many requirements regarding the more common gases. For air, oxygen, and nitrogen the first of these has provided the basis for the tabulations and charts of Williams (1)[3] and Curtiss and Hirschfelder (2). In addition, a direct independent empirical correlation was used by Claitor and Crawford (3) to prepare accurate charts for these gases.

Each of these contributions has been dependent on an empirical correlation which was associated directly with the experimental data. Aside from the trivial fact that the perfect-gas domain is approached at sufficiently low pressures or densities, no physical characteristic of the imperfect gas was involved in establishing the empirical equation. This makes any valid extension of the properties beyond the narrow confines of experimental data essentially fortuitous and not dependable.

Basis for Extension of Gas-Property Data

Recent theoretical developments in regard to intermolecular forces have established a basis by which a more fundamentally valid extension of gas-property data may be prepared. These intermolecular forces modify the perfectly elastic impacts of a simple kinetic theory gas model and thereby produce deviations from perfect-gas behavior. As the molecules of a gas are pushed closer together at higher densities the effect of the molecular interaction increases. Consequently, the deviation from perfect-gas behavior is expressed fundamentally by the compressibility factor

$$Z = \frac{p}{RT\rho} \qquad [1]$$

expressed as a power series in the density

$$Z = 1 + B\rho + C\rho^2 + D\rho^3 + \ldots \qquad [2]$$

The second, third, and fourth virial coefficients B, C, D, and so on, are temperature functions, dependent primarily on interactions of groups of two, three, and four molecules, respectively.

The interaction between molecules can be represented by a potential from which the force or any effect due to the force may be derived. This intermolecular potential has the general form shown in Fig. 1 where the potential energy E is given as a function of the radial distance r. For small r the slope of the potential curve is large and negative corresponding to the repulsion due to molecular interference. At larger distances the potential curve slope becomes positive, indicating a small attraction between the molecules. At still larger distances this attractive force becomes negligible. An approximate formulation of the potential has been given by Lennard-Jones (4) in the form

$$E(r) = 4\epsilon\left[\left(\frac{r_0}{r}\right)^{12} - \left(\frac{r_0}{r}\right)^{6}\right] \qquad [3]$$

---

[1] Professor of Mechanical Engineering, Heat Power Division, University of Minnesota. Mem. ASME.

[2] Assistant Professor of Mechanical Engineering, Heat Power Division, University of Minnesota. Assoc. Mem. ASME.

Contributed by the Heat Transfer Division and presented at the Annual Meeting, New York, N. Y., November 29–December 4, 1953, of The American Society of Mechanical Engineers.

Note: Statements and opinions advanced in papers are to be understood as individual expressions of their authors and not those of the Society. Manuscript received at ASME Headquarters, May 4, 1953. Paper No. 53—A-5.

[3] Numbers in parentheses refer to the Bibliography at the end of the paper.

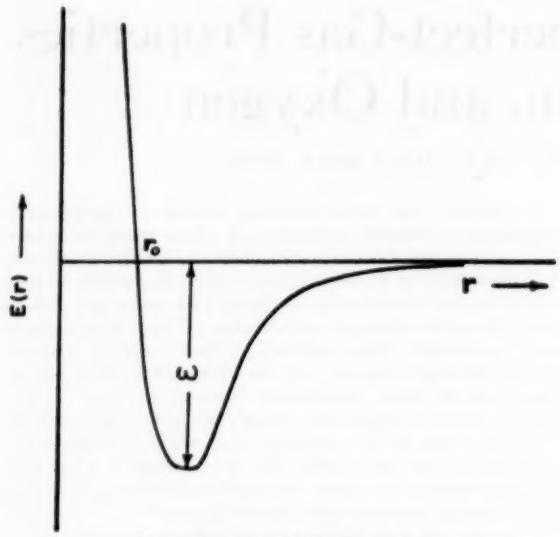

FIG. 1 LENNARD-JONES POTENTIAL

where

r_0 = low-energy-collision diameter, i.e., the distance at which low-energy molecular encounters occur, or essentially the molecular diameter; ϵ = minimum potential energy corresponding to state of equilibrium between attractive and repulsive forces.

This formulation contains the essential elements of the physical interactions and is justified by more refined physical theories as well as being confirmed by experimental data (5, 6, 7, 8, 9).

The virial coefficients may be expressed as integrals of the interaction potential and have been evaluated recently together with temperature derivatives by Bird and Spotz (10). This potential assumes a spherical, nonpolar molecule, conditions which are closely satisfied by oxygen and nitrogen. Accordingly, the tabulation of Bird and Spotz may be used to obtain specific properties for these gases as well as for air as a mixture.

For a two-component mixture the virial coefficients are given according to Mayer (11) by

$$\left.\begin{aligned} B_{\text{mixture}} &= B_1X_1^2 + 2B_{12}X_1X_2 + B_2X_2^2 \\ &= B_1X_1 + B_2X_2 - 2\beta_{12}X_1X_2 \end{aligned}\right\} \quad \ldots\ldots [4]$$

$$\left.\begin{aligned} C_{\text{mixture}} &= C_1X_1^3 + 3C_{112}X_1^2X_2 + 3C_{122}X_1X_2^2 + C_2X_2^3 \\ &= C_1X_1 + C_2X_2 - 3\,\gamma_{112}X_1^2X_2 - 3\,\gamma_{122}\,X_1X_2^2 \end{aligned}\right\} \quad \ldots [5]$$

where X_1 and X_2 are the mol fractions for the two components, and B_1, B_2, and C_1, C_2 are their respective virial coefficients. B_{12} and C_{112} and C_{122} are interaction coefficients corresponding to groups of two and three unlike molecules and

$$\beta_{12} = \frac{1}{2}(B_1 + B_2) - B_{12} \quad \ldots\ldots [6]$$

$$\gamma_{112} = \frac{1}{3}(2C_1 + C_2) - C_{112} \quad \ldots\ldots [7]$$

$$\gamma_{122} = \frac{1}{3}(C_1 + 2C_2) - C_{122} \quad \ldots\ldots [8]$$

The interaction coefficients are computed in a manner similar to the virial coefficients from an interaction potential. The Lennard-Jones form may be used with the characteristic constants computed by the rule according to Hirschfelder, et al. (8)

$$r_{0_{12}} = \frac{1}{2}\left[r_{0_1} + r_{0_2}\right] \quad \ldots\ldots [9]$$

$$\epsilon_{12} = \sqrt{\epsilon_1\epsilon_2} \quad \ldots\ldots [10]$$

The calculations of Bird and Spotz (10) are reported in the form

$$B(T) = b_0\,B^{(0)}(\tau) \quad \ldots\ldots [11]$$

$$B^{(1)}(\tau) = \tau\,\frac{dB^{(0)}}{d\tau} \quad \ldots\ldots [12]$$

$$B^{(2)}(\tau) = \tau^2\,\frac{d^2B^{(0)}}{d\tau^2} \quad \ldots\ldots [13]$$

$$C(T) = b_0^2\,C^{(0)}(\tau) \quad \ldots\ldots [14]$$

$$C^{(1)}(\tau) = \tau\,\frac{dC^{(0)}}{d\tau} \quad \ldots\ldots [15]$$

$$C^{(2)}(\tau) = \tau^2\,\frac{d^2C^{(0)}}{d\tau^2} \quad \ldots\ldots [16]$$

where

$$b_0 = \frac{2}{3}\pi\,Nr_0^3, \quad \tau = kT/\epsilon$$

$N = 6.0235 \times 10^{23}$ Avogadro's number, number of molecules per gram mole

$k = 1.38032 \times 10^{-16}$ Boltzmann's constannt, ergs per deg K

The first of these relations provides the primary means of determining the molecular constants r_0 and ϵ. Writing

$$b_0 = B(T)_{\text{exp}}/B^{(0)}(\tau) \quad \ldots\ldots [17]$$

a series of values of b_0 can be computed from available data on the second virial coefficient and for selected choices of ϵ. A certain value of ϵ will give the minimum deviation from a constant value of b_0 for varying T. This optimum value determined ϵ and b_0 as follows:

Gas	ϵ/k (deg K)	b_0 (cc/mol)
Nitrogen	95.36	64.13
Oxygen	117.04	54.35

A similar determination of b_0 from empirically determined quantities other than the second virial coefficient confirms these results closely. The correlation with experimental data is reported in full in reference (12).

COMPOSITION OF AIR

Air as a mixture has been defined by the Aerological Commission of the International Meteorological Organization (13) as having the following composition:

	Mol fraction, per cent	Mol weight
Nitrogen	78.09	28.016
Oxygen	20.95	32.000
Argon	0.93	39.944
Carbon dioxide	0.03	44.010

with a resulting apparent molecular weight of 28.966.

Considering the interaction of the several types of molecules, it appears that interaction terms β and γ are either essentially zero owing to similarities in the molecules or provide a negligible contribution in view of the small amount present (12). Accordingly, in computing the virial coefficients for air it was assumed that only oxygen and nitrogen were present, distributed in proportion to their actual occurrence. Thus

$$B_{\text{air}} = (X'B)_{N_2} + (X'B)_{O_2} \quad \ldots\ldots [18]$$

$$C_{\text{air}} = (X'C)_{N_2} + (X'C)_{O_2} \quad \ldots\ldots [19]$$

TABLE 1 AIR-VIRIAL COEFFICIENTS AND TEMPERATURE DERIVATIVES

T °R	B	$T\frac{dB}{dT}$	$T^2\frac{d^2B}{dT^2}$	$C\,10^3$	$T\frac{dC}{dT}10^3$	$T^2\frac{d^2C}{dT^2}10^3$
100	-0.2446	0.4574	-1.464			
105	-0.2235	0.4106	-1.296			
110	-0.2054	0.3721	-1.150			
115	-0.1895	0.3395	-1.029			
120	-0.1757	0.3114	-0.9275			
125	-0.1635	0.2880	-0.8438			
130	-0.1526	0.2670	-0.7713			
140	-0.1338	0.2330	-0.6548			
150	-0.1190	0.2061	-0.5661	-0.5610	10.928	-86.4
160	-0.1064	0.1843	-0.4966	-0.0142	6.640	-56.6
170	-0.09581	0.1665	-0.4413	+0.3083	4.142	-37.6
180	-0.08669	0.1518	-0.3956	0.4964	2.550	-25.7
190	-0.07884	0.1393	-0.3585	0.6100	1.5124	-17.7
200	-0.07196	0.1285	-0.3271	0.6636	0.8268	-12.2
210	-0.06598	0.1193	-0.3003	0.6919	0.5914	- 8.51
220	-0.06055	0.1112	-0.2774	0.7017	0.06462	- 5.86
230	-0.05577	0.1041	-0.2576	0.6996	- 0.1383	- 4.03
240	-0.05150	0.09787	-0.2401	0.6908	- 0.2716	- 2.71
260	-0.04407	0.08736	-0.2112	0.6627	- 0.4106	- 0.622
280	-0.03795	0.07857	-0.1883	0.6303	- 0.4536	+ 0.241
300	-0.03279	0.07140	-0.1696	0.5989	- 0.4516	0.680
320	-0.02837	0.06534	-0.1542	0.5705	- 0.4282	0.891
340	-0.02457	0.06011	-0.1413	0.5474	- 0.3944	0.977
360	-0.02126	0.05580	-0.1298	0.5238	- 0.3610	0.985
380	-0.01835	0.05195	-0.1207	0.5052	- 0.3272	0.959
400	-0.01576	0.04852	-0.1124	0.4892	- 0.2950	0.909
420	-0.01347	0.04553	-0.1051	0.4756	- 0.2658	0.850
440	-0.01142	0.04286	-0.09870	0.4637	- 0.2394	0.784
460	-0.009567	0.04044	-0.09298	0.4537	- 0.2158	0.724
480	-0.007896	0.03826	-0.08787	0.4450	- 0.1950	0.664
500	-0.006370	0.03629	-0.08325	0.4373	- 0.1766	0.608
550	-0.003118	0.03199	-0.07354	0.4225	- 0.1396	0.484
600	-0.0004780	0.02867	-0.06574	0.4114	- 0.1129	0.385
650	+0.001704	0.02583	-0.05936	0.4033	- 0.09308	0.311
700	0.003528	0.02348	-0.05405	0.3970	- 0.07904	0.249
750	0.005077	0.02145	-0.04943	0.3918	- 0.06900	0.200
800	0.006405	0.01970	-0.04573	0.3877	- 0.06144	0.162
850	0.007565	0.01816	-0.04237	0.3840	- 0.05602	0.131
900	0.008570	0.01680	-0.03939	0.3810	- 0.05238	0.105
950	0.009459	0.01556	-0.03679	0.3780	- 0.04998	0.0858
1000	0.01025	0.01454	-0.03454	0.3765	- 0.04860	0.0708
1100	0.01150	0.01279	-0.03076	0.3710	- 0.04774	0.0488
1200	0.01255	0.01130	-0.02758	0.3669	- 0.04824	0.0360
1300	0.01341	0.01005	-0.02493	0.3630	- 0.04952	0.0284
1400	0.01411	0.008995	-0.02270	0.3594	- 0.05124	0.0249
1500	0.01470	0.008085	-0.02077	0.3556	- 0.05324	0.0234
1600	0.01520	0.007296	-0.01910	0.3522	- 0.05536	0.0230
1700	0.01562	0.006601	-0.01765	0.3488	- 0.05728	0.0239
1800	0.01598	0.005989	-0.01637	0.3455	- 0.05904	0.0255
1900	0.01629	0.005444	-0.01523	0.3421	- 0.06100	0.0272
2000	0.01656	0.004956	-0.01420	0.3390	- 0.06280	0.0293
2200	0.01699	0.004118	-0.01245	0.3328	- 0.06600	0.0339
2400	0.01730	0.003430	-0.01100	0.3271	- 0.06864	0.0386
2600	0.01757	0.002847	-0.009788	0.3214	- 0.07098	0.0433
2800	0.01776	0.002354	-0.008749	0.3160	- 0.07280	0.0477
3000	0.01789	0.001945	-0.007902	0.3110	- 0.07470	0.0518
3200	0.01802	0.001559	-0.007086	0.3061	- 0.07616	0.0556
3400	0.01810	0.001234	-0.006405	0.3014	- 0.07718	0.0591
3600	0.01814	0.0009486	-0.005803	0.2970	- 0.07848	0.0612
3800	0.01816	0.0006935	-0.005263	0.2927	- 0.07904	0.0642
4000	0.01817	0.0004656	-0.004779	0.2886	- 0.07960	0.0669
4200	0.01819	0.0002611	-0.004346	0.2847	- 0.08022	0.0693
4400	0.01819	0.00007537	-0.003949	0.2811	- 0.08052	0.0712
4600	0.01820	-0.00008975	-0.003595	0.2776	- 0.08096	0.0736
4800	0.01821	-0.0002453	-0.003262	0.2740	- 0.08112	0.0751
5000	0.01822	-0.0003842	-0.002962	0.2706	- 0.08150	0.0768

TABLE 2 NITROGEN-VIRIAL COEFFIGIENTS AND TEMPERATURE DERIVATIVES

T °R	B	$T\frac{dB}{dT}$	$T^2\frac{d^2B}{dT^2}$	C 10^3	$T\frac{dC}{dT}10^3$	$T^2\frac{d^2C}{dT^2}10^3$
100	-0.2396	0.4393	-1.382			
105	-0.2194	0.3960	-1.219			
110	-0.2019	0.3601	-1.087			
115	-0.1865	0.3296	-0.9768			
120	-0.1731	0.3030	-0.8833	-4.539	38.56	-295.3
125	-0.1612	0.2810	-0.8067	-3.206	29.64	-228.1
130	-0.1505	0.2612	-0.7399	-2.179	22.70	-177.4
140	-0.1321	0.2288	-0.6317	-0.8618	13.63	-109.4
150	-0.1176	0.2030	-0.5486	-0.1166	8.304	- 69.75
160	-0.1052	0.1821	-0.4833	+0.3074	5.072	- 45.57
170	-0.09467	0.1649	-0.4309	+0.5492	3.050	- 30.34
180	-0.08562	0.1506	-0.3872	0.6846	1.760	- 20.41
190	-0.07784	0.1384	-0.3520	0.7627	0.9285	- 13.97
200	-0.07099	0.1279	-0.3219	0.7887	0.3862	- 9.480
210	-0.06505	0.1189	-0.2962	0.7982	0.3146	- 6.439
220	-0.05962	0.1109	-0.2741	0.7941	- 0.1999	- 4.303
230	-0.05485	0.1040	-0.2549	0.7814	- 0.3480	- 2.809
240	-0.05060	0.09782	-0.2380	0.7646	- 0.4397	- 1.745
260	-0.04316	0.08731	-0.2099	0.7255	- 0.5221	0.05300
280	-0.03703	0.07876	-0.1875	0.6862	- 0.5306	0.7017
300	-0.03184	0.07164	-0.1692	0.6503	- 0.5061	1.008
320	-0.02742	0.06563	-0.1540	0.6189	- 0.4675	1.128
340	-0.02359	0.06035	-0.1413	0.5917	- 0.4230	1.154
360	-0.02026	0.05609	-0.1300	0.5687	- 0.3827	1.117
380	-0.01734	0.05225	-0.1209	0.5491	- 0.3435	1.060
400	-0.01474	0.04884	-0.1127	0.5323	- 0.3076	0.9872
420	-0.01243	0.04582	-0.1055	0.5182	- 0.2755	0.9102
440	-0.01036	0.04316	-0.09914	0.5059	- 0.2471	0.8325
460	-0.008499	0.04074	-0.09346	0.4956	- 0.2220	0.7618
480	-0.006816	0.03853	-0.08836	0.4866	- 0.1999	0.6935
500	-0.005280	0.03656	-0.08378	0.4788	- 0.1806	0.6300
550	-0.001881	0.03233	-0.07405	0.4637	- 0.1423	0.4961
600	+0.0006571	0.02890	-0.06624	0.4524	- 0.1152	0.3924
650	0.002856	0.02604	-0.05983	0.4441	- 0.09490	0.3135
700	0.004693	0.02365	-0.05454	0.4376	- 0.08120	0.2499
750	0.006254	0.02161	-0.04986	0.4322	- 0.01719	0.1991
800	0.007590	0.01984	-0.04616	0.4280	- 0.06416	0.1600
850	0.008748	0.01829	-0.04282	0.4242	- 0.05899	0.1279
900	0.009750	0.01693	-0.03982	0.4210	- 0.05562	0.1012
950	0.01063	0.01568	-0.03724	0.4179	- 0.05368	0.08213
1000	0.01142	0.01466	-0.03500	0.4153	- 0.05260	0.06750
1100	0.01272	0.01284	-0.03106	0.4102	- 0.05247	0.04671
1200	0.01377	0.01132	-0.02784	0.4056	- 0.05364	0.03485
1300	0.01463	0.01006	-0.02515	0.4013	- 0.05538	0.02822
1400	0.01533	0.008987	-0.02289	0.3972	- 0.05754	0.02568
1500	0.01592	0.008062	-0.02094	0.3930	- 0.05985	0.02475
1600	0.01642	0.007261	-0.01926	0.3891	- 0.06224	0.02514
1700	0.01683	0.006555	-0.01778	0.3853	- 0.06460	0.02662
1800	0.01719	0.005933	-0.01648	0.3816	- 0.06660	0.02877
1900	0.01750	0.005379	-0.01532	0.3778	- 0.06878	0.03105
2000	0.01776	0.004884	-0.01428	0.3743	- 0.07080	0.03360
2200	0.01819	0.004033	-0.01250	0.3673	- 0.07414	0.03901
2400	0.01850	0.003331	-0.01103	0.3609	- 0.07728	0.04452
2600	0.01875	0.002740	-0.009795	0.3545	- 0.07982	0.04975
2800	0.01893	0.002239	-0.008742	0.3485	- 0.08176	0.05472
3000	0.01905	0.001828	-0.007887	0.3428	- 0.08370	0.05931
3200	0.01918	0.001431	-0.007047	0.3373	- 0.08512	0.06349
3400	0.01925	0.001102	-0.006354	0.3321	- 0.08636	0.06728
3600	0.01927	0.0008107	-0.005742	0.3272	- 0.08748	0.06934
3800	0.01924	0.0005518	-0.005193	0.3224	- 0.08816	0.07278
4000	0.01928	0.0003204	-0.004701	0.3178	- 0.08880	0.07568
4200	0.01929	0.0001126	-0.004260	0.3135	- 0.08946	0.07832
4400	0.01929	-0.00007568	-0.003856	0.3094	- 0.08976	0.08073
4600	0.01930	-0.0002430	-0.003498	0.3056	- 0.09016	0.08316
4800	0.01931	-0.0004011	-0.003159	0.3016	- 0.09024	0.08479
5000	0.01932	-0.0005415	-0.002852	0.2978	- 0.09050	0.08650

TABLE 3 OXYGEN-VIRIAL COEFFICIENTS AND TEMPERATURE DERIVATIVES

T °R	B	$T\frac{dB}{dT}$	$T^2\frac{d^2B}{dT^2}$	$C\,10^3$	$T\frac{dC}{dT}\,10^3$	$T^2\frac{d^2C}{dT^2}\,10^3$
100	-0.2628	0.5224	-1.760			
105	-0.2385	0.4636	-1.572			
110	-0.2181	0.4155	-1.377			
115	-0.2006	0.3755	-1.218			
120	-0.1853	0.3418	-1.087			
125	-0.1720	0.3131	-0.9767			
130	-0.1602	0.2883	-0.8842			
140	-0.1403	0.2484	-0.7383			
150	-0.1243	0.2174	-0.6293	-2.148	30.31	-145.8
160	-0.1111	0.1928	-0.5453	-1.162	12.24	- 95.49
170	-0.1000	0.1726	-0.4792	-0.5511	8.053	- 64.16
180	-0.09062	0.1564	-0.4257	-0.1745	5.377	- 44.39
190	-0.08254	0.1426	-0.3823	+0.06565	3.599	- 31.15
200	-0.07552	0.1309	-0.3461	0.2178	2.400	- 22.20
210	-0.06940	0.1210	-0.3156	0.3135	1.580	- 15.96
220	-0.06398	0.1123	-0.2895	0.3730	1.009	- 11.52
230	-0.05915	0.1048	-0.2675	0.4084	0.6097	- 8.411
240	-0.05479	0.09814	-0.2480	0.4283	0.3278	- 6.163
260	-0.04739	0.08767	-0.2163	0.4395	- 0.01273	- 3.035
280	-0.04130	0.07801	-0.1914	0.4317	- 0.1802	- 1.403
300	-0.03621	0.07071	-0.1715	0.4164	- 0.2575	- 0.4869
320	-0.03180	0.06448	-0.1549	0.3984	- 0.2883	+ 0.05161
340	-0.02810	0.05930	-0.1414	0.3809	- 0.2930	0.3491
360	-0.02484	0.05483	-0.1297	0.3643	- 0.2844	0.5158
380	-0.02198	0.05092	-0.1199	0.3494	- 0.2689	0.5993
400	-0.01942	0.04748	-0.1112	0.3359	- 0.2504	0.6320
420	-0.01721	0.04448	-0.1038	0.3240	- 0.2313	0.6350
440	-0.01520	0.04184	-0.09722	0.3139	- 0.2123	0.6156
460	-0.01339	0.03945	-0.09141	0.3049	- 0.1944	0.5925
480	-0.01176	0.03732	-0.08622	0.2970	- 0.1778	0.5622
500	-0.01027	0.03537	-0.08155	0.2900	- 0.1624	0.5275
550	-0.007102	0.03082	-0.07178	0.2761	- 0.1301	0.4416
600	-0.004530	0.02791	-0.06397	0.2659	- 0.1050	0.3672
650	-0.002407	0.02517	-0.05767	0.2583	- 0.08600	0.3017
700	-0.0006263	0.02288	-0.05243	0.2525	- 0.07140	0.2479
750	+0.0008843	0.02092	-0.04800	0.2479	- 0.06045	0.2053
800	0.002185	0.01924	-0.04424	0.2443	- 0.05200	0.1709
850	0.003354	0.01771	-0.04084	0.2411	- 0.04556	0.1423
900	0.004372	0.01638	-0.03790	0.2386	- 0.04095	0.1183
950	0.005290	0.01517	-0.03524	0.2364	- 0.03714	0.09928
1000	0.006072	0.01413	-0.03297	0.2345	- 0.03450	0.08290
1100	0.007182	0.01265	-0.02974	0.2318	- 0.03069	0.05651
1200	0.008227	0.01122	-0.02667	0.2292	- 0.02904	0.04046
1300	0.009073	0.01004	-0.02415	0.2269	- 0.02886	0.02941
1400	0.009783	0.009036	-0.02199	0.2248	- 0.02912	0.02254
1500	0.01037	0.008178	-0.02018	0.2228	- 0.02970	0.01814
1600	0.01088	0.007430	-0.01859	0.2208	- 0.03056	0.01554
1700	0.01131	0.006774	-0.01721	0.2189	- 0.03145	0.01442
1800	0.01168	0.006197	-0.01599	0.2171	- 0.03240	0.01377
1900	0.01200	0.005683	-0.01491	0.2153	- 0.03340	0.01361
2000	0.01228	0.005220	-0.01394	0.2136	- 0.03460	0.01408
2200	0.01274	0.004435	-0.01229	0.2102	- 0.03674	0.01578
2400	0.01303	0.003782	-0.01092	0.2069	- 0.03840	0.01786
2600	0.01337	0.003234	-0.009782	0.2038	- 0.04004	0.02021
2800	0.01360	0.002767	-0.008804	0.2007	- 0.04144	0.02274
3000	0.01377	0.002367	-0.007966	0.1978	- 0.04290	0.02352
3200	0.01392	0.002018	-0.007237	0.1950	- 0.04384	0.02754
3400	0.01403	0.001711	-0.006595	0.1923	- 0.04488	0.02971
3600	0.01412	0.001442	-0.006026	0.1897	- 0.04572	0.03188
3800	0.01419	0.001200	-0.005523	0.1873	- 0.04636	0.03379
4000	0.01425	0.0009848	-0.005069	0.1848	- 0.04720	0.03552
4200	0.01429	0.0007917	-0.004660	0.1825	- 0.04746	0.03722
4400	0.01430	0.0006147	-0.004288	0.1803	- 0.04796	0.03794
4600	0.01430	0.0004570	-0.003950	0.1782	- 0.04830	0.03957
4800	0.01430	0.0003102	-0.003643	0.1761	- 0.04848	0.04101
5000	0.01431	0.0001768	-0.003360	0.1741	- 0.04900	0.04225

TABLE 4 AIR COMPRESSIBILITY FACTOR $Z = 1 + B\rho + C\rho^2$

T °R	ρ=0.0200	ρ=0.0600	ρ=0.1000	ρ=0.1400	ρ=0.1800	ρ=0.2200	ρ=0.2600	ρ=0.3000	ρ=0.4000
100									
105									
110	0.9959								
115	0.9962								
120	0.9965	0.9894							
125	0.9967	0.9902							
130	0.9969	0.9908	0.9847						
140	0.9973	0.9920	0.9866	0.9813	0.9759	0.9706	0.9652		
150	0.9976	0.9929	0.9881	0.9833	0.9786	0.9738	0.9690	0.9642	0.9523
160	0.9979	0.9936	0.9894	0.9851	0.9808	0.9766	0.9723	0.9681	0.9574
170	0.9981	0.9942	0.9904	0.9866	0.9828	0.9789	0.9751	0.9713	0.9617
180	0.9983	0.9948	0.9913	0.9879	0.9844	0.9810	0.9775	0.9740	0.9654
190	0.9984	0.9953	0.9921	0.9890	0.9858	0.9827	0.9795	0.9764	0.9686
200	0.9986	0.9957	0.9928	0.9899	0.9871	0.9842	0.9813	0.9785	0.9713
210	0.9987	0.9960	0.9934	0.9908	0.9881	0.9855	0.9829	0.9803	0.9737
220	0.9988	0.9964	0.9940	0.9915	0.9891	0.9867	0.9843	0.9819	0.9759
230	0.9989	0.9966	0.9944	0.9922	0.9900	0.9878	0.9855	0.9833	0.9778
240	0.9990	0.9969	0.9948	0.9928	0.9908	0.9887	0.9866	0.9846	0.9795
260	0.9991	0.9974	0.9956	0.9938	0.9921	0.9903	0.9886	0.9868	0.9825
280	0.9992	0.9977	0.9962	0.9947	0.9932	0.9917	0.9902	0.9887	0.9849
300	0.9993	0.9980	0.9967	0.9954	0.9941	0.9928	0.9915	0.9902	0.9870
320	0.9994	0.9983	0.9972	0.9960	0.9949	0.9938	0.9927	0.9915	0.9887
340	0.9995	0.9985	0.9975	0.9966	0.9956	0.9946	0.9936	0.9927	0.9902
360	0.9996	0.9987	0.9979	0.9970	0.9962	0.9953	0.9945	0.9937	0.9916
380	0.9996	0.9989	0.9982	0.9974	0.9967	0.9960	0.9953	0.9945	0.9927
400	0.9997	0.9990	0.9984	0.9978	0.9972	0.9966	0.9959	0.9953	0.9938
420	0.9997	0.9992	0.9986	0.9981	0.9976	0.9970	0.9965	0.9960	0.9947
440	0.9998	0.9993	0.9987	0.9984	0.9980	0.9975	0.9971	0.9966	0.9955
460	0.9998	0.9994	0.9990	0.9987	0.9983	0.9979	0.9975	0.9972	0.9962
480	0.9998	0.9995	0.9992	0.9989	0.9986	0.9983	0.9980	0.9977	0.9969
500	0.9999	0.9996	0.9994	0.9991	0.9989	0.9986	0.9984	0.9981	0.9975
550	0.9999	0.9998	0.9997	0.9996	0.9994	0.9993	0.9992	0.9991	0.9988
600	1.000	1.000	1.000	0.9999	0.9999	0.9999	0.9999	0.9999	0.999
650	1.000	1.000	1.000	1.000	1.000	1.000	1.000	1.000	1.001
700	1.000	1.000	1.000	1.000	1.001	1.001	1.001	1.001	1.001
750	1.000	1.000	1.000	1.001	1.001	1.001	1.001	1.002	1.002
800	1.000	1.000	1.001	1.001	1.001	1.001	1.002	1.002	1.003
850	1.000	1.000	1.001	1.001	1.001	1.002	1.002	1.002	1.003
900	1.000	1.001	1.001	1.001	1.002	1.002	1.002	1.003	1.004
950	1.000	1.000	1.001	1.001	1.002	1.002	1.002	1.003	1.004
1000	1.000	1.001	1.001	1.001	1.002	1.002	1.003	1.003	1.004
1100	1.000	1.001	1.001	1.002	1.002	1.002	1.003	1.003	1.005
1200	1.000	1.001	1.001	1.002	1.002	1.003	1.003	1.004	1.005
1300	1.000	1.001	1.001	1.002	1.002	1.003	1.004	1.004	1.005
1400	1.000	1.001	1.001	1.002	1.002	1.003	1.004	1.004	1.006
1500	1.000	1.001	1.001	1.002	1.003	1.003	1.004	1.004	1.006
1600	1.000	1.001	1.001	1.002	1.003	1.003	1.004	1.004	1.006
1700	1.000	1.001	1.001	1.003	1.003	1.003	1.004	1.005	1.006
1800	1.000	1.001	1.002	1.002	1.003	1.004	1.004	1.005	1.006
1900	1.000	1.001	1.002	1.002	1.003	1.004	1.004	1.005	1.006
2000	1.000	1.001	1.002	1.002	1.003	1.004	1.004	1.005	1.007
2200	1.000	1.001	1.002	1.002	1.003	1.004	1.004	1.005	1.007
2400	1.000	1.001	1.002	1.002	1.003	1.004	1.004	1.005	1.007
2600	1.000	1.001	1.002	1.002	1.003	1.004	1.004	1.005	1.007
2800	1.000	1.001	1.002	1.002	1.003	1.004	1.005	1.005	1.007
3000	1.000	1.001	1.002	1.002	1.003	1.004	1.005	1.005	1.007
3200	1.000	1.001	1.002	1.002	1.003	1.004	1.005	1.005	1.007
3400	1.000	1.001	1.002	1.002	1.003	1.004	1.005	1.005	1.007
3600	1.0004	1.0011	1.0018	1.0025	1.0033	1.0040	1.0047	1.0055	1.0073
3800	1.000	1.001	1.002	1.002	1.003	1.004	1.005	1.005	1.007
4000	1.000	1.001	1.002	1.002	1.003	1.004	1.005	1.005	1.007
4200	1.000	1.001	1.002	1.002	1.003	1.004	1.005	1.005	1.007
4400	1.000	1.001	1.002	1.002	1.003	1.004	1.005	1.005	1.007
4600	1.000	1.001	1.002	1.002	1.003	1.004	1.005	1.005	1.007
4800	1.000	1.001	1.002	1.002	1.003	1.004	1.005	1.005	1.007
5000	1.000	1.001	1.002	1.002	1.003	1.004	1.005	1.005	1.007

TABLE 4 (*Continued*)

T °R	ρ=0.6000	ρ=0.8000	ρ=1.000	ρ=1.200	ρ=1.800	ρ=2.400	ρ=3.000	ρ=3.600	ρ=4.200
100									
105									
110									
115									
120									
125									
130									
140									
150									
160	0.9362	0.9149							
170	0.9426	0.9235	0.9045	0.8855					
180	0.9482	0.9310	0.9138	0.8967	0.8456				
190	0.9529	0.9373	0.9218	0.9063	0.8601	0.8143			
200	0.9571	0.9428	0.9287	0.9146	0.8726	0.8311	0.7901	0.7495	
210	0.9607	0.9476	0.9347	0.9218	0.8835	0.8456	0.8083	0.7714	0.7351
220	0.9639	0.9520	0.9402	0.9284	0.8933	0.8587	0.8247	0.7911	0.7581
230	0.9668	0.9558	0.9449	0.9341	0.9019	0.8702	0.8390	0.8083	0.7781
240	0.9693	0.9592	0.9492	0.9392	0.9095	0.8804	0.8517	0.8236	0.7959
260	0.9738	0.9652	0.9566	0.9481	0.9228	0.8980	0.8738	0.8499	0.8266
280	0.9774	0.9700	0.9627	0.9554	0.9337	0.9126	0.8918	0.8715	0.8517
300	0.9805	0.9742	0.9678	0.9615	0.9429	0.9248	0.9070	0.8897	0.8728
320	0.9832	0.9777	0.9722	0.9668	0.9508	0.9352	0.9200	0.9053	0.8909
340	0.9854	0.9807	0.9760	0.9713	0.9575	0.9442	0.9312	0.9186	0.9065
360	0.9874	0.9833	0.9793	0.9752	0.9634	0.9520	0.9409	0.9302	0.9199
380	0.9892	0.9856	0.9822	0.9787	0.9686	0.9539	0.9495	0.9405	0.9318
400	0.9907	0.9877	0.9847	0.9818	0.9732	0.9650	0.9571	0.9496	0.9424
420	0.9921	0.9895	0.9870	0.9845	0.9773	0.9704	0.9639	0.9577	0.9518
440	0.9933	0.9912	0.9890	0.9870	0.9809	0.9753	0.9699	0.9648	0.9602
460	0.9944	0.9926	0.9909	0.9892	0.9842	0.9796	0.9754	0.9714	0.9678
480	0.9954	0.9940	0.9925	0.9912	0.9872	0.9836	0.9803	0.9773	0.9747
500	0.9963	0.9952	0.9941	0.9930	0.9900	0.9872	0.9848	0.9827	0.9810
550	0.9983	0.9978	0.9973	0.9969	0.9958	0.9950	0.9944	0.9942	0.9944
600	0.9999	0.9999	0.9999	1.000	1.000	1.001	1.002	1.004	1.005
650	1.001	1.002	1.002	1.003	1.004	1.006	1.009	1.011	1.014
700	1.002	1.003	1.004	1.005	1.008	1.011	1.014	1.018	1.022
750	1.003	1.004	1.005	1.007	1.010	1.014	1.019	1.023	1.028
800	1.004	1.005	1.007	1.008	1.013	1.018	1.023	1.028	1.034
850	1.005	1.006	1.008	1.010	1.015	1.020	1.026	1.032	1.038
900	1.005	1.007	1.009	1.011	1.017	1.023	1.029	1.036	1.043
950	1.006	1.008	1.010	1.012	1.018	1.025	1.032	1.039	1.046
1000	1.006	1.008	1.011	1.013	1.020	1.027	1.034	1.042	1.050
1100	1.007	1.009	1.012	1.014	1.022	1.030	1.038	1.046	1.055
1200	1.008	1.010	1.013	1.016	1.024	1.032	1.041	1.050	1.059
1300	1.008	1.011	1.014	1.017	1.025	1.034	1.043	1.053	1.063
1400	1.008	1.012	1.014	1.017	1.026	1.036	1.046	1.055	1.066
1500	1.009	1.012	1.015	1.018	1.028	1.037	1.047	1.058	1.068
1600	1.009	1.012	1.016	1.019	1.028	1.038	1.049	1.059	1.070
1700	1.009	1.013	1.016	1.019	1.029	1.039	1.050	1.061	1.072
1800	1.010	1.013	1.016	1.020	1.030	1.040	1.051	1.062	1.073
1900	1.010	1.013	1.017	1.020	1.030	1.041	1.052	1.063	1.074
2000	1.010	1.013	1.017	1.020	1.031	1.042	1.053	1.064	1.076
2200	1.010	1.014	1.017	1.021	1.032	1.043	1.054	1.065	1.077
2400	1.010	1.014	1.018	1.021	1.032	1.043	1.055	1.066	1.078
2600	1.011	1.014	1.018	1.022	1.033	1.044	1.056	1.067	1.079
2800	1.011	1.014	1.018	1.022	1.033	1.044	1.056	1.068	1.080
3000	1.011	1.014	1.018	1.022	1.033	1.045	1.056	1.068	1.081
3200	1.011	1.015	1.018	1.022	1.033	1.045	1.057	1.069	1.081
3400	1.011	1.015	1.018	1.022	1.034	1.045	1.057	1.069	1.081
3600	1.011	1.015	1.018	1.022	1.034	1.045	1.057	1.069	1.081
3800	1.011	1.015	1.018	1.022	1.034	1.045	1.057	1.069	1.081
4000	1.011	1.015	1.018	1.022	1.034	1.045	1.057	1.069	1.081
4200	1.011	1.015	1.018	1.022	1.034	1.045	1.057	1.069	1.081
4400	1.011	1.015	1.018	1.022	1.034	1.045	1.057	1.069	1.081
4600	1.011	1.015	1.018	1.022	1.034	1.045	1.057	1.069	1.081
4800	1.011	1.015	1.018	1.022	1.034	1.045	1.057	1.069	1.081
5000	1.011	1.015	1.018	1.022	1.034	1.045	1.057	1.069	1.081

TABLE 4 (*Continued*)

T °R	P=5.000	P=6.000	P=7.000	P=8.000	P=9.000
100					
105					
110					
115					
120					
125					
130					
140					
150					
160					
170					
180					
190					
200					
210	0.6874	0.6290			
220	0.7148	0.6620	0.6086	0.5605	0.5119
230	0.7386	0.6906	0.6439	0.5986	0.5547
240	0.7598	0.7159	0.6733	0.6322	0.5924
260	0.7962	0.7594	0.7240	0.6898	0.6570
280	0.8260	0.7950	0.7652	0.7367	0.7095
300	0.8510	0.8248	0.7998	0.7760	0.7534
320	0.8724	0.8503	0.8294	0.8096	0.7909
340	0.8908	0.8723	0.8548	0.8385	0.8232
360	0.9068	0.8913	0.8768	0.8634	0.8511
380	0.9209	0.9081	0.8963	0.8855	0.8758
400	0.9334	0.9230	0.9136	0.9052	0.8978
420	0.9445	0.9363	0.9290	0.9227	0.9173
440	0.9545	0.9482	0.9428	0.9383	0.9348
460	0.9635	0.9589	0.9553	0.9525	0.9506
480	0.9716	0.9686	0.9665	0.9653	0.9650
500	0.9791	0.9775	0.9768	0.9770	0.9781
550	0.9950	0.9945	0.9949	1.002	1.008
600	1.008	1.013	1.017	1.022	1.029
650	1.019	1.025	1.032	1.039	1.048
700	1.028	1.035	1.044	1.054	1.064
750	1.035	1.044	1.055	1.066	1.077
800	1.042	1.052	1.064	1.076	1.089
850	1.047	1.059	1.072	1.085	1.099
900	1.052	1.065	1.079	1.093	1.108
950	1.057	1.070	1.085	1.100	1.116
1000	1.061	1.075	1.090	1.106	1.123
1100	1.067	1.082	1.099	1.116	1.134
1200	1.072	1.088	1.106	1.124	1.143
1300	1.076	1.094	1.112	1.130	1.150
1400	1.080	1.098	1.116	1.136	1.156
1500	1.082	1.101	1.120	1.140	1.161
1600	1.085	1.104	1.124	1.144	1.165
1700	1.087	1.106	1.126	1.147	1.169
1800	1.088	1.108	1.129	1.150	1.172
1900	1.090	1.110	1.131	1.152	1.174
2000	1.091	1.112	1.132	1.154	1.176
2200	1.093	1.114	1.135	1.157	1.180
2400	1.095	1.116	1.137	1.159	1.182
2600	1.096	1.117	1.139	1.161	1.184
2800	1.097	1.118	1.140	1.162	1.185
3000	1.097	1.118	1.140	1.163	1.186
3200	1.098	1.119	1.141	1.164	1.187
3400	1.098	1.119	1.141	1.164	1.187
3600	1.098	1.119	1.141	1.164	1.187
3800	1.098	1.119	1.141	1.164	1.187
4000	1.098	1.119	1.141	1.164	1.187
4200	1.098	1.119	1.141	1.164	1.187
4400	1.098	1.119	1.141	1.164	1.186
4600	1.098	1.119	1.141	1.163	1.186
4800	1.098	1.119	1.141	1.163	1.186
5000	1.098	1.119	1.141	1.163	1.186

TABLE 5 NITROGEN COMPRESSIBILITY FACTOR $Z = 1 + B\rho + C\rho^2$

T °R	ρ=0.0200	ρ=0.0500	ρ=0.1000	ρ=0.1500	ρ=0.2000	ρ=0.2500	ρ=0.3000	ρ=0.4000	ρ=0.6000
100									
105									
110	0.99591								
115	0.99627								
120	0.99654	0.9913							
125	0.9968	0.9919	0.9838						
130	0.9970	0.9925	0.9849	0.9774					
140	0.9974	0.9934	0.9868	0.9802	0.9735	0.9669			
150	0.9976	0.9941	0.9882	0.9824	0.9765	0.9706	0.9647	0.9529	
160	0.9979	0.9947	0.9895	0.9842	0.9790	0.9737	0.9685	0.9580	0.9370
170	0.9981	0.9953	0.9905	0.9858	0.9811	0.9764	0.9716	0.9622	0.9434
180	0.9983	0.9957	0.9914	0.9872	0.9829	0.9786	0.9744	0.9659	0.9489
190	0.9984	0.9961	0.9922	0.9883	0.9845	0.9806	0.9767	0.9690	0.9536
200	0.9986	0.9964	0.9929	0.9894	0.9858	0.9823	0.9788	0.9717	0.9577
210	0.9987	0.9967	0.9935	0.9903	0.9870	0.9838	0.9806	0.9741	0.9613
220	0.9988	0.9970	0.9940	0.9911	0.9881	0.9851	0.9822	0.9763	0.9645
230	0.9989	0.9972	0.9945	0.9918	0.9891	0.9863	0.9836	0.9782	0.9674
240	0.9990	0.9975	0.9949	0.9924	0.9899	0.9874	0.9849	0.9799	0.9699
260	0.9991	0.9978	0.9957	0.9935	0.9914	0.9892	0.9871	0.9828	0.9744
280	0.9992	0.9982	0.9963	0.9945	0.9926	0.9908	0.9890	0.9853	0.9780
300	0.9994	0.9984	0.9968	0.9952	0.9936	0.9921	0.9905	0.9874	0.9811
320	0.9994	0.9986	0.9973	0.9959	0.9945	0.9932	0.9918	0.9891	0.9838
340	0.9995	0.9988	0.9976	0.9965	0.9953	0.9941	0.9930	0.9908	0.9860
360	0.9996	0.9990	0.9980	0.9970	0.9960	0.9950	0.9940	0.9920	0.9880
380	0.9996	0.9991	0.9983	0.9974	0.9966	0.9957	0.9948	0.9932	0.9898
400	0.9997	0.9993	0.9985	0.9978	0.9971	0.9963	0.9956	0.9942	0.9913
420	0.9998	0.9994	0.9988	0.9981	0.9975	0.9969	0.9963	0.9951	0.9927
440	0.9998	0.9995	0.9990	0.9984	0.9979	0.9974	0.9969	0.9959	0.9940
460	0.9998	0.9996	0.9992	0.9987	0.9983	0.9979	0.9975	0.9967	0.9951
480	0.9999	0.9997	0.9993	0.9990	0.9986	0.9983	0.9980	0.9974	0.9961
500	0.9999	0.9997	0.9995	0.9992	0.9990	0.9987	0.9984	0.9980	0.9970
550	1.000	0.9999	0.9998	0.9997	0.9996	0.9996	0.9995	0.9993	0.9990
600	1.000	1.0000	1.000	1.000	1.000	1.000	1.000	1.000	1.000
650	1.000	1.000	1.000	1.000	1.000	1.001	1.001	1.001	1.002
700	1.000	1.000	1.000	1.001	1.001	1.001	1.001	1.002	1.003
750	1.000	1.000	1.000	1.001	1.001	1.002	1.002	1.002	1.004
800	1.000	1.000	1.001	1.001	1.002	1.002	1.002	1.003	1.005
850	1.000	1.000	1.001	1.001	1.002	1.002	1.003	1.004	1.005
900	1.000	1.000	1.001	1.001	1.002	1.002	1.003	1.004	1.006
950	1.000	1.001	1.001	1.002	1.002	1.003	1.003	1.004	1.006
1000	1.000	1.001	1.001	1.002	1.002	1.003	1.003	1.005	1.007
1100	1.000	1.001	1.001	1.002	1.002	1.003	1.004	1.005	1.008
1200	1.000	1.001	1.001	1.002	1.003	1.003	1.004	1.006	1.008
1300	1.000	1.001	1.001	1.002	1.003	1.004	1.004	1.006	1.009
1400	1.000	1.001	1.002	1.002	1.003	1.004	1.005	1.006	1.009
1500	1.000	1.001	1.002	1.002	1.003	1.004	1.005	1.006	1.010
1600	1.000	1.001	1.002	1.002	1.003	1.004	1.005	1.007	1.010
1700	1.000	1.001	1.002	1.002	1.003	1.004	1.005	1.007	1.010
1800	1.000	1.001	1.002	1.002	1.003	1.004	1.005	1.007	1.010
1900	1.000	1.001	1.002	1.003	1.004	1.004	1.005	1.007	1.011
2000	1.000	1.001	1.002	1.003	1.004	1.004	1.005	1.007	1.011
2200	1.000	1.001	1.002	1.003	1.004	1.004	1.005	1.007	1.011
2400	1.000	1.001	1.002	1.003	1.004	1.005	1.006	1.007	1.011
2600	1.000	1.001	1.002	1.003	1.004	1.005	1.006	1.008	1.011
2800	1.000	1.001	1.002	1.003	1.004	1.005	1.006	1.008	1.011
3000	1.000	1.001	1.002	1.003	1.004	1.005	1.006	1.008	1.012
3200	1.000	1.001	1.002	1.003	1.004	1.005	1.006	1.008	1.012
3400	1.000	1.001	1.002	1.003	1.004	1.005	1.006	1.008	1.012
3600	1.000	1.001	1.002	1.003	1.004	1.005	1.006	1.008	1.012
3800	1.000	1.001	1.002	1.003	1.004	1.005	1.006	1.008	1.012
4000	1.000	1.001	1.002	1.003	1.004	1.005	1.006	1.008	1.012
4200	1.000	1.001	1.002	1.003	1.004	1.005	1.006	1.008	1.012
4400	1.000	1.001	1.002	1.003	1.004	1.005	1.006	1.008	1.012
4600	1.000	1.001	1.002	1.003	1.004	1.005	1.006	1.008	1.012
4800	1.000	1.001	1.002	1.003	1.004	1.005	1.006	1.008	1.012
5000	1.000	1.001	1.002	1.003	1.004	1.005	1.006	1.008	1.012

TABLE 5 (*Continued*)

T °R	p=0.8000	p=1.000	p=1.500	p=2.000	p=2.500	p=3.000	p=3.500	p=4.000	p=4.500
100									
105									
110									
115									
120									
125									
130									
140									
150									
160	0.9160								
170	0.9246	0.9059							
180	0.9319	0.9151	0.8731						
190	0.9382	0.9229	0.8850	0.8474	0.8102				
200	0.9437	0.9298	0.8953	0.8612	0.8274	0.7941	0.7612	0.72866	
210	0.9485	0.9357	0.9042	0.8731	0.8424	0.8120	0.7821	0.7526	0.7234
220	0.9528	0.9412	0.9124	0.8839	0.8559	0.8283	0.8010	0.7742	0.7478
230	0.9566	0.9459	0.9195	0.8934	0.8678	0.8425	0.8176	0.7930	0.7690
240	0.9600	0.9502	0.9258	0.9018	0.8783	0.8551	0.8323	0.8098	0.7878
260	0.9659	0.9576	0.9369	0.9166	0.8966	0.8770	0.8578	0.8390	0.8205
280	0.9708	0.9636	0.9460	0.9287	0.9117	0.8951	0.8788	0.8628	0.8473
300	0.9749	0.9688	0.9537	0.9389	0.9245	0.9103	0.8965	0.8830	0.8699
320	0.9785	0.9732	0.9603	0.9476	0.9353	0.9233	0.9116	0.9002	0.8891
340	0.9815	0.9770	0.9659	0.9552	0.9447	0.9346	0.9247	0.9151	0.9058
360	0.9842	0.9803	0.9709	0.9618	0.9529	0.9443	0.9360	0.9280	0.9203
380	0.9865	0.9832	0.9752	0.9675	0.9601	0.9529	0.9460	0.9394	0.9331
400	0.9885	0.9858	0.9791	0.9726	0.9665	0.9606	0.9549	0.9496	0.9444
420	0.9904	0.9881	0.9825	0.9772	0.9722	0.9674	0.9628	0.9586	0.9546
440	0.9920	0.9901	0.9856	0.9813	0.9773	0.9735	0.9699	0.9666	0.9636
460	0.9935	0.9920	0.9884	0.9850	0.9818	0.9790	0.9763	0.9739	0.9718
480	0.9948	0.9937	0.9909	0.9883	0.9860	0.9839	0.9821	0.9805	0.9792
500	0.9961	0.9952	0.9932	0.9914	0.9898	0.9885	0.9874	0.9865	0.9859
550	0.9988	0.9986	0.9982	0.9981	0.9982	0.9985	0.9991	0.9999	1.001
600	1.001	1.001	1.002	1.003	1.004	1.006	1.008	1.010	1.012
650	1.002	1.003	1.005	1.007	1.010	1.012	1.015	1.018	1.023
700	1.004	1.005	1.008	1.011	1.014	1.018	1.022	1.026	1.030
750	1.005	1.007	1.010	1.014	1.018	1.023	1.027	1.032	1.037
800	1.006	1.008	1.012	1.017	1.022	1.027	1.032	1.037	1.043
850	1.007	1.009	1.014	1.019	1.024	1.030	1.036	1.042	1.048
900	1.008	1.010	1.016	1.021	1.027	1.033	1.039	1.046	1.052
950	1.009	1.011	1.017	1.023	1.029	1.036	1.042	1.049	1.056
1000	1.009	1.012	1.018	1.024	1.031	1.038	1.045	1.052	1.060
1100	1.010	1.013	1.020	1.027	1.034	1.042	1.050	1.057	1.066
1200	1.011	1.014	1.022	1.029	1.037	1.045	1.053	1.062	1.070
1300	1.012	1.015	1.023	1.031	1.039	1.048	1.056	1.065	1.074
1400	1.012	1.016	1.024	1.032	1.041	1.050	1.058	1.068	1.077
1500	1.013	1.016	1.025	1.033	1.042	1.051	1.060	1.070	1.080
1600	1.013	1.017	1.026	1.034	1.043	1.053	1.062	1.072	1.082
1700	1.014	1.017	1.026	1.035	1.044	1.054	1.064	1.073	1.084
1800	1.014	1.018	1.027	1.036	1.045	1.055	1.065	1.075	1.085
1900	1.014	1.018	1.027	1.036	1.046	1.056	1.066	1.076	1.086
2000	1.014	1.018	1.027	1.037	1.047	1.057	1.067	1.077	1.087
2200	1.015	1.018	1.028	1.038	1.048	1.058	1.068	1.079	1.089
2400	1.015	1.019	1.028	1.038	1.048	1.059	1.069	1.080	1.090
2600	1.015	1.019	1.029	1.039	1.049	1.059	1.070	1.081	1.092
2800	1.015	1.019	1.029	1.039	1.050	1.060	1.070	1.081	1.092
3000	1.015	1.019	1.029	1.039	1.050	1.060	1.071	1.082	1.093
3200	1.016	1.020	1.030	1.040	1.050	1.060	1.071	1.082	1.093
3400	1.016	1.020	1.030	1.040	1.050	1.061	1.071	1.082	1.093
3600	1.016	1.020	1.030	1.040	1.050	1.061	1.071	1.082	1.093
3800	1.016	1.020	1.030	1.040	1.050	1.061	1.071	1.082	1.093
4000	1.016	1.020	1.030	1.040	1.050	1.061	1.071	1.082	1.093
4200	1.016	1.020	1.030	1.040	1.050	1.061	1.071	1.082	1.093
4400	1.016	1.020	1.030	1.040	1.050	1.061	1.071	1.082	1.093
4600	1.016	1.020	1.030	1.040	1.050	1.061	1.071	1.082	1.093
4800	1.016	1.020	1.030	1.040	1.050	1.061	1.071	1.082	1.093
5000	1.016	1.020	1.030	1.040	1.050	1.061	1.071	1.082	1.093

TABLE 5 (*Continued*)

T °R	ρ=5.000	ρ=6.000	ρ=7.000	ρ=8.000
100				
105				
110				
115				
120				
125				
130				
140				
150				
160				
170				
180				
190				
200				
210	0.6947	0.6384		
220	0.7218	0.6709	0.6216	0.5739
230	0.7453	0.6990	0.6543	0.6112
240	0.7661	0.7239	0.6833	0.6441
260	0.8023	0.7672	0.7334	0.7012
280	0.8320	0.8025	0.7749	0.7477
300	0.8570	0.8324	0.8090	0.7869
320	0.8784	0.8578	0.8384	0.8202
340	0.8968	0.8798	0.8639	0.8491
360	0.9129	0.8989	0.8860	0.8743
380	0.9270	0.9157	0.9055	0.8964
400	0.9396	0.9307	0.9229	0.9161
420	0.9508	0.9441	0.9384	0.9337
440	0.9608	0.9560	0.9523	0.9495
460	0.9699	0.9668	0.9648	0.9637
480	0.9781	0.9766	0.9761	0.9766
500	0.9856	0.9856	0.9865	0.9884
550	1.002	1.005	1.010	1.015
600	1.014	1.020	1.027	1.034
650	1.025	1.033	1.042	1.051
700	1.034	1.044	1.054	1.066
750	1.042	1.053	1.065	1.078
800	1.049	1.061	1.074	1.088
850	1.054	1.068	1.082	1.097
900	1.059	1.074	1.089	1.105
950	1.064	1.079	1.095	1.112
1000	1.067	1.083	1.100	1.118
1100	1.074	1.091	1.109	1.128
1200	1.079	1.097	1.116	1.136
1300	1.083	1.102	1.122	1.143
1400	1.086	1.106	1.127	1.148
1500	1.089	1.110	1.131	1.152
1600	1.092	1.112	1.134	1.156
1700	1.094	1.115	1.137	1.159
1800	1.095	1.117	1.139	1.162
1900	1.097	1.119	1.141	1.164
2000	1.098	1.120	1.143	1.166
2200	1.100	1.122	1.145	1.169
2400	1.102	1.124	1.147	1.171
2600	1.103	1.125	1.149	1.173
2800	1.103	1.126	1.150	1.174
3000	1.104	1.127	1.150	1.174
3200	1.104	1.127	1.151	1.175
3400	1.104	1.127	1.151	1.175
3600	1.104	1.127	1.151	1.175
3800	1.104	1.127	1.151	1.175
4000	1.104	1.127	1.150	1.174
4200	1.104	1.127	1.150	1.174
4400	1.104	1.127	1.150	1.174
4600	1.104	1.127	1.150	1.174
4800	1.104	1.127	1.150	1.174
5000	1.104	1.127	1.150	1.174

TABLE 6 OXYGEN COMPRESSIBILITY FACTOR $Z = 1 + B\rho + C\rho^2$

T °R	ρ=0.0200	ρ=0.0500	ρ=0.1000	ρ=0.1500	ρ=0.2000	ρ=0.2500	ρ=0.3000	ρ=0.4000	ρ=0.6000
100									
105									
110									
115									
120									
125									
130	0.99680								
140	0.99719	0.99298							
150	0.99751	0.99378	0.98755						
160	0.99778	0.99444	0.98888	0.98331	0.97773				
170	0.99800	0.99500	0.98999	0.98499	0.97998	0.97496	0.96995	0.95991	
180	0.99819	0.99547	0.99094	0.98640	0.98187	0.97733	0.97280	0.96372	0.94556
190	0.99835	0.99587	0.99175	0.98762	0.98349	0.97937	0.97524	0.96699	0.95050
200	0.99849	0.99622	0.99245	0.98868	0.98490	0.98113	0.97736	0.96983	0.95477
210	0.99861	0.99653	0.99306	0.98960	0.98613	0.98267	0.97921	0.97229	0.95847
220	0.99872	0.99680	0.99361	0.99042	0.98723	0.98404	0.98085	0.97448	0.96177
230	0.99882	0.99704	0.99409	0.99114	0.98819	0.98524	0.98229	0.97640	0.96466
240	0.99890	0.99726	0.99452	0.99179	0.98906	0.98633	0.98360	0.97815	0.96728
260	0.99905	0.99763	0.99526	0.99290	0.99054	0.98818	0.98582	0.98111	0.97172
280	0.99917	0.99794	0.99587	0.99381	0.99176	0.98970	0.98765	0.98355	0.97538
300	0.99928	0.99819	0.99638	0.99458	0.99277	0.99097	0.98917	0.98558	0.97843
320	0.99936	0.99841	0.99682	0.99524	0.99366	0.99207	0.99050	0.98734	0.98106
340	0.99944	0.99860	0.99719	0.99579	0.99440	0.99300	0.99160	0.98882	0.98328
360	0.99950	0.99876	0.99752	0.99628	0.99505	0.99381	0.99258	0.99012	0.98523
380	0.99956	0.99890	0.99780	0.99671	0.99562	0.99453	0.99344	0.99126	0.98694
400	0.99961	0.99903	0.99806	0.99709	0.99613	0.99516	0.99420	0.99228	0.98847
420	0.99966	0.99914	0.99828	0.99742	0.99657	0.99572	0.99487	0.99317	0.98979
440	0.99970	0.99924	0.99848	0.99773	0.99697	0.99622	0.99547	0.99397	0.99099
460	0.99973	0.99933	0.99866	0.99800	0.99733	0.99667	0.99601	0.99469	0.99208
480	0.99976	0.99941	0.99883	0.99824	0.99766	0.99708	0.99650	0.99534	0.99305
500	0.99979	0.99949	0.99898	0.99847	0.99796	0.99745	0.99694	0.99594	0.99394
550	0.99986	0.99964	0.99929	0.99894	0.99859	0.99824	0.99789	0.99720	0.99584
600	0.99991	0.99977	0.99955	0.99933	0.99910	0.99887	0.99866	0.99823	0.99738
650	0.99995	0.99988	0.99976	0.99964	0.99953	0.99941	0.99930	0.99908	0.99865
700	0.99999	0.99997	0.99994	0.99991	0.99988	0.99986	0.99983	0.99979	0.99972
750	1.00002	1.00004	1.00009	1.00014	1.00019	1.00024	1.00029	1.00039	1.00062
800	1.00004	1.00011	1.00022	1.00033	1.00045	1.00056	1.00068	1.00091	1.00140
850	1.00007	1.00017	1.00034	1.00051	1.00068	1.00085	1.00103	1.00138	1.00210
900	1.00009	1.00022	1.00044	1.00066	1.00088	1.00111	1.00133	1.00179	1.00271
950	1.00010	1.00026	1.00053	1.00080	1.00107	1.00134	1.00161	1.00215	1.00326
1000	1.00012	1.00030	1.00061	1.00092	1.00122	1.00153	1.00184	1.00247	1.00373
1100	1.00014	1.00036	1.00072	1.00108	1.00144	1.00181	1.00218	1.00291	1.00439
1200	1.00016	1.00041	1.00082	1.00124	1.00165	1.00207	1.00249	1.00333	1.00502
1300	1.00018	1.00045	1.00091	1.00137	1.00182	1.00228	1.00274	1.00366	1.00552
1400	1.00020	1.00050	1.00098	1.00147	1.00196	1.00246	1.00296	1.00395	1.00595
1500	1.00021	1.00052	1.00104	1.00156	1.00208	1.00261	1.00313	1.00418	1.00630
1600	1.00022	1.00054	1.00109	1.00164	1.00218	1.00273	1.00328	1.00439	1.00661
1700	1.00023	1.00057	1.00113	1.00170	1.00227	1.00284	1.00341	1.00456	1.00686
1800	1.00023	1.00058	1.00117	1.00176	1.00234	1.00293	1.00352	1.00471	1.00709
1900	1.00024	1.00060	1.00120	1.00180	1.00241	1.00301	1.00362	1.00483	1.00728
2000	1.00024	1.00061	1.00123	1.00185	1.00246	1.00308	1.00370	1.00495	1.00744
2200	1.00025	1.00063	1.00127	1.00191	1.00255	1.00319	1.00383	1.00512	1.00770
2400	1.00026	1.00065	1.00130	1.00196	1.00261	1.00327	1.00393	1.00524	1.00789
2600	1.00027	1.00067	1.00134	1.00201	1.00268	1.00335	1.00403	1.00538	1.00819
2800	1.00027	1.00068	1.00136	1.00204	1.00273	1.00341	1.00410	1.00547	1.00823
3000	1.00028	1.00069	1.00138	1.00207	1.00276	1.00345	1.00415	1.00554	1.00833
3200	1.00028	1.00070	1.00139	1.00209	1.00279	1.00349	1.00419	1.00560	1.00842
3400	1.00028	1.00070	1.00140	1.00211	1.00281	1.00352	1.00423	1.00564	1.00849
3600	1.00028	1.00071	1.00141	1.00212	1.00283	1.00354	1.00425	1.00568	1.00854
3800	1.00028	1.00071	1.00142	1.00213	1.00284	1.00356	1.00427	1.00570	1.00858
4000	1.00028	1.00071	1.00143	1.00214	1.00286	1.00357	1.00429	1.00573	1.00862
4200	1.00028	1.00071	1.00143	1.00215	1.00286	1.00358	1.00430	1.00574	1.00864
4400	1.00029	1.00072	1.00143	1.00215	1.00287	1.00359	1.00431	1.00575	1.00864
4600	1.00029	1.00072	1.00143	1.00215	1.00287	1.00359	1.00431	1.00575	1.00864
4800	1.00029	1.00072	1.00143	1.00215	1.00287	1.00359	1.00431	1.00575	1.00864
5000	1.00029	1.00072	1.00143	1.00215	1.00287	1.00359	1.00431	1.00575	1.00865

TABLE 6 (*Continued*)

T °R	ρ=0.8000	ρ=1.000	ρ=1.500	ρ=2.000	ρ=2.500	ρ=3.000	ρ=3.500	ρ=4.000	ρ=4.500
100									
105									
110									
115									
120									
125									
130									
140									
150									
160									
170									
180									
190	0.93401								
200	0.93972	0.92470							
210	0.94468	0.93091	0.89660	0.86245					
220	0.94909	0.93643	0.90493	0.87361	0.84248				
230	0.95294	0.94126	0.91219	0.88262	0.85468	0.82622	0.79798		
240	0.95644	0.94564	0.91878	0.89213	0.86570	0.83948	0.81348	0.78769	0.76212
260	0.96237	0.95305	0.92990	0.90698	0.88427	0.86178	0.83952	0.81747	0.79564
280	0.96724	0.95913	0.93902	0.91913	0.89945	0.87998	0.86074	0.84171	0.82289
300	0.97130	0.96421	0.94662	0.92924	0.91208	0.89512	0.87836	0.86182	0.84549
320	0.97481	0.96860	0.95320	0.93799	0.92299	0.90818	0.89358	0.87917	0.86497
340	0.97777	0.97229	0.95873	0.94536	0.93219	0.91921	0.90643	0.89384	0.88145
360	0.98036	0.97552	0.96356	0.95178	0.94018	0.92878	0.91752	0.90647	0.89560
380	0.98264	0.97837	0.96782	0.95744	0.94723	0.93720	0.92735	0.91767	0.90816
400	0.98468	0.98092	0.97162	0.96250	0.95355	0.94478	0.93614	0.92789	0.91941
420	0.98644	0.98311	0.97491	0.96688	0.95900	0.95129	0.94374	0.93635	0.92913
440	0.98804	0.98511	0.97791	0.97088	0.96396	0.95722	0.95064	0.94423	0.93798
460	0.98948	0.98691	0.98060	0.97444	0.96843	0.96257	0.95687	0.95133	0.94593
480	0.99078	0.98854	0.98303	0.97767	0.97246	0.96739	0.96248	0.95771	0.95309
500	0.99197	0.99002	0.98525	0.98062	0.97614	0.97180	0.96761	0.96358	0.95968
550	0.99450	0.99317	0.98997	0.98690	0.98397	0.98118	0.97852	0.97601	0.97363
600	0.99655	0.99574	0.99380	0.99200	0.99034	0.98880	0.98740	0.98613	0.98500
650	0.99824	0.99785	0.99697	0.99622	0.99560	0.99510	0.99474	0.99450	0.99440
700	0.99966	0.99963	0.99963	0.99976	1.00001	1.00039	1.00090	1.00157	1.00229
750	1.00087	1.00113	1.00188	1.00276	1.00376	1.00488	1.00613	1.00750	1.00900
800	1.00190	1.00243	1.00383	1.00535	1.00699	1.00875	1.01064	1.01265	1.01478
850	1.00284	1.00360	1.00557	1.00767	1.00989	1.01223	1.01469	1.01727	1.01998
900	1.00365	1.00461	1.00709	1.00970	1.01242	1.01526	1.01822	1.02130	1.02450
950	1.00438	1.00553	1.00847	1.01152	1.01470	1.01800	1.02141	1.02494	1.02859
1000	1.00501	1.00631	1.00964	1.01308	1.01664	1.02033	1.02412	1.02804	1.03207
1100	1.00589	1.00741	1.01129	1.01529	1.01940	1.02363	1.02798	1.03244	1.03701
1200	1.00673	1.00846	1.01286	1.01737	1.02200	1.02674	1.03160	1.03658	1.04166
1300	1.00740	1.00930	1.01412	1.01905	1.02410	1.02926	1.03454	1.03992	1.04542
1400	1.00797	1.01001	1.01518	1.02046	1.02586	1.03137	1.03699	1.04273	1.04858
1500	1.00844	1.01059	1.01606	1.02163	1.02732	1.03312	1.03902	1.04504	1.05118
1600	1.00884	1.01110	1.01682	1.02264	1.02858	1.03463	1.04078	1.04705	1.05343
1700	1.00919	1.01153	1.01746	1.02350	1.02964	1.03590	1.04227	1.04874	1.05533
1800	1.00948	1.01190	1.01801	1.02423	1.03056	1.03699	1.04354	1.05019	1.05696
1900	1.00974	1.01222	1.01848	1.02486	1.03134	1.03794	1.04464	1.05144	1.05836
2000	1.00996	1.01249	1.01890	1.02541	1.03204	1.03876	1.04560	1.05254	1.05958
2200	1.01033	1.01295	1.01958	1.02632	1.03316	1.04011	1.04716	1.05432	1.06159
2400	1.01056	1.01324	1.02001	1.02689	1.03387	1.04095	1.04814	1.05543	1.06282
2600	1.01083	1.01357	1.02051	1.02756	1.03470	1.04194	1.04929	1.05674	1.06429
2800	1.01101	1.01380	1.02085	1.02800	1.03525	1.04261	1.05006	1.05761	1.06526
3000	1.01114	1.01397	1.02110	1.02833	1.03566	1.04309	1.05062	1.05824	1.06597
3200	1.01126	1.01412	1.02132	1.02862	1.03602	1.04352	1.05111	1.05880	1.06659
3400	1.01135	1.01422	1.02148	1.02883	1.03628	1.04382	1.05146	1.05920	1.06703
3600	1.01142	1.01431	1.02161	1.02900	1.03648	1.04407	1.05174	1.05952	1.06738
3800	1.01147	1.01438	1.02171	1.02913	1.03664	1.04426	1.05196	1.05976	1.06765
4000	1.01152	1.01443	1.02179	1.02924	1.03678	1.04441	1.05214	1.05996	1.06787
4200	1.01155	1.01447	1.02184	1.02931	1.03686	1.04451	1.05225	1.06008	1.06800
4400	1.01156	1.01448	1.02186	1.02932	1.03688	1.04452	1.05226	1.06008	1.06800
4600	1.01155	1.01448	1.02185	1.02931	1.03686	1.04450	1.05223	1.06005	1.06796
4800	1.01155	1.01448	1.02185	1.02930	1.03685	1.04448	1.05221	1.06002	1.06792
5000	1.01156	1.01448	1.02186	1.02932	1.03686	1.04450	1.05222	1.06002	1.06792

TABLE 6 (*Continued*)

T °R	ρ=5.000	ρ=6.000	ρ=7.000	ρ=8.000	ρ=9.000
100					
105					
110					
115					
120					
125					
130					
140					
150					
160					
170					
180					
190					
200					
210					
220					
240	0.73676				
260	0.77404	0.73148	0.68980	0.64901	0.60909
280	0.80429	0.76774	0.73205	0.69723	0.66327
300	0.82936	0.79773	0.76693	0.73697	0.70784
320	0.85096	0.82354	0.79692	0.77110	0.74607
340	0.86925	0.84544	0.82241	0.80017	0.77870
360	0.88491	0.86407	0.84397	0.82460	0.80595
380	0.89884	0.88070	0.86326	0.84652	0.83048
400	0.91130	0.89557	0.88052	0.86614	0.85243
420	0.92206	0.90841	0.89542	0.88307	0.87137
440	0.93185	0.92010	0.90898	0.89849	0.88862
460	0.94067	0.93064	0.92121	0.91239	0.90419
480	0.94862	0.94013	0.93223	0.92493	0.91822
500	0.95590	0.94882	0.94232	0.93640	0.93106
550	0.97139	0.96733	0.96381	0.96085	0.95845
600	0.98400	0.98239	0.98132	0.98078	0.98077
650	0.99442	0.99486	0.99581	0.99728	0.99926
700	1.00318	1.00533	1.00799	1.01115	1.01482
750	1.01062	1.01423	1.01834	1.02294	1.02804
800	1.01703	1.02190	1.02726	1.03312	1.03945
850	1.02280	1.02880	1.03529	1.04226	1.04972
900	1.02782	1.03482	1.04230	1.05025	1.05867
950	1.03236	1.04025	1.04861	1.05745	1.06676
1000	1.03622	1.04487	1.05399	1.06358	1.07364
1100	1.04170	1.05144	1.06163	1.07229	1.08341
1200	1.04686	1.05761	1.06882	1.08048	1.09261
1300	1.05104	1.06261	1.07463	1.08710	1.10004
1400	1.05454	1.06679	1.07950	1.09265	1.10626
1500	1.05742	1.07024	1.08351	1.09722	1.11138
1600	1.05992	1.07323	1.08698	1.10117	1.11580
1700	1.06202	1.07574	1.08990	1.10449	1.11952
1800	1.06383	1.07790	1.09240	1.10733	1.12270
1900	1.06538	1.07975	1.09455	1.10978	1.12544
2000	1.06674	1.08137	1.09643	1.11191	1.12782
2200	1.06896	1.08401	1.09948	1.11537	1.13169
2400	1.07032	1.08563	1.10135	1.11748	1.13403
2600	1.07194	1.08756	1.10358	1.12000	1.13684
2800	1.07302	1.08882	1.10503	1.12164	1.13866
3000	1.07380	1.08974	1.10608	1.12282	1.13995
3200	1.07448	1.09054	1.10700	1.12384	1.14108
3400	1.07496	1.09110	1.10763	1.12455	1.14185
3600	1.07534	1.09155	1.10814	1.12510	1.14244
3800	1.07563	1.09188	1.10851	1.12551	1.14288
4000	1.07587	1.09215	1.10880	1.12583	1.14322
4200	1.07601	1.09231	1.10897	1.12600	1.14339
4400	1.07601	1.09229	1.10893	1.12594	1.14330
4600	1.07596	1.09222	1.10883	1.12580	1.14313
4800	1.07590	1.09214	1.10873	1.12567	1.14296
5000	1.07590	1.09213	1.10870	1.12562	1.14289

where

$$X'_{N_2} = X_{N_2} + X_A \left(\frac{X_{N_2}}{X_{N_2} + X_{O_2}} \right),$$

$$X'_{O_2} = X_{O_2} + X_A \left(\frac{X_{O_2}}{X_{N_2} + X_{O_2}} \right)$$

Using the force constants for O_2 and N_2 and the adjusted composition for air, a basic set of values for virial coefficients for nitrogen, oxygen, and air were computed from the tables of Bird and Spotz (10). These tabulations are given in Tables 1, 2, and 3.

These tables may be used to calculate the compressibility factor and hence the pressure according to Equations [2] and [1]. The compressibility factors thus obtained are given by Tables 4, 5, and 6.

Corrections to Thermodynamic Properties

Corrections to the zero-density thermodynamic properties as given for the several gases as perfect gases (10, 12) are obtained in terms of the virial coefficients and their temperature derivatives. The most important of these are

$$h - h^0 = RT \left[(B - TB')\rho - \left(C - \frac{1}{2} TC' \right) \rho^2 \right] \quad \ldots [20]$$

$$S - S^* + R \ln p = -R \left[TB'\rho + \frac{1}{2} (B - C + TC')\rho^2 \right] \quad \ldots [21]$$

$$C_v - C_v^0 = -R \left[(2TB' + T^2B'')\rho + \left(TC' + \frac{1}{2} T^2C'' \right) \rho^2 \right] \quad \ldots [22]$$

$$C_p - C_v = R \left\{ 1 + 2TB'\rho + [(B - TB')^2 - C + 2TC']\rho^2 \right\} \quad \ldots [23]$$

where h^0 and C_v^0 represent the zero-density properties, and S^* the gas entropy at 1 atm pressure. These corrections for the three gases are tabulated for the same range of temperatures and density as Tables 4 to 6.

In addition to these corrections many others such as Joule-Thompson coefficient, specific-heat ratio, and velocity of sound may be computed to comparable degrees of accuracy by use of the same set of virial coefficients and temperature derivatives.

The only comparative results available are recent tables published by the National Bureau of Standards (14). For the range in which the two tables are comparable the agreement is always within $\frac{1}{2}$ per cent in compressibility factor. Similar agreement exists with Curtiss and Hirschfelder (2) for the range of applicability of the Beattie-Bridgman equation used in their tabulation.

There is one essential difference between the present tabulation and that of the National Bureau of Standards data. At high temperatures NBS considers the effect of dissociation while the present data do not. The question of which is the more correct procedure can be answered adequately only by reference to the application to be made. It is desirable accordingly to have properties available in both forms.

The tabulations are carried out to a constant limiting density of about 40 per cent of the critical density. This limit was determined by the point at which the contribution of the fourth virial coefficient increases to a degree comparable to the uncertainties inherent in the available experimental data. It is of course possible to obtain rough estimates to much higher densities but reliable tabulations must depend on obtaining data from more refined experiments.

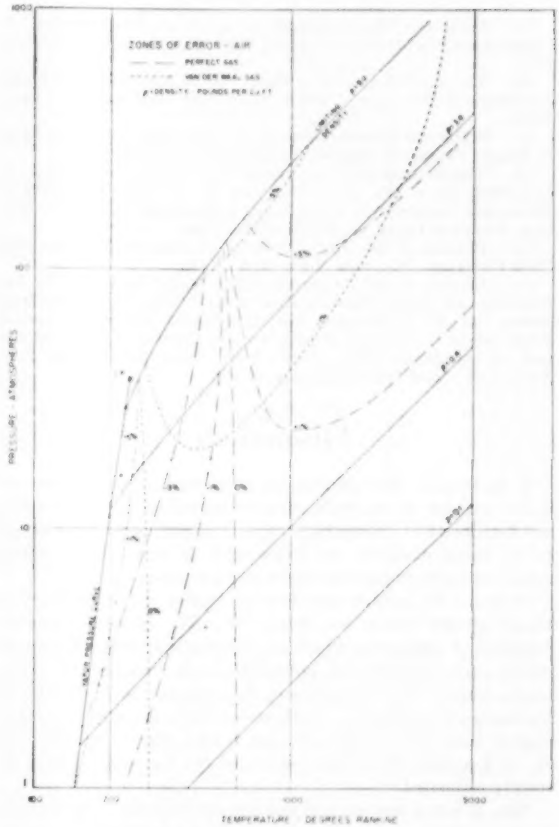

Fig. 2 Zones of Error—Air

This tabular limit is shown for air in Fig. 2. Also for comparative purposes are shown the limits of applicability within certain values of error for the perfect-gas equation and for the van der Waals equation. Aside from a narrow singular region where both equations are fortuitously quite accurate, the error bounds correspond approximately to lines of constant density. In general, density is the fundamental quantity determining the limit of validity of an equation of state rather than pressure.

BIBLIOGRAPHY

1 "The Thermodynamic Properties of Air at Low Temperatures," by V. C. Williams, Trans. AIChE, vol. 38, 1943, p. 93.

2 "Thermodynamic Properties of Air," by C. F. Curtiss and J. O. Hirschfelder, University of Wisconsin, Madison, Wis., CM-472 NOrd 9938, June 1, 1948.

3 "Thermodynamic Properties of Oxygen, Nitrogen, and Air at Low Temperatures," by L. C. Claitor and D. B. Crawford, Trans. ASME, vol. 71, 1949, pp. 885–895.

4 "On the Determination of Molecular Fields, II. From the Equation of State of a Gas," by J. E. Lennard-Jones, Proceedings of the Royal Society of London, series A, vol. 106, 1924, p. 463.

5 "Communication From the Physical Laboratory of the University of Leiden," by W. H. Keesom, Supplement No. 24, 1912.

6 "Über einiger Eigenschaften und Anwendungen der Molekularkräfte," by F. London, *Zeitschrift für Physikalische Chemie*, vol. B11, 1930, p. 222.

7 "The Equation of State and Critical Phenomena," by J. E. Lennard-Jones, *Physica*, vol. 4, 1937, p. 941.

8 "The Transport Properties of Gases and Gaseous Mixtures, II," by J. O. Hirschfelder, B. Bird, and E. L. Spotz, *Chemical Reviews*, vol. 44–1, 1949, p. 205.

9 "Statistical Thermodynamics," by R. H. Fowler and E. A. Guggenheim, Cambridge University Press, New York, N. Y., 1949, p. 279.

10 "The Virial Equation of State," by B. Bird and E. L. Spotz, University of Wisconsin, CM-599 NOrd 9938 Task Wis—1—c May, 1950.

11 "Statistical Thermodynamics of Condensing Systems," by J. E. Mayer, *Journal of Physical Chemistry*, vol. 43, 1939, p. 71.

12 "Thermodynamic Properties of Air, Nitrogen, and Oxygen as Imperfect Gases," by N. A. Hall and W. E. Ibele, University of Minnesota, Institute of Technology, Engineering Experiment Station, Technical Paper No. 85, December, 1951.

13 "Physics of the Air," by W. J. Humphreys, McGraw-Hill Book Company, Inc., New York, N. Y., 1940.

14 "Density of Air;" "Compressibility Factor for Air;" "Dry Air, Enthalpy, Entropy;" "Specific Heat of Air;" "Dry Air, Specific Heat Ratios," by W. S. Benedict, The NBS–NACA Tables of Thermal Properties of Gases, U. S. Departments of Commerce, National Bureau of Standards, 1951: Table 2.18; Table 2.20; Table 2.22; Table 2.24; and Table 2.26, respectively.

Discussion

R. B. Bird.[4] The calculations performed by the authors are a nice example of the applications of statistical mechanics which are described in a companion paper.[5] Constant progress is currently being made in the preparation of usable tables which relate bulk properties with molecular parameters.

It should be pointed out that the neglect of the "interaction terms" β and γ may not always be valid. In calculations for mixtures of substances which are structurally quite different or which have very different potential-energy functions, the interaction terms may be significant, for example, in a mixture of hydrogen and methane. Furthermore, there is really no need to neglect these terms inasmuch as it is very easy to calculate the B_{12} of Equation [6] of the paper and the C_{112} and C_{122} may be readily estimated.[6,7]

Also, it is not necessary to restrict the contents of the air mixture to nitrogen and oxygen, inasmuch as calculations for multicomponent mixtures present no difficulties.[5,6] In addition, if moisture content needs to be taken into account, this also can be done easily, since tables are available for calculating the virial coefficients of polar gases and mixtures of polar and nonpolar gases.[5,8]

In connection with the use of the Lennard-Jones potential it should be pointed out that the agreement between the calculated and experimental third virial coefficients is not exceptionally good.[9,10] This lack of agreement puts a definite restriction on the validity of the results. Also, the Lennard-Jones potential is not sufficiently good to describe the temperature dependence of the second virial coefficient over the great range of temperatures in the authors' calculation. It would be worth while to compare the values of the second virial coefficient of nitrogen and oxygen at 5000 R as calculated by means of the Lennard-Jones potential, the modified Buckingham (6-exp) potential,[11,12] and the Kihara potential[13] (which takes into account the "ellipsoidal" or "spherocylindrical" shape of diatomic molecules).

L. C. Nelson.[14] This paper presents a convenient tabulation of the compressibility factors and temperature derivatives for air, oxygen, and nitrogen based upon new values of the force constants for the Bird and Spotz equation of state.

The questions immediately arise: What evidence is there to show the accuracy of the Bird and Spotz equation as well as the effects of the Hall and Ibele constants? Since the tables of compressibility factors are complete to four and five significant figures, won't the reader assume an accuracy which is not supported by the experimental data throughout the regions of the tables?

The effects of changing the force constants of the Bird and Spotz tabulations will be reflected in the correlation of the theoretical equation with the experimental data. Each particular set of force constants will allow better correlation in certain pvT regions while decreasing the accuracy in other regions. A simple method for obtaining force constants for most gases with adequate accuracy is shown in the writer's paper.[15] The over-all effects of the force constants listed by Bird and Spotz have not been demonstrated conclusively to the writer's knowledge.

However, the validity of the authors' constants, as reflected by the agreement of their tables with the experimental data, can be illustrated by Fig. 3 of this discussion. This chart illustrates Z, the compressibility factor, as a function of the reduced pressure

$$p_r' = \frac{pb_0}{R\,\dfrac{\epsilon}{k}}$$

and the reduced temperature $\tau = Tk/\epsilon$. The solid lines of constant τ were constructed using the authors' force constants in the Bird and Spotz tabulations. Thus these lines also represent the authors' tabulated compressibility data. The dash lines represent the experimental nitrogen data and the points represent the experimental oxygen data. (The sources of these data are given in the Bibliography of the writer's paper.[15])

The authors chose 8 lb_m/ft^3 as the maximum density for nitrogen and 9 lb_m/ft^3 as the maximum density for oxygen. These limits correspond to a reduced density $\rho_r' = b_0\rho$ of approximately 0.25 for oxygen and 0.30 for nitrogen and are shown in Fig. 3, herewith, along with one other line of constant density to facilitate comparison with the authors' tables.

Fig. 3 shows very clearly the limits of the Bird and Spotz equation of state as well as the effects of the force constants. In the region below a reduced density of $\rho_r' = 0.15$ and for temperatures near and above the critical point ($\tau = 1.4$ is approximately the critical temperature) the experimental data are reproduced accurately by the equation of state. This same excellent agreement with the experimental data exists at and above reduced

4 Department of Chemical Engineering, College of Engineering The University of Wisconsin, Madison, Wis.

5 "The Theoretical Calculation of the Equation of State and Transport Properties of Gases and Liquids," by R. B. Bird, J. O. Hirschfelder, and D. F. Curtiss, published in this issue, pp. 1011–1038.

6 "The Molecular Theory of Gases and Liquids," by J. O. Hirschfelder, C. F. Curtiss, and R. B. Bird, John Wiley & Sons, Inc., New York, N. Y., 1954—Virial-coefficient calculations for mixtures are described on pp. 168, 173, and 223.

7 "The Third Virial Coefficient for Nonpolar Gases," by R. B. Bird, Ellen L. Spotz, and J. O. Hirschfelder, *Journal of Chemical Physics*, vol. 18, 1950, pp. 1395–1402.

8 See, for example, §2d of footnote 6, or §3.10f of footnote 7.

9 "Intermolecular Forces and the Virial Equation of State," by R. B. Bird, Doctoral Dissertation, University of Wisconsin, 1950.

10 "Het Principe van Overeenstemmende Toestanden," by R. J. Lunbeck, Doctoral Dissertation, University of Amsterdam, The Netherlands.

11 "Second Virial Coefficient of Gases Obeying a Modified Buckingham (Exp-Six) Potential," by W. E. Rice and J. O. Hirschfelder, University of Wisconsin Report ONR-2, June 22, 1953 (to be published in the *Journal of Chemical Physics*).

12 "The Intermolecular Potentials for Some Simple Nonpolar Molecules," by E. A. Mason and W. E. Rice, University of Wisconsin Report ONR-6, November 6, 1953 (to be published soon in the *Journal of Chemical Physics*). . . see also footnote 6, pp. 180 et seq.

13 "Virial Coefficients and Models of Molecules in Gases," by Taro Kihara, University of Wisconsin Report OOR-7, June 5, 1953; see also footnote 6, §3.7.

14 Lecturer in Mechanical Engineering, Northwestern Technological Institute, Evanston, Ill.

15 "Generalized pvT Properties of Gases," by L. C. Nelson and E. F. Obert, published in this issue, pp. 1057–1066.

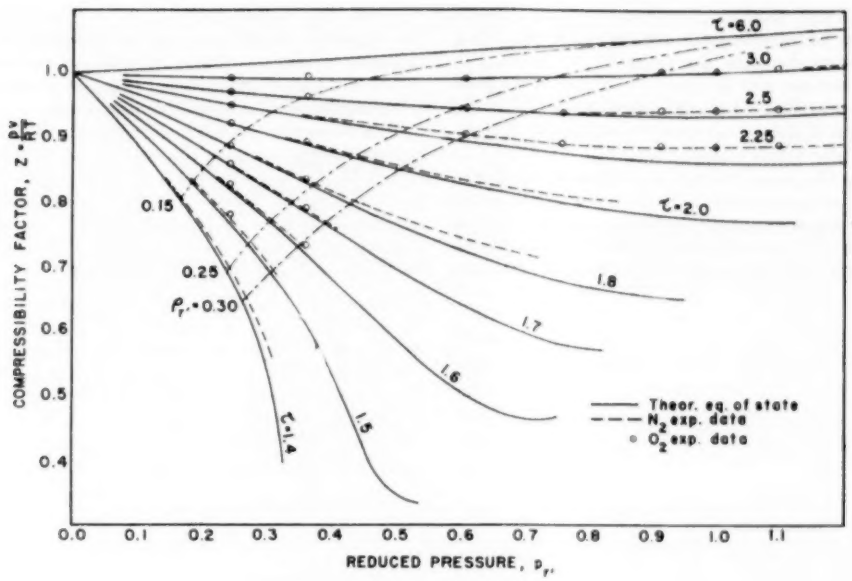

FIG. 3

temperatures of $\tau = 2.5$ up to the limiting density selected by the authors. No experimental data are available above $\tau = 6$ to establish that the correlation continues (a good probability). At temperatures below $\tau = 2.5$ in the higher-density region, however, note that deviations of the order of 1.5 per cent are encountered; thus significant figures greater than three are unwarranted. It is suggested that the tables might have been improved by allowing the number of signficant figures to change to agree with the accuracy of the experimental data. Also, a common reduced density should be the limit of validity of the equation of state. Hence the oxygen tables could have been extended to a density of $\rho_r' = 0.30$ ($\rho = 11$ lb_m/ft^3) to match the accuracy of the nitrogen tables.

Since Fig. 3 of this discussion is expressed in reduced coordinates, the nitrogen data serve to show the limits of the Bird and Spotz three virial equations of state for any gas whose pvT properties can be expressed adequately in terms of the Lennard-Jones force potential.

Note particularly that the O_2 and N_2 experimental data correlate each other exceptionally well in their corresponding states and in regions beyond the validity of the three virial equations of state. This is very gratifying since it provides a means of extending the limited O_2 data. In light of this good correlation at the higher densities, the writer is of the opinion that the theory is sound enough to warrant the labor necessary to calculate the fourth virial coefficient.

In addition to the questions raised in the discussion, the writer is curious to ascertain why the oxygen data are reported to five significant figures and the nitrogen to four? It would seem that the sparse oxygen data in the literature would not yield an accuracy greater than that of nitrogen. Also, the writer is not clear whether or not data for argon and CO_2 were included in the various calculations for air. The authors' comments on these questions would be appreciated.

AUTHORS' CLOSURE

The authors wish to express their appreciation for the comments by Messrs. Bird and Nelson.

The interaction terms β and γ between unlike molecules, mentioned by Mr. Bird, were carefully studied before undertaking the tabulation of mixture properties for air. The possible interaction coefficients for the four-component analysis of air employed were calculated in order to determine their probable effect on the various properties. The method of accounting for argon and carbon-dioxide contributions, given in the paper and in detail (12), was then designed in the light of these calculations. While it is true that the second virial coefficient for unlike molecules is easy to calculate and the third readily estimated, some saving of time and effort was realized without introducing inaccuracies greater than those for the intermolecular force constants ϵ/k and b_0.

The validity of the Lennard-Jones potential, while not entirely satisfactory with respect to experimental third virial coefficients, nevertheless represented for the gases involved, the most acceptable compromise between faithful reproduction of the experimental data and a mathematical characteristic amenable to physical-property calculations. That this is accomplished within a maximum error of 1.5 per cent in compressibility factor is, in the authors' opinion, a vindication of the reasonableness of the original choice and an indication of the utility of the resulting tabulations.

It is not clear from either the discussion or the paper by Nelson and Obert (discussion footnote 15) what particular experimental data of nitrogen and oxygen are used in establishing the behavior shown in Fig. 3. Among the thirty-one and nineteen sources of original data listed (discussion, footnote 15) for nitrogen and oxygen, respectively, not all are of equal reliability. While one appreciates the work of early experimenters in view of the obstacles confronting them, their results cannot be given equal weight with those obtained by the Leiden and Berlin groups, for example. The most reliable experimental compressibility data were used in obtaining the intermolecular force constants reported in the paper, and further confirmation was obtained by comparing predicted and experimental Joule-Thomson and pressure coefficients of velocity of sound measurements. Reference (12) contains a detailed comparison of the predicted thermo-

dynamic properties with those of other studies, several of which are based entirely on experimental measurements, and close agreement was obtained within the range of the tables, i.e., within one half of one per cent in density. In view of the foregoing, it would appear that, within the range of the tables, the graphical correlation of Nelson and Obert represents no improvement over the tabular values reported.

In all discussions of gas properties, it is pertinent to recall that a semitheoretical extension into regions where experimental measurements are sparse or nonexistent is best accomplished by means of a pattern of theoretical behavior which is shown to be consistent with existing experimental data. Thus in reference (12), not only compressibility factor, but enthalpy, entropy, and heat capacity values are given at elevated temperatures and moderate pressures. These tabulations represent, then, the results of a logical extrapolation of gas-property data that could be accomplished with reasonable confidence.

With respect to the tables themselves, the exercise of normal prudence would preclude the assumption of accuracy not warranted by the experimental evidence, despite the number of significant figures listed. The tabulations given here and in reference (12) were constructed primarily for utility and convenience in engineering applications. The authors are hopeful that their original purpose will be realized.

Generalized pvT Properties of Gases

By L. C. NELSON[1] and E. F. OBERT,[2] EVANSTON, ILL.

In this paper two sets of generalized compressibility charts are presented: One set is based upon critical temperatures and pressures as in the past; the other set is based upon pseudo-reduced co-ordinates obtainable from the Lennard-Jones force potential. In both sets the underlying data are more extensive than those used in constructing older charts since a complete survey of existing pvT data was made. The results of this survey for 30 gases are contained in a Bibliography of 275 items which has been constructed to show the extent of the experimental data by including the ranges of pressure and temperature for each item. Although the charts are intended for engineering computations, the chart for the low-pressure region (p_r = 0 to 1), for example, has a deviation of 1 per cent for 26 gases.

Introduction

In engineering practice, reasonable approximations to the pvT relationships of a fluid are required frequently, especially for the case, more usual than unusual, where pvT data are entirely nonexistent. To fulfill this need, several generalized charts (276–288)[3] have been developed and are in use, principally in the chemical industries. Comparison of these charts reveals that either large differences are present or else the charts are closely similar. In the first instance, the divergences arose from the assumptions made in generalizing the pvT data or from the choice of data. In the second instance, the charts were based primarily upon one or two gases (usually, hydrogen and nitrogen) and the same compressibility data were used by the several authors. It is understandable that the validity of the older charts has not been too well established when it is considered that the charts were developed some years ago, and even today high-pressure data are extremely meager.

When it was decided to construct new generalized charts, it was discovered, somewhat surprisingly, that no complete bibliography of experimental pvT data was available in the literature (1952). For this reason, the Bibliography in this article has been expanded to show both the fluid and the ranges covered by the experiments.

In constructing the new charts, the various methods of reducing the properties into generalized properties were studied. It was concluded that, for most engineering applications, the usual generalizations based upon the critical temperature and pressure were preferable for best correlation of data for all gases over wide ranges of temperature and pressure. Specifically, gases with elongated molecules are best treated by a reduction based upon the critical constants. The compressibility factor is defined

$$Z = \frac{pv}{RT} \quad \ldots\ldots [1]$$

The reduced properties for the first set of charts are

$$p_r = \frac{p}{p_c}, \quad T_r = \frac{T}{T_c} \quad \ldots\ldots [2]$$

where p_c and T_c are the critical values. A set[4] of three charts presents Z as a function of p_r and T_r for the regions illustrated in Fig. 1:

1 Low-pressure region (p_r = 0 to 1, T_r = 0.6 to 15.0) (T_r from 0.60 to 1.15 by 0.05 increment, 1.2, 1.3, 1.4, 1.6, 2.0, 2.5, 3.0, 5, 10, and 15)

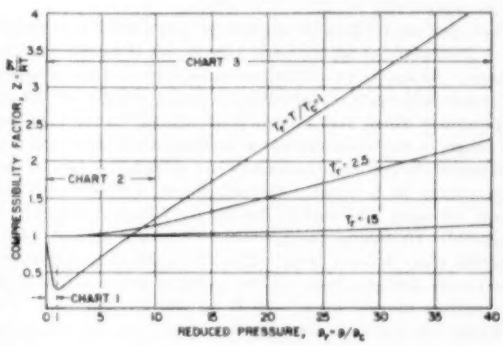

Fig. 1 Ranges of Generalized Compressibility Charts

2 Intermediate-pressure region (p_r = 0 to 10, T_r = 1 to 15) (T_r from 1.0 to 1.2 by 0.05 increment, 1.2 to 1.6 by 0.10 increment, and 1.8, 2.0, 2.5, 3.5, 5, 7, 10, and 15)

3 High-pressure region (p_r = 0 to 40, T_r = 1 to 15) (T_r from 1.0 to 1.2 by 0.05 increment, 1.2 to 1.6 by 0.10 increment, 1.8, 2.0 to 4.0 by 0.5 increment, and 5, 6, 8, 10, and 15)

However, the rigor of the work of Bird, Spotz, Hirschfelder, and Curtiss (289–291), and based upon the Lennard-Jones force potential, showed that a more fundamental method of analysis was available for nonpolar gases with symmetrical molecular structure. It will be shown that pseudo-reduced parameters p_r' and τ (see Equations [10] and [15]) allow Z to be defined with relatively great accuracy. These parameters do not bear a universal relationship to the critical constants else a new chart would be useless. In effect, the new parameters shift the gases relative to each other so that some loss of correlation occurs near the critical point but greater over-all accuracy is obtained in other regions. A set[4] of two charts was constructed:

1 Low-pressure region (p_r' = 0 to 0.3, τ = 1.0 to 20) (τ from 1 to 2 by 0.10 increment, and 2, 2.25, 2.5, 3.0, 3.5, 4.5, 6, 10, 15, and 20)

2 Intermediate-pressure region (p_r' = 0 to 1.8, τ = 1.4 to 20) (τ from 1.4 to 2.0 by 0.1 increment, 2.25, 2.5, 3.0, 3.5, 4.5, 6.5, 10, 15, and 20)

---

[1] Royal Cabell Fellow, Department of Mechanical Engineering, Northwestern Technological Institute.

[2] Professor of Mechanical Engineering, Northwestern Technological Institute. Mem. ASME.

[3] Numbers in parentheses refer to the Bibliography at the end of the paper.

Contributed by the Heat Transfer Division and presented at the Annual Meeting, New York, N. Y., November 29–December 4, 1953, of The American Society of Mechanical Engineers.

Note: Statements and opinions advanced in papers are to be understood as individual expressions of their authors and not those of the Society. Manuscript received at ASME Headquarters, September 2, 1953. Paper No. 53—A-194.

[4] The charts are 8½ in. × 11 in., and 11 in. × 17 in. in size and can be obtained from the authors.

This second set of charts is recommended for nonpolar (and slightly polar) gases with essentially spherical symmetry and with negligible quantum effects.

Experimental Data

The experimental data for 52 gases were investigated but the data for only 30 gases were in sufficient amounts to aid in constructing charts. It would involve too great an extension of the purpose of this paper to discuss the individual fluids. For this reason, the Bibliography has been constructed to allow data for a specific fluid to be ascertained readily. Note that the Bibliography has been divided into 32 parts and only original sources of data have been included. The first 30 parts are in alphabetical order by gases and each part is pertinent only to one fluid. The ranges of temperature and pressure covered by the experimental work are shown under each entry. In this form the Bibliography is useful to extend previous papers on pvT properties. Gratch (292) gave an excellent review of nine fluids in 1948. His data on argon, for example, are represented by (27, 28, 29, 30, 32, 35) of the Bibliography (25 to 37 for argon). Gratch's survey can be extended to include later work (26, 33, 34, 36) and to include work not mentioned (25, 31, 37).

The experimental data are surprisingly few when it is considered that a generalized chart demands wide ranges of temperature and pressure. At low and medium pressures most of the experiments were made with small increments of pressure, but for only several temperatures which may be widely separated; in the high-pressure range, even the increments of pressure are widely separated. Such points do not lend themselves to interpolation for the fixed temperatures of a chart. Certain fluids, notably hydrogen, helium, nitrogen, and carbon dioxide have been extensively investigated: Hydrogen, from —259.2 C to 400 C, and from 0 to 12,600 atm; helium, from —271.5 C to 600 C, and from 0 to 14,500 atm; nitrogen, from —175 C to 400 C, and from 0 to 14,500 atm; carbon dioxide from —70 C to 500 C, and from 0 to 3000 atm. In recent years, considerable data on the compressibility of hydrocarbons have been obtained: Ethylene, from 0 C to 200 C and from 0 to 3000 atm; methane, from —70 C to 200 C, and from 0 to 1000 atm; ethane, from 14 C to 275 C, and from 0 to 680 atm; propane, from 20 C to 336 C, and from 0 to 680 atm; butane, from 0 C to 300 C, and from 0 to 680 atm.

Generalized Charts Based Upon Critical Constants

The van der Waals law of corresponding states assumes that the pvT regions of all gases are symmetrical with respect to the critical point. Thus the reduced properties are defined by the ratios p/p_c, T/T_c, and v/v_c, and

$$f(p_r, T_r, v_r) = 0 \quad [3]$$

However, data usually are plotted in the form of reduced isotherms on a chart with Z as the ordinate and p_r as the abscissa, Fig. 1. The accuracy of this diagram indicates that a better approximation than Equation [3] is a law corresponding to

$$Z = f(p_r, T_r) \quad [4]$$

Su (286) introduced an ideal reduced volume which is defined

$$v_r' = \frac{v}{RT_c/p_c} = \frac{ZRT/p}{RT_c/p_c} = Z\frac{T_r}{p_r} \quad [5]$$

A chart with lines of constant v_r' was published by Obert (285) that allows interpolation for T_r-values which do not fall upon the chart isotherms. Trial calculations also are avoided when data are for volume and temperature (or pressure) and pressure (or temperature) is the unknown variable. This feature also was employed in the new charts.

To construct the generalized charts, it was first necessary to obtain a tabulation of compressibility factors at common selected values of reduced temperature and pressure. A graphical, rather than an analytical, method was selected since accuracy to only three figures was considered necessary. Two construction charts were required for each gas. The first chart was a plot of reduced isotherms on Z and reduced-pressure co-ordinates. The second chart was a cross plot of the first, of isobars at selected values plotted against Z and reduced temperature. A division on the co-ordinates corresponded to a value of 0.0025 increments with 20 divisions per in.

Rectilinear co-ordinates were chosen for the charts because normally straight isotherms (especially true in the high-pressure region) suffer distortion when plotted on logarithmic co-ordinates. The curved isotherms make extrapolation and interpolation more difficult. Note, too, that with a logarithmic ordinate the greatest magnification is in the neighborhood of the critical point where correlation of data is the poorest.

The critical constants of the fluids that were used for computing the reduced temperature T_r and the reduced pressure p_r are listed in Table 1. Corrections to the critical constants of H_2 and He, as recommended by Newton (309) for his generalized activity coefficients, should not be used for compressibility data at temperatures below the Boyle point isotherm but are recommended for higher temperatures.

The low-pressure chart was drawn on a large scale with divisions of 0.01 unit. The data correlated by the chart are listed in Table 2. Note, in Fig. 2, that the maximum deviations from the average curves for 26 gases are of the order of 1 per cent. The worst

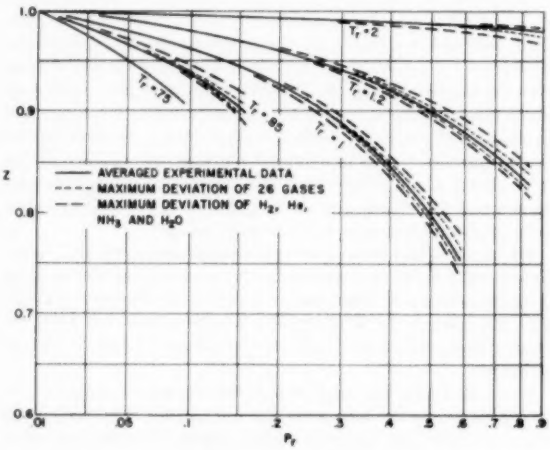

Fig. 2 Deviation of Experimental Data in Low-Pressure Region

offenders are H_2, He (with uncorrected critical constants from Table 1), NH_3, and H_2O and the extent of their deviations are also indicated in Fig. 2. No data exist for NH_3 and H_2O at temperatures near or above the Boyle point isotherm. But for H_2 and He, from the data available, it appears that correlation within 1 per cent can be obtained by using the so-called Newton corrections (at or above the Boyle point isotherm). The Boyle point isotherm can be considered to be the $Z = 1.00$ co-ordinate with probable accuracy of 0.004 units (based upon data for A, air, CH_4, O_2, CO, H_2, N_2, and Ne). Maximum Z-values are attained in the neighborhood of $T_r = 5$. The isotherms then descend, for example, the isotherms $T_r = 3$ and $T_r = 15$ closely coincide within 0.004 unit (data for H_2, He, and Ne).

TABLE 1 CRITICAL CONSTANTS

(Absolute zero at —273.16 C)

Substance	T, K	p_c atm	Reference	Substance	T, K	p_c atm	Reference
Air	132.53	37.17	(293)	n-Hexane	507.9	29.94	(301)
Ammonia	405.4	111.3	(294)	Hydrogen	33.24	12.797	(299)
Argon	150.72	47.996	(295)	Hydrogen sulphide	373.7	88.8	(181)
Benzene	562.7	48.7	(38)	Methane	191.05	45.79	(302)
n-Butane	425.17	37.47	(39)	Methyl fluoride	317.71	58.0	(303)
Isobutane	408.14	36.00	(296)	Neon	44.39	26.86	(298)
1-Butene	419.6	39.7	(48)	Nitrogen	126.26	33.54	(304)
Carbon dioxide	304.20	72.85	(66)	Nitric oxide	180.3	64.6	(306)
Carbon monoxide	132.91	34.529	(298)	Oxygen	154.78	50.14	(305)
n-Deuterium	38.35	16.432	(299)	n-Pentane	471.0	33.0	(253)
Ethane	305.43	48.20	(79)	Isopentane	461.0	32.92	(307)
Ethyl ether	467.8	35.6	(300)	Propane	370.01	42.1	(263)
Ethylene	283.06	50.50	(93)	Propylene	364.92	45.61	(266)
Helium	5.19	2.26	(298)	Water	647.27	218.167	(308)
n-Heptane	540.17	27.00	(127)	Xenon	289.81	57.89	(274)

TABLE 2 DATA REFERENCES FOR CHARTS

Chart No. 1 p_r (0–1.0) T_r(0.65–15)

7–9, 12, 14, 16, 18, 19, 22, 24, 26, 31–33, 35, 37, 38, 40–44, 46–49, 54–58, 60, 62–64, 66, 69–75, 77, 79–82, 84, 88, 91, 92, 95, 108, 109, 112, 114, 117, 125, 129, 130, 135, 137, 138, 143, 150–152, 155, 157, 160, 161, 168, 170, 171, 178, 180–182, 184, 185, 187–189, 194, 204, 206, 207, 218, 221, 229, 230, 232, 233, 237, 245, 246, 250, 251, 254–257, 259, 261, 263, 265, 266, 268, 269, 273, 274.

Chart No. 2 p_r(1–10) T_r(1–15)

7, 9, 12–14, 16, 18, 19, 23, 26, 31–33, 35, 37, 38, 40–44, 46–49, 54, 60, 64–66, 70–75, 77, 79–82, 84, 88, 92, 95, 96, 108, 109, 115–117, 122, 124, 128–130, 135, 137, 138, 142, 143, 150, 152, 155, 157, 160, 161, 164, 168, 170, 171, 175, 178, 180–182, 184, 185, 187–189, 191, 194–196, 198, 204, 206, 207, 218, 221, 225, 227, 229, 230, 232, 233, 237, 245, 246, 250, 251, 254–257, 259, 261, 263, 265, 266, 268, 269, 273, 274.

Chart No. 3 p_r(10–40) T_r(1–15)

7, 13, 33, 41, 42, 49, 54, 65, 70, 71, 73, 75, 82, 88, 95, 96, 108, 115, 124, 126, 135, 137, 138, 152, 157, 171, 180, 185, 188, 196, 204, 206, 207, 209, 222, 225, 227, 230, 237, 255, 256, 265.

Chart No. 4 p_r(0–0.3) v(1–20)

7–9, 12, 14, 16, 18, 26, 31–33, 35, 37, 71–75, 135, 137, 138, 150, 152, 155, 157, 160, 161, 168, 170, 171, 178, 182, 184, 185, 187, 188, 194, 204, 206, 207, 218, 221, 229, 230, 237, 245, 246, 250, 251, 274.

Chart No. 5 p_r(0.3–1.8) v(1–20)

7, 9, 13, 14, 16, 18, 26, 31–33, 35, 37, 71–75, 135, 137, 138, 142, 150, 152, 155, 157, 160, 161, 168, 170, 171, 175, 178, 182, 184, 186, 187, 188, 191, 194–196, 198, 204, 206, 207, 218, 221, 225, 227, 229, 230, 237, 245, 246, 250, 251, 274.

The intermediate-pressure chart also is based on data for 30 gases with the extent shown by Table 2. For 26 of the gases studied (excluding H_2, He, NH_3, and CH_2F), the correlation was found to be within a maximum deviation of 2½ per cent (except near the critical region). The worst offender was NH_3 which could not be correlated satisfactorily on this chart above p_r = 1.0; CH_2F correlated within 2½ per cent above T_r = 1.3 but had deviations at the lower temperatures as much as 7 per cent. Both H_2 and He exhibited erratic correlation below the Boyle point isotherm, but, at higher temperatures both these gases correlated the chart (with the use of the Newton corrections).

The high-pressure chart was constructed from the data for 17 fluids (Table 2) but for only a few of these fluids could the data be called extensive. In those regions where several gases could be compared, the maximum deviation was less than 5 per cent (T_r = 1 to 3.5; p_r = 10 to 20). In this same pressure region, but above the Boyle point isotherm, H_2 and He (with the Newton corrections) correlated all the available data (N_2, air, and CO) within 2½ per cent. Because of this, and because no other data were available, the data for H_2 and He (with the Newton corrections) were used to construct all isotherms above T_r = 5.0. No data are available for NH_3 and CH_2F in the high-pressure region; H_2 and He (uncorrected) again exhibited erratic correlation below the Boyle point isotherm with maximum deviation of 10 per cent.

The effects of the Newton corrections are illustrated in Fig. 3 for T_r = 1.3 and T_r = 3.0. Note, at T_r = 1.3, that the uncorrected constants (H_2 isotherm) allow better correlation of the experimental data than do the corrected constants (H_2' isotherm) which cause errors as much as 40 per cent. Above the Boyle point isotherm on all charts H_2 and He could be correlated with

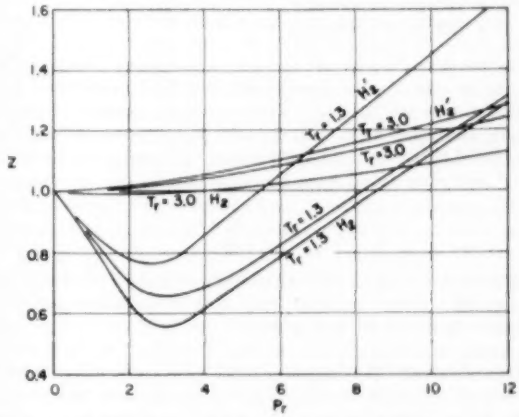

FIG. 3 EFFECT OF NEWTON CORRECTIONS ON HYDROGEN AT TWO REDUCED TEMPERATURES

other gases within the accuracy stated for the chart by using the Newton corrections.

VIRIAL EQUATION OF STATE

A virial equation of state can be derived from the fundamental principles of either kinetic theory or statistical mechanics to relate the pvT behavior of a gas to the forces between molecules. The form of the equation is a power series in $(1/v)$

$$\frac{pv}{RT} = 1 + \frac{B}{v} + \frac{C}{v^2} + \frac{D}{v^3} + \ldots \quad [6]$$

The coefficients B, C, D, etc., are called, respectively, the second, third, fourth, etc., virial coefficients and each virial is a function of temperature alone. Each virial also corresponds to a summation of the effects of the interactions of n-molecules: two-molecular interactions for B; three-molecular interactions for C; etc.

To evaluate the virial coefficients, an assumption must be made as to the nature of the intermolecular forces. For spherical nonpolar molecules the intermolecular potential energy usually is represented by the Lennard-Jones potential function

$$E(r) = 4\epsilon[(r_0/r)^{12} - (r_0/r)^6] \quad [7]$$

The two constants, ϵ and r_0, in this equation are called *force constants*

ϵ = maximum energy of attraction

r_0 = collision diameter for encounters between two molecules with negligible kinetic energy

Lennard-Jones (310) has shown that Equation [7] allows the second virial to be expressed as a rapidly converging infinite series. Bird and Spotz (289) extended this work by an original

evaluation of the third virial and prepared tables that allow the second and third virial coefficients to be evaluated. The Bird and Spotz tables list values of the temperature functions B^0 and C^0 versus a reduced temperature τ. A virial equation with the same form as Equation [6] can be fitted to the experimental data and the virials B, C, etc., determined. The empirical virials B and C are equal to

$$B = b_0 B^0 \qquad C = b_0^2 C^0 \ldots\ldots\ldots [8]$$

where

$$b_0 = 2/3\pi N r_0^3 \ldots\ldots\ldots [9]$$

$$\tau = kT/\epsilon \ldots\ldots\ldots [10]$$

N = number of molecules per gram mole
k = Boltzmann constant
T = Kelvin temperature

The fourth and higher virials were not calculated. Note that the force constants ϵ and r_0 must be known before the Bird and Spotz relationships can be used. Values of these constants for several gases, and based upon both viscosity and experimental pvT data, are listed in the Bird and Spotz tables. The values obtained from pvT data were found from Equation [8].

$$b_0 = \frac{B_{exp}}{B^0} \ldots\ldots\ldots [11]$$

To solve this equation, an estimate of the constant ϵ must be made to enable τ to be computed; a method of successive approximations is described by Hall and Ibele (311). To avoid the initial estimate, note that the second virial B must be zero for the Boyle point isotherm. This factor enables the corresponding temperature to be obtained from the experimental data by interpolation. The function B^0 differs from B only by a constant factor. Then the reduced temperature τ where B^0 passes through zero should correspond to the actual temperature where B also passes through zero. The tables of Bird and Spotz, on interpolation, show τ for $B^0 = 0$ to be 3.416. The force constant ϵ can now be directly computed by Equation [10] and b_0 found from Equation [9]. A comparison of the force constants obtained for nitrogen by, apparently, three methods is as follows

Nitrogen	Bird and Spotz (289)	Hall and Ibele (311)	Boyle Isotherm
ϵ/k	95.05, 95.9	95.36	95.1
b_0	63.78, 64.42	64.13	63.9

The Lennard-Jones force potential presupposes essentially spherical, nonpolar gases with negligible quantum effects. The quantum effects are small except for light gases (H_2, He, D_2, Ne) at low temperatures. The quantum effects could be taken into account by a three-constant force potential but then comparison could only be made between molecules with the same quantum mechanical parameters (312). Similarly, three-constant force potentials can be derived theoretically for polar molecules (313) and for nonspherical molecules but comparison is again restricted by the introduction of new parameters for dipole moments and length-width ratios. Thus a third parameter severely restricts the number of fluids which can be compared, and a generalized chart would be of only limited use. But for many fluids, quantum effects and dipole moments are small in magnitude. For such fluids, reduced parameters based upon a two-constant potential may be more valuable than the older reductions based upon critical constants. This supposition is the basis for the second set of generalized charts.

A Virial Law of Corresponding States

A physical picture of the virial equation is shown by the compressibility chart, Fig. 1. Note that the region in the vicinity of $Z = 1$ corresponds to the concept of the perfect gas with negligible force interactions between molecules. As the pressure is increased at constant temperature, binary collisions between molecules become more frequent and the second virial exerts an increasing effect on the compressibility factor Z. This effect may be either positive or negative: Positive values imply a predominance of repulsion between the molecules (in general, above the Boyle point isotherm); and negative values imply attraction. Note that descending isotherms ($T_r < T_{Boyle}$) would continue to fall if the virial equation did not include the third, and higher, virial coefficients. It can be surmised that when the second virial is negative, the third and succeeding virials must have positive sign, if the isotherms are to break upward at high pressures, as shown by the chart. The point of the discussion is this: Virial equations founded upon theory cannot represent the entire range of experimental values in Fig. 1, unless the temperature functions of C^0, D^0, E^0, and probably F^0, are evaluated accurately (and the Bird and Spotz tables include only B^0 and C^0).

Although Bird and Spotz limit their results to "regions of high temperature and moderate pressure," the compressibility chart serves to define these terms. To illustrate this point, Equation [6] can be converted into a power series in p

$$Z = \frac{pv}{RT} = 1 + B'p + C'p^2 + \ldots\ldots\ldots [12]$$

where it is readily shown that

$$B' = B/RT \qquad C' = (C - B^2)/(RT)^2 \ldots\ldots [13]$$

The terms specific to one gas can be replaced by their generalized equivalents with the help of Equations [8], [9], and [10], and a dimensionless equation obtained

$$Z = 1 + 2/3\pi \left(\frac{B^0}{\tau}\right) \frac{r_0^3 p}{\epsilon} + (2/3\pi)^2 \left(\frac{C^0 - B^{0^2}}{\tau^2}\right) \frac{r_0^6 p^2}{\epsilon^2} + \ldots\ldots [14]$$

A reduced pressure can be defined

$$p_r' = \frac{p}{\epsilon/r_0^3} = \frac{p}{R(\epsilon/kb_0)} \ldots\ldots\ldots [15]$$

to supplement the reduced temperature τ, Equation [10]. Along a reduced isotherm

$$Z = 1 + C_1 p_r' + C_2 p_r'^2 + \ldots]_{\tau = C} \ldots\ldots [16]$$

where C_1 and C_2 are functions of the reduced temperature. Equations [10], [14], and [15] can be called a virial law of corresponding states. A generalized compressibility chart could be constructed from these equations.

To illustrate the regions where the Bird and Spotz values will depart from the experimental data, Fig. 4 has been constructed from Equation [14] for several values of T_r and plotted against p_r'. Note that each value of T_r will correspond to a value τ for one particular fluid. For this reason the substance must also be shown when representation is made in the manner of Fig. 4. The points of divergence, which are approximately[5] located in Fig. 4, are a good estimate of the areas where the Bird and Spotz integrations are not sufficiently complete to reproduce adequately the experimental data. For example, at $T_r \approx 1.2$, $p_r \approx 1.3$, the Bird and Spotz tables will begin to diverge from the experimental data (for all nonpolar, spherically symmetrical fluids).

[5] Note that Fig. 4 implies a constant relationship between the kinetic parameters and the critical constants. This approximation serves for the purpose of Fig. 4 but not for the virial charts presented here.

Although the Bird and Spotz tables are inadequate for isotherms below the Boyle point isotherm at high pressures, still, the form of Equation [16] indicates that the virial law of corresponding states should apply at all pressures. In other words, a correlation between τ and p_r' should exist such that

$$Z = f(\tau, p_r') \quad [17]$$

at any pressure. To illustrate this statement, Fig. 5 was constructed for specified ranges of pressure and temperature for N_2 such that $T_r = 1.8$ and $\tau = 2.38$ are equivalent, and $p_r = 0$ to 6 is equivalent to $p_r' = 0$ to 1.65. (The equivalence is valid only for N_2 since τ and p_r' do not bear a constant relationship to T_r and p_r for all fluids.) Fig. 5 indicates that the law expressed by Equation [17] is more accurate than the law expressed by Equation [4]. Therefore, the second set of charts is more precise than the first set if the gases essentially are nonpolar and spherical, and with slight quantum effects. (This conclusion has been substantiated by the correlation of data in constructing the charts.) For example, in Fig. 5 note that at $T_r = 1.8$, CO and CH_4 deviate by 3.1 per cent while in essentially the same temperature range, $\tau = 2.38$, the deviation is less than 1 per cent on the virial chart. Note, too, that H_2 (uncorrected) does not correlate well with other data at $T_r = 3.5$ but on the virial chart, at $\tau = 4.63$, the deviation is less than 1 per cent. But at lower temperatures the deviation for hydrogen (also, He and D_2) becomes greater. Fig. 5 illustrates that the virial law of corresponding states is more accurate than the Bird and Spotz tables when the regions of interest are beyond those indicated in Fig. 4.

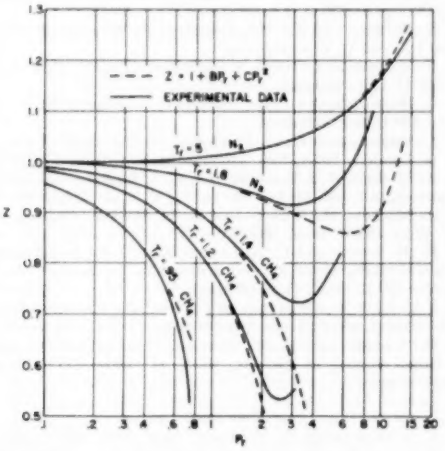

FIG. 4 CORRELATION OF VIRIAL EQUATION WITH EXPERIMENTAL DATA

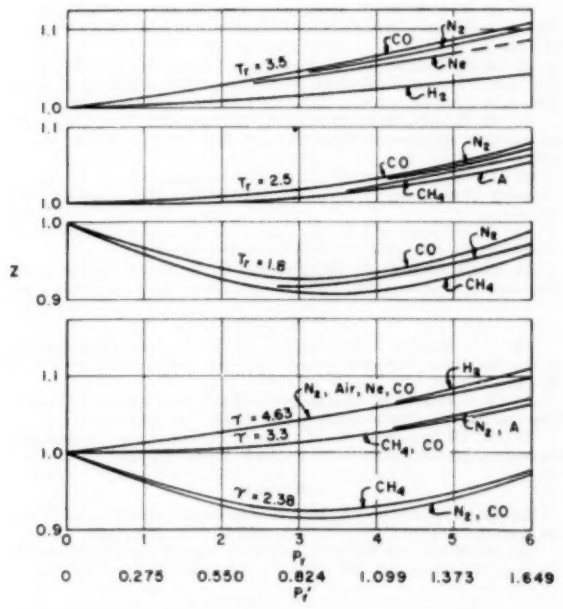

FIG. 5 EFFECT OF KINETIC VERSUS CRITICAL CONSTANT PARAMETERS ON CORRELATION AT THREE REDUCED TEMPERATURES

TABLE 3 FORCE CONSTANTS

Substance	ϵ/k, K	b_0, cc/mol	Reference
Air	102	60.34	(291)
Argon	119.8	49.80	(291)
Carbon monoxide	100.2	67.22	(291)
Hydrogen	29.2	29.76	(291)
Methane	148.2	70.16	(291)
Neon	34.9	27.10	(291)
Nitrogen	95.36	64.13	(311)
Oxygen	117.04	54.35	(311)
Xenon	221	86.94	(291)

If Equation [17] were exactly true, it would be necessary only to plot the data for one gas to obtain a chart valid for all spherical, nonpolar gases. However, as shown by Fig. 5, there are some divergences between gases, although considerably less than when plotted on the co-ordinates of Equation [4]. Hence it was considered best to average the available data to obtain the chart isotherms.

The construction of the virial charts followed the same procedures already described for the critical-constant charts and the references are listed in Table 2. For the second set, only the essentially nonpolar gases were correlated: A, Ne, Xe, air, N_2, O_2, CO, and CH_4. Above the Boyle point isotherm (approximately $\tau = 3.4$), H_2 correlated N_2, O_2, A, and CO within 1 per cent up to a reduced pressure of $p_r' = 1.45$ (essentially $p_r = 5.5$). At lower pressures where more data were available, the same degree of correlation was obtained with these gases and also with air and Ne. The excellence of correlation increased with increasing temperature. For this reason, the hydrogen data were used to construct the isotherms above $\tau = 6.5$ since no other data are available. The force constants that were used are listed in Table 3.

When the gases are highly polar or when nonsymmetry is present, the first set of charts is superior. In Fig. 6 are shown two hydrocarbons and nitrogen plotted for one reduced temperature. Note that extreme divergences are encountered—a result to be expected from theoretical considerations.

SUMMARY AND CONCLUSIONS

This paper has summarized two laws of corresponding states for the construction of generalized compressibility charts. Two new sets of charts are presented along with a complete Bibliography of original compressibility data for 30 gases. Specific points of the discussion indicated the following:

1 Generalized pvT data should be based upon critical constants when the molecular structure of the fluid is complex or for polar molecules.

2 Generalized pvT data can be correlated better by kinetic parameters when the molecular structures of the fluids are essentially spherical, and the molecules are essentially nonpolar, and quantum effects are negligible. This correlation is obtained in regions where theoretical kinetic equations cannot be applied.

3 The regions where the Bird and Spotz tables are applicable have been indicated in terms of the critical-constant parameters of reduced pressure and reduced temperature.

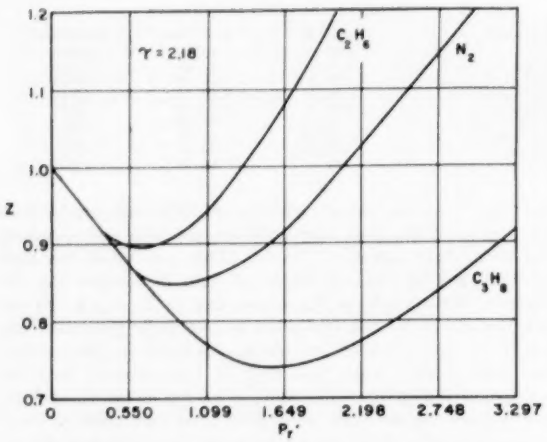

FIG. 6 EFFECT OF KINETIC PARAMETERS ON CHAIN MOLECULES

4 At temperatures below the Boyle point isotherm, H_2, He, and D_2 exhibit erratic behavior on either set of charts and the *pvT* relationships should be obtained from compressibility data for the individual gases.

ACKNOWLEDGMENT

The help of Mr. William McLean is acknowledged who assisted in the calculations and in the correlation of data.

BIBLIOGRAPHY

AIR

1 E. H. Amagat, *Annales de Chimie*, (4), 28, 274 (1873)—(250 and 320 C, 1 atm).

2 E. H. Amagat, *Annales de Chimie*, (5), 8, 270 (1876)—(10 to 12 C, 0.0085 to 0.0165 atm).

3 E. H. Amagat, Comptes Rendus des Séances de l'Academie des Sciences, 82, 914 (1876)—(10 to 12 C, 0.0085 to 0.0165 atm).

4 E. H. Amagat, *Annales de Chimie*, (5), 19, 345 (1880)—(0 C, 31.7 to 401 atm).

5 E. H. Amagat, *Annales de Chimie*, (5), 28, 464 (1883)—(100 to 290 C, 0.89 to 3.78 atm).

6 E. H. Amagat, Comptes Rendus des Séances de l'Academie des Sciences, 107, 522 (1888)—(15 C, 750 to 3000 atm).

7 E. H. Amagat, *Annales de Chimie*, 29, (6), 68 (1893)—(0 to 200 C, 1 to 3000 atm).

8 C. Antoine, Comptes Rendus des Séances de l'Academie des Sciences, 108, 141 (1889)—(144 to 191 C, 15.1 atm).

9 E. S. Burnett, Trans. ASME, vol. 58, A-136 (1936)—(30 C, 0 to 60 atm).

10 L. Holborn and H. Schultze, *Annalen der Physik*, (4), 47, 1089 (1915)—(0 to 200 C, 25 to 99 atm).

11 L. Holborn and J. Otto, *Zeitschrift für Physik*, 23, 77 (1924)—(0 to 100 C, 0 to 99 atm).

12 L. Holborn and J. Otto, *Zeitschrift für Physik*, 33, 1 (1925)—(0 to 200 C, 0 to 105 atm).

13 R. Kiyama, Review of Physical Chemistry of Japan, 19, 38 (1945)—(30 C, 97 to 4490 atm).

14 P. P. Koch, *Annalen der Physik*, 27, 311 (1908)—(—79 and 0 C, 26 to 200 atm).

15 J. Oishi, Tokyo Institute of Physical and Chemical Research, Scientific Papers, 43, 22 (June, 1949)—(0 and 100 C, 1.2 to 1.5 atm).

16 F. M. Penning, Communications From the Physical Laboratory of the University of Leiden, 166, 1 (1923)—(—145 to 20 C, 27.7 to 61.4 atm).

17 F. R. S. Rayleigh, Philosophical Transactions of the Royal Society of London, 204A, 351 (1905)—(11.4 C, 0.5 to 1 atm).

18 A. W. Witkowski, *Philosophical Magazine*, 41, 288 (1896)—(—145 to +100 C, 1 to 130 atm).

AMMONIA

19 J. A. Beattie and C. K. Lawrence, *Journal of the American Chemical Society*, 52, 6 (1930)—(75 to 325 C, 14.4 to 130.4 atm).

20 P. W. Bridgman, Proceedings of the American Academy of Arts and Sciences, 59, 173 (1924)—(30 C, 968 to 11,600 atm).

21 G. Holst, *Bulletin Association Internationale du Froid*, 6, 48 (1915)—(24 to 100 C, 3 to 21 atm).

22 F. G. Keyes, *Journal of the American Society of Refrigerating Engineers*, 7, 371 (1921)—(56 to 164 C, 22 to 40 atm).

23 F. G. Keyes, *Journal of the American Chemical Society*, 53, 965 (1931)—(0 to 210 C, 100 to 1100 atm).

24 C. H. Meyers and R. S. Jessup, *Refrigerating Engineering*, 11, 345 (1925)—(—35 to 300 C, 0.8 to 28 atm).

ARGON

25 P. W. Bridgman, Proceedings of the American Academy of Arts and Sciences, 59, 173 (1924)—(55 C, 1,936 to 14,520 atm).

26 J. Du Claux, Comptes Rendus des Séances de l'Academie des Sciences, 226, n14, 1113 (1948)—(116.62 C, 13.9 to 60.7 atm).

27 V. W. Heuse and J. Otto, *Annalen der Physik*, (5), 2, 1012 (1929)—(0 C, 0.394 to 1.182 atm).

28 L. Holborn and H. Schultze, *Annalen der Physik*, (4), 47, 1089 (1915)—(0 to 200 C, 0 to 99 atm).

29 L. Holborn and J. Otto, *Zeitschrift für Physik*, 30, 320 (1924)—(—100 to —50 C, 0 to 105 atm).

30 L. Holborn and J. Otto, *Zeitschrift für Physik*, 23, 77 (1924)—(300 to 400 C, 25 to 100 atm).

31 L. Holborn and J. Otto, *Zeitschrift für Physik*, 33, 1 (1925)—(—100 to 400 C, 0 to 105 atm).

32 I. Masson and L. G. F. Dolley, Proceedings of the Royal Society of London, 103A, 524 (1923)—(24.95 C, 5 to 125 atm).

33 A. Michels, R. J. Lunbeck, and G. J. Wolkers, Applied Scientific Research, A2, 345 (1951)—(0 to 150 C, 0 to 2500 atm).

34 A. Michels, H. Wijker, and H. K. Wijker, *Physica*, 15, 627 (1949)—(0 to 150 C, 18 to 3000 atm).

35 H. K. Onnes and C. A. Crommelin, Communications From the Physical Laboratory of the University of Leiden, No. 118b (1910)—(—150 to 20 C, 11 to 60 atm).

36 J. Oishi, Tokyo Institute of Physical and Chemical Research, Scientific Papers, 43, 22 (June 1949)—(0 and 100 C, 1.2 to 1.5 atm).

37 W. Ramsey and M. W. Travers, Philosophical Transactions of the Royal Society of London, 197A, 47 (1901)—(11.2 and 237.3 C, 30 to 100 atm).

BENZENE

38 E. J. Gornowski, E. H. Amick, and A. N. Hixon, *Industrial and Engineering Chemistry*, 39, 1348 (1947)—(240 to 355 C, 26 to 66 atm).

n-BUTANE

39 J. A. Beattie, G. L. Simard, and G. J. Su, *Journal of the American Chemical Society*, 61, 24 (1939)—(152.1 to 159.9 C, 37.3 to 37.7 atm).

40 J. A. Beattie, G. L. Smith, and G. J. Su, *Journal of the American Chemical Society*, 61, 26 (1939)—(150 to 300 C, 14.68 to 358.53 atm).

41 R. H. Olds, H. H. Reamer, B. H. Sage, and W. N. Lacey, *Industrial and Engineering Chemistry*, 36, 282 (1944)—(100 to 460 F, 0.68 to 680 atm).

42 H. W., Prengle, Jr., L. R. Greenhaus, and R. York, Jr., *Chemical Engineering Progress*, 44, 863 (1948)—(31.1 to 540 F, 0 to 300 atm).

43 B. H. Sage and W. N. Lacey, *Industrial and Engineering Chemistry*, 28, 106 (1936)—(70 to 220 F, 0 to 204 atm).

44 B. H. Sage, D. C. Webster, and W. N. Lacey, *Industrial and Engineering Chemistry*, 29, 1188 (1937)—(70 to 250 F, 1 to 204 atm).

ISOBUTANE

45 J. A. Beattie, H. G. Ingersoll, and W. H. Stockmeyer, *Journal of the American Chemical Society*, 64, 548 (1942)—(150 to 275 C, 25.7 to 254 atm).

46 J. A. Beattie, S. Marple, and J. Edwards, *Journal of Chemical Physics*, 18, 127 (1950)—(150 to 300 C, 25.7 to 303.8 atm).

47 B. H. Sage and W. N. Lacey, *Industrial and Engineering Chemistry*, 30, 673 (1938)—(70 to 250 F, 0.6 to 275 atm).

1-BUTENE

48 J. A. Beattie and S. Marple, *Journal of the American Chemical Society*, 72, 4143 (1950)—(150 to 250 C, 25 to 250 atm).

49 R. H. Olds, B. H. Sage, and W. N. Lacey, *Industrial and Engineering Chemistry*, 38, 301 (1946)—(100 to 340 F, 1 to 680 atm).

CARBON DIOXIDE

50 E. H. Amagat, *Annales de Chimie*, (5), 19, 345 (1880)—(0 C, 32 to 400 atm).

51 E. H. Amagat, Comptes Rendus des Séances de l'Academie des Sciences, (1), 93, 306 (1881)—(50 to 300 C, 0.73 to 2.85 atm).

52 E. H. Amagat, *Annales de Chimie*, (5), 22, 353 (1881)—(18.2 to 100 C, 39.5 to 416 atm).

53 E. H. Amagat, *Annales de Chimie*, (5), 28, 464 (1883)—(50 to 300 C, 1 to 4 atm).

54 E. H. Amagat, *Annales de Chimie*, (6), 29, 68 (1893)—(0 to 258 C, 30 to 1000 atm).

55 C. Antoine, Comptes Rendus des Séances de l'Academie des Sciences, (1), 108, 896 (1889)—(5 to 80 C, 1 to 20.4 atm).

56 O. C. Bridgman, *Journal of the American Chemical Society*, 49, 1130 (1927)—(0 to 100 C, 11.16 to 59.35 atm).

57 W. Cawood and H. S. Patterson, *Journal of the Chemical Society of London*, 619 (1933)—(0 to 31 C, 1.32 to 3.95 atm).

58 P. A. Guye and T. Batuecas, *Helvetica Chim Acta*, 5, 532 (1922)—(0 C, 0.2 to 1.2 atm).

59 P. A. Guye and T. Batuecas, *Journal de Chimie Physique*, 20, 308 (1923)—(0 C, 0.2 to 1.2 atm).

60 W. H. Keesom, Communications From the Physical Laboratory of the University of Leiden, No. 88 (1903)—(25 to 57 C, 63 to 138 atm).

61 C. G. Knott, Proceedings of the Royal Physical Society of Edinburgh, 30, 1 (1910)—(31 to 48 C, 1 atm).

62 O. Maass and J. H. Mennie, Proceedings of the Royal Society of London, 110A, 198 (1926)—(−70.2 to 99.9 C, 0.2 to 0.9 atm).

63 K. E. MacCormack and W. G. Schneider, *Journal of Chemical Physics*, 18, 1269 (1950)—(0 to 500 C, 1 to 50 atm).

64 A. Michels and C. Michels, Proceedings of the Royal Society of London, 153A, 201–214 (1935)—(0 to 150 C, 16 to 250 atm).

65 A. Michels, C. Michels, and H. Wouters, Proceedings of the Royal Society of London, 153A, 214–224 (1935)—(0 to 150 C, 75 to 3000 atm).

66 A. Michels, B. Blaisse, and C. Michels, Proceedings of the Royal Society of London, 160A, 358–375 (1937)—(2.85 to 40 C, 36 to 98 atm).

67 G. P. Nyhoff, A. Michels, and A. J. Gerver, Proceedings of the Koninklijke Akademie van Wetenshappen te Amsterdam, 33, 72 (1930).

68 J. Oishi, Tokyo Institute of Physical and Chemical Research, Scientific Papers, 43, 22 (June, 1949)—(0 and 100 C, 1.2 to 1.5 atm).

69 L. Rayleigh, Philosophical Transactions of the Royal Society of London, 204A, 351 (1905)—(13.8 C, 0.5 to 1 atm).

70 H. H. Reamer, B. H. Sage, and W. N. Lacey, *Industrial and Engineering Chemistry*, 36, 88 (1944)—(100 to 460 F, 0 to 680 atm).

CARBON MONOXIDE

71 E. P. Bartlett, H. C. Hetherington, H. M. Kvalnes, and T. H. Tremearne, *Journal of the American Chemical Society*, 52, 1374 (1930)—(—70 to 200 C, 0.1 to 1000 atm).

72 S. Goig, Comptes Rendus des Séances de l'Academie des Sciences, 189, 246 (1929)—(0 C, 53 to 127 atm).

73 A. Michels, J. M. Lupton, T. Wassenaar, and W. De Graff, *Physica*, 18, 121 (1952)—(0 to 150 C, 20 to 3000 atm).

74 G. A. Scott, Proceedings of the Royal Society of London, 125A, 330 (1929)—(25 C, 1 to 170 atm).

75 D. T. A. Townsend and L. A. Bhatt, Proceedings of the Royal Society of London, 134A, 502 (1931)—(0 and 25 C, 1 to 600 atm).

DEUTERIUM

76 H. J. Hoge and J. W. Lassiter, United States National Bureau of Standards *Journal of Research*, 47, 75 (1951)—(37.2 to 41.2 K, 141 to 223 atm).

77 A. Michels and M. Goudeket, *Physica*, 8, 353 (1941)—(0 to 150 C, 9 to 3000 atm).

ETHANE

78 J. A. Beattie, G. J. Su, and G. L. Simard, *Journal of the American Chemical Society*, 61, 924 (1939)—(32.2 to 32.3 C, 48.09 to 48.3 atm).

79 J. A. Beattie, G. J. Su, and G. L. Simard, *Journal of the American Chemical Society*, 61, 926 (1939)—(50 to 275 C, 60 to 350 atm).

80 J. A. Beattie, N. Poffenberger, and C. Hadlock, *Journal of Chemical Physics*, 3, 93 (1935)—(25 to 250 C, 11.1 to 192.3 atm).

81 N. Quint, *Zeitschrift für Physikalische Chemie*, 39, 14 (1902)—(14 to 50 C, 32 to 56 atm).

82 H. H. Reamer, R. H. Olds, B. H. Sage, and W. N. Lacey, *Industrial and Engineering Chemistry*, 36, 956 (1944)—(100 to 460 F, 0 to 680 atm).

83 B. H. Sage, D. C. Webster, and W. N. Lacey, *Industrial and Engineering Chemistry*, 29, 658 (1937)—(70 to 250 F, 1 to 240 atm).

ETHYL ETHER

84 J. A. Beattie, *Journal of the American Chemical Society*, 46, 342 (1924)—(150 to 325 C, 11 to 200 atm).

85 J. A. Beattie, *Journal of the American Chemical Society*, 49, 1123 (1927)—(150 to 325 C, 11.2 to 66 atm).

ETHYLENE

86 E. H. Amagat, *Annales de Chimie*, (5), 19, 345 (1880)—(0 C, 32 to 400 atm).

87 E. H. Amagat, *Annales de Chimie*, (5), 22, 353 (1881)—(16.3 to 100 C, 32.9 to 421 atm).

88 E. H. Amagat, *Annales de Chimie*, 29, 68 (1893)—(0 to 198.5 C, 1 to 1000 atm).

89 T. Batuecas, *Helvetica Chim. Acta*, 5, 544 (1922)—(0 C, 0.34 to 1.1 atm).

90 W. Cawood and H. S. Patterson, *Journal of the Chemical Society of London*, p. 619 (June, 1933)—(0 and 21 C, 1.32 to 3.95 atm).

91 C. A. Crommelin and G. H. Watts, Communications From the Physical Laboratory of the University of Leiden, No. 189C (1927)—(—1.3 to 20 C, 21 to 36 atm).

92 I. Masson and L. G. F. Dolley, Proceedings of the Royal Society of London, 103A, 524 (1923)—(24.95 C, 5 to 125 atm).

93 R. L. McIntosh, J. R. Dacey, and O. Maass, *Canadian Journal of Research*, 17B, 241 (1939)—(8.92 to 10 C, 49.45 to 50.79 atm).

94 A. Michels, J. de Grogter, and F. Niesen, *Physica*, 3, 347 (1936)—(0 to 150 C, 20 to 270 atm).

95 A. Michels and M. Geldermans, *Physica*, 9, 967 (1942)—(0 to 150 C, 20 to 270 atm).

HELIUM

96 J. D. A. Boks and H. K. Onnes, Communications From the Physical Laboratory of the University of Leiden, No. 170a (1924)—(—259 to 20 C, 15 to 65 atm).

97 P. W. Bridgman, Proceedings of the American Academy of Arts and Sciences, 59, 173 (1924)—(65 C, 2900 to 14,520 atm).

98 E. Buchmann, *Zeitschrift für Physikalische Chemie*, 163A, 461 (1933)—(13.5 to 20.4 C, 197 to 1740 atm).

99 E. S. Burnett, Trans. ASME, 58, A-136(1936)—(0 and 50 C, 0 to 140 atm).

100 F. P. Burt, Transactions of the Faraday Society, 6, 19 (1910)—(0 C, 0.194 to 1.1 atm).

101 C. W. Gibby, C. C. Tanner, and I. Masson, Proceedings of the Royal Society of London, 122A, 283 (1929)—(25 to 175 C, 30 to 125 atm).

102 W. Heuse, *Zeitschrift für Physik*, 37, 157 (1926)—(0 to 100 C, 0.5 to 1.5 atm).

103 V. W. Heuse and J. Otto, *Annalen der Physik*, 2, 1012 (1929)—(0 and 100 C, 0.394 to 1.79 atm).

104 L. Holborn and H. Schultze, *Annalen der Physik*, (4), 47, 1089 (1915)—(0 to 100 C, 0 to 52.6 atm).

105 L. Holborn and J. Otto, *Zeitschrift für Physik*, 10, 367 (1922)—(0 to 100 C, 0 to 105 atm).

106 L. Holborn and J. Otto, *Zeitschrift für Physik*, 30, 320 (1924)—(—183 to 50 C, 0 to 105 atm).

107 L. Holborn and J. Otto, *Zeitschrift für Physik*, 23, 77 (1924)—(200 to 400 C, 0 to 105 atm).

108 L. Holborn and J. Otto, *Zeitschrift für Physik*, 33, 1 (1925)—(—183 to 400 C, 0 to 105 atm).

109 L. Holborn and J. Otto, *Zeitschrift für Physik*, 38, 359 (1926)—(—258 to —183 C, 0 to 105.1 atm).

110 W. H. Keesom and J. J. M. Van Santen, Communications From the Physical Laboratory of the University of Leiden, No. 227b (1933)—(0 to 100 C, 5.5 to 16.5 atm).

111 W. H. Keesom and H. H. Kraak, Communications From the Physical Laboratory of the University of Leiden, 234e (1935)—(2.6 to 4.2 K, 0.07 to 0.34 atm).

112 W. H. Keesom and W. K. Walstra, Communications From the Physical Laboratory of the University of Leiden, No. 260e (1940)—(2.61 to 4.24 K, 0.036 to 0.93 atm).

113 J. Kistemaker and W. H. Keesom, *Physica*, 12, 227 (1946)—(1.7 to 2.7 K, 0.003 to 0.022 atm).

114 J. P. Martinez and H. K. Onnes, Communications From the Physical Laboratory of the University of Leiden, No. 164 (1923)—(20.5 C, 0.04 to 0.8 atm).

115 A. Michels and H. Wouters, *Physica*, 8, 923 (1941)—(0 to 150 C, 9 to 292 atm).

116 G. P. Nijhoff and W. H. Keesom, Communications From the Physical Laboratory of the University of Leiden, No. 188b (1927)—(—183.07 to —201.52 C, 3 to 8 atm).

117 G. P. Nijhoff, W. H. Keesom, and B. Iliin, Communications From the Physical Laboratory of the University of Leiden, 188c (1927)—(—259 to —103.6 C, 1.5 to 14 atm).

118 H. K. Onnes, Communications From the Physical Laboratory of the University of Leiden, No. 102 (1908)—(—216 to 100 C, 9 to 60 atm).

119 H. K. Onnes and J. D. A. Boks, Communications From the Physical Laboratory of the University of Leiden, No. 170b (1924)—(2.57 to 4.21 K, 0.065 to 1 atm).

120 J. Oishi, Tokyo Institute of Physical and Chemical Research, Scientific Papers, 43, 22 (June, 1949)—(0 and 100 C, 1.2 to 1.5 atm).

121 J. Otto, Handbuch der Experimental Physik, 8 (2), 143 (1929)—(0 and 100 C, 101 to 190 atm).

122 F. M. Penning and H. K. Onnes, Communications From the Physical Laboratory of the University of Leiden, No. 165c (1923)—(—258 to —205 C, 8.6 to 50 atm).

123 W. Ramsey and M. W. Travers, Philosophical Transactions of the Royal Society of London, 197A, 47 (1901)—(11.2 and 237.3 C, 28 to 100 atm).

124 W. G. Schneider, *Canadian Journal of Research*, 27B, 339 (1949)—(0 and 600 C, 6 to 80 atm).

125 F. P. G. A. J. van Agt and H. K. Onnes, Communications From the Physical Laboratory of the University of Leiden, No. 176b (1925)—(14 to 90 K, 0.05 to 1.6 atm).

126 R. Wiebe, V. L. Gaddy, and C. Heins, Jr., *Journal of the American Chemical Society*, 53, 1721 (1931)—(—70 to 200 C, 100 to 1000 atm).

n-Heptane

127 J. A. Beattie and W. C. Kay, *Journal of the American Chemical Society*, 59, 1586 (1937)—(266.8 to 267 C, 26.92 to 27.04 atm).

128 L. B. Smith, J. A. Beattie, and W. C. Kay, *Journal of the American Chemical Society*, 59, 1587 (1937)—(30 to 250 C, 7 to 351 atm).

n-Hexane

129 E. A. Kelso and W. A. Felsing, *Journal of the American Chemical Society*, 62, 3132 (1940)—(100 to 275 C, 0.1 to 10 atm).

130 G. L. Thomas and S. Young, *Journal of the Chemical Society of London*, 67, 1071 (1895)—(170 to 280 C, 9.3 to 35.9 atm).

Hydrogen

131 E. H. Amagat, *Annales de Chimie*, (4), 28, 274 (1873)—(249 to 252 C, 1 atm).

132 E. H. Amagat, *Annales de Chimie*, (5), 19, 345 (1880)—(0 C, 32 to 400 atm).

133 E. H. Amagat, *Annales de Chimie*, (5), 22, 353 (1881)—(17.7 to 100.1 C, 39.5 to 421 atm).

134 E. H. Amagat, Comptes Rendus des Séances de l'Academie des Sciences, 107, 522 (1888)—(15 C, 750 to 3000 atm).

135 E. H. Amagat, *Annales de Chimie*, (6), 29, 68 (1893)—(0 to 200 C, 1 to 3000 atm).

136 E. P. Bartlett, *Journal of the American Chemical Society*, 49, 687 (1927)—(0 C, 50 to 1000 atm).

137 E. P. Bartlett, H. L. Cupples, and T. M. Tremearne, *Journal of the American Chemical Society*, 50, 1275 (1928)—(0 to 400 C, 1 to 1000 atm).

138 E. P. Bartlett, H. C. Hetherington, H. M. Kvalnes, and T. H. Tremearne, *Journal of the American Chemical Society*, 52, 1363 (1930)—(—70 to 20 C, 0 to 1000 atm).

139 J. Bassett and R. Dupinay, Comptes Rendus des Séances de l'Academie des Sciences, 191, 1295 (1930)—(0 and 16 C, 1000 to 5000 atm).

140 P. W. Bridgman, Recueil des Travaux Chimiques des Pays-Bas, 42, 568 (1923)—(30 and 65 C, 1940 to 12,600 atm).

141 P. W. Bridgman, Proceedings of the American Academy of Arts and Sciences, 59, 173 (1924)—(30 and 65 C, 1940 to 12,600 atm).

142 C. A. Crommelin and J. C. Swallow, Communications From the Physical Laboratory of the University of Leiden, No. 172a (1924)—(—240 to —217 C, 12 to 60 atm).

143 C. A. Crommelin and J. C. Swallow, Proceedings of the Fourth International Congress of Refrigeration, 1, 53a (1924)—(—240 to —217 C, 12 to 60 atm).

144 W. J. de Haas, Communications From the Physical Laboratory of the University of Leiden, No. 127A (1912)—(20 C, 0.16 to 1.13 atm).

145 P. A. Guye and T. Batuecas, *Helvetica Chim Acta*, 5, 532 (1922)—(0 C, 0.2 to 1.2 atm).

146 P. A. Guye and T. Batuecas, *Journal de Chimie Physique*, 20, 308 (1923)—(0 C, 0.2 to 1.2 atm).

147 V. Heuse and J. Otto, *Annalen der Physik* (5), 2,1012 (1929)—(0 and 100 C, 0.5 to 1.8 atm).

148 L. Holborn, *Annalen der Physik*, 63, 674 (1920)—(0 to 100 C, 0 to 100 atm).

149 L. Holborn and J. Otto, *Zeitschrift für Physik*, 23, 77 (1924)—(200 C, 0 to 105.2 atm).

150 L. Holborn and J. Otto, *Zeitschrift für Physik*, 33, 1 (1925)—(—183 to 400 C, 0 to 105.2 atm).

151 L. Holborn and J. Otto, *Zeitschrift für Physik*, 38, 359 (1926)—(207 C, 20 to 100 atm).

152 H. L. Johnson and D. White, Trans. ASME, 72, 785 (1950)—(35 to 300 K, 1 to 200 atm).

153 P. Kohnstamm and K. W. Walstra, Proceedings of the Koninklijke Academie van Wetenschappen te Amsterdam, 17, (1), 203 (1914)—(15.5 and 20 C, 125 to 2285 atm).

154 S. H. Maran and D. Turnbull, *Industrial and Engineering Chemistry*, 34, 544 (1942)—(0 C, 100 to 1000 atm).

155 J. P. Martines and H. R. Onnes, Communications From the Physical Laboratory of the University of Leiden, No. 164 (1923)—(20.5 C, 0.09 to 0.8 atm).

156 A. Michels, G. P. Nijhoff, and A. J. J. Gervery, *Annalen der Physik*, 12, 562 (1932)—(0 to 100 C, 75 to 1200 atm).

157 A. Michels and M. Goudeket, *Physica*, 8, 347 (1941)—(0 to 150 C, 10 to 3000 atm).

158 G. P. Nijhoff and W. H. Keesom, Communications From the Physical Laboratory of the University of Leiden, No. 188d (1927)—(0 to 100 C, 32 to 60 atm).

159 G. P. Nijhoff and W. H. Keesom, Communications From the Physical Laboratory of the University of Leiden, No. 188e (1928)—(—248.3 to —225.5 C, 1.6 to 4.2 atm).

160 H. K. Onnes and H. H. F. Hyndman, Communications From the Physical Laboratory of the University of Leiden, No. 78c (1902)—(0 and 20 C, 45 to 56 atm).

161 H. K. Onnes and C. Braak, Communications From the Physical Laboratory of the University of Leiden, No. 97a (1906)—(—217 to —104 C, 0.3 to 60 atm).

162 H. K. Onnes and C. Braak, Communications From the Physical Laboratory of the University of Leiden, No. 99a (1907)—(—217 to 104 C, 14.6 to 58.3 atm).

163 H. K. Onnes and C. Braak, Communications From the Physical Laboratory of the University of Leiden, No. 100a (1908)—(—217 to —104 C, 14.6 to 58.3 atm).

164 H. K. Onnes and C. Braak, Communications From the Physical Laboratory of the University of Leiden, No. 100b (1908)—(0 and 100 C, 27.3 to 50 atm).

165 H. K. Onnes and W. J. de Haas, Communications From the Physical Laboratory of the University of Leiden, No. 127c (1912)—(—257.3 to —252.6 C, 0.07 to 0.6 atm).

166 H. K. Onnes, C. A. Crommelin, and E. I. Smid, Communications From the Physical Laboratory of the University of Leiden, No. 146b (1914)—(20 C, 60 to 100 atm).

167 H. K. Onnes, C. Dorsman, and G. Holst, Communications From the Physical Laboratory of the University of Leiden, No. 146a (1915)—(20 C, 60 to 90 atm).

168 H. K. Onnes and F. M. Penning, Communications From the Physical Laboratory of the University of Leiden, No. 165b (1923)—(—243.9 to —103.6 C, 6 to 50 atm).

169 J. Otto, Handbuch der Experimental Physik, 8 (2) 161 (1929)—(0 and 100 C, 102 to 189 atm).

170 F. M. Penning, Communications From the Physical Laboratory of the University of Leiden, No. 166 (1923)—(—244 to —104 C, 6 to 50 atm).

171 G. A. Scott, Proceedings of the Royal Society of London, 125A, 330 (1929)—(25 C, 1 to 170 atm).

172 J. C. Schalkwijk, Communications From the Physical Laboratory of the University of Leiden, No. 70 (1901)—(20 C, 1 to 60 atm).

173 D. T. A. Townend and L. A. Bhatt, Proceedings of the Royal Society of London, 134A, 502 (1931)—(0 and 25 C, 1 to 600 atm).

174 F. P. G. A. J. van Agt and H. K. Onnes, Communications From the Physical Laboratory of the University of Leiden, No. 176b (1925)—(14 to 90 K, 0.04 to 1.6 atm).

175 T. T. H. Verschoyle, Proceedings of the Royal Society of London, 111A, 552 (1926)—(0 and 20 C, 46 to 205 atm).

176 K. W. Walstra, Proceedings of the Koninklijke Academie Wetenshappen te Amsterdam, 17,203 (1914)—(15.5 and 20 C, 1 to 2200 atm).

177 R. Wiebe and V. L. Gaddy, *Journal of the American Chemical Society*, 60, 2300 (1938)—(0 to 300 C, 25 to 1000 atm).

178 A. W. Witkowski, *Krakauer Anzeiger*, 305 (1905)—(—212 to 100 C, 0 to 60 atm).

179 V. Wroblewski, *Weiner Bericht*, 11A, 97, 1346 (1888)—(—182 to 100 C, 14 to 70 atm).

180 S. A. Zhunitsyn and N. S. Rudenko, Journal of Experimental

and Theoretical Physics (U.S.S.R.), 16, 776 (1946)—(65.7 to 90.6 K, 7 to 1000 atm).

HYDROGEN SULPHIDE

181 H. H. Reamer, B. H. Sage, and W. N. Lacey, *Industrial and Engineering Chemistry*, 42, 140 (1950)—(40 to 340 F, 0 to 681 atm).

METHANE

182 E. H. Amagat, *Annales de Chimie*, (5), 22, 353 (1881)—(14.7 to 100.1 C, 39 to 300 atm).

183 F. A. Freeth and T. T. H. Verschoyle, Proceedings of the Royal Society of London, 130A, 453 (1931)—(0 and 20 C, 17.2 to 215 atm).

184 F. G. Keyes and N. G. Burk, *Journal of the American Chemical Society*, 49, 1403 (1927)—(0 to 200 C, 32.3 to 254.4 atm).

185 H. N. Kvalnes and V. L. Gaddy, *Journal of the American Chemical Society*, 53, 394 (1931)—(—70 to 200 C, 0 to 1000 atm).

186 A. Michels and G. W. Nederbragt, *Physica*, 2, 1001 (1935)—(0 to 150 C, 20 to 60 atm).

187 A. Michels and G. W. Nederbragt, *Physica*, 3, 569 (1936)—(0 to 150 C, 25 to 380 atm).

188 R. H. Olds, H. H. Reamer, W. N. Lacey, and B. H. Sage, *Industrial and Engineering Chemistry*, 35, 922 (1943)—(70 to 460 F, 0 to 686 atm).

METHYL FLUORIDE

189 A. Michels, A. Visser, R. J. Lunbeck, and G. J. Volkeas, *Physica*, 18, 114 (1952)—(0 to 150 C, 0 to 150 atm).

NEON

190 F. P. Burt, Transactions of the Faraday Society, 6, 19 (1910)—(0 C, 0.18 to 1.1 atm).

191 C. A. Crommelin, J. P. Martinez, and H. K. Onnes, Communications From the Physical Laboratory of the University of Leiden, No. 154A (1919)—(— 217 to 20 C, 22 to 93 atm).

192 V. W. Heuse and J. Otto, *Annalen der Physik*, (5), 2, 1012 (1929)—(0 C, 0.4 to 1 atm).

193 L. Holborn and J. Otto, *Zeitschrift für Physik*, 23, 77 (1924)—(0 to 400 C, 0 to 105 atm).

194 L. Holborn and J. Otto, *Zeitschrift für Physik*, 33, 1 (1925)—(—183 to 400 C, 0 to 105 atm).

195 L. Holborn and J. Otto, *Zeitschrift für Physik*, 38, 359 (1926)—(—207.9 C, 20 to 90 atm).

196 A. Michels and R. O. Gibson, *Annalen der Physik*, (4), 87, 850 (1928)—(0 to 100.8 C, 32 to 494 atm).

197 J. Oishi, Tokyo Institute of Physical and Chemical Research, Scientific Papers, 43, 22 (1949)—(0 and 100 C, 1.2 to 1.5 atm).

198 H. K. Onnes and C. A. Crommelin, Communications From the Physical Laboratory of the University of Leiden, No. 147d (1917)—(—217 to 20 C, 22 to 93 atm).

199 W. Ramsey and M. S. Travers, Philosophical Transactions of the Royal Society of London, 197A, 47 (1901)—(11.2 and 237.3 C, 39 to 94 atm).

NITROGEN

200 E. H. Amagat, *Annales de Chimie*, (5), 19, 345 (1880)—(0 C, 27.3 to 430.1 atm).

201 E. H. Amagat, *Annales de Chimie*, (5), 22, 353 (1881)—(17.7 to 100 C, 39 to 417 atm).

202 E. H. Amagat, Comptes Rendus des Séances de l'Academie des Sciences, 95, 638 (1882)—(0 to 260 C, 0 to 442 atm).

203 E. H. Amagat, Comptes Rendus des Séances de l'Academie des Sciences, 107, 552 (1888)—(15 C, 750 to 3000 atm).

204 Amagat, E. H., *Annales de Chimie et de Physique*, (6), 29, 68 (1893)—(0 to 199.5 C, 1 to 3000 atm).

205 E. P. Bartlett, *Journal of the American Chemical Society*, 49, 687 (1927)—(0 C, 50 to 1000 atm).

206 E. P. Bartlett, H. L. Cupples, and T. H. Tremearne, *Journal of the American Chemical Society*, 50, 1275 (1928)—(0 to 400 C, 1 to 1000 atm).

207 E. P. Bartlett, H. C. Hetherington, H. M. Kvalnes, and T. H. Tremearne, *Journal of the American Chemical Society*, 52, 1363 (1930)—(—70 to 20 C, 0 to 1000 atm).

208 J. Basset and R. Dupinay, Comptes Rendus des Séances de l'Academie des Sciences, 191, 1295 (1930)—(0 and 16 C, 1000 to 5000 atm).

209 M. Benedict, *Journal of the American Chemical Society*, 59, 2224 (1937)—(—175 to 200 C, 980 to 5800 atm).

210 P. W. Bridgman, Proceedings of the American Academy of Arts and Sciences, 59, 173 (1924)—(68 C, 2400 to 14,500 atm).

211 G. A. Bottomly, D. S. Massie, and F. R. S. Whytlaw-Gray, Proceedings of the Royal Society of London, 200A, 201 (1950)—(22.05 C, 0.3 to 1.1 atm).

212 J. Duclaux, Comptes Rendus des Séances de l'Academie des Sciences, 226, 2034 (1948)—(—102 C, 28.5 to 54.7 atm).

213 V. W. Heuse, *Zeitschrift für Physik*, 37, 157 (1926)—(0 and 100 C, 0.5 to 1.8 atm).

214 V. W. Heuse and J. Otto, *Annalen der Physik*, (5), 2, 1012 (1929)—(0 C, 0.5 to 1.8 atm).

215 L. Holborn and J. Otto, *Zeitschrift für Physik*, 10, 367 (1922)—(0 to 100 C, 0 to 100 atm).

216 L. Holborn and J. Otto, *Zeitschrift für Physik*, 23, 77 (1924)—(0 to 400 C, 0 to 105 atm).

217 L. Holborn and J. Otto, *Zeitschrift für Physik*, 30, 320 (1924)—(—130 to —50 C, 0 to 105 atm).

218 L. Holborn and J. Otto, *Zeitschrift für Physik*, 33, 1 (1925)—(—130 to 400 C, 0 to 105 atm).

219 F. Henning and W. Heuse, *Zeitschrift für Physik*, 5, 285 (1921)—(0 and 100 C, 0.3 to 1.8 atm).

220 S. H. Maran and D. Turnbull, *Industrial and Engineering Chemistry*, 34, 544 (1942)—(0 C, 100 to 1000 atm).

221 A. Michels, H. Wouters, and J. DeBoer, *Physica*, 1, 587 (1934)—(0 to 150 C, 19 to 85 atm).

222 A. Michels, H. Wouters, and J. DeBoer, *Physica*, 3, 585 (1936)—(0 to 150 C, 200 to 3000 atm).

223 H. K. Onnes and A. Th. van Urk, Communications From the Physical Laboratory of the University of Leiden, No. 169D (1924)—(—150 to 20 C, 23 to 60 atm).

224 J. Otto, Handbuch der Experimental Physik, 8 (2), 168 (1929)—(0 and 100 C, 99 to 189 atm).

225 J. Otto, A. Michels, and H. Wouters, *Physikalische Zeitschrift*, 35, 97 (1934)—(0 to 150 C, 45 to 415 atm).

226 W. Ramsey and M. W. Travers, Philosophical Transactions of the Royal Society of London, 197A, 47 (1901)—(11.2 and 237.3 C, 53 to 105 atm).

227 L. B. Smith and R. S. Taylor, *Journal of the American Chemical Society*, 45, 2107 (1923)—(0 to 200 C, 34 to 320 atm).

228 C. Schlatter, T. Batuecas, and G. Maverick, *Journal de Chemie Physique*, 26, 548 (1929)—(0 C, 0.3 to 1 atm).

229 T. T. H. Verschoyle, Proceedings of the Royal Society of London, 111A, 552 (1926)—(0 and 20 C, 25 to 205 atm).

230 R. Wiebe and V. L. Gaddy, *Journal of the American Chemical Society*, 60, 2300 (1938)—(0 to 300 C, 25 to 1000 atm).

NITRIC OXIDE

231 T. Batuecas, *Journal de Chimie Physique*, 22, 101 (1925)—(0 C, 0.3 to 1 atm).

232 E. Briner, H. Biedermann, and A. Rothen, *Journal de Chimie Physique*, 23, 157 (1926)—(—78.6 to 9 C, 30 to 160 atm).

233 B. H. Golding and B. H. Sage, *Industrial and Engineering Chemistry*, 43, 160 (1951)—(40 to 220 F, 0 to 170 atm).

OXYGEN

234 E. H. Amagat, *Annales de Chimie*, (5), 19, 345 (1880)—(0 C, 31 to 400 atm).

235 E. H. Amagat, Comptes Rendus des Séances de l'Academie des Sciences, 91, 812 (1880)—(14.7 and 100 C, 113 to 418 atm).

236 E. H. Amagat, Comptes Rendus des Séances de l'Academie des Sciences, 107, 522 (1888)—(15 C, 750 to 3000 atm).

237 E. H. Amagat, *Annales de Chimie et de Physique*, (6), 29, 68 (1893)—(0 to 200 C, 1 to 3000 atm).

238 E. Baxter and G. Starkweather, Proceedings of the National Academy of Science, 12, 699 (1926)—(0 C, 0.25 to 1 atm).

239 R. W. Grey and F. P. Burt, *Journal of the Chemical Society of London*, 95, 1633 (1909)—(0 C, 0.2 to 1.2 atm).

240 P. A. Guye and T. Batuecas, *Helvetica Chim. Acta*, 5, 532 (1922)—(0 C, 0.2 to 1.2 atm).

241 P. A. Guye, and T. Batuecas, *Journal de Chimie Physique*, 20, 308 (1923)—(0 C, 0.2 to 1.2 atm).

242 V. W. Heuse, *Zeitschrift für Physik*, 37, 157 (1926)—(0 and 100 C, 0.5 to 1.8 atm).

243 V. W. Heuse and J. Otto, *Annalen der Physik*, (5), 2, 1012 (1929)—(0 C, 0.4 to 1 atm).

244 L. Holborn and J. Otto, *Zeitschrift für Physik*, 10, 367 (1922)—(0 to 100 C, 0 to 105 atm).

245 L. Holborn and J. Otto, *Zeitschrift für Physik*, 33, 1 (1925)—(0 to 100 C, 0 to 105 atm).

246 H. A. Kuypers and H. K. Onnes, Communications From the Physical Laboratory of the University of Leiden, 165A (1923)—(0 and 20 C, 20 to 60 atm).

247 S. H. Maran and D. Turnbull, *Industrial and Engineering Chemistry*, 35, 544 (1942)—(0 C, 100 to 1000 atm).

248 I. Masson and L. G. F. Dolley, Proceedings of the Royal

Society of London, 103A, 524 (1923)—(24.95 C, 5 to 125 atm).

249 G. P. Nijhoff and W. H. Keesom, Communications From the Physical Laboratory of the University of Leiden, No. 179B (1925)—(—152 to —40 C, 3 to 9 atm).

250 H. K. Onnes and H. H. F. Hyndman, Communications From the Physical Laboratory of the University of Leiden, No. 78b (1902)—(0 to 20 C, 22 to 66 atm).

251 H. K. Onnes and H. A. Kuypers, Communications From the Physical Laboratory of the University of Leiden, No. 169A (1924)—(—117 to —40 C, 20 to 60 atm).

252 A. T. van Urk and G. P. Nijhoff, Communications From the Physical Laboratory of the University of Leiden, No. 169C (1925)—(0 to 20 C, 35 to 66 atm).

n-Pentane

253 J. Rose-Innes and S. Young, *Philosophical Magazine*, (5), 47, 353 (1899)—(40 to 280 C, 1 to 60 atm).

254 B. H. Sage, W. N. Lacey, and J. G. Schaafsma, *Industrial and Engineering Chemistry*, 27, 48 (1935)—(70 to 220 F, 0.7 to 205 atm).

255 B. H. Sage and W. N. Lacey, *Industrial and Engineering Chemistry*, 34, 730 (1942)—(100 to 460 F, 1 to 680 atm).

Iso-Pentane

256 P. W. Bridgman, Proceedings of the American Academy of Arts and Sciences, 66, 185 (1930)—(0 to 95 C, 0 to 9000 atm).

257 E. A. Kelso and W. A. Felsing, *Journal of the American Chemical Society*, 62, 3132 (1940)—(100 to 225 C, 5.6 to 312 atm).

258 S. Young, Proceedings of the Physical Society of London, 13, 602 (1894)—(10 to 280 C, 5.5 to 60 atm).

259 S. Young, *Zeitschrift für Physikalische Chemie*, 29, 193 (1899)—(10 to 280 C, 5.5 to 60 atm).

Propane

260 J. A. Beattie, N. Poffenberger, and C. Hadlock, *Journal of Chemical Physics*, 3, 96 (1935)—(96 to 97.2 C, 41.4 to 42.4 atm).

261 J. A. Beattie, W. C. Kay, and J. Kaminsky, *Journal of the American Chemical Society*, 59, 1589 (1937)—(96.8 to 275 C, 23 to 305 atm).

262 B. J. Chenery, H. Marchman, and R. York, *Industrial and Engineering Chemistry*, 41, 2653 (1949)—(50 to 125 C, 10 to 50 atm).

263 W. W. Deschner and G. G. Brown, *Industrial and Engineering Chemistry*, 32, 836 (1940)—(30 to 336 C, 1 to 140 atm).

264 B. A. Sage, J. G. Schaafsma, and W. N. Lacey, *Industrial and Engineering Chemistry*, 26, 1218 (1934)—(70 to 220 F, 1.5 to 204 atm).

265 B. A. Sage and W. N. Lacey, *Industrial and Engineering Chemistry*, 41, 482 (1949)—(100 to 460 F, 0 to 680 atm).

Propylene

266 H. Marchman, H. W. Prengle, and R. L. Motard, *Industrial and Engineering Chemistry*, 41, 2658 (1949)—(30 to 250 C, 10 to 215 atm).

267 W. E. Vaughn and N. P. Graves, *Industrial and Engineering Chemistry*, 32, 1252 (1940)—(0 to 300 C, 2 to 80 atm).

Water

268 H. L. Callendar, Proceedings of the Institution of Mechanical Engineers, 116, 507 (1929)—(100 to 550 C, 1 to 50 atm).

269 J. Havlicek and L. Miskovsky, *Helvetica Physica Acta*, 9, 161 (1936)—(100 to 550 C, 1 to 400 atm).

270 F. G. Keyes, L. B. Smith, and H. T. Gerry, Proceedings of the American Academy of Arts and Sciences, 69, 137 (1934)—(150 to 374 C, 4.7 to 218.2 atm).

271 F. G. Keyes, L. B. Smith, and H. T. Gerry, Proceedings of the American Academy of Arts and Sciences, 70, 319 (1936)—(100 to 550 C, 1 to 390 atm).

272 O. Maass and J. H. Mennie, Proceedings of the Royal Society of London, 110A, 198 (1926)—(94.3 to 200 C, 0.4 to 1.05 atm).

273 L. B. Smith and F. G. Keyes, Proceedings of the American Academy of Arts and Sciences, 69, 285 (1934)—(30 to 374 C, 24.2 to 344.6 atm).

Xenon

274 J. A. Beattie, R. J. Barriault, and J. S. Brierly, *Journal of Chemical Physics*, 19, 1219 (1941)—(16.7 to 300 C, 20.7 to 406.1 atm).

275 W. Ramsey and M. W. Travers, Philosophical Transactions of the Royal Society of London, 197A, 47 (1901)—(11.2 and 237.3 C, 25 to 102 atm).

Compressibility Charts

276 G. G. Brown, M. Sauders, and R. L. Smith, *Industrial and Engineering Chemistry*, 24, 512 (1932).

277 J. A. Beattie and W. H. Stockmeyer, Physical Society Report, *Progress Physics*, 7, 195 (1940).

278 W. C. Edmister, *Industrial and Engineering Chemistry*, 30, 352 (1938).

279 W. K. Lewis, *Industrial and Engineering Chemistry*, 28, 259 (1936).

280 B. F. Dodge, *Industrial and Engineering Chemistry*, 24, 1353 (1932).

281 B. F. Dodge, "Chemical Engineering Thermodynamics," McGraw-Hill Book Company, New York, N. Y., 1944.

282 R. A. Morgan and J. H. Childs, *Industrial and Engineering Chemistry*, 37, 669 (1945).

283 W. K. Lewis and C. D. Luke, *Industrial and Engineering Chemistry*, 25, 725 (1933).

284 H. C. Weber, "Thermodynamics for Chemical Engineers," John Wiley and Sons, New York, N. Y., 1939.

285 E. F. Obert, *Industrial and Engineering Chemistry*, 40, 2185 (1948).

286 G. J. Su, *Industrial and Engineering Chemistry*, 38, 803 (1946).

287 K. M. Watson and R. L. Smith, *National Petroleum News*, 28, No. 27 (1936).

288 F. D. Maslan and T. M. Littman, *Industrial and Engineering Chemistry*, 45, 1566 (1953).

Miscellaneous

289 R. B. Bird and E. L. Spotz, University of Wisconsin, CM-599 (10 May 1950).

290 J. O. Hirschfelder, R. B. Bird, and E. L. Spotz, Trans. ASME, 71, 921 (1949).

291 R. B. Bird, J. O. Hirschfelder, and E. L. Spotz, University of Wisconsin, CM-758 (15 November 1952).

292 S. Gratch, Trans. ASME, 70, 631 (1948).

293 J. P. Kuenen and A. L. Clark, Communications From the Physical Laboratory of the University of Leiden, No. 150b (1917).

294 S. Postma, Recueil des Travaux Chimiques des Pays-Bas, 39, 515 (1920).

295 C. A. Crommelin, Communications From the Physical Laboratory of the University of Leiden, No. 115 (1910).

296 J. A. Beattie, D. G. Edwards, and S. Marple, *Journal of Chemical Physics*, 17, 576 (1949).

297 J. A. Beattie, D. R. Douslin, and S. W. Levine, *Journal of Chemical Physics*, 19, 948 (1951).

298 E. Mathias and C. A. Crommelin, *Annales de Physique*, 5, 137 (1936).

299 A. S. Friedman, D. White, and H. L. Johnson, *Journal of the American Chemical Society*, 73, 1310 (1951).

300 E. Shroer, *Zeitschrift für Physikalische Chemie*, 140, 379 (1929).

301 W. B. Kay, *Journal of the American Chemical Society*, 68, 1336 (1946).

302 F. G. Keyes, R. S. Taylor, and R. L. Smith, *Journal of Mathematics and Physics*, 1, 211 (1922).

303 W. Cawood and H. S. Patterson, *Journal of the Chemical Society of London*, 1932, 2180 (1932).

304 D. White, A. S. Friedman, and H. L. Johnston, *Journal of the American Chemical Society*, 73, 5713 (1951).

305 H. J. Hoge, National Bureau of Standards, *Journal of Research*, 44, 321 (1950).

306 S. F. Pickering, National Bureau of Standards Scientific Paper No. 541 (1926).

307 S. Young, Scientific Proceedings Royal Society of Dublin, 12. 374 (1909–1910).

308 F. G. Keyes, L. B. Smith, and H. T. Gerry, Proceedings of the American Academy of Arts and Sciences, 69, 137(1934).

309 R. H. Newton, *Industrial and Engineering Chemistry*, 27, 302 (1935).

310 J. E. Lennard-Jones, Proceedings of the Royal Society of London, 106A, 463 (1924).

311 N. A. Hall and W. E. Ibele, University of Minnesota, Technical Paper No. 85 (December, 1951).

312 J. DeBoer and B. S. Blaisse, *Physica*, 14, 149 (1948).

313 W. H. Stockmeyer, *Journal of Chemical Physics*, 9, 398 (1941).

Survey of Experimental Determinations of Heat Capacity of Ten Technically Important Gases

By JOSEPH F. MASI,[1] WASHINGTON, D. C.

All of the literature reports of determinations of heat capacity of gases in the period 1925–1952, inclusive, are reviewed, and those pertaining to any of the ten gases—air, NH_3, CO_2, CO, H_2, CH_4, NO, N_2, O_2, and H_2O—are tabulated. The four direct and six indirect methods used in these measurements are described briefly. By means of graphs, the reported results for several of the gases are compared with values calculated from molecular data and an equation of state. There is included a table of the most recent values of heat capacity at 1 atm for the ten gases.

Introduction

THE specific heat is one of the most important thermodynamic properties of pure substances, and at the same time it is one of those measurable in the laboratory to a degree of confidence proportional to the expenditure of care and the refinement of technique. In the particular case of gases, accurate heat-capacity measurements, at several pressures and over a range of temperatures, are valuable in at least two ways: (*a*) They may be extrapolated to zero pressure at the several temperatures to obtain a set of values of ideal-gas heat capacities. For gases of any complexity the heat capacities thus obtained frequently may be used to decide questions of structure or vibration frequency. Once a reliable set of molecular constants is available, the zero-pressure thermodynamic properties may be calculated over a temperature range far larger than that of the heat-capacity experiments. (*b*) The values obtained for the change of heat capacity with pressure may be an order of magnitude more accurate than the same quantity calculated from data of state of good accuracy. Thus there is provided an opportunity to check or modify existing equations of state.

In the past two decades it has gradually become accepted that ideal-gas heat capacities of diatomic molecules and others of very simple structure can be calculated statistically with at least as good reliability as they can be obtained from experimental measurements. For this reason, heat capacities of several of the gases which were selected for this survey probably will not again be measured at low pressures, unless for purposes of checking an apparatus. This does not mean, however, that gas-heat-capacity measurements are no longer necessary; on the contrary, they are becoming more important both in regard to C_p^0 and equation of state, for the vast majority of substances in the vapor state, which are too complex for reliable statistical calculations.

An important milestone in the history of gas heat capacities was the publication in 1924 of Partington and Shilling's "Specific Heats of Gases" (1).[2] That volume not only gave a detailed description of each worker's method and apparatus, but also tabulated the results obtained by all workers, for a large number of gases. The present survey therefore attempts to include only the experiments which have been done since the appearance of the Partington and Shilling work. The reader should consult it for discussion of some of the classical experiments and more detailed description of apparatus and methods than can be given in this brief paper.

Experimental Methods

The quantity desired in heat-capacity measurements is generally

$$C_p = \left(\frac{\partial H}{\partial T}\right)_p$$

or

$$C_v = \left(\frac{\partial U}{\partial T}\right)_v$$

Thus, by direct measurement, the quantity of energy at constant pressure ΔH or at constant volume ΔU necessary to raise a measured mass of gas through a temperature interval ΔT is obtained. The increments are kept small so that their ratio, with small correction, can be set equal to the appropriate derivative.

For the purpose of this paper, direct determinations of the heat capacity are those which involve a calorimeter. The four methods to be described separately are the constant-flow calorimeter method, the constant-volume method, the heat-exchanger method, and the explosion method.

Indirect determinations of heat capacity are those in which another variable is measured, and may be converted to C_p or C_v only with knowledge of the equation of state, or of the heat capacity of a calibrating gas. The six methods which are to be described briefly are those which have been used for the gases discussed in this survey. They are the methods involving isentropic expansion, velocity of sound, resonance, self-sustained oscillations, flow comparison, and constant-volume comparison.

Direct Methods

Flow Calorimeter. The constant-flow electric-heating method is the only way yet devised of measuring directly absolute values of C_p. In simplest terms, the method consists in obtaining a constant, measured rate of flow of gas through a tube, then measuring the temperature of the gas at two points along the tube between which a constant measured electric power is being applied. Obtaining and measuring a constant flow rate to the desired precision, measuring temperatures which accurately represent the state of the gas, and reducing the heat leak of the calorimeter to manageable proportions are only three of the problems which are encountered, and which tend to make extremely complicated any flow calorimeter built for precision work.

Several of the early flow calorimeters are described by Partington and Shilling (1). One of the most refined of this type of ap-

---

[1] Thermodynamics Section, National Bureau of Standards; present address: Callery Chemical Company, Callery, Pa.

[2] Numbers in parentheses refer to Bibliography at end of paper.

Contributed by the Heat Transfer Division and presented at the Annual Meeting, New York, N. Y., November 29–December 4, 1953, of The American Society of Mechanical Engineers.

Note: Statements and opinions advanced in papers are to be understood as individual expressions of their authors and not those of the Society. Manuscript received at ASME Headquarters, October 23, 1953. Paper No. 53—A-206.

paratus was built by Osborne, Stimson, and Sligh (2) and used for the work on ammonia (3). A simplified version of this apparatus was described by Wacker, Cheney, and Scott (4), and shown by them to be accurate to 0.1 per cent. The apparatus now in use at the National Bureau of Standards has been shown to give similar accuracy. It is drawn in cross section in Fig. 1 and is described in detail in the Appendix. It is this apparatus which was used for recent determinations of the heat capacity of oxygen and carbon dioxide (5), Freon-12 (6), and fluorinated hydrocarbons (7, 8).

Waddington, Todd, and Huffman (9) described an all-glass flow calorimeter which has been employed extensively by the Bartlesville group of the United States Bureau of Mines, for investigations, with an accuracy of 0.1 to 0.2 per cent, of vapors of hydrocarbons and related compounds (10, 11, 12). McCullough, et al., have recently published revisions of this calorimeter (13)

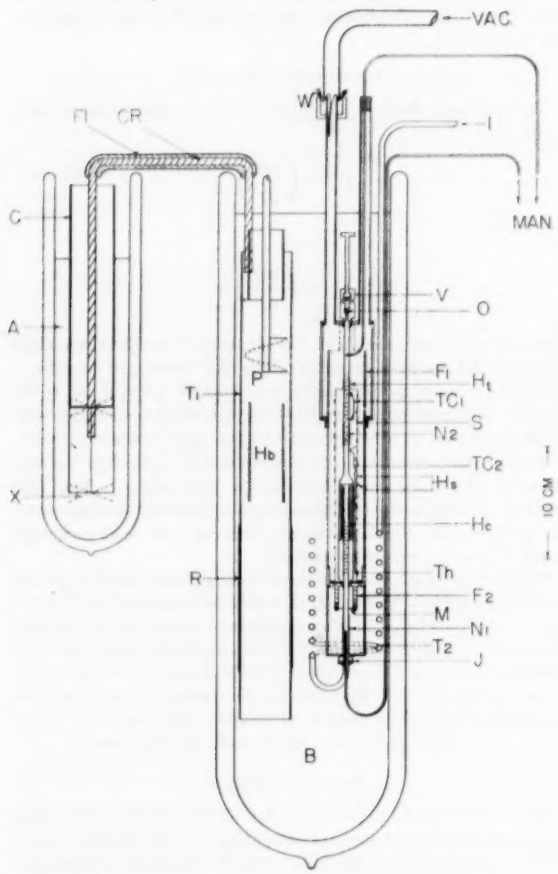

A, Liquid nitrogen
B, Constant-temperature bath
C, Protecting cylinder
CR, Copper rod
F_1, Flange
F_2, Flange
Fl, Felt insulation
H_b, Bath heater
H_c, Calorimeter heater
H_s, Shield heater
H_t, Tube heater
I, Inlet
J, Bellows seal
M, Mica spacer
MAN, Manometer tubes
N_1, Nickel thermometer
N_2, Nickel thermometer
O, Outlet
P, Propeller
R, Bath-control thermometer
S, Radiation shield
T_1, Stirrer tube
T_2, Helical tube
TC_1, Tube thermel
TC_2, Shield thermel
Th, Metal thimble
V, Throttle valve
VAC, Vacuum line
W, Wax seal
X, Vanes

FIG. 1 DIAGRAM OF NBS FLOW CALORIMETER

and precise data on the heat capacity of water vapor (14).

Other flow calorimeters in United States laboratories are those of DeVries and co-workers at Purdue University (15, 16) and Pitzer at the University of California (17). These also are of glass, operating generally at 1 atm or below, with somewhat less precision than the Bartlesville apparatus.

The flow calorimeter of Bennewitz and Schulze (18) and a modification of it built by Dailey and Felsing (19) were of a different type. In this, the temperature difference ΔT along the flow tube is maintained by two massive metal blocks, and there is measured the power required to be added to the center portion of the tube to keep the gradient linear between the two blocks. Precision is somewhat lower with this method.

Constant Volume. The method of adiabatic calorimetry, customarily applied to determination of heat capacity of solids and liquids, has not been used very much for gases because the precision is poor at ordinary densities where the heat capacity of the sample is small compared to that of the container. There is a certain appeal, however, in the simplicity of placing a weighed amount of sample in a closed container, isolating it, adding measured energy, and measuring the resultant temperature rise. Fair accuracy can be obtained if the gas is compressed to high density. A recent series of determinations of C_v of carbon dioxide has been made by Michels and Strijland (20) using this method.

Heat Exchanger. This method was devised by Workman and was used to measure the ratio of the heat capacity at a selected pressure to that at some standard pressure (e.g., 1 atm) for hydrogen, oxygen, and nitrogen (21). The method involves exchanging heat between the flowing gas at high pressure and the same gas stream after throttling to the lower pressure. The only measurements required are the temperatures of the high and low-pressure gas before and after the heat exchanger and the pressures.

Explosion. This method is no longer very often used because the corrections required are usually large and uncertain. However, the temperature range for which it yields data is above that of any other method, and so the data have importance even if the accuracy is poor. Essentially, the method consists in observing the temperature and pressure changes in a high-pressure constant-volume container during and after the occurrence of an exothermic reaction. The gas whose heat capacity is to be measured is either a compound not taking part in the reaction, or is an excess of one of the reactants. By varying the amounts of this inert gas, the mean heat capacity of the container and reaction products can be eliminated by extrapolation. The method, as can be seen, gives a mean C_v value, between the starting and maximum temperatures of the explosion. Nevitt (22) and Wohl and Magat (23) are among the workers with this method.

INDIRECT METHODS

Isentropic Expansion. In an adiabatic (isentropic) expansion of an ideal gas, the quantity $PT^{\gamma/1-\gamma}$ is a constant, and the value of γ can be obtained from an experiment in which the pressure and temperature are measured carefully just before and just after an adiabatic expansion. In the case of a real gas, however, the exponent β in the expression $PT^{\beta} = \text{const}$ can be shown readily to be

$$\beta = -\frac{C_p}{R[Z + (\partial Z/\partial T)_p]} \quad \ldots\ldots\ldots\ldots [1]$$

where $Z = PV/RT$.

Using such an expression, or equivalent ones involving γ or C_v, and appropriate equations of state, various workers have investigated the isentropic expansions of a number of gases. In

these experiments the volume of gas involved should be large and the container and temperature-measuring device should have as little mass as possible. Consequently, nearly all work has been done near 1 atm. Brinkworth (24, 25), Eucken and von Lude (26), and Kistiakowsky and Rice (27) are among the modern workers in this method.

Velocity of Sound. The velocity of sound a in a gas, when measured at sufficiently low frequency so that dispersion is not encountered, is related to the heat-capacity ratio by the equation

$$\gamma = a^2 \left(\frac{\partial \rho}{\partial P} \right)_T \quad \ldots\ldots\ldots\ldots\ldots\ldots [2]$$

Thus a knowledge of the equation of state is again required. The experimental determination of a consists usually of measuring the distance between nodes of standing waves set up by a vibration of known frequency. Partington and Shilling and their co-workers (28, 29, 30, 31, 32) were advocates of this method. Sherratt and Griffiths (33, 34), Hubbard and Hodge (35), and Cornish and Eastman (36) have improved the method and obtained greater precision. In the latter reference there is a detailed discussion of the method.

Resonance. Closely akin to the sound-velocity method is the method developed by Clark and Katz (37) in which the natural frequency of two cylindrical volumes of gas is determined by varying the frequency of vibration of a piston between them until maximum amplitude is obtained. The frequency thus found is used in the equation

$$\gamma = \frac{mV_0W_m^2}{2a^2P_0} DEGH \quad \ldots\ldots\ldots\ldots\ldots\ldots [3]$$

where m and a are the mass and area of the piston, P_0 and V_0 are the volume and pressure at equilibrium on each side of the piston, W_m is the frequency of maximum amplitude, E is the effective mass of piston and moving gas, and D, G, and H are correction factors for friction, nonideality, and nonadiabaticity (heat leak), respectively. The method was used by Katz, Leverton, and Woods (38) to determine γ for carbon dioxide and methane.

Self-Sustained Oscillations. Only slightly different from the method of Clark and Katz is that of Koehler (39) for self-sustained oscillations. In this method a ball is supported on a vertical column of gas in a smooth, uniform tube and oscillates at a frequency which is characteristic of the gas and the system. Equation [3] applies except that the factor 2 is eliminated from the denominator, and the frequency used is that of the self-sustained oscillation of the ball.

Flow Comparison. This method was developed by Blackett, Henry, and Rideal (40, 41) and used by Henry to obtain the values of C_v for air, nitrogen, and oxygen (42). In this experiment the gas flows through a tube which is thermostatted at the same constant temperature at both ends and heated at the center. Two principal measurements are taken; the rate of flow through the tube and the difference in temperature between two points placed symmetrically, as indicated by $\pm\lambda$ in Fig. 2. Measurements on two gases permit calculation of the ratio of their heat capacities to about 1 per cent.

Constant-Volume Comparison. The method developed by Trautz and Kaufmann (43) and Trautz and Blum (44) was for comparing C_v for two different gases at the same temperature. Essentially, the method involves adjusting the number of moles of the gas under investigation in a known volume until the temperature rise is the same as that of an identical vessel containing a known quantity of a standard gas, the two containers being heated with the same energy input. This method was not used extensively, since the calculations are cumbersome and the assumptions are of undetermined effect.

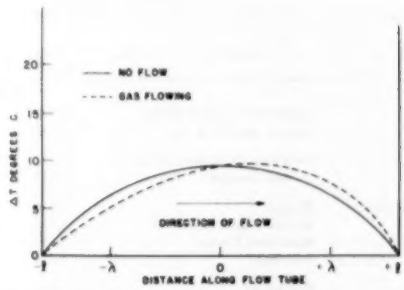

FIG. 2 FLOW-COMPARISON METHOD OF BLACKETT, HENRY, AND RIDEAL

THE EXPERIMENTS

Table 1 lists all of the literature reports giving results of heat-capacity measurements on the ten gases selected for this survey, published since 1924, the year of Partington and Shilling's book (1). The list is intended to be complete in so far as the open literature is concerned. The entries are arranged chronologically for each gas. In addition to temperature and pressure ranges of each set of experiments, estimates are given in most cases of the accuracy of the reported values of the quantity shown in the penultimate column. Great caution should prevail in the application of these estimates of accuracy. Most are those of the original authors but occasionally an estimate has been inserted on the basis of the apparent precision of the data.

The results reported by these experiments, taken as a whole, are rather sparse in the pressure direction and abbreviated in temperature range. Moreover, in the case of the uncomplicated molecules discussed here, it has now become the accepted practice to calculate statistically the zero-pressure thermodynamic properties of each gas and then apply corrections for the effect of pressure, calculated from the equation of state. For these two reasons it has seemed that this survey would possibly perform a service by presenting, in necessarily abbreviated form, a set of the latest heat-capacity values, calculated from statistics and equations of state, and then showing some examples of the comparison of the experimental heat capacities with the tabulated values.

Table 2 lists values of the dimensionless heat capacity C_p/R at 1 atm, for air, NH_3, CO_2, CO, H_2, CH_4, NO, N_2, O_2, and H_2O. The values for all except NH_3 and CH_4 are those that appear in the "NBS–NACA Tables of Thermal Properties of Gases (51)." For those eight gases, the correction for nonideality is based on equations of state which are arrived at by considering all of the experimental data including any available changes of heat capacity with pressure.

The values in Table 2 for ammonia are taken from a recent critical survey and correlation by P. Davies (52). Those for methane are from the experimental work of Eucken and von Lude (26).

Fig. 3 shows the deviations of some of the experimental heat capacities of carbon dioxide from those of Table 2. Only experiments which reported C_p are shown. Work which appeared before 1925 is plotted but is not referenced in this survey, since it is discussed thoroughly in reference (1).

Fig. 4 shows the departure of the experimental values for carbon monoxide from the NBS–NACA Tables.

Fig. 5 is a plot of C_p/R against temperature at 1 atm for nitric oxide. The values of Eucken and d'Or (50) are presented from the original work and also as recalculated, using a later equation of state (51). The curve represents the calculated values as presented in Table 2. For comparison, a portion of the ideal-gas curve is also shown.

TABLE 1 MEASUREMENTS OF GAS HEAT CAPACITY, 1925–1952

Gas	Authors	Date	Method*	Temperatures or Range °C	Pressure or Range Atm	Estimated Accuracy %	Quantity Reported	Ref.
			DIRECT DETERMINATIONS					
Air	Bennewitz and Schulze	1940	Flow	52.2, 73.5, 77.5	1		Cp	18
	Dailey and Felsing	1943	Flow	70 to 330	1	1	Cp	19
Ammonia	Osborne, Stimson, Sligh and Cragoe	1925	Flow	-15 to 150	0.5 to 20	0.1	Cp	3
Carbon Dioxide	Newitt	1929	Expl.	2900	?	2	Cv (mean)	22
	Michels and Strijland	1950	Cv	20 to 40	60 to 190	1	Cv	20
	Masi and Petkof	1952	Flow	-30 to 90	0.5 to 1.5	0.1	Cp	5
	Schrock	1952	Flow	35 to 550	1 to 67	0.5	Cp	45
Hydrogen	Workman	1931	Exch.	50	10 to 130	0.2	$Cp/(Cp)_o$	21
	Wohl and Magat	1932	Expl.	2200 to 2550	1 and 3	1	Cv (mean)	23
Nitrogen	Newitt	1929	Expl.	2327 to 2727	?	2	Cv (mean)	22
	Mackey and Krase	1930	Flow	30 to 150	50 to 800	1	Cp	46
	Workman	1931	Exch.	26 and 60	10 to 130	0.2	$Cp/(Cp)_o$	21
Oxygen	Workman	1931	Exch.	26 and 60	10 to 130	0.2	$Cp/(Cp)_o$	21
	Wacker, Cheney and Scott	1947	Flow	-30 to 90	1	0.1	Cp	4
	Masi and Petkof	1952	Flow	-30 to 50	1	0.1	Cp	5
Steam	Newitt	1929	Expl.	2327 to 2727	?	2	Cv (mean)	22
	Wohl and Magat	1932	Expl.	2000 to 2600	1	1	Cv (mean)	23
	Maxwell and Wheeler	1933	Expl.	1400 to 2450	?	5	Cv (mean)	47
	McCullough, Bennington and Waddington	1952	Flow	90 to 215	0.2 to 1	0.1	Cp	14
			INDIRECT DETERMINATIONS					
Air	Brinkworth	1925	Exp.	-118°, -78, 17	1		γ	24
	Shilling and Partington	1928	Vel.	0 to 1300	1		γ, Cp, Cv	31
	Eucken and von Lude	1929	Exp.	0 to 210	1	0.3	Cp	26
	Trautz and Kaufmann	1930	Cv Comp.	20	1	0.2	Cv	43
	Henry	1931	Flow Comp.	20 to 370	1	1	Cv	42
	Hubbard and Hodge	1937	Vel.	27	1 to 100	0.5	γ	35
	Kistiakowsky and Rice	1939	Exp.	0 to 100	1	0.3	Cp	27
Carbon Dioxide	Eucken and von Lude	1929	Exp.	0 to 270	1	0.5	Cp	26
	King and Partington	1930	Vel.	15 to 1000	1		γ, Cp, Cv	32
	Trautz and Blum	1933	Cv Comp.	15.3, 18, 19	1	0.3	Cv	44
	Sherratt and Griffiths	1936	Vel.	0 to 1000	1	1	Cv	34
	Hubbard and Hoge	1937	Vel.	27	1 to 60	0.5	γ	35
	Kistiakowsky and Rice	1939	Exp.	27, 58, and 95	1	0.3	Cp	27
	Katz, Leverton and Woods	1949	Res.	29.9	1.2 to 8.2	0.2	γ, γ_o	38
	Koehler	1950	Osc.	25	1	0.2	γ	39
	Noury	1952	Vel.	31	60 to 100	5	γ	48
Carbon Monoxide	Partington and Carroll	1925	Vel.	10.3	1	1	γ, Cp, Cv	28
	Eucken and von Lude	1929	Exp.	24 to 207	1	0.3	Cp	26
	Sherratt and Griffiths	1934	Vel.	1000 to 1800	1	0.5	C_v^o	33
Hydrogen	Brinkworth	1925	Exp.	-183, -78, 17	1	0.5	γ	24
	Partington and Howe	1925	Vel.	25	1		γ	29
	Cornish and Eastman	1928	Vel.	-192 to 100	< 1	0.5	C_v^o/R	36
	Eucken and Mucke	1932	Exp.	203, 354, 514	10	0.5	Cp	49
	Koehler	1950	Osc.	25	1	0.1	γ	39
Methane	Eucken and von Lude	1929	Exp.	25 to 207	1	1	Cp	26
	Katz, Leverton and Woods	1949	Res.	25.1	1.5 to 5.3	0.1	γ, γ_o	38
	Koehler	1950	Osc.	25	1	0.1	γ	39
Nitric Oxide	Eucken and d'Or	1932	Exp.	-146 to -95	1	1	C_p^o	50
Nitrogen	Brinkworth	1926	Exp.	-183, -78, 17	1		γ	25
	Shilling and Partington	1928	Vel.	20 to 1000	1	1	γ, Cp, Cv	31
	Eucken and von Lude	1929	Exp.	31 to 207	1	0.3	Cp	26
	Henry	1931	Flow Comp.	20 to 370	1	1	Cv	42
	Koehler	1950	Osc.	25	1	0.1	γ	39
Oxygen	Shilling and Partington	1928	Vel.	20 to 1000	1	1	γ, Cp, Cv	31
	Eucken and von Lude	1929	Exp.	27 to 207	1	0.3	Cp	26
	King and Partington	1930	Vel.	950 to 1200	1	1	γ, Cp, Cv	32
	Henry	1931	Flow Comp.	20 to 370	1	1	Cv	42
	Koehler	1950	Osc.	25	1	0.1	γ	39

*The methods listed in the text are abbreviated in this column as follows:

Cv = Constant Volume. Cv comp. = Constant-volume comparison. Exch. = Heat exchanger; Exp. = Isentropic expansion; Expl = Explosion. Flow = Flow calorimetry. Flow comp. = Flow comparison. Osc. = Self-sustained oscillations. Res. = Resonance. Vel. = Velocity of sound.

TABLE 2 C_p/R AT 1-ATM FOR TEN GASES

T, °K	Air	Ammonia	Carbon Dioxide	Carbon Monoxide	Hydrogen	Methane	Nitric Oxide	Nitrogen	Oxygen	Steam
100	3.5824				2.722			3.613	3.647	
150	3.5205				3.056		3.871	3.5288	3.5347	
200	3.5062			3.517	3.282		3.686	3.5146	3.5190	
250	3.5027		4.261	3.512	3.408		3.626	3.5094	3.5214	
300	3.5059	4.424	4.512	3.511	3.470	4.35	3.599	3.5058	3.5403	
350	3.5160	4.521	4.753	3.517	3.499	4.74	3.594	3.5115	3.5759	
400	3.5333	4.685	4.933	3.532	3.511	5.10	3.607	3.5207	3.6243	4.355
450	3.5577	4.866	5.188	3.554	3.516	5.44	3.634	3.5365	3.6811	4.284
500	3.5882	5.056	5.373	3.585	3.519	5.77	3.670	3.5595	3.7415	4.294
550	3.6230	5.242	5.542	3.622	3.523		3.713	3.5884	3.8023	4.335
600	3.6626	5.423	5.695	3.662	3.527		3.760	3.6225	3.8611	4.391
700	3.7455		5.963	3.750	3.541		3.854	3.6998	3.9681	4.522
800	3.8281		6.187	3.838	3.563		3.943	3.7812	4.0583	4.665
900	3.906		6.375	3.919	3.594		4.021	3.8600	4.1332	4.8096
1000	3.979		6.532	3.991	3.633		4.089	3.9329	4.1952	4.9607
1100	4.046		6.664	4.054	3.678		4.147	3.9985	4.2472	5.1807
1200	4.109		6.775	4.110	3.727		4.196	4.0564	4.2915	5.2510
1300	4.171		6.871	4.158	3.780		4.238	4.1074	4.3302	5.3856
1400	4.230		6.952	4.199	3.833		4.274	4.1520	4.3653	5.5125
1500	4.289		7.021	4.236	3.885		4.306	4.1910	4.3976	5.6282
1600	4.352			4.267	3.936		4.332	4.2253	4.4283	5.7357
1700	4.418			4.294	3.985		4.356	4.2555	4.4579	5.8346
1800	4.487			4.319	4.033		4.377	4.2822	4.4869	5.9255
1900	4.566			4.340	4.080		4.395	4.3058	4.5154	6.0088
2000	4.662			4.359	4.124		4.412	4.3269	4.5437	6.0854
2100	4.781			4.376	4.165		4.426	4.3458	4.5716	6.1560
2200	4.947			4.391	4.204		4.440	4.3627	4.5993	6.2212
2300	5.179			4.405	4.241		4.452	4.3780	4.6268	6.2816
2400	5.484			4.418	4.276		4.464	4.3920	4.6540	6.3378
2500	5.882			4.429	4.310		4.474	4.4047	4.6808	6.3902
2600	6.40			4.440	4.342		4.484	4.4163	4.7071	6.4392
2700	7.06			4.450	4.373		4.493	4.4270	4.7328	6.4851
2800	7.87			4.459	4.402		4.502	4.4369	4.7579	6.5282
2900	8.86			4.468	4.430		4.510	4.4460	4.7824	6.5690
3000	9.96			4.476	4.458		4.518	4.4545	4.8062	6.6074
R, cal.g^{-1} deg K^{-1}	.068604	.116674	.045153	.070946	.985709	.123874	.066222	.070930	.062100	.110301
R, Btu lb^{-1} deg R^{-1}	.068559	.116598	.045123	.070899	.985059	.123798	.066179	.070884	.062059	.110229

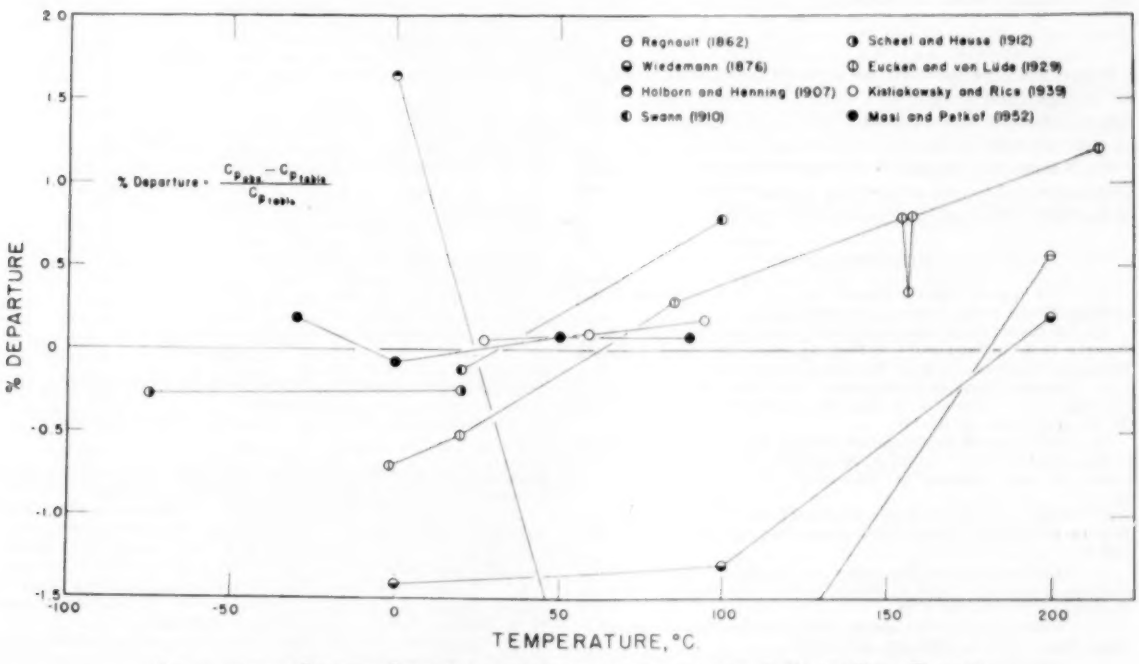

FIG. 3 CARBON DIOXIDE—DEVIATION OF SOME EXPERIMENTAL 1-ATM C_p VALUES FROM TABLE 2

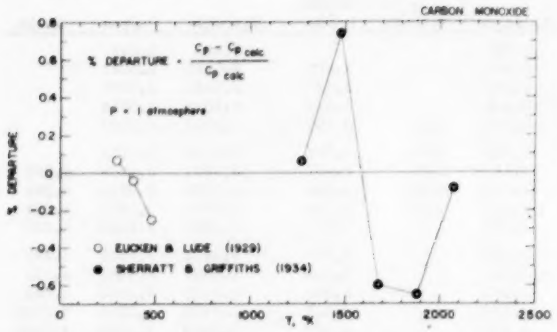

FIG. 4 CARBON MONOXIDE—DEVIATION OF EXPERIMENTAL 1-ATM C_p VALUES FROM TABLE 2

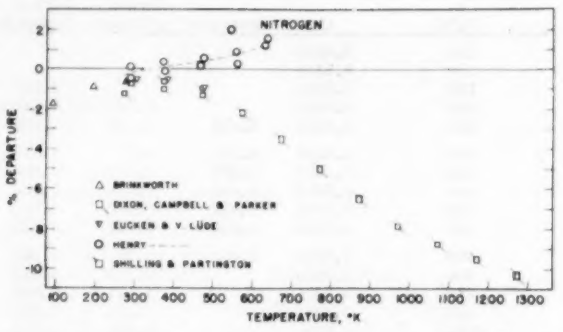

FIG. 6 NITROGEN—DEVIATION OF EXPERIMENTAL 1-ATM C_p VALUES FROM TABLE 2

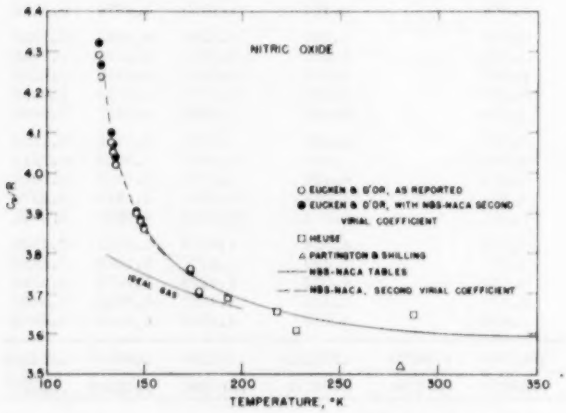

FIG. 5 NITRIC OXIDE—EXPERIMENTAL AND CALCULATED VALUES OF C_p AT 1 ATM

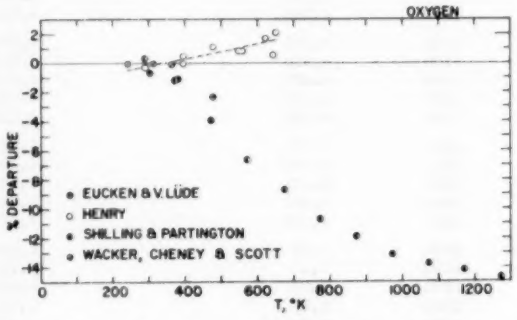

FIG. 7 OXYGEN—DEVIATION OF EXPERIMENTAL 1-ATM C_p VALUES FROM TABLE 2

Figs. 6 and 7 are the deviation plots for the experimental data for nitrogen and oxygen at 1 atm. The low values for the velocity-of-sound method appear to be caused chiefly by use of an incorrect value of the velocity of sound in air as a reference.

Fig. 8 shows the comparison between Workman's experimental heat capacity of oxygen at moderate pressure (21) and the values of the NBS–NACA tables, represented by the curves.

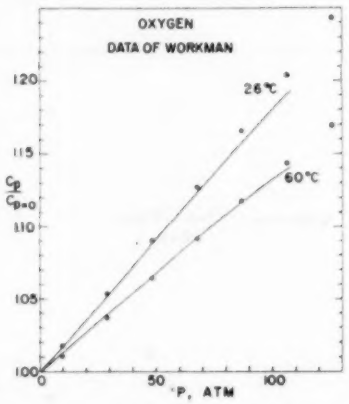

FIG. 8 OXYGEN—SHOWING DEPENDENCE OF HEAT CAPACITY UPON PRESSURE
(Circles are data of Workman; curves from NBS–NACA Tables.)

BIBLIOGRAPHY

1 "The Specific Heats of Gases," by J. R. Partington and W. G. Shilling, Ernest Penn, London, England, 1924.

2 "A Flow Calorimeter for Specific Heats of Gases," by N. S. Osborne, H. F. Stimson, and T. S. Sligh, Jr., Scientific Papers, National Bureau of Standards, vol. 20, No. 503, 1925, pp. 119–151.

3 "Specific Heat of Superheated Ammonia Vapor," by N. S. Osborne, H. F. Stimson, T. S. Sligh, Jr., and C. S. Cragoe, Ibid., vol. 20, No. 501, 1925, pp. 65–110.

4 "Heat Capacities of Gaseous Oxygen, Isobutane, and 1-Butene From −20 to 90° C," by P. F. Wacker, R. K. Cheney, and R. B. Scott, National Bureau of Standards, Ibid., vol. 38, 1947, p. 651.

5 "Heat Capacity of Gaseous Carbon Dioxide," by J. F. Masi and B. Petkof, National Bureau of Standards, Ibid., vol. 48, 1952, pp. 179–187.

6 "Thermodynamic Properties of Gaseous Difluorodichloromethane (Freon-12)," by J. F. Masi, *Journal of the American Chemical Society*, vol. 74, 1952, p. 4738.

7 "Heat Capacity of Gaseous Perfluorocyclobutane," by J. F. Masi, Ibid., vol. 75, 1953, pp. 5082–5084.

8 "Heat Capacity of Gaseous Hexafluoroethane," by J. S. Wicklund, H. W. Flieger, Jr., and J. F. Masi, National Bureau of Standards, *Journal of Research*, vol. 51, 1953, pp. 91-92.

9 "An Improved Flow Calorimeter. —Experimental Vapor Heat Capacities and Heats of Vaporization of Heptane and 2, 2, 3-Trimethylbutane," by G. Waddington, S. S. Todd, and H. M. Huffman *Journal of the American Chemical Society*, vol. 69, 1947, pp. 22–30.

10 "Experimental Vapor Heat Capacities and Heats of Vaporization of Hexane and 2, 2-Dimethylbutane," by G. Waddington and D. R. Douslin, Ibid., vol. 69, 1947, pp. 2275–2279.

11 "Experimental Vapor Heat Capacities and Heats of Vaporization of 2-Methylpentane, 3-Methylpentane, and 2, 3-Dimethylbu-

tane," by G. Waddington, J. C. Smith, D. W. Scott, and H. M. Huffman, *Journal of the American Chemical Society*, vol. 71, 1949, pp. 3902–3906.

12 "Thiacyclobutane: Heat Capacity, Heat of Transition, Fusion and Vaporization, Vapor Pressure, Entropy, Heat of Formation, and Thermodynamic Functions," by D. W. Scott, H. L. Finke, W. N. Hubbard, J. P. McCullough, C. Katz, M. E. Gross, J. F. Messerly, R. E. Pennington, and G. Waddington, Ibid., vol. 75, 1953, p. 2795.

13 "The Thermodynamic Properties of 2-Methyl-2-Propanethiol from 0° to 1000° K," by J. P. McCullough, D. W. Scott, H. L. Finke, W. N. Hubbard, M. E. Gross, C. Katz, R. E. Pennington, J. F. Messerley, and G. Waddington, Ibid., vol. 75, 1953, pp. 1818–1824.

14 "A Calorimetric Determination of the Vapor, Heat Capacity, and Gas Imperfection of Water," by J. P. McCullough, R. E. Pennington, and G. Waddington, Ibid., vol. 74, 1952, p. 4439.

15 "Heat Capacity of Organic Vapors, III. A Comparison of Flow Calorimeters," by J. B. Montgomery and T. DeVries, Ibid., vol. 64, 1942, p. 2372.

16 "Heat Capacity of Organic Vapors. VIII. Data for Some Aliphatic Alcohols Using an Improved Flow Calorimeter Requiring Only 25 ml. of Sample," by G. C. Sinke and T. DeVries, Ibid., vol. 75, 1953, p. 1815.

17 "The Heat Capacity of Gaseous Paraffin Hydrocarbons, Including Experimental Values for n-Pentane and 2, 2-Dimethylbutane," by K. S. Pitzer, Ibid., vol. 63, 1941, p. 2413.

18 "A New Method for Determining Specific Heats of Gases and Vapors," by K. Bennewitz and O. Schulze, *Zeitschrift für Physikalische Chemie*, vol. A186, 1940, pp. 299–313.

19 "Heat Capacities at Higher Temperatures of Ethane and Propane," by B. P. Dailey, with W. A. Felsing, *Journal of the American Chemical Society*, vol. 65, 1943, p. 42.

20 "Specific Heat at Constant Volume of Carbon Dioxide in the Neighborhood of the Critical Point," by A. Michels and J.C. Strijland, *Physica*, vol. 16, 1950, p. 813.

21 "The Variation of the Specific Heats (C_p) of Oxygen, Nitrogen, and Hydrogen With Pressure," by E. J. Workman, *The Physical Review*, vol. 37, 1931, pp. 1345–1355.

22 "Heats of Nitrogen, Steam, and Carbon Dioxide at High Temperatures," by D. M. Nevitt, Proceedings of the Royal Society, London, England, series A, vol. 125, 1929, pp. 119–134.

23 "Specific Heat and Dissociation of Gases at High Temperatures," by K. Wohl and M. Magat, *Zeitschrift für Physikalische Chemie*, vol. B19, 1932, pp. 117–138.

24 "The Measurement of the Ratio of the Specific Heats Using Small Volumes of Gas. The Ratios of the Specific Heats of Air and of Hydrogen at Atmospheric Pressure and at Temperatures Between 20° and —183° C," by J. H. Brinkworth, Proceedings of the Royal Society, London, England, series A, vol. 107, 1925, pp. 510–543.

25 "The Ratios of the Specific Heats of Nitrogen at Atmospheric Pressure and at Temperatures Between 10° and —183° C," by J. H. Brinkworth, Proceedings of the Royal Society, London, England, series A, vol. 111, 1926, pp. 124–133.

26 "The Specific Heats of Gases at Medium and High Temperatures. I. The Specific Heat of the Gases: Air, Nitrogen, Oxygen, Carbon Monoxide, Carbon Dioxide, Nitrous Oxide, and Methane," by A. Eucken and K. von Lude, *Zeitschrift für Physikalische Chemie* vol. B5, 1929, pp. 413–441.

27 "Gaseous Heat Capacities. I. The Method and Heat Capacities of C_2H_4 and C_2D_4," by G. B. Kistiakowsky and W. W. Rice, *Journal of Chemical Physics*, vol. 7, 1931, pp. 281–288.

28 "The Specific Heats of Carbon Monoxide and Hydrocyanic Acid Vapor," by J. R. Partington and J. F. Carroll, *The Philosophical Magazine*, London, England, (6), vol. 49, 1925, pp. 1665–1680.

29 "The Ratio of the Specific Heats of Hydrogen," by J. R. Partington and A. B. Howe, Proceedings of the Royal Society, London, England, series A, vol. 109, 1925, pp. 286–291.

30 "Velocity of Sound in Steam, Nitrous Oxide, and Carbon Dioxide With Reference to the Temperature Coefficients of the Molecular Heats," by W. G. Shilling, *The Philosophical Magazine*, (7), vol. 3, 1927, pp. 273–301.

31 "Measurements of the Velocity of Sound in Air, Nitrogen, and Oxygen, With Special Reference to the Temperature Coefficients of the Molecular Heats," by W. G. Shilling and J. R. Partington, *The Philosophical Magazine* (7), vol. 6, 1928, pp. 920–929.

32 "Measurement of Sound Velocity in Air, Oxygen, and Carbon Dioxide at Temperatures From 900° to 1200° C With Special Reference to the Temperature Coefficient of the Molecular Heats," by F. E. King and J. R. Partington, *The Philosophical Magazine* (7), vol. 9, 1930, pp. 1020–1026.

33 "The Determination of the Specific Heats of Gases at High Temperatures by the Velocity of Sound Method. V. Carbon Monoxide," by G. G. Sherratt and E. Griffiths, Proceedings of the Royal Society, London, England, series A, vol. 147, 1934, pp. 292–308.

34 "The Determination of the Specific Heat of Gases at High Temperatures by the Sound Velocity Method. II. Carbon Dioxide," by G. G. Sherratt and E. Griffiths, Proceedings of the Royal Society, London, England, series A, vol. 156, 1936, pp. 504–517.

35 "Ratio of Specific Heats of Air, N_2, and CO_2 as a Function of Pressure by the Ultrasonic Method," by J. C. Hubbard and A. H. Hodge, *Journal of Chemical Physics*, vol. 5, 1937, pp. 978-979.

36 "The Specific Heat of Hydrogen Gas at Low Temperature From the Velocity of Sound, and Precision Method of Measuring the Frequency of An Oscillating Circuit," by R. E. Cornish and E. D. Eastman, *Journal of the American Chemical Society*, vol. 50, 1928, pp. 627–652.

37 "Resonance Method for Measuring the Ratio of the Specific Heats of a Gas, C_p/C_v," by A. L. Clark and L. Katz, *Canadian Journal of Research*, vol. 18A, 1940, pp. 23–38; vol. 21A, 1943, pp. 1–17.

38 "The Resonance Method of Measuring the Ratio of the Specific Heats of a Gas, C_p/C_v. VI. Carbon Dioxide, Nitrous Oxide, and Methane," by L. Katz, W. F. Leverton, and S. B. Woods, *Canadian Journal of Research*, vol. 27A, 1949, pp. 39–44.

39 "The Ratio of the Specific Heats of Gases, C_p/C_v, by a Method of Self-Sustained Oscillations," by W. F. Koehler, *Journal of Chemical Physics*, vol. 18, 1950, pp. 465–472.

40 "A Flow Method for Comparing the Specific Heats of Gases. I. The Experimental Method," by P. M. S. Blackett, P. S. H. Henry, and E. K. Rideal, Proceedings of the Royal Society, London, England, series A, vol. 126, 1930, pp. 319–332.

41 "A Flow Method for Comparing the Specific Heats of Gases. II. The Theory of the Method," by P. M. S. Blackett, P. S. H. Henry, and E. K. Rideal, Ibid., series A, vol. 126, 1930, pp. 333–354.

42 "Specific Heats of Air, Oxygen, and Nitrogen, From 20° to 370° C," by P. S. H. Henry, Ibid., series A, vol. 133, 1931, pp. 492–506.

43 "Criticism of the Electrical Difference Method of Measuring C_v of Gases. IV. Measurements, the Standardization With Argon," by M. Trautz and F. Kaufmann, *Annalen der Physik* (5), vol. 5, 1930, pp. 581–605.

44 "Criticism of the Electrical Differential Method of Measuring C_v of Gases. V. New Measurements; C_v of Carbon Dioxide," by M. Trautz and H. Blum, *Annalen der Physik* (5), vol. 16, 1933, pp. 362–376.

45 "Calorimetric Determination of Constant-Pressure Specific Heats of Carbon Dioxide at Elevated Pressures and Temperatures," by V. E. Shrock, NACA Technical Note 2838, December, 1952.

46 "Specific Heats of Gases at High Pressures. III. Results for Nitrogen to 150° C and 700 Atmospheres," by B. H. Mackey and N. W. Krase, *Industrial and Engineering Chemistry*, vol. 22, 1930, pp. 1060–1062.

47 "Explosions of Mixtures of Hydrogen and Air. The Specific Heats of Steam at High Temperatures," by G. B. Maxwell and R. V. Wheeler, *Journal of the Chemical Society*, 1933, pp. 882–885.

48 "The Specific Heat Ratio, γ, for Carbon Dioxide in the Critical Region," by Jack Noury, Compte Rendus, vol. 234, 1952, 1036.

49 "The Determination of True Specific Heats of Several Gases at High Temperatures by the Lummer-Pringsheim Method," by A. Eucken and O. Mucke, *Zeitschrift für Physikalische Chemie*, vol. B18, 1932, pp. 167–188.

50 "The Molecular Heats of Gaseous Nitric Oxide at Low Temperatures," by A. Eucken and L. d'Or. *Nachreisen die Gesellschaften der Wissenschaft, Göttingen*, vol. 1932, p. 107.

51 "NBS–NACA Tables of Thermal Properties of Gases," Joseph Hilsenrath, editor, National Bureau of Standards, Washington, D. C., to be published.

52 "The Thermodynamic Properties of Ammonia to 1100 Atmospheres," by P. Davies, Heat Division Paper No. 26, Mechanical Engineering Research Organization, DSIR, London, England.

53 "Note on the Resonance Method of Measuring the Ratio of the Specific Heats of a Gas, C_p/C_v," by H. W. Woolley, *Canadian Journal of Physics*, vol. 31, 1953, pp. 604–612.

Appendix

Description of Flow Calorimeter. As an example of the method and apparatus which is now most favored for obtaining precise heat-capacity measurements, the flow calorimeter in use at the National Bureau of Standards is described briefly. The calorimeter proper, with its constant-temperature bath, is shown in Fig. 1.

The necessary heater, refrigeration, control thermometer, and stirrer for the bath are shown in the left part of the large Dewar

flask in the figure. The temperature of the bath is controlled automatically and remains constant within ±0.001 deg for the period of a heat-capacity determination or longer.

The flow calorimeter is made of metal. The center tube, which is the calorimeter, is thin-walled Monel. The calorimeter is protected as much as possible from heat leaks by polishing the various surfaces, by having high vacuum in the jacket, and by maintaining the surrounding radiation shield S and the upper tube very near the calorimeter temperature.

The gas entering the calorimeter at I is brought to bath temperature in the helix, its temperature is measured at N_1, electrical energy is added by means of the heater H_c, and the temperature is again measured at N_2. N_1 and N_2 are nickel-resistance thermometers. The power and rate of flow are adjusted so that the rise in temperature is close to a selected value, usually 10 deg C.

If the gas under investigation has a vapor pressure at 0 C in excess of 3 atm, the sample is contained in a steel cylinder in an ice-water bath (not shown in Fig. 1). Reduction in pressure is accomplished, and the rate of flow is controlled accurately by means of a sensitive diaphragm valve. The mean pressure and pressure drop in the calorimeter are observed by means of a three-column manometer, two columns of which are connected to the calorimeter as shown in Fig. 1.

The gas is led from the calorimeter at O to a receiver at liquid-nitrogen temperature, through a snap-throw valve which is used to divert the flow, within 0.1 sec, from one receiver to another.

A heat-capacity experiment consists of taking data during a steady-state period when the gas is removing heat at the same rate it is being added. Nearly continuous measurements are made of the exit temperature at N_2, and slight adjustments of the flow are made to keep that temperature as constant as possible. The experiment is begun and ended by directing the flow of gas into and away from a weighed receiver by means of the snap-throw valve. The readings of N_2 are identical at these two moments so that there is no gain or loss of energy by the calorimeter. Readings of the current and potential in the heater, the resistance of N_1 and a platinum-resistance thermometer in the bath, height of the manometer columns, barometer, time interval to 0.01 sec, and weight of sample to 1 mg are the other data obtained. A G-2 Mueller bridge is used for the measurement of resistances, and a sensitive five-dial potentiometer, with calibrated standard resistor and volt box, is used for the energy measurements.

In order to eliminate, as far as possible, the effect of residual heat leaks, the heat capacity is determined at a number of different flow rates at each temperature and pressure of measurement and extrapolated to zero reciprocal rate of flow. Also, "blank" determinations are made at several rates at each temperature and pressure, to measure the small amount of cooling δT experienced by the gas in passing through the calorimeter when no heat is applied.

If W is the power supplied to the heater, F is the rate of flow of the gas, ΔT is the observed rise in temperature, and δT is the fall in temperature in a corresponding blank experiment, the apparent heat capacity is calculated by

$$C = \frac{W}{F(\Delta T + \delta T)}$$

The value of C is corrected for the deviation of the observed mean pressure and mean temperature from the nominal values. The corrected values of C are then plotted against the reciprocal of the rate of flow and extrapolated linearly to infinite rate to eliminate the small heat leak (if any) and arrive at the correct C_p for the temperature and pressure being considered.

Results of Service Test Program on Transition Welds Between Austenitic and Ferritic Steels at the Philip Sporn and Twin Branch Plants

By G. E. LIEN,[1] F. EBERLE,[2] and R. D. WYLIE[3]

A test program was set up to give advance operating information on the dissimilar-metal welds installed on the American Gas and Electric Company (AG&E) System in the units of the Philip Sporn Plant of Appalachian Electric Power Company, The Ohio Power Company, and in unit No. 5 of the Twin Branch Plant of the Indiana & Michigan Electric Company. After cycling weld-test vessels, small surface notches and subsurface cracks have formed at the fusion line between the austenitic weld metal and the ferritic pipe. The program and findings to date are described in this paper.

Introduction

TRANSITION welds between austenitic and ferritic steels have been a source of interest and discussion as to their suitability and strength for high-temperature service. The difference in expansion coefficients has been the main disturbing element which would tend to promote failure of a welded joint under temperature variations. A number of excellent test programs conducted on welds of this type have been reported to ASME, ASTM, and AWS[4] and we believe this report of the AG&E tests will add to published information on the reliability of these welds.

Design Considerations

When the American Gas and Electric Service Corporation was designing the first of the series of seven 150,000-kw, 1050-F, 1000-F reheat units, the General Electric Company was using stainless type 347 material for high-temperature turbine shells, steam leads, and stop valves. Economical design of the superheater-outlet tubes and the main steam header from The Babcock & Wilcox boiler called for using 2¼ Cr 1 Mo material, ASME Spec. A213grT22. The piping arrangement is shown in Fig. 1. To join the ferritic header to the austenitic stop valves then required a joint which would withstand the operating conditions of 2000 psi and 1050 F in addition to the stresses resulting from the wide difference in coefficient of expansion between the two materials. Flanged joints, cast transition joints, and other types were reviewed and after careful study the conventional butt weld was decided on.

Short stubs of the 2¼ Cr 1 Mo pipe were sent to the General Electric Company by The Babcock & Wilcox Company and the transition welds to the stop-valve nozzles were made under carefully controlled shop conditions. The field welds attaching the stop valves to the header were then made between corresponding materials.

In general, the welding procedure used for the transition welds was as follows: 20-deg U-bevel welding groove, tapered type 347 backing rings, 480–750 F preheat and interpass temperature during welding, type 347 filler metal, 1100–1200 F stress relief for the benefit of the ferritic side, gamma-ray and fluorescent-penetrant postweld inspection.

Weld-Test Vessel and Cycling Procedure

In order to study the behavior of these transition butt welds

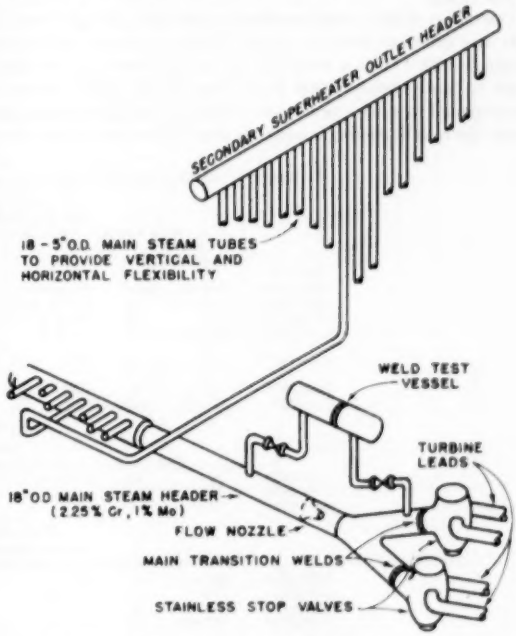

Fig. 1 Schematic Diagram of Main Steam Piping for Philip Sporn Plant and Twin Branch Plant Unit No. 5

[1] Senior Engineer, Piping and Metallurgy Section, Mechanical Engineering Division, American Gas and Electric Service Corporation, New York, N. Y. Mem. ASME.

[2] Chief Metallurgist, Research Center, The Babcock & Wilcox Company, Alliance, Ohio.

[3] Metallurgist, The Works Control Laboratory, The Babcock & Wilcox Company, Barberton, Ohio.

[4] Some papers on related tests listed in References at end of paper.

Contributed by the Joint ASTM-ASME Committee on Effect of Temperature on the Properties of Metals and presented at a joint session with the Power Division at the Annual Meeting, New York, N. Y., November 29–December 4, 1953, of The American Society of Mechanical Engineers.

Note: Statements and opinions advanced in papers are to be understood as individual expressions of their authors and not those of the Society. Manuscript received at ASME Headquarters, October 9, 1953. Paper No. 53—A-150

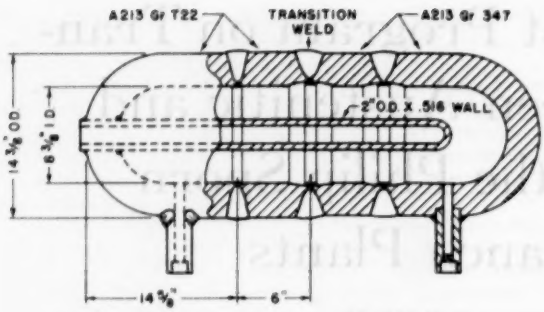

FIG. 2 CROSS SECTION OF WELD TEST VESSEL

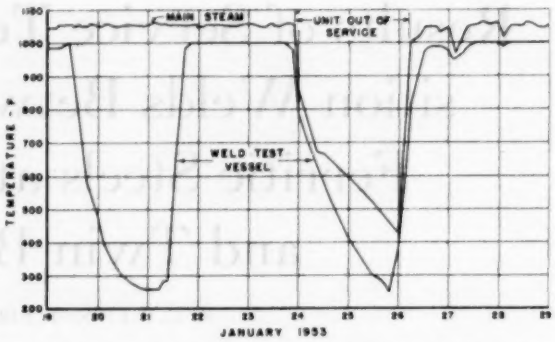

FIG. 3 SECTION OF RECORD ON TEMPERATURES OF WELD TEST VESSEL AND MAIN STEAM

under operating conditions, a test vessel as shown in Fig. 2 was made from sections of TP 347 stainless and 2¼ Cr 1 Mo pipe of the same dimensions as the pipe at the main welds. The vessel was closed with end caps and the center weld was made an exact duplicate of the main transition welds at the stop valves. A 1½-in-ID blind pipe nipple was expanded and seal-welded into a hole in the ferritic end cap to provide a means for inserting a radiograph capsule into the center of the vessel for making inspections of the weld.

The vessel was then piped up to receive steam from a connection upstream of the main steam-flow nozzle and discharge it downstream. A pressure drop of up to 200 in. of water was thus available at high loads to produce steam flow through the vessel for heating it. Heavy insulation was used to cut down heat loss and help maintain as high a temperature as possible in the vessel. The high average temperature at the surface of the vessels has been between 980 F and 1010 F. The steam connections are valved so that the vessel can be cooled independently of the main header and the cooling can be accelerated by blowing air through a small tube into the open end of the inspection pipe at one end of the vessel.

Operation of the vessel consists of exposing it to high temperature and pressure with the steam connections open to the main steam header. Once a week the valves are closed and the vessel cools to approximately 300 F in about 22 hr. The valves are then opened to start a new cycle. Through the high-temperature range the rate of cooling is equal to that of the main header which cools with decreasing steam temperature when the load is reduced. At lower temperatures the vessel cools faster than the header. By this method the test joint is aged at high temperature while being subjected to more frequent wide temperature changes which would produce the highest stresses in the weld. A thermo-couple is peened into the surface of the test-vessel weld and the temperature is recorded along with the corresponding one of the main steam. A typical record of these temperatures is shown in Fig. 3.

METHODS OF INSPECTION

The dissimilar welds in the three installations were inspected periodically by the fluorescent-penetrant method and by radiographic examination. For this purpose the surface along the austenitic-ferritic weld junction was sandpapered thoroughly to remove all oxide before the penetrant liquid was applied. The radiographic inspections were made with cobalt 60 because it offers the smallest source for gamma rays and, therefore, gives a more clearly defined image of any defects present. Exposures with the cobalt were made at the weld center line to reveal defects normal to the surface, and other exposures 1¼ in. off center so that the rays followed the angle of the scarf of the weld groove on the ferritic side where cracks due to thermal-expansion stresses were most likely to form. Whenever defects were found, they were disclosed by the fluorescent-penetrant method, but were not indicated by gamma-ray inspection.

TABLE 1 SUMMARY OF DISSIMILAR WELDS AND RECORD OF INSPECTIONS

Date of inspection	Number of cycles — Header	Number of cycles — Test vessel	Type of inspection	Results of inspection of header welds and test-vessel welds
Philip Sporn Unit No. 1				
Date of installation, January 1, 1950				
High average temperature of header 1050 F; of vessel 980 F				
4-26-1950	NI[a]	15	FP[b] & R[c]	Intermittent shallow surface defects ground out.
9-15-1950	11	34	FP & R	No defects found in header or test vessel.
2-28-1952	27	78	FP & R	Intermittent short cracks in test vessel. No defects in header welds.
4-24-1952	NI	84	FP	Intermittent short cracks in test vessel. First sample removed from test vessel.
7-28-1952	NI	84	FP	Second sample removed from test vessel.
7-1-1953	37 NI	102	FP	Third sample removed from test vessel.
Philip Sporn Unit No. 2				
Date of installation, July 1, 1950				
High average temperature of header 1050 F; of vessel 1000 F				
3-16-1952	10	32	FP & R	No defects found.
2-23-1953	NI	56 NI	...	Vessel removed to add new welds.
4-2-1953	19	NI	FP	No defects found.
Twin Branch Unit No. 5				
Date of installation, August 22, 1949				
High average temperature of header 1050 F; of vessel 1010 F				
3-23-1950	13	NI	FP	Intermittent shallow surface defects ground out.
4-6-1951	NI	47	FP & R	No defects found.
12-22-1951	34	92	FP & R	No defects found in header or test vessel.
3-13-1953	NI 45	158	FP & R	Intermittent surface cracks. First sample removed.

[a] Not inspected.
[b] Fluorescent penetrant.
[c] Radiograph.

A summary of the history of the various dissimilar welds and a record of the periodic inspections are given in Table 1.

History of Periodic Inspections and Discovery of Cracks in Test Vessel of Philip Sporn Unit No. 1

The details of examinations which led to the verification of the presence of cracks in the test vessel at Philip Sporn unit No. 1 were as follows: The dissimilar weld was first inspected on April 26, 1950, when the test vessel had undergone fifteen thermal cycles; fluorescent-penetrant examination of the test vessel revealed a number of short intermittent cracks along the edge of the cover bead on the austenitic-ferritic weld junction. In order to ascertain the depth of these cracks, two were ground and inspected repeatedly until they had disappeared. This occurred after less than $^1/_{32}$ in. of metal had been removed. The weld was then radiographed with cobalt 60, with the radioactive source located in five different positions. However, the gamma-ray films failed to reveal the defects found by the fluorescent-penetrant method. The remaining cracks were then ground out and the locations re-examined to make sure that the cracks had been removed completely. This was done since consideration had to be given to the possibility that these shallow surface defects might have originated in the fabrication of the weld joints.

The second inspection of the dissimilar welds in the Philip Sporn unit No. 1 was made some 5 months later, on September 15, 1950. The test vessel had then accumulated 34 thermal cycles, and the main-line welds 11 cycles. Neither Zyglo nor radiographic examination revealed any sign of defects in the vessel or in the main-line welds. The cracks which had been found by the previous examination and which subsequently had been removed by grinding had not re-formed.

A third inspection by the fluorescent-penetrant method, made on February 28, 1952, after 78 cycles in the test vessel and 27 cycles in the main-line welds, again disclosed the presence of a number of short intermittent cracks, about $^1/_8$ to $^3/_{16}$ in. long each, along the dissimilar-weld junction of the test vessel, but no defects in the main-line welds. Radiographic examination did not reveal these defects. The location of the defects along the weld circumference is indicated with other information in Fig. 9. All cracks were along the line of fusion on the ferritic side of the weld.

Metallographic Examination of First Two Boat Samples Removed From Test Vessel of Philip Sporn Unit No. 1 After 84 Thermal Cycles

It then was decided to remove a boat sample containing one of the indicated defects in order to determine metallographically the condition of the dissimilar-weld junction. Fig. 4 illustrates the location of the transverse sample in the cross section of the weld. Fig. 5 shows a top view and section through the sample.

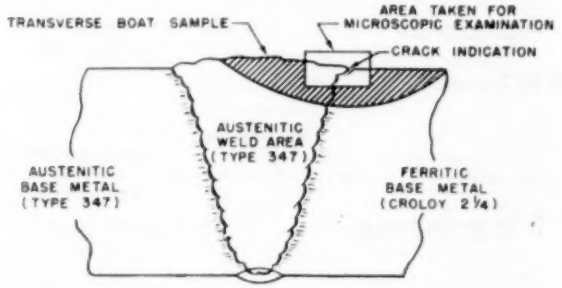

Fig. 4 Schematic Diagram Illustrating Position of Area Taken for Microscopic Examination in Relation to Ferritic-Austenitic Weld Junction

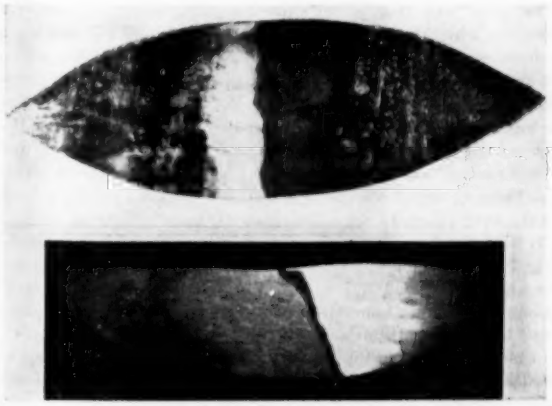

Fig. 5 Top View and Section Through First Weld-Probe Boat Sample From Philip Sporn Unit No. 1 Test Vessel Removed After 84 Cycles

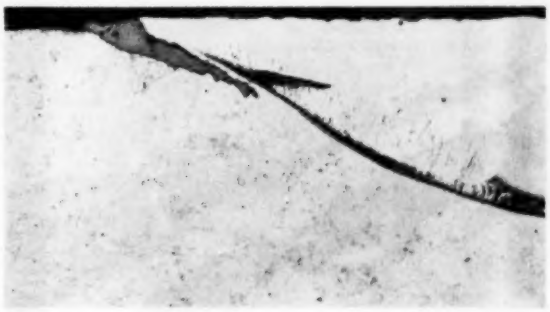

Fig. 6 Surface Stress-Oxidation Notch in Croloy 2¼ (*left*) Adjacent to Fusion Interface With 19-9 Cb Weld Metal (*right*) of Boat Sample Fig. 5; ×100

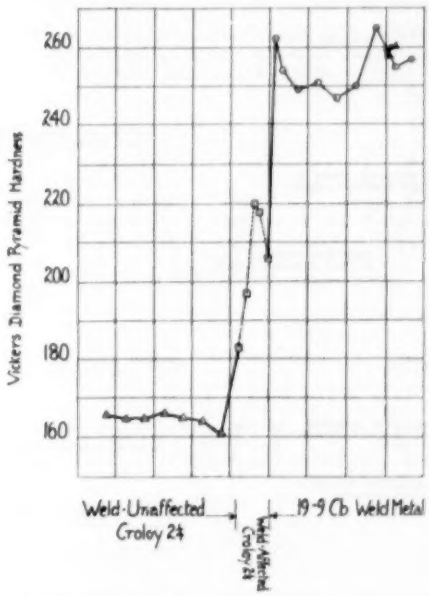

Fig. 7 Weld-Hardness Survey of Dissimilar-Weld Junction (First boat sample Philip Sporn Unit No. 1.)

The boat was then sliced into several additional transverse sections which were polished, etched, and examined under the microscope. Two of the sections revealed an oxide-filled notch in the Croloy $2^1/_4$ base metal directly adjacent to the fusion interface as shown in the photomicrographs, Fig. 6. This notch had a total depth of 0.009 in. perpendicular to the surface and displayed the serrated contours frequently found in cracks of dissimilar-weld junctions subjected to cyclic operations. A weld-hardness survey of the fusion interface revealed a hardness drop in the weld-affected Croloy $2^1/_4$ and a hardness increase in the 19-9 Cb weld metal, indicative of carbon migration. This is shown in Fig. 7. Carbon migration was not recognizable in the microstructure of the Croloy $2^1/_4$, but was indicated by a carbide accumulation in the grain boundaries of the austenitic weld metal adjacent to the fusion interface, Fig. 8.

Considering the possibility that the boat sample was not representative of the worst condition along the circumference of the dissimilar-weld junction, it was decided to remove a second sample which was done on July 28, 1952. Prior to the sampling the surface was ground lightly to remove tightly adhering oxide and then examined. The defects revealed by this examination and the location of the removed boat sample are indicated in Fig. 9. Metallographic examination of this second sample disclosed the presence of an oxide notch in the Croloy $2^1/_4$ metal which in every respect was similar to that found in the first boat sample, Fig. 10. Its depth of penetration, perpendicular to the surface, was about 0.010 in. as compared to the 0.009 in. observed in the first boat sample.

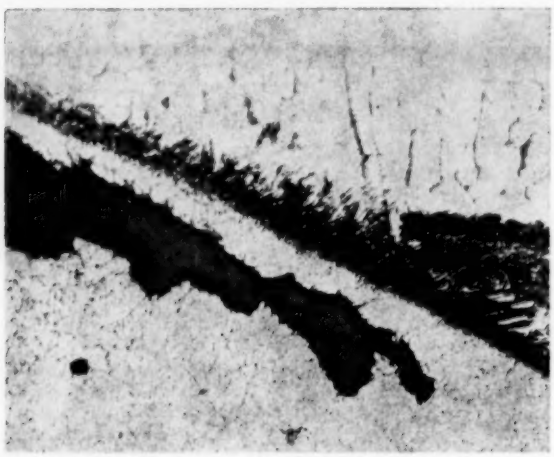

FIG. 8 FUSION ZONE NEAR SURFACE OXIDATION NOTCH OF FIG. 6, SHOWING CARBIDE CLUSTERS IN GRAIN BOUNDARIES OF 19-9 Cb WELD METAL (*top*); ×500

REPAIR WELDING OF CAVITIES LEFT BY REMOVAL OF BOAT SAMPLES

The boat-sample cavities were ground to round out the sharp Vee at the bottom of the cavity and the saw-tooth marks on the sides. The cavity was then inspected with fluorescent oil to insure against the presence of cracks before welding. All traces of oil were removed and a 6-in. band on either side of the cavity was preheated to a minimum of 400 F which was maintained throughout the welding. Electrodes of 19-9 Cb were used with string beads, craters were chipped or ground, and the finished weld was ground smooth and flush with the pipe surface. After cooling the welded area was again checked with fluorescent oil.

INVESTIGATION OF PROTECTIVE WELD OVERLAYS

Considerable thought had been given to means of protecting ferritic-austenitic weldments against the type of surface cracking observed in laboratory and field studies of dissimilar-weld behavior. Experiments conducted by The Babcock & Wilcox Company had indicated that the formation of the type of notch or crack found at the dissimilar-weld junction of the two removed boat samples could be retarded greatly by covering the surface area on both sides of the dissimilar-weld interface with nickel-chromium weld metal of a coefficient of thermal expansion between those of the low-alloy steel and the austenitic weld metal of the joint. The test vessel at Philip Sporn unit No. 1 offered an opportunity to try out such protective weld overlays on a large-sized pipe under operating conditions.

For this purpose, all defects indicated by fluorescent-penetrant examination along the dissimilar-weld seam were ground out on the top half of the circumference of the vessel while for comparison the bottom half was left with cracks undisturbed. Along three sections of top-half dissimilar-weld seam, weld overlays

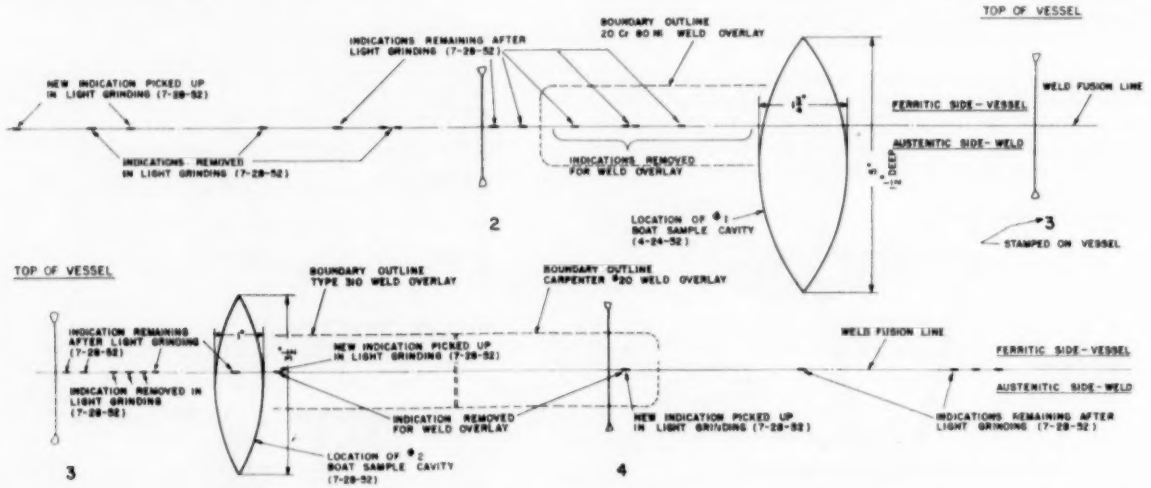

FIG. 9 TEST VESSEL AT PHILIP SPORN PLANT UNIT NO. 1; LOCATION OF DEFECTS INDICATED BY FLUORESCENT-PENETRANT INSPECTION AND OF PROBE SAMPLES TAKEN

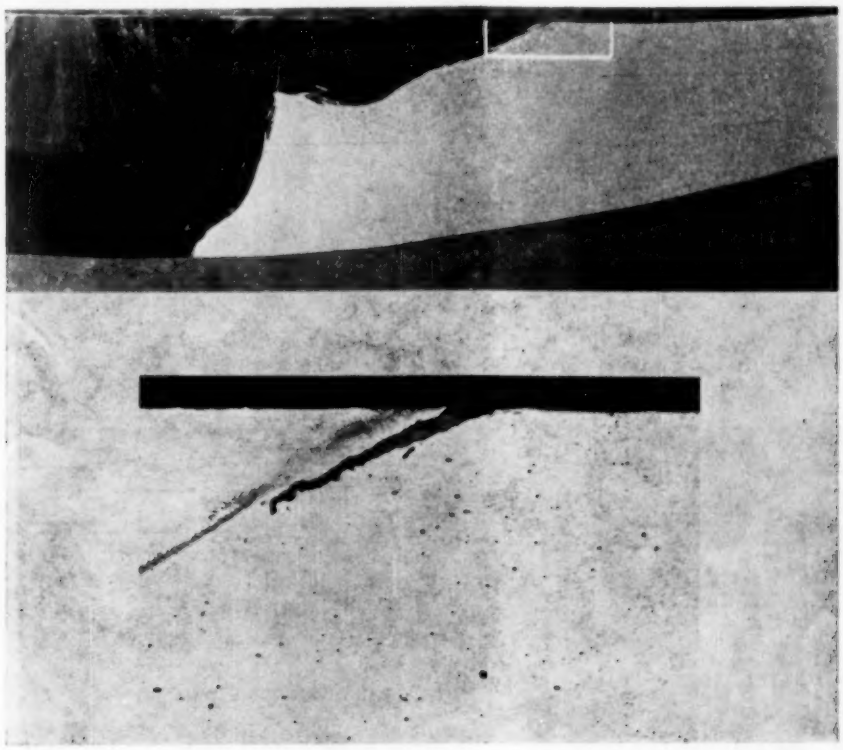

FIG. 10 SURFACE STRESS-OXIDATION NOTCH FOUND IN SECOND BOAT SAMPLE REMOVED FROM PHILIP SPORN UNIT NO. 1 AFTER 84 CYCLES; (*top*) ×8; (*bottom*) ×100

with 20 Cr 80 Ni, Carpenter stainless No. 20 (20 Cr 29 Ni 2 Mo 3 Cu) and 25 Cr 20 Ni electrodes, respectively, were then deposited as shown in Fig. 9. The top center section was left unprotected for comparison. The position of the weld overlay relative to the ferritic-austenitic weld-fusion line is indicated in Fig. 11. Each of the overlays consisted of two circumferential layers of weld metal 4 in. long extending 3/4 in. on each side of the ferritic-austenitic junction. Preheat and interpass temperatures were maintained at 400 F. The finished welds were ground to a smooth surface contour and examined again. No defects were found along the new ferritic-austenitic fusion line. These overlay-protected weld-seam sections will be examined by means of boat samples after a suitable number of thermal cycles have again accumulated on the test vessel.

EXAMINATION OF THIRD BOAT SAMPLE REMOVED FROM TEST VESSEL OF PHILIP SPORN UNIT NO. 1 AFTER 102 CYCLES

The last inspection of the test vessel at Philip Sporn unit No. 1 was made on July 1, 1953, after completion of 102 thermal cycles. Examination by the fluorescent-penetrant method revealed that the previously reported defects on the lower half of the vessel were still present, but had not progressed in the additional service time since April 24, 1952. No evidence of cracking was found in the top center area where the cracks had been removed by grinding or in the areas of the weld overlays. As a further check, a boat sample was removed from the top center of the vessel. Five photographs showing the vessel and removal of the third sample with the weld-probe machine are shown in Fig. 12.

The boat sample was later cut into six longitudinal slices,

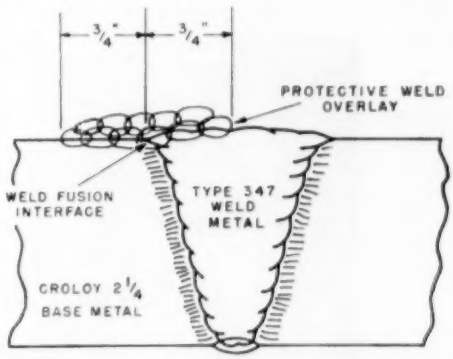

FIG. 11 POSITION OF WELD OVERLAY RELATIVE TO FERRITIC-AUSTENITIC WELD FUSION LINE

transverse to the weld junction, and the slices polished, etched, and microscopically examined. No crack or oxide notch was found at the surface of the dissimilar-weld junction although there was a steplike abrupt change from the austenitic-weld-metal surface to the surface of the 2 1/4 Cr 1 Mo pipe, caused by the more rapid oxidation of the latter, Fig. 13. However, with careful polishing, some very fine intergranular fissures as shown in Fig. 14, became apparent in the Croloy 2 1/4 metal adjacent to the dissimilar-weld interface. These fissures were located in a small area at the base of the top shoulder bead and did not extend to the surface.

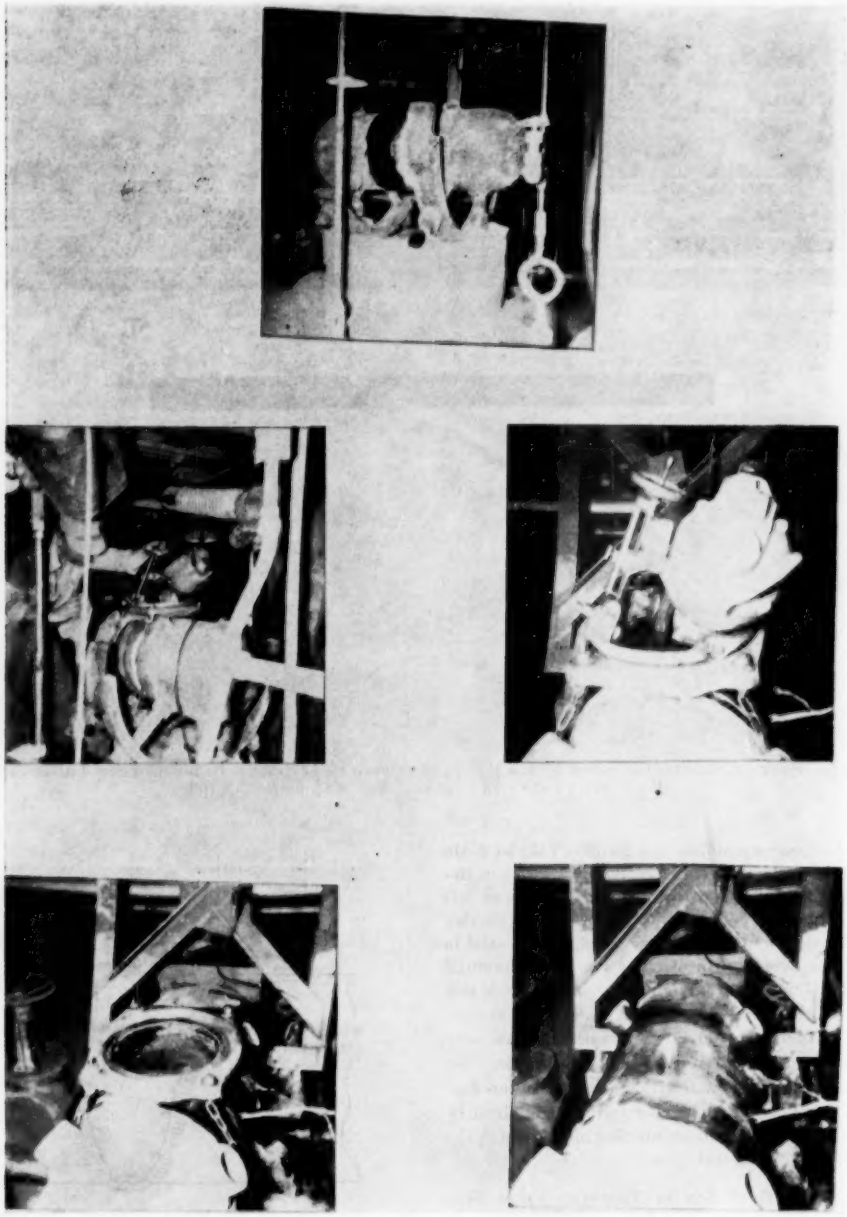

FIG. 12 PHILIP SPORN UNIT NO. 1 WELD TEST VESSEL AND WELD-PROBE MACHINE REMOVING THIRD BOAT SAMPLE

EXAMINATION OF BOAT SAMPLE REMOVED FROM TEST VESSEL AT TWIN BRANCH UNIT NO. 5 AFTER 158 THERMAL CYCLES

The test vessel at the Twin Branch Plant also had been examined periodically up to March, 1953, by the fluorescent-penetrant and by radiographic methods without indications of defects at the dissimilar-weld junction. However, at an inspection on March 13, after the vessel had undergone 158 thermal cycles, Zyglo examination revealed a notch extending around the entire dissimilar-weld junction. This notch could not be removed with light polishing and, therefore, it was decided to remove a boat sample. A macroetched longitudinal section through the latter is shown in Fig. 15.

Four transverse-weld slices cut from the boat were subjected to a microscopic examination which revealed the presence of a blunt-nosed stress-oxidation notch, about 0.010 in deep, in the Croloy $2^1/_4$ metal adjacent to the weld-fusion interface, Fig. 16. This notch extended over the entire width of the boat sample. About 0.020 in. below the root of this surface notch, a narrow zone adjacent to the fusion line containing fine intergranular cracks was noted as shown in Figs. 17 and 18. This cracked zone extended down to a depth of 0.110 in. below the vessel surface,

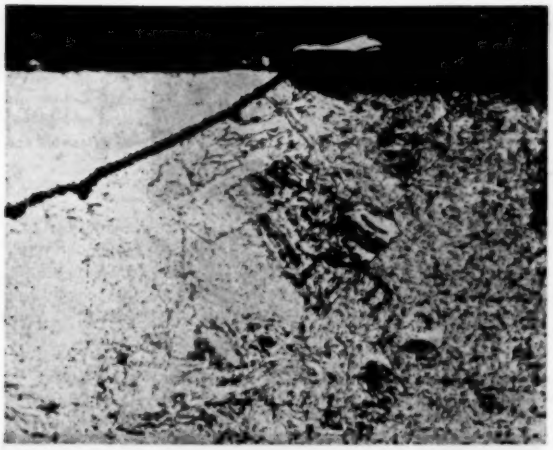

FIG. 13 WELDED JUNCTION AT SURFACE OF THIRD BOAT SAMPLE REMOVED FROM PHILIP SPORN UNIT NO. 1 TEST VESSEL AFTER 102 CYCLES; ×250

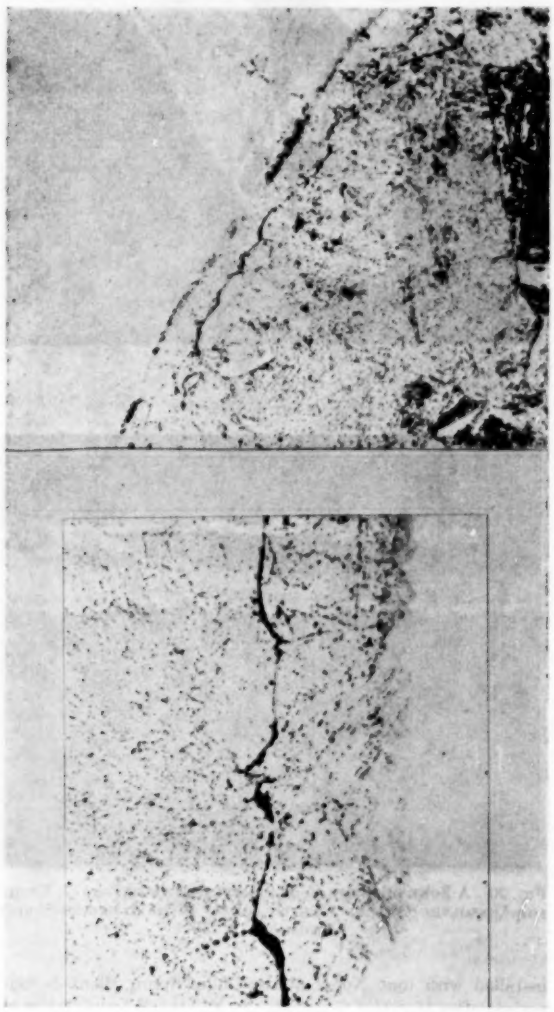

FIG. 14 SUBSURFACE CRACKS IN CROLOY 2¼ ADJACENT TO WELD INTERFACE IN THIRD WELD PROBE SHOWN IN FIG. 13; *(top)* ×250; *(bottom)* ×1000

FIG. 15 SECTION THROUGH FIRST WELD PROBE REMOVED FROM TWIN BRANCH UNIT NO. 5 TEST VESSEL AFTER 158 CYCLES

FIG. 16 SURFACE STRESS-OXIDATION NOTCH AT WELD-FUSION INTERFACE AT SURFACE OF SECTION SHOWN IN FIG. 15; ×250

but did not reach the latter at any location over the width of the boat sample. The boat-sample slices were repolished and etched with alkaline sodium chromate, an etchant which indicates regions of dissolved oxygen as white areas in a dark background. Fig. 19 depicts the cracked zone after etching with the chromate reagent. No oxygen-containing areas were indicated in this zone. However, dissolved oxygen was evident at the periphery of the surface notch and along the surface of the Croloy 2¼ metal, Fig. 20. The subsurface cracking along the dissimilar-weld junction therefore may be mechanical in nature and not of the stress-oxidation type represented by the surface notches.

SUMMARY AND CONCLUSIONS

The experience gained with the test vessels at Philip Sporn unit No. 1 and at the Twin Branch unit No. 5 has demonstrated that ferritic-austenitic weld joints subjected to thermal cycles between about 980–1010 F and 300 F may develop not only oxide notches or cracks at the surface, but also cracks below the surface. Both types of cracks seem to occur only in the less oxidation-resistant and weaker low-alloy steel in a region directly adjacent to the dissimilar weld-fusion interface. The notches or cracks occurring at the surface are undoubtedly of the stress-oxidation type whereas those below the surface have been shown to originate in the absence of oxygen. It is believed that the differential expansion stresses are primarily responsible for the development of these dissimilar weld cracks.

The propagation of the cracks under the operating conditions existing at the Philip Sporn and Twin Branch plants appears to be rather slow and encourages the belief that the dissimilar welds in the main steam lines which are subjected to much less frequent thermal cycles than the test vessels are in no danger and will give many years of safe operation.

The test vessels have proved to be a most valuable means of studying and anticipating the dissimilar-weld behavior in the main steam lines. The fact that radiographic examination does not seem to indicate the presence of surface cracks or subsurface cracks of the type observed in the two test vessels and the fluorescent-penetrant method reveals only cracks at the surface, but not below the surface, deserves attention. The only reliable

FIG. 17 SURFACE STRESS-OXIDATION NOTCH AND SUBSURFACE INTERGRANULAR CRACKS IN CROLOY 2¼ ALONG WELD-FUSION INTERFACE OF SECTION SHOWN IN FIG. 15; ×100

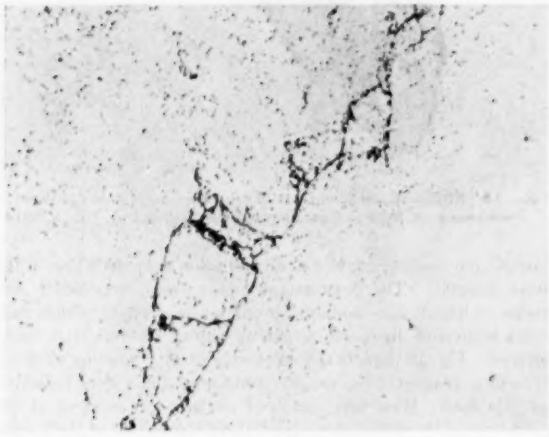

FIG. 18 A ZONE OF SUBSURFACE INTERGRANULAR CRACKS SHOWN IN FIG. 17; ×750

FIG. 19 A ZONE OF SUBSURFACE CRACKS SHOWN IN FIG. 17, ETCHED FOR DISSOLVED OXYGEN WITH ALKALINE-SODIUM-CHROMATE; ×250

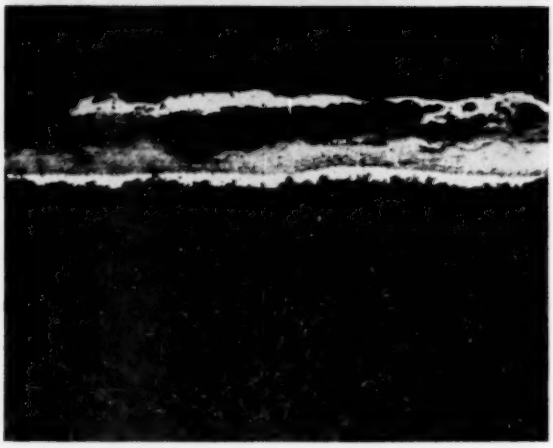

FIG. 20 A ZONE OF SURFACE OF SAMPLE SHOWN IN FIG. 17, ETCHED FOR DISSOLVED OXYGEN (WHITE ZONES) WITH ALKALINE-SODIUM-CHROMATE; ×250

method of detecting the presence of both types of cracks appears to be the removal and metallographic examination of weld-boat samples.

Both test vessels covered by this paper are back in service and being cycled weekly. They will be inspected in September, 1954, to follow the progress of the cracks. The test vessel installed with unit No. 2 at the Philip Sporn Plant is being revised after 56 cycles to include two additional transition welds. One of these is being made by General Electric Company using Inconel filler material and the other by The Babcock & Wilcox

Company using a ferritic electrode called B&W Croloy 2LC. The addition of these new welds to the program will bring into service testing the latest techniques in butt-welding austenitic and ferritic steels for steam piping.

Acknowledgments

The authors wish to express their gratitude to the staffs of the Philip Sporn and Twin Branch Plants for their work in operating the test program and to the staffs of The Babcock & Wilcox Company, Barberton and Alliance laboratories for their guidance and help in testing and metallurgical analysis.

References

"The Basic Concept Behind Philip Sporn Station," by Philip Sporn; "Condenser and Piping Fit Objectives," by S. N. Fiala, *Electrical World*, vol. 133, June 5, 1950, pp. 81–108.

"Cyclic Heating Test of Main Steam Piping Joints Between Ferritic and Austenitic Steels—Sewaren Generating Station," by H. Weisberg, Trans. ASME, vol. 71, 1949, pp. 643–664.

"Welds Between Dissimilar Alloys in Full-Size Steam Piping," by R. V. Blaser, F. Eberle, and J. T. Tucker, Proceedings of the ASTM, vol. 50, 1950, pp. 789–808.

"Some Considerations in the Joining of Dissimilar Metals for High-Temperature, High-Pressure Service," by O. R. Carpenter, N. C. Jessen, J. L. Oberg, and R. D. Wylie, Proceedings of the ASTM, vol. 50, 1950, pp. 809–860.

"Thermal-Shock and Other Comparison Tests of Austenitic and Ferritic Steels for Main Steam Piping," by W. C. Stewart and W. G. Schreitz, Trans. ASME, vol. 72, 1950, pp. 1043–1060.

"Welded Joints Between Dissimilar Metals in High-Temperature Service," by R. W. Emerson and W. R. Hutchinson, Welding Research Supplement, vol. 17, March, 1953, No. 3.

Discussion

H. J. Robar.[8] It is gratifying to find that the test results on austenitic-ferritic transition welds of the American Gas and Electric Service Corporation program, as reported by the authors are, in general, similar to those obtained in the Public Service cyclic-heating test.

We question the authors' conclusion as to the origin of the subsurface cracking adjacent to the fusion line of their transition weld. Cracking of this nature was present in our test after 100 thermal cycles, as shown in Fig. 21 of this discussion. It was, however, present before cycling, as shown in Fig. 22, although not revealed by radiographic examination. We therefore concluded that the cracking occurred during welding. Some propagation of the initial cracks may have occurred as a result of thermal cycling so far. Further contemplated tests may disclose more conclusively to what extent propagation does occur.

In view of these results, we would like to ask if the authors made any examination other than radiographic to determine the presence of any subsurface cracking before cycling.

[8] Metallurgist, Maplewood Laboratory, Public Service Electric and Gas Company, Maplewood, N. J.

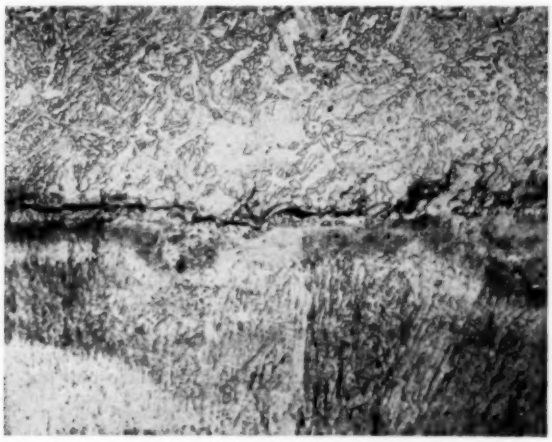

Fig. 21 After 100 Thermal Cycles; ×100

Fig. 22 Before 100 Thermal Cycles; ×100

Authors' Closure

The authors would like to thank Mr. Robar for his discussion of this paper. The Public Service Electric and Gas Company of New Jersey has done a considerable amount of work in this field and therefore the questions that he poses are based on sound facts.

It is interesting that cracking similar to that discussed in the paper was found prior to thermal cycling. No nondestructive test now known will disclose cracking of this nature, and it was felt that removing a plug or a boat sample from the original test bottle may alter the stress pattern at the weld junction and thus produce erroneous conclusions after cycling. Therefore no samples were taken prior to service. Examination of many other welds of this type on tubular specimens, both before and after exposure to cyclic conditions, has disclosed that welds examined prior to exposure showed no evidence of subsurface cracking, whereas welds examined after exposure showed such defects. Therefore we believe that our conclusion is valid that such defects may also occur as a result of cyclic stresses during test.

It will be interesting to follow the progress of the cracking described by Mr. Robar in future examinations of their test vessel.

Cyclic Heating Test of Main Steam Piping Materials and Welds at the Sewaren Generating Station

By H. WEISBERG[1] and H. M. SOLDAN,[2] NEWARK, N. J.

This paper describes a continuation of previously reported cyclic heating tests of austenitic and ferritic piping and welds, representing the main steam piping installed at Sewaren Generating Station. In the current test, a section made up of these materials was subjected to thermal cycling from room temperature to 1100 F, and from atmospheric pressure to the operating pressure of 1500 psi. The heating and cooling rates were somewhat more severe than are experienced during regular starting and shutting-down conditions in the actual piping systems. The results show that 100 cycles did not produce any cracking. It is proposed to continue the test to destruction by further cycling and the addition of external bending forces.

Introduction

WELDED joints between austenitic and ferritic piping have been the subject of considerable discussion because of differences in thermal expansion, conductivity, and other physical properties of these materials. To obtain information for the design of the steam-piping system between the boilers and turbines of the Sewaren Generating Station, a preliminary cyclic heating and cooling test of welded joints between these dissimilar materials was conducted in 1947.[3] Briefly, this test indicated that no failures would occur after 100 cycles representing normal operation and 10 cycles simulating boiler carry-over conditions.

After installation of the Sewaren piping, a second cyclic heating test, which is the subject of this paper, was initiated using the various materials and types of welds actually installed in the station piping systems which included welds between austenitic steels made by various practices, as well as welds between austenitic and ferritic steels. This test differed from the first test in that the test section was heated by steam and was subjected to internal pressure.

The General Electric Company, Westinghouse Electric Corporation, and The M. W. Kellogg Company participated in the test and furnished the pieces of piping, in so far as possible, to the same specifications as the piping which was furnished with the equipment.

The first two units in the station have now been in operation about five years. Early in the operation, some cracks were observed and two failures occurred in the austenitic turbine piping.[4] The failures occurred in the third unit, which started a year after the first two units. The defects have been attributed to improper detail design or faulty installation of the various piping components rather than to materials or types of welds.

Description of Test

The test section is shown in Figs. 1 and 2. It consists of nine pieces—3 forged-ferritic, 2 forged-austenitic, and 3 cast-austenitic pieces (one centrifugally cast) each approximately 10 in. long, 12 in. nominal diam, and 2¼ in. in wall thickness, also one austenitic-ferritic (Kelcaloy) transition piece. The centrifugal casting furnished by the United States Pipe and Foundry Company is included to obtain information on this material and does not represent any piping in the actual installation at Sewaren. The chemicals and physicals of the individual pieces are shown in Table 1.

Welded joints represent actual shop and field welds made with the techniques used in the installed station piping. Welds were preheated and postheated as shown in Fig. 2 and represent variations in practice at the time. Later work demonstrated that 1350 F postheat is preferable for the 3 Cr 1 Mo material to avoid possibility of forming martensite. Also that a 1900–2000 F solution heat-treatment is desirable for the austenitic material to minimize sigmatization in operation. Welds heat-treated in accordance with this later practice were incorporated in the tests as the work proceeded (see Appendix).

The test section was provided with a steel core to reduce the internal steam volume, and distributing internals were installed to insure uniform heating and cooling as shown in Fig. 3. It was connected to the main steam piping of No. 1 Unit, Sewaren, operating at 1500 psig, 1050 F, and the outlet was piped to the main condenser of that unit. A diagram of the piping connections is shown in Fig. 4.

The arrangement of equipment is shown in Fig. 5. The test section was imbedded in an open-top steel box filled with expanded vermiculite. A gas-fired furnace was installed in which the steam feed was heated to 1250 F maximum before admission to the test section. A desuperheater was provided for use in the cooling cycles. Thermocouples with recorders were provided for continuous temperature readings during the test.

During the test, 100 thermal cycles were applied. The first 5 cycles were to simulate rapid heating, equivalent to the maximum heating rate observed in operation of the station piping, approximately ½ deg per sec. The section was to be maintained at 1100 F for 1 hr during each cycle and was to be cooled rapidly at approximately 0.6 deg per sec by introducing boiler feedwater, simulating boiler-water carry-over conditions. The next 95 cycles were to simulate the maximum heating and cooling rates encountered during normal start-up and shutdown periods, approximately ½ deg per sec. The test section was to be held at 1100 F, 1500 psi for 1 hr during each cycle. An additional overnight

---

[1] Mechanical Engineer, Electric Engineering Department, Public Service Electric and Gas Company. Fellow ASME.

[2] Senior Engineer, Electric Engineering Department, Public Service Electric and Gas Company. Mem. ASME.

[3] "Cyclic Heating Test of Main Steam Piping Joints Between Ferritic and Austenitic Steels—Sewaren Generating Station," by H. Weisberg, Trans. ASME, vol. 71, 1949, pp. 643–644.

Contributed by the Joint ASTM-ASME Committee on Effect of Temperature on the Properties of Metals and presented at a joint session with the Power Division at the Annual Meeting, November 29–December 4, 1953, of The American Society of Mechanical Engineers.

Note: Statements and opinions advanced in papers are to be understood as individual expressions of their authors and not those of the Society. Manuscript received at ASME Headquarters, October 9, 1953. Paper No. 53—A-151.

[4] "Metallurgy and Piping," Edison Electric Institute, Publications No. 50-10, February, 1951, and No. 52-13, 1953.

TABLE 1 CHEMICALS AND PHYSICALS OF TEST PIECES AND WELDS

PIECES	SPECIFICATION	MATERIAL (1)	HEAT TREATMENT DEGREES F	CHEMICALS C	Mn	P	S	Si	Cr	Ni	Mo	Cb	W	PHYSICALS TENSILE p.s.i.	YIELD p.s.i.	PER CENT ELONG	PER CENT R of A
INLET CAP	A213-T21(A182)	F 3Cr - 1Mo	1,725 Normalize 1,250 Stress relief	0.180	—	0.034	0.029	0.290	2.36	—	1.010	—	—	103,000	78,500	20.0	51.9
h - e	A213-T21(A182)	F 3Cr - 1Mo	1,550 Anneal	0.080	0.500	0.026	0.029	0.360	2.90	—	0.880	—	—	66,500	33,000	31.5	—
e - d	A182-F8C	F 18/8 Cb	1,950 Solution	0.080	1.140	0.019	0.010	0.500	17.68	11.44	—	0.990	—	None	None	—	—
d - i	A182-F8C	F 18/8 Cb	1,950 Solution	0.080	1.140	0.019	0.010	0.500	17.68	11.44	—	0.990	—	None	None	—	—
i - b	AISI 316 + Cb	CC 18/8 Mo Cb	1,950 Solution	0.067	1.130	0.014	0.011	0.930	15.86	14.50	1.860	1.000	—	76,000	27,200	27.5	24.6
b - a	AISI 347	C 18/8 Cb		0.095	1.380	0.022	0.022	0.721	18.60	12.50	0.202	0.741	—	66,500	35,500	17.0	19.2
a - c	AISI 316 + Cb	C 18/8 Mo Cb	1,950 Solution 1,600 Stress relief	0.078	1.960	0.019	0.016	0.716	15.90	14.90	1.940	1.310	—	69,600	38,500	18.0	8.5
f TRANSITION	A213-T21 (A182)	F 3Cr-1Mo	1,550 Anneal	0.100	0.460	0.030	0.028	0.330	3.20	—	0.920	—	—	74,000	42,000	33.5	—
	AISI 347	C 18/8 Cb	1,550 Anneal	0.060	1.550	0.020	0.011	0.400	18.50	10.50	—	0.840	—	← No data before test		—	—
OUTLET CAP	A213-T21(A182)	F 3Cr - 1Mo		0.123	0.417	0.038	0.018	1.050	2.99	0.358	0.860	—	—	97,800	70,000	18.5	65.7

NOTES

1. F-FORGED
   C-CAST
   CC-CAST CENTRIFUGALLY
2. FILLER RODS:
   h f g MUREX
   e d i i ARCOS CHROMEND
   b a c c GENERAL ELECTRIC
3. SECOND WELD

WELDS	FILLER (2)	PREHEAT DEGREES F	POSTHEAT DEGREES F	C	Mn	P	S	Si	Cr	Ni	Mo	Cb	W	WELDS h f g AFTER HEAT TREATMENT. ALL OTHERS AS WELDED.			
h	6215	600	1,550	0.090	0.631	0.015	0.007	0.265	3.173	—	1.000	—	—	66,400	—	31.3	—
e	19/9 Cb	600	1,350	0.068	1.676	0.017	0.005	0.469	20.04	10.07	—	0.920	—	92,500	68,000	34.0	51.0
d	19/9 Cb	70	1,600	0.068	1.676	0.017	0.005	0.469	20.04	10.07	—	0.920	—	92,500	68,000	34.0	51.0
i (3)	9/9 WMo	1,000	1,350	0.090	1.176	0.016	0.005	0.858	19.80	8.78	0.600	—	1.11	110,000	75,000	35.0	30.8
b	W 1347	70	—	0.033	1.850	0.010	0.019	0.531	19.70	9.60	—	0.874	—	101,500	—	29.0	48.0
a	W 1347	70	—	0.092	1.850	0.018	0.010	0.552	20.10	9.94	—	0.960	—	101,500	—	29.0	48.0
c	W 1347	70	1,600	0.092	1.850	0.018	0.010	0.552	20.10	9.94	—	0.960	—	101,500	—	29.0	48.0
g	6215	600	1,400	0.120	0.620	0.019	0.015	0.240	3.28	—	1.010	—	—	69,700	—	43.0	—

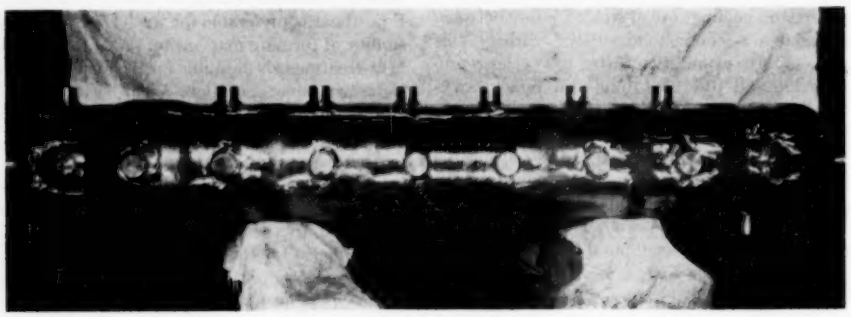

FIG. 1 TEST SECTION

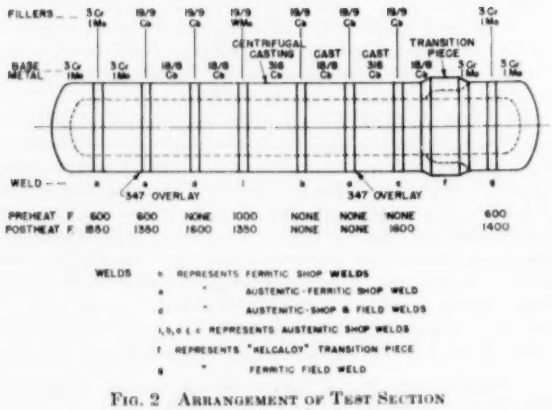

FIG. 2 ARRANGEMENT OF TEST SECTION

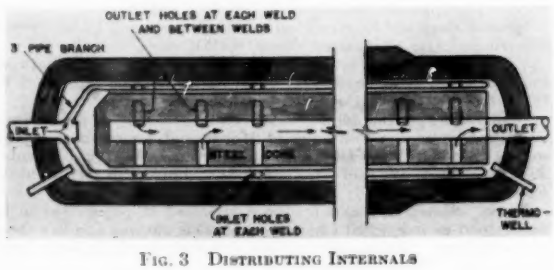

FIG. 3 DISTRIBUTING INTERNALS

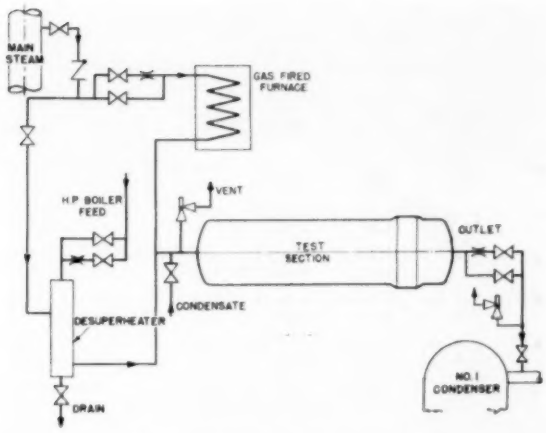

FIG. 4 DIAGRAM OF CONNECTIONS

control of the gas furnace. Pressure was controlled manually at the inlet and outlet of the test section. The heating-steam flow was limited arbitrarily to 2000 lb per hr maximum and was controlled by a metering orifice.

Temperatures during a typical cycle are shown in Figs. 6 and 7, from which it may be noted that the maximum differential between the inside and outside wall during heating was 80 F and during cooling was 270 F.

Intended rates of heating and cooling were somewhat exceeded. The maximum rate of heating was 0.5 deg per sec. The maximum rate of cooling during the first five cycles was 1.8 deg per sec and the average was 0.48 deg per sec. The maximum rate of cooling for cycles No. 6 to 100, inclusive, was 0.8 deg per sec and the average was 0.234 deg per sec. Heating rates at the start and at the finish of a heating period were low owing to the test section being full of water at the start and because of the decreasing temperature differential between the test section and the inlet steam at the finish.

Cooling of the test section was at times erratic because the

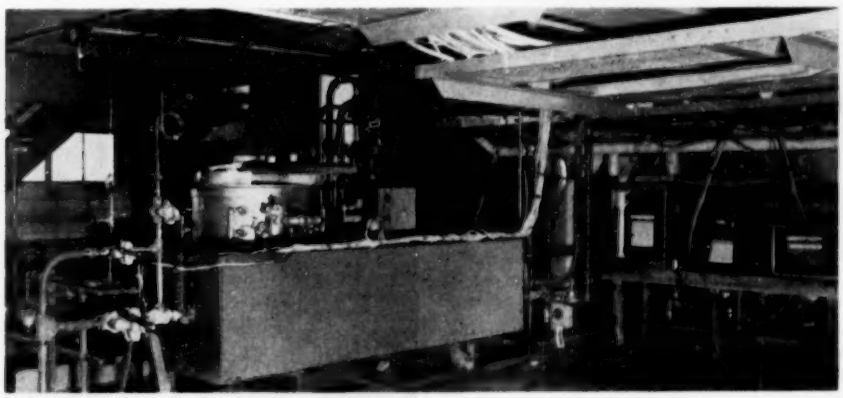

FIG. 5 ARRANGEMENT OF EQUIPMENT

soak at 1000 F, 1500 psi was included during alternate cycles to simulate aging to a moderate extent.

Cooling was controlled by injecting boiler feedwater into the superheated steam. The temperature of the steam entering the test section was limited to a maximum of 1250 F by automatic feedwater and steam mixture was difficult to control. Feedwater flow was increased as the test-section temperature decreased. At 450 to 500 F the test section was cooled entirely by feedwater. At 350 to 400 F, the feedwater was shut off and the condensate was admitted to cool down to 150 F.

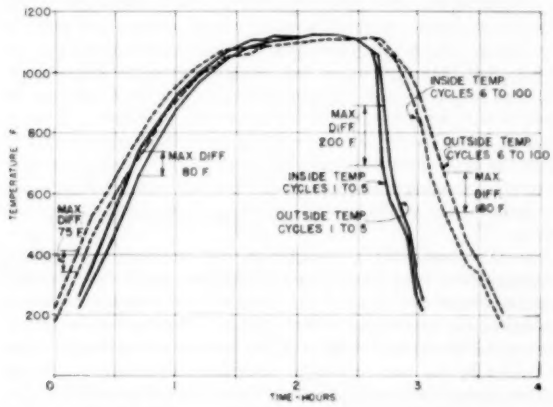

FIG. 6 TYPICAL HEATING AND COOLING CYCLE WELD (e) BETWEEN AUSTENITIC AND FERRITIC WROUGHT PIPE

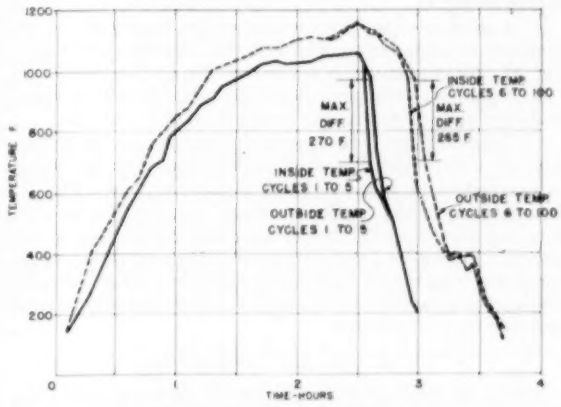

FIG. 7 TYPICAL HEATING AND COOLING CYCLE AT f AUSTENITIC-FERRITIC TRANSITION PIECE

The total cycling time for 100 cycles was 2803 hr of which 140 hr were heating, 105 hr holding at 1100 F, 2456 hr holding at 1000 F, and 102 hr cooling.

Examination

Before testing, welds in the section were radiographed to Boiler Code requirements and the surface of the section was examined by the red dye-fluid penetrant method. An ultrasonic inspection also was made. Ultrasonic inspection of the centrifugal casting was unsuccessful because of the large grain size. Some microfissures, Fig. 8, and star cracks, which were found, were not repaired in order to study the effect of thermal cycling upon them. Trepanned plugs were removed from all welds and examined. A few very small cracks were found in weld metal.

Fig. 8 Typical Microfissures; ×1

The test section was examined with red dye after 5, 30, 76, and 100 cycles. The section was inspected with ultrasonic flaw-detection equipment after five cycles. After 100 cycles, trepanned plugs were removed and examined. Typical macrographs of trepanned plugs are shown in Fig. 9. Ferrite and hardness values are shown in Table 2.

Results

The following results were noted:

1 No cracking was observed in any of the pieces which could be attributed to thermal cycling.

2 Microfissures and star cracks visible at the start of the test did not propagate.

3 A notch resulting from scaling on the ferritic side of the junctions between ferritic and austenitic materials was found, Fig. 10. No propagation of cracks from the notch appeared.

4 No defects were found in the (Kelcaloy) ferritic-austenitic transition piece other than the scaling previously mentioned.

5 The centrifugal casting satisfactorily withstood the cycling; however, a band of shallow checking 0.03 in. deep on the outside surface and 1/2 in. wide was found adjacent to weld *i*, Fig. 11. It could be removed readily by filing. The checking was not apparent after the 1900 F heat-treatment and its cause is not known. It may be a local progression from a mottled effect, which was observed on the outside surface in random locations, resulting from insufficient machining to remove the effects of the mold spray used for traction.

Conclusions and Further Tests

Two cyclic heating and cooling tests of materials and welded joints used in the Sewaren piping installation have shown that failures will not occur under conditions which may be encountered in normal operation during periods representing a major portion of the unit's life. Five years of operation on the first units in the plant itself have not resulted in failures of materials or welds in the piping systems which may be attributed to thermal cycling. It is apparent that a condition more severe than subjecting test sections in a free state to thermal cycling at the rates expected in operation is necessary to produce cracking or failure. It is intended, therefore, to continue cycling the section now under test with the application of external bending forces. Also under consideration is aging of the test section at some higher temperature, to simulate the condition of the piping after considerably more service.

Another possibility is to subject the test section to even greater thermal shock than heretofore until failure occurs. While these proposed tests are more severe than will be encountered in the actual piping installation, it is hoped that by this procedure it will be possible to evaluate ability of the various materials and joints included in the test section to withstand abnormal conditions which cannot be avoided entirely in the actual installation, and also possibly to indicate the effects of time and temperature under normal stress.

TABLE 2 FERRITE CONTENT AND HARDNESS OF WELDS
(Readings taken on outside surface of welds.)

Weld	Ferrite Content %			Hardness - Brinell		
	Before Test	After 30 Cycles	After 100 Cycles	Before Test	After 30 Cycles	After 100 Cycles
a	14.8 to 18.4	8.85 to 12.9	9.8 to 11.0	215 to 248	-	197 to 203
b	13.9 to 17.5	5.7 to 9.8	9.5 to 10.1	241	-	205 to 218
c	-	6.0 to 8.2	8.9 to 9.8	205 to 255	197	204 to 210
d	2.1 to 7.0	5.7 to 7.3	5.3 to 6.4	229	-	190 to 213
e	2.9 to 5.6	2.5 to 3.8	2.5 to 4.2	241	-	225 to 237
g	-	-	-	143 to 195	-	163 to 172
h	-	-	-	140	-	163 to 177
i	-	2.5 to 7.0	12.0 to 12.9	205 to 214	217 to 228	202 to 217

Fig. 9(*a*) Typical Macrograph of Trepanned Plug Before Cycling; ×2

Fig. 9(*b*) Typical Macrograph of Trepanned Plug After Cycling; ×2

FIG. 10 OXIDATION AT AUSTENITIC-FERRITIC JUNCTION; ×100

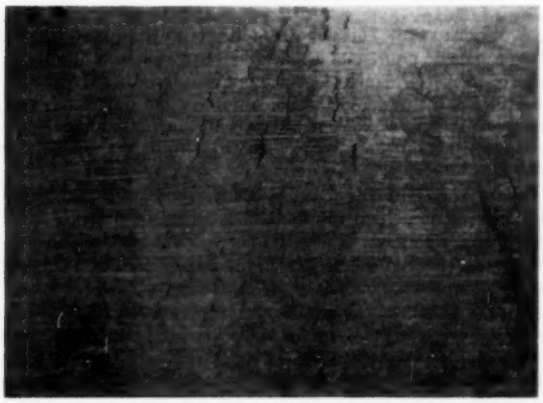

FIG. 11 CHECKING IN CENTRIFUGAL CASTING; ×5

ACKNOWLEDGMENTS

The co-operation and helpful advice of Messrs. E. L. Robinson and A. W. Rankin of the General Electric Company, N. L. Mochel of the Westinghouse Electric Corporation, W. B. Bunn of The M. W. Kellogg Company, and Dr. Schuh of United States Pipe and Foundry Company are acknowledged. The authors also are indebted to several associates in Public Service Electric and Gas Company, and particularly Mr. H. J. Robar, metallurgist, Maplewood Laboratory, for metallurgical examinations and interpretations.

Appendix

SOLUTION HEAT-TREATMENT OF AUSTENITIC WELDS

Laboratory tests indicate that a 1900 to 2000 F heat-treatment is beneficial in maintaining the impact resistance of welds in high-temperature service. It was therefore decided, after 30 cycles, to experiment with a 1900-F solution heat-treatment of one of the welds. Weld *c* was selected and heated to 1900 F with natural gas.

The heating and cooling rates were 400 deg per hr up to 1100 F, hold for 2 hr; 270 deg per hr from 1100 to 1900 F, hold for 2 hr. The weld was cooled rapidly. (It is believed that the 1100 F hold reduces the chance of developing cracks during heat-treatment.)

Owing to the narrowness of the heated band, the wall-temperature gradient was excessive, i.e., 300 F. This was sufficient to produce stress rupture in the weld metal, resulting in cracks at the outer surface of the weld. No evidence of carburization due to the use of natural gas for the heat-treatment was found.

The cracks consisted of an interrupted series of parallel lines, three or four wide, extending completely around the section in the weld metal. They were gouged out to a depth of $^3/_4$ in. and rewelded with 19/9 Cb. The reweld was not heat-treated.

In a second attempt, it was decided to solution heat-treat weld *i* (19/9 WMo) by electric induction. Cooling coils were applied at the extremities of the windings to avoid possible sigmatization of adjacent joints. Heating rates for this treatment were: 300 deg per hr up to 1100 F, hold for 2 hr; 600 deg per hr from 1100 to 1900 F, hold 2 hr; cool rapidly. This method proved successful as shown by trepanned specimens removed for examination following heat-treatment.

Discussion

R. H. CAUGHEY.[5] By fostering a test program which subjects typical piping materials and welded joints to conditions approaching the service requirements of increased high-temperature and high-pressure steam encountered in modern electric-generating plants, the authors have contributed greatly to our knowledge of the behavior of certain of these materials. It is gratifying to learn that this program will be extended to include other possible service conditions and that a future report on added results may be expected.

The behavior of weld joints composed of Type 347 stainless-steel deposits and wrought piping materials for steam-pipe service at temperatures of 1050 F and above has been under investigation by the writer's company in co-operation with Public Service of New Jersey service plants and certain of the turbine and electrode manufacturers, for the past several years. Particular interest has centered on the fact that satisfactory electrodes available up until now, in order to produce "crack-free" deposits, necessarily have been balanced, from a chemical-composition standpoint, to produce deposits which are "ferrite" bearing. However, the more rapid conversion of ferrite than austenite in these deposits to a brittle "sigma" phase, as the result of aging at the higher steam temperatures, and the accompanying liability that the mechanical strength of the weld joints could be impaired soon became the chief concern.

Objectively, therefore, efforts have been directed toward the development of improved electrode compositions which would deposit either fully austenitic welds or welds containing lesser amounts of ferrite, both of which would be insensitive to cracking. Also, and at the same time, practical postheat-treatments of weld joints which might inhibit sigma formations were explored.[6]

One result of this work, as it relates to the results described in the present paper, showed that the relative levels of ferrite in weld deposits compared by magne gage techniques, both before and after exposure to elevated temperatures, was a reliable indication of the progress of sigma formation, sigma being nonmagnetic whereas ferrite is highly magnetic. By reference to Table 2 of the paper, wherein the residual ferrite after cycling is compared with the initial rating, it is noticeable that the ferrite

[5] Assistant Chief Metallurgist, The M. W. Kellogg Company, Jersey City, N. J.

[6] "Fabrication of Austenitic Stainless Steel Piping for Operation at 1100 F," by W. G. Benz and R. H. Caughey, ASME paper No. 53—SA-58, presented at the Semi-Annual Meeting, Los Angeles, Calif., June 28–July 2, 1953.

evidence has not changed markedly. It seems evident therefore that the approximate 2400-hr exposure at 1000 F has not been long enough to convert the ferrite completely to sigma; accordingly, embrittlement of the weld deposits to any serious degree probably has not resulted.

This may be one explanation for the absence of any failure at this stage in testing. The results of any laboratory mechanical tests which the authors may have completed on each of the construction materials both before and after cycling should shed some light on this question. It is noted that the authors contemplate the application of an aging treatment at some higher temperature to simulate the conditions of the materials after extended service. In our opinion this is a step which should be taken to establish whether or not complete conversion of ferrite to sigma in austenitic (and ferrite-bearing) weld joints may be expected to result in early failures. Comparative laboratory tests at this stage also would be important.

L. F. Kooistra.[7] This paper constitutes a timely contribution to a welding problem in power-plant engineering that has been of tremendous importance during the past several years. Of particular interest in the series of welds tested are those which make up the joints between dissimilar metals, in the sense that one of the members in these joints is ferritic and the other austenitic.

This type of joint in some form or other will appear inevitably in high-temperature installations where austenitic materials are employed on the high-temperature end of the cycle. In general, they are more difficult to handle because of metallurgical dissimilarity as well as differences in coefficient of thermal expansion between these two types of steel. Representatives of these combinations are welds *e* and *f* in Fig. 2 of the paper.

Thermal-cycling tests have been conducted by the writer's company continuously since 1947. These tests were reviewed in a progress report in 1950.[8] It might be of value to discuss the results obtained with those reported in the paper.

Two types of tests are being conducted, namely, rotating-beam fatigue tests on full-size joints in superheater tubes, and the other, thermal cycles on a $10^3/_4$-in-diam steam pipe simulating service-operating cycles.

The rotating-beam fatigue tests constitute a rather severe stress cycle at constant operating temperature, with a frequency of about 350 cycles per min (cpm), where the thermal simulated service cycle on the $10^3/_4$-in-diam pipe was conducted at a rate of 1 thermal cycle a week—5 days at operating temperature of 1100 F and 2 days for cooling, inspection, and reheating. The results are widely different. Where the tube joints in the rotating-beam test can withstand hundreds of thousands, sometimes millions of cycles, the dissimilar-weld joint in the simulated-service test failed after 47 full weekly cycles. The difference in these results can be attributed largely to the extended time at temperature for the simulated service test, which will promote plastic deformation at the interface between the dissimilar metals. During the holding cycle at maximum temperature, plastic deformation will take place as a result of creep. In the cooling part of the cycle this plastic deformation may be reversed by yielding at or near room temperature. This severe treatment produces failure in the weakest (ferritic) metal at the interface.

If the holding time at operating temperature is too short to allow for creep to progress to any great extent or the temperature is so low that relaxation due to creep is insignificant, no reversible plastic deformation takes place and strains in the joint will remain largely elastic. Although the thermal cycle described in the paper closely approaches the weekly simulated-service cycle, the holding time at maximum temperature of 1100 F was only 1 hr. When the holding time was more extensive the temperature level was reduced to 1000 F so that the two principal factors inducing failure did not coincide.

It is believed that the longer cycling life exhibited by the welds described in the paper as compared with that of the weekly thermal cycle can be attributed to this fundamental difference.

As the authors are contemplating further and more severe tests it would be interesting to determine what the effect of a longer holding time at 1100 F would have on the cycling life of the dissimilar-metals joints. If any metallurgical investigation is made of the various welds after the cycling tests have been completed, a series of microphotographs of typical sections would be a valuable addition to the data presented.

A. W. Rankin.[9] This paper, together with the preceding companion paper,[8] represents a valuable contribution to our knowledge of the performance of welded joints at the current high temperatures of the power-generation industry. Testing of this type, involving as it does a considerable expenditure in time and money, is necessary if our industry is to proceed to higher temperature levels.

That no cracking was observed in any of the components which could be attributed to the thermal cycling and that the initial microfissures and star cracks did not propagate even under the severe test conditions described in this paper indicates that these materials and welding joints are inherently capable of reliable operation. That cracking in service has been encountered, however, indicates that the specific and severe test conditions necessary to duplicate actual service have not yet been introduced, and the authors should be encouraged to proceed with further tests to simulate both bending stress and time-temperature aging. Thermal shocks could be used of sufficient severity to produce weldment cracking, but the results of such tests would be difficult of interpretation since the thermal shocks already employed are sufficiently severe to represent any normally encountered in service.

The 1950 F postweld treatment of austenitic welds described in the Appendix has shown considerable promise in minimizing the deleterious effects of sigma formation. By utilizing a low-ferrite electrode in conjunction with 1950 F treatment not only is the amount of ferrite in the weld deposit considerably reduced in actual magnitude, but that which is present is essentially spheroidized by the 1950 F treatment so that its conversion to sigma cannot seriously affect the properties of the weld deposit. Room-temperature keyhole charpy tests of some type 347 weld deposits illustrate the value of this newly developed procedure. A 347 weld deposit of normal ferrite content with no postweld treatment initially had 12 per cent ferrite and 28 ft-lb charpy; after exposure to 1200 F for 300 hr the charpy had dropped to 7 ft-lb. A 347 weld deposit made with the low-ferrite electrodes and the 1950 F postweld treatment initially had approximately 3 per cent ferrite and 35 ft-lb charpy; after exposure to 1200 F for 6400-hr, the charpy value was still 24 ft-lb.

The changes in Brinell values which occur in austenitic weld deposits after long-time high-temperature exposure can be difficult

[7] Superintendent of Materials Development, Research Center, The Babcock & Wilcox Company, Alliance, Ohio. Mem. ASME.

[8] Progress reports on this work were presented at the 53rd Annual Meeting of the ASTM at Atlantic City, N. J., June 26–30, 1950.

"Some Considerations in the Joining of Dissimilar Metals for High-Temperature, High-Pressure Service," by O. R. Carpenter, N. C. Jesson, J. L. Oberg, and R. D. Wylie, Proceedings of the ASTM, vol. 50, 1950, pp. 809–860.

"Welds Between Dissimilar Alloys in Full Size Steam Piping," by R. U. Blaser, F. Eberle, and J. T. Tucker, Jr., Proceedings of the ASTM, vol. 50, 1950, pp. 789–808.

[9] Turbine Structural Engineer, Large Steam Turbine-Generator Department, General Electric Co., Schenectady, N. Y. Mem. ASME

of interpretation. Since the hardness is basically due to the sigma formation, and since this occurs only in the small percentage of ferrite present, a Brinell reading may not give a clear picture since it tends to give an average of the hardness of the sigma formed and the hardness of the grains themselves. Accordingly, a significant hardening of the ferrite constituents may be masked by the relative lack of hardening of the matrix.

With respect to austenitic-to-ferritic welds, the writer's company has conducted relatively long cycling tests on three such welds. Neither steam pressure nor bending stresses were employed in these cycling tests, but the temperature was cycled between 300 and 1100 F for a total of 254 cycles. During the last 130 cycles, a hold of 6 hours was maintained at both the 300 and 1100 F levels. These welds were between pipe stubs of Type 347 and $2^1/_4$ chrome—1 molybdenum with an outside diameter of $14^3/_8$ in. and a wall thickness of 3 in. One weld deposit was of $2^1/_4$ chrome—1 molybdenum, and this cracked severely on the austenitic side of the weld deposit after only 50 cycles; a second weld deposit was of Type 347 (1160 F postweld treatment, normal-ferrite electrode), and after 191 cycles, a crack of only 0.020 in. depth appeared on the ferritic side of the weld deposit; a third weld deposit was of Inconel, and this showed no defects whatsoever after the entire 254 cycles. All these three welds were austenitic-to-ferritic joints, and the Inconel deposit was employed because it has both superior high-temperature properties and a coefficient of expansion matching that of the ferritic steel. The minor cracking which was noted in the 347 weld deposit indicates that such welds should give many years of reliable service; our field experience to date on a number of such welds made with this procedure supports this expectation.

As a matter of interest to the power-generation industry, part of the program being conducted by the writer's company on austenitic weldments in general, is an investigation into the hot-shortness of some of the austenitic steels at the welding temperatures. Such hot-shortness may be one of the primary causes for the cracking which sometimes occurs in cast base materials, during the welding operation, adjacent to the weld deposit. It is planned that these results will be made available to the industry as soon as this investigation has proceeded to a point at which significant results are being obtained.

Authors' Closure

Mr. Caughey's suggestion that the test section be aged at elevated temperatures to promote the formation of sigma and more closely simulate the effects of service in the actual piping system is considered part of the test program. Aging is expected to follow the second phase of the test in which the test section will be subjected to external bending stresses in addition to thermocycling stresses. At the conclusion of the test, complete mechanical and metallurgical tests will be made.

It is proposed to apply bending stresses during the next 50 cycles equal to the maximum stress value permitted by the ASME Boiler Code for type 347 material.

If failure does not occur, it is then proposed to apply bending stresses comparable with the maximum combined bending-stress value permitted by the proposed revision to the ASA Piping Code.

Mr. Kooistra's comparison with the Babcock & Wilcox tests is interesting and it is our intention in the second phase of the tests, by altering the heating equipment, to hold the test section at 1100 F for longer periods, more closely simulating actual service conditions.

Mr. Rankin's observations concerning the beneficial effects resulting from 1950 F postheat-treatment of austenitic weldments are in agreement with our tests. Correlation of the physical properties and microstructure of the parts which cracked during the General Electric cyclic tests, with the cracking currently observed in the parent-metal heat-affected zones of entire type 347 weldments, both prior to and following service, would be interesting.

The investigation, which the General Electric Company is now conducting, to determine the cause of cracking in the heat-affected zones of austenitic weldments is most opportune. It appears that weld-metal deposits as now made with low-ferrite electrodes, and close control of the silicon-carbon and columbium-carbon ratios and with additional manganese, are better able to withstand the effects of welding, heat-treatment, and service conditions than is the parent metal. If cracking is due to hot-shortness in type 347 cast or wrought base metal as postulated, modification in the chemistry of the base metal for application in high-temperature-pressure steam-turbine parts and piping should be considered.

Stress-Rupture Properties of Some Chromium-Nickel Stainless-Steel Weld Deposits

By R. D. WYLIE,[1] C. L. COREY,[2] AND W. E. LEYDA[3]

The use of higher steam temperatures in central-station generating plants has required the manufacturer of power-boiler equipment to use austenitic chromium-nickel steels for the outlet sections of the superheater where metal temperatures are in the order of 1200–1250 F. Since these tubular materials must be fabricated by welding, The Babcock & Wilcox Company has been conducting a test program on the high-temperature strength of chromium-nickel stainless-steel welded joints. The first work to be completed is data on the strength of all-weld-metal coupons of eleven compositions of commercial stainless-steel weld deposits. It is hoped that the data in this report, together with those presented in subsequent discussion by other industrial organizations, will serve as a guide to the Subcommittee on Stress Allowances for Ferrous Materials of the ASME Boiler Code Committee in the selection of allowable stresses for the chromium-nickel stainless steels.

Introduction

IN central-station power-boiler equipment, the outlet-steam temperatures and pressures have been raised consistently in recent years in order to increase the efficiency of power production. Boilers in operation at the present time deliver superheated steam to the turbine at 1050 F and 2300 psi pressure. Installations are being built with 1100 F steam temperature, and, in the future, when higher-strength tube materials are available, units delivering steam at 1200 F may be possible. With this increase in outlet steam temperature, it has been necessary to use high-strength austenitic-alloy tubing for the outlet ends of the superheater. Superheater-metal temperatures are now in the range of 1200–1250 F, and in the 1100–1150 F steam units are predicted to be 1300–1400 F.

Many investigators, foreseeing the need for high-temperature-strength data on wrought austenitic alloys, have been performing creep-rupture tests on these materials for many years. The ASME Subcommittee for Allowable Stresses has collected sufficient data to establish design stresses for most wrought austenitic alloys, and additional data are still being obtained. Since these materials are employed in tubular form and are joined together by welding in the construction of superheaters, The Babcock & Wilcox Company, in 1949, undertook a comprehensive program at both the Works Control Laboratory in Barberton, Ohio, and the Research and Development Center in Alliance, Ohio, to determine the high-temperature strength of stainless-steel weld deposits as produced and used at the present time.

The selection of electrodes for welding austenitic alloys is usually governed by the analysis of the base material. For welding the 18 Cr-8 Ni type alloys, a 19 Cr-9 Ni electrode is used which normally deposits a partially ferritic weld. A small amount of delta ferrite has been found necessary to produce sound weld deposits at 0.08 maximum carbon content. For welding the titanium- and columbium-stabilized alloys of the 18 Cr-8 Ni type, 19 Cr-9 Ni-Cb electrodes usually are employed, since the columbium in the coating is transferred through the arc in sufficient quantities to insure a stabilized weld deposit. Another popular stainless-steel electrode is 25 Cr-20 Ni which has been used extensively for welding stainless steels of all types and in many cases for joining hardenable ferritic materials.

In addition to the electrodes just discussed, the following weld-metal compositions were included in this investigation:

(1) 19 Cr-9 Ni-LC
(2) 19 Cr-9 Ni-Cb-Ta
(3) 19 Cr-9 Ni-DW
(4) 18 Cr-12 Ni-3 Mo
(5) 18 Cr-12 Ni-3 Mo-LC
(6) 18 Cr-12 Ni-3 Mo-Cb
(7) 25 Cr-20 Ni-Cb

Some of these materials may be satisfactory for service at metal temperatures of 1300–1400 F, whereas others, such as the extra-low-carbon grades, may find use in special applications. The actual chemical analyses of the weld deposits are presented in Table 1.

Testing Procedure

The tests to be described in this paper were made on nondilution all-weld-metal pads produced by depositing multilayer pads of weld-metal on a base plate. From these pads two types of stress-rupture specimens were prepared. One type, employed by the Alliance Research Laboratory is shown in Fig. 1(*a*). The specimens were prepared so that the direction of applied stress in the rupture test would be normal to the direction of weld-bead deposition. This would represent the direction of the major stress axis in a longitudinal weld seam in a drum or header or in a seal weld. The specimen was machined with a 0.252-in. reduced diameter. The other specimen, used by the Barberton Laboratory, is illustrated in Fig. 1(*b*). This specimen was prepared in such a manner that the direction of applied stress would be parallel to the direction of weld-bead deposition. This would represent the direction of major stress in a circumferential tube or pipe weld. The specimen used for these tests was machined with a 0.505-in. reduced diameter. A summary of welding procedures used in preparing the weld pads for this examination is given in Table 2. Most of the electrodes used in this investigation were commercial-quality welding rods.

The stress-rupture tests described in this report were made by

[1] Metallurgist, The Babcock & Wilcox Company, Barberton, Ohio.
[2] Research Engineer, Engineering Research Institute, University of Michigan, Ann Arbor, Mich.
[3] Senior Test Engineer, The Babcock & Wilcox Research Center, Alliance, Ohio.

Contributed by the Joint ASTM-ASME Committee on Effect of Temperature on the Properties of Metals, and presented at a joint session with the Power Division at the Annual Meeting, November 29–December 4, 1953, of THE AMERICAN SOCIETY OF MECHANICAL ENGINEERS.

NOTE: Statements and opinions advanced in papers are to be understood as individual expressions of their authors and not those of the Society. Manuscript received at ASME Headquarters, October 9, 1953. Paper No. 53—A-152.

TABLE 1 CHEMICAL ANALYSES OF DEPOSITED WELD METAL

Material	Laboratory	C	Mn	Si	Cr	Ni	Mo	W	Cb	Ta
19Cr-9Ni	A	.07	1.62	0.51	19.36	9.63	-	-	-	-
	B	.09	2.23	0.49	18.74	9.06	-	-	-	-
19Cr-9Ni LC	A	.03	1.02	0.16	19.77	10.57	-	-	-	-
19Cr-9Ni Cb	B	.09	1.62	0.53	19.96	9.78	-	-	1.06	-
	B	.08	1.52	0.46	19.47	10.06	-	-	1.43	-
	A	.07	1.81	0.52	19.88	9.90	.10	-	.91	-
19Cr-9Ni Cb Ta	B	.09	2.20	1.06	18.59	8.86	-	-	.68	.17
19Cr-9Ni DW	A	.29	1.61	.94	20.79	7.98	1.21	1.49	.62	-
18Cr-12Ni-3Mo	B	.14	1.60	.40	19.65	13.58	3.22	-	-	-
	A	.10	1.94	.59	18.68	13.82	2.09	-	-	-
18Cr-12Ni-3Mo LC	A	.03	1.08	.19	18.62	13.28	1.70	-	-	-
18Cr-12Ni-3Mo Cb	A	.07	1.97	.50	19.10	12.21	2.25	-	.74	-
25Cr-20Ni	B	.22	2.10	.45	25.23	21.14	-	-	-	-
	A	.18	2.65	.33	24.78	18.92	-	-	-	-
	A	.12	1.48	.42	25.92	22.12	-	-	-	-
25Cr-20Ni Cb	A	.11	1.97	.65	25.39	18.16	-	-	1.15	-
	B	.13	1.84	.65	25.36	20.25	-	-	1.20	-

TABLE 2 SUMMARY OF WELDING-PROCEDURE DATA

Electrode Material	19Cr-9Ni		19Cr-9Ni Cb		19Cr-9Ni LC	19Cr-9Ni Cb
	A	B	A	B		
Manufacturer	B&W	Arcos	Arcos	Arcos	Arcos Chromend KLC	B&W
Heat No.	-	Chromend K E1579L308	F1567A308	-	E1874R308	B875
Process No.	-	D94921A	D124717	-	54917-2	-
Electrode Dia.	5/32	5/32	3/16	5/32	5/32	5/32
Current	125	160	150	130	130	125
Preheat	-	-	-	70	70	-
Interpass Temp.	350	-	350	-	-	350

Electrode Material	19Cr-9Ni DW		18Cr-12Ni-3Mo			18Cr-12Ni-3Mo LC
	A	B	A	B	C	
Manufacturer	Arcos	Arcos	Arcos	Chromend	KMo	Arcos Chromend KMoLC
Heat No.	4313	4314	E-1618L316	-	-	E1942L316
Process No.	-	-	34826	-	-	D12496-1
Electrode Dia.	1/8	1/8 & 5/32	5/32	1/8	1/8	5/32
Current	90	1/8 - 90 5/32-105	125	90	95	130
Preheat	70	70	-	70	70	70
Interpass Temp.	-	-	350	-	-	-

Electrode	18Cr-12Ni-3Mo Cb	25Cr-20 Ni				25Cr-20Ni Cb	
		A	B	C	D	A	B
Manufacturer	Arcos	B&W	B&W	Arcos	Arcos	Arcos	Arcos
Heat No.	-	B2HT1890	-	-	-	F1074L310	D1552L310
Process No.	-	-	-	-	-	94517E	-
Electrode Diameter	1/8	3/16	1/8	1/8	1/8	3/16	1/8
Current	95	150	90	85	90	150	90
Preheat	70	-	70	70	70	-	70
Interpass Temp.	-	-	-	-	-	350	-

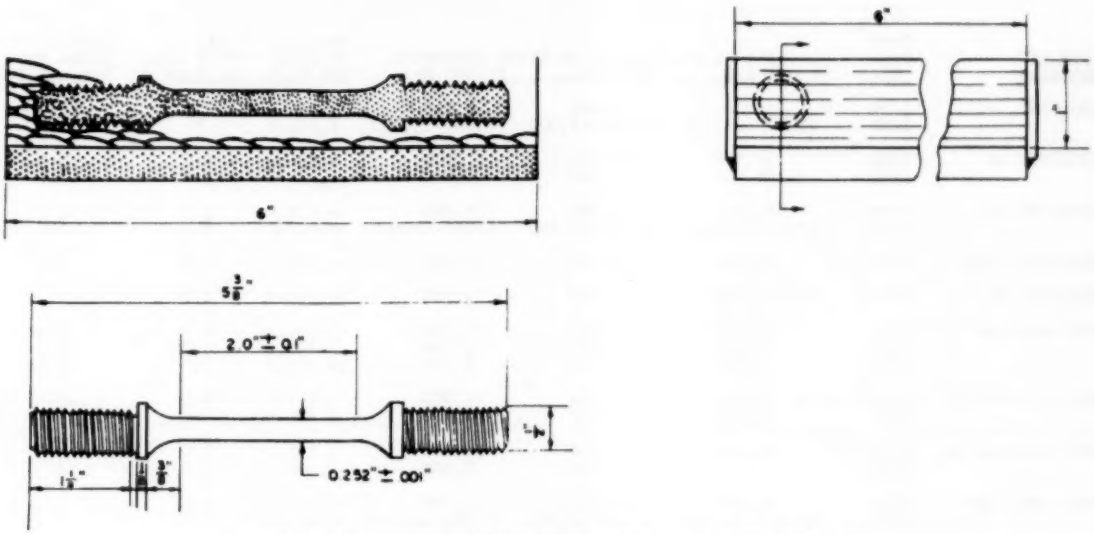

FIG. 1(a) SPECIMEN TAKEN TRANSVERSE TO DIRECTION OF WELD BEADS

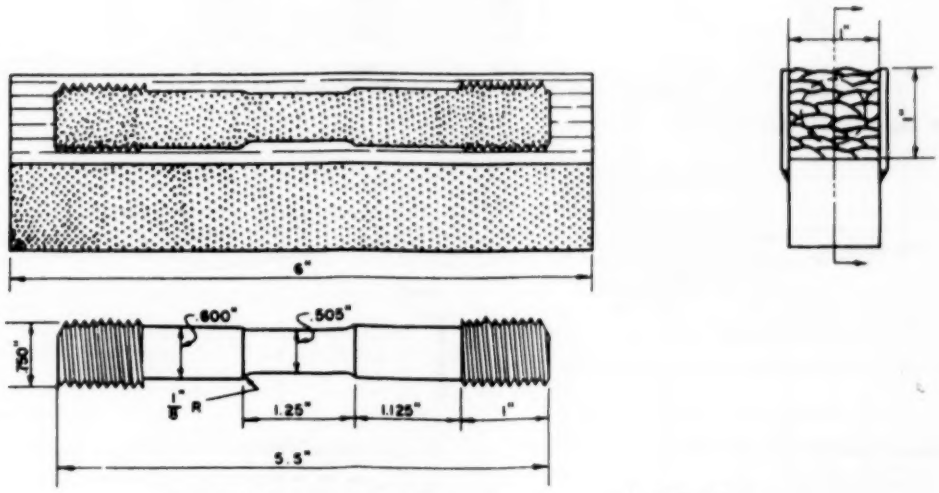

FIG. 1(b) SPECIMEN TAKEN PARALLEL TO DIRECTION OF WELD BEADS

the two co-operating laboratories. The tests at the Alliance Laboratory were made in the 12-station multiple-unit stress-rupture machines. These facilities recently were described (1).[4] The tests at Barberton were made in single-station units with a constant-input type of power control.

The tests were conducted at several temperatures selected with respect to the intended operation. The principal test temperature employed was 1200 F. The duration of the longest test at each temperature is listed in Table 3. Many of these tests were continued for longer than 10,000 hr. This reflects the policy of the company in studying the high-temperature properties of the materials used for steam generation with long-time creep and stress-rupture tests.

The data obtained in these tests were plotted on logarithmic co-ordinate chart paper. From these charts values were selected for the stress to produce rupture in 100, 1000, and 10,000 hr.

[4] Numbers in parentheses refer to the Bibliography at the end of the paper.

The fractured specimens were examined metallographically for structural changes which may have occurred during tests. These studies were supplemented by magnetic permeability and Vickers hardness tests on many of the compositions investigated. These tests were used to determine the extent and, in certain cases, the rate of structural transformations brought about by long-time exposure to elevated temperatures under stress.

PRESENTATION OF DATA

The test data obtained on the weld-metal compositions investigated are plotted in Figs. 2 to 12. There was perhaps more scatter experienced in these tests than generally encountered in wrought materials of corresponding chemical analysis. This may be due partly to the less homogeneous nature of the deposited weld metal. A tabulation of stress to produce rupture in 100, 1000, and 10,000 hr is given in Table 3. As a matter of further interest, a column was added to this table showing the percentage of elongation obtained at rupture for the longest test.

TABLE 3 SUMMARY OF STRESS-RUPTURE DATA FOR DEPOSITED WELD METALS

Type of Material	Test Temp °F.	Stress for Rupture in Times Indicated 100 Hrs.	1000 Hrs.	10,000 Hrs.	Duration of Longest Test	% El. in 2" of Longest Test	Similar Value for Wrought Steel
19Cr-9Ni	1050	36,000	28,000	20,000	5,336.2	0.5	6.0
	1200	21,000-24,000	14,200-18,000	7,800-13,000	5,921.0	*	14.5
19Cr-9Ni LC	1050	35,500	27,000	20,500	6,934.3	3.5	9.5
	1200	19,500	14,000	9,000	6,037.2	3.0	27.0
19Cr-9Ni Cb	1050	55,000	44,000	27,000	6,424.4	5.5	6.0
	1200	29,000-35,000	21,000-25,000	16,000-18,000	6,928.0	6.1	16.0
18Cr-8Ni-CbTa	1200	46,000	31,000	20,000	4,328.0	5.0	6.5
19Cr-9Ni DW	1500	9,600	5,600	3,300	16,354.3	2.0	
18Cr-12Ni Mo	1200	28,000	19,500	10,500	3,592.0	6.0	38.0
	1350	12,500	7,200	3,100	3,427.8	0.0	22.0
	1500	6,000	3,000	2,100	14,055.6	1.0	41.0
18Cr-12Ni-Mo-LC	1200	22,000	16,500	7,700	5,192.2	4.5	18.0
	1350	12,800	6,800	2,900	5,624.6	*	-
18Cr-12Ni-Mo Cb	1200	42,000	34,500	27,000	5,601.3	1.0	-
	1350		16,000	8,600	2,020.3	0.0	31.5
25Cr-20Ni B&W	1050	39,500	27,500	16,500	4,704.8	1.0	
	1200	21,000-29,000	12,000-17,500	7,000-10,500	6,270.0	5.0	
25Cr-20Ni Arcos	1050		25,000	14,000	6,512.1	0.5	-
	1200		9,200	5,000	10,673.9	1.0	-
	1350		4,800	2,700	6,802.7	3.5	18.8
	1500		2,500	1,400	10,470.6	4.0	34.0
25Cr-20Ni Cb	1050		51,000	43,000	8,494.8	1.5	-
	1200	35,000	25,500-32,300	14,500-20,500	12,679.6	*	-

*Unable to measure ductility

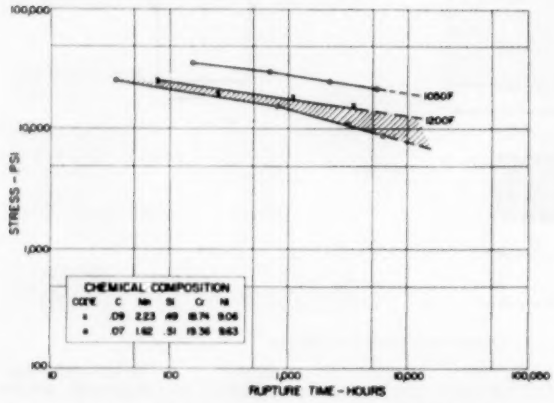

FIG. 2 STRESS-RUPTURE CURVES FOR 19 CR-9 NI WELD METAL

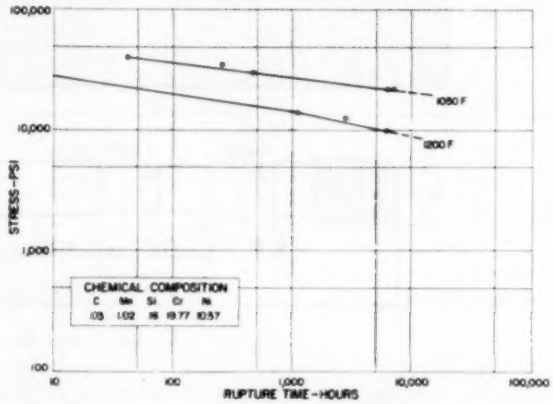

FIG. 3 STRESS-RUPTURE CURVES FOR 19 CR-9 NI (LOW-CARBON) WELD METAL

These materials exhibited very low rupture ductility in the long-time tests, which appears to be a characteristic of the austenitic weld metals. A companion column was added showing comparable ductility values for rupture-test specimens of wrought materials of similar chemical composition and approximately the same rupture time. Where enough data were available to indicate the extent of scatter, this was indicated on the chart by a shaded band. As an example, reference is made to Fig. 2 which is the charted data for unstablized 19 Cr-9 Ni weld deposits. The area between the curves has been shaded to indicate variations in strength which have been observed in this material tested at 1200 F.

If enough test data had been available on each of the materials tested, it is believed that all of the curves would have been represented by such a scatter band.

A comparison of the rupture strength of the weld metals with wrought products of similar composition is shown in Fig. 13. The information on the wrought material was taken from various sources given in the Bibliography (2, 3, 4), as well as from unpublished data obtained by the company. It can be seen from this chart that most weld deposits are weaker than the equivalent wrought material. The columbium-stabilized weld metals appeared to be the principal exception to this.

The strengths of the weld metals investigated are compared in Table 4. The metals are listed at each test temperature employed in order of decreasing stress-rupture strength. The strongest weld metals at each temperature were those stabilized with columbium and the weakest was 25 Cr-20 Ni. The extra-low-carbon grades of weld deposit were weaker at 1100 F than the

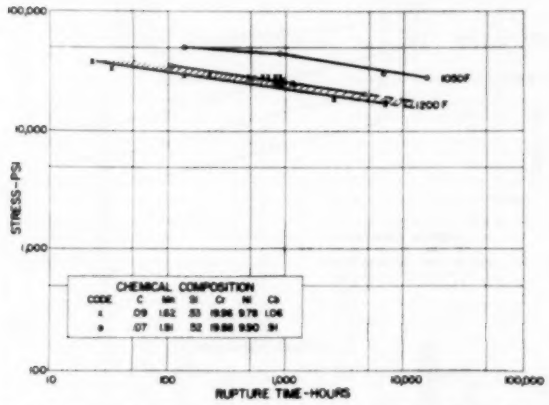

FIG. 4 STRESS-RUPTURE CURVES FOR 19 Cr-9 Ni-Cb WELD METAL

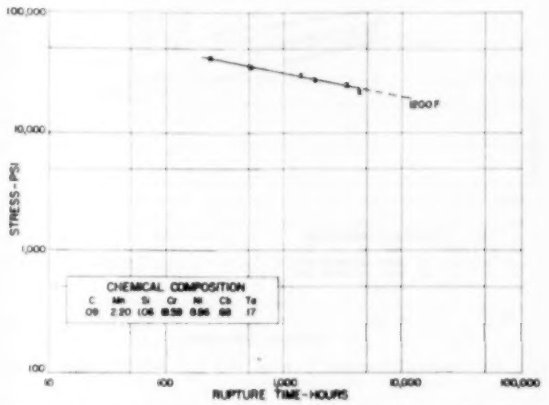

FIG. 5 STRESS-RUPTURE CURVES FOR 18 Cr-9 Ni-Cb-Ta WELD METAL

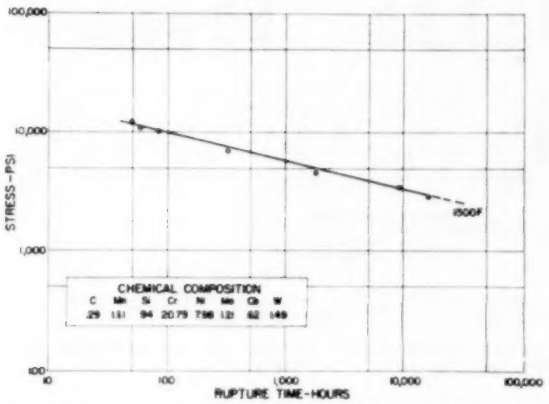

FIG. 6 STRESS-RUPTURE CURVES FOR 19 Cr-9 Ni-DW WELD METAL

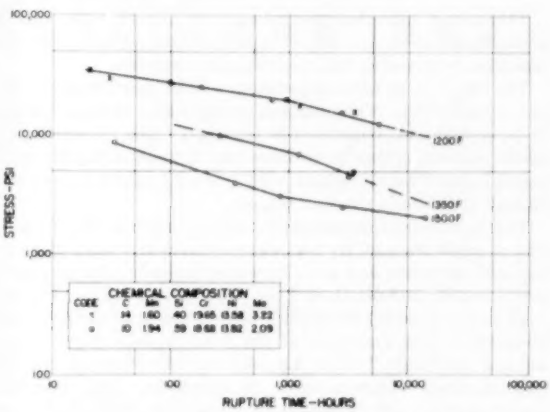

FIG. 7 STRESS-RUPTURE CURVES FOR 18 Cr-12 Ni-Mo WELD METAL

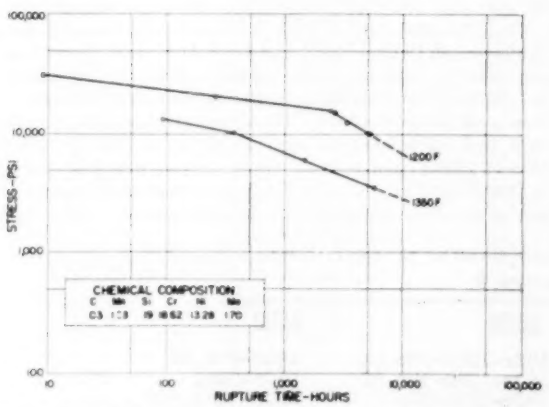

FIG. 8 STRESS-RUPTURE CURVES FOR 18 Cr-12 Ni-Mo (LOW-CARBON) WELD METAL

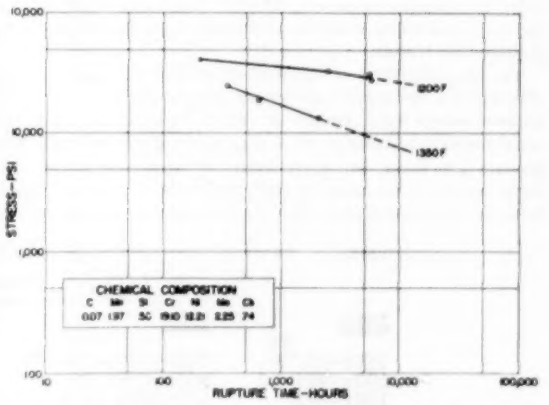

FIG. 9 STRESS-RUPTURE CURVES FOR 18 Cr-12 Ni-Mo-Cb WELD METAL

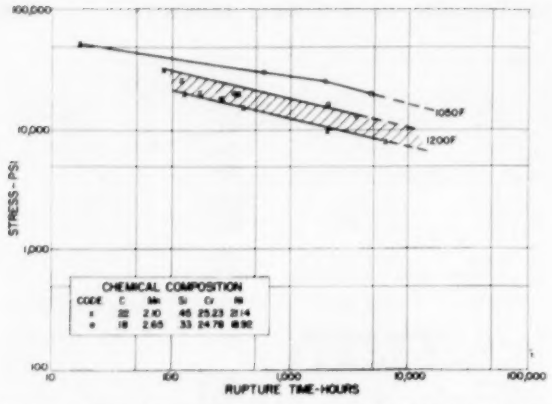

FIG. 10 STRESS-RUPTURE CURVES FOR 25 CR-20 NI(B&W) WELD METAL

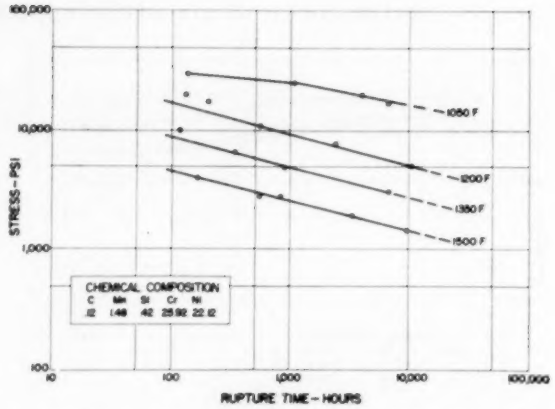

FIG. 11 STRESS-RUPTURE CURVES FOR 25 CR-20 NI(ARCOS) WELD METAL

same analysis at standard carbon levels. This is also true for the extra-low-carbon wrought metals.

METALLURGICAL CONSIDERATIONS

The factors affecting the strength of a weld deposit at a given temperature are chemical composition, soundness of the deposited weld metal, and metallurgical structure.

The effect of chemical composition was discussed briefly in the preceding section. The principal strengthening elements appear to be carbon and columbium or tantalum. The chromium and nickel contents appear to be important in maintaining the weld-metal balance and, together with carbon content, govern the amount of ferrite in the weld deposit.

The soundness of the austenitic weld deposits has been a subject of much research by the manufacturers and users of stainless-steel electrodes and there have been several technical papers written on the subject (5, 6, 7, 8). It is obvious that unless the weld metal is sound it will not have consistent stress-rupture properties. The soundness of the weld depends largely upon welding procedure, weld-metal analysis, and electrode coating characteristics. Defects such as entrapped slag, porosity, microfissuring, and crater-cracking, if not eliminated may produce poor high-temperature strength. The welds used in this investigation were made with high-quality electrodes with the chemistry such as to insure freedom from microfissuring. In order to eliminate crater-cracking the pads were made so that the stops and starts would be discarded when the samples were prepared for testing.

The microstructure of the weld deposit is the third criterion affecting the sustained high-temperature strength. In order to produce sound weld deposits of the 19 Cr-9 Ni type it is the usual practice to balance the composition of the weld metal to produce 2 to 6 per cent delta ferrite in the microstructure. At temperatures in the range of 1100–1600 F this ferrite may transform to sigma phase and affect the high-temperature properties.

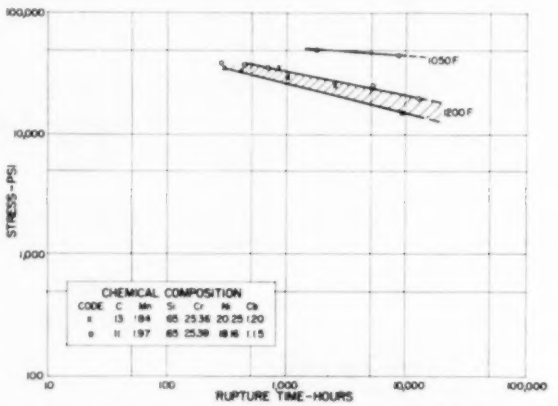

FIG. 12 STRESS-RUPTURE CURVES FOR 25 CR-20 NI-CB WELD METAL

Sigma phase also may form in totally austenitic weld deposits such as 25 Cr-20 Ni. In both of these cases the particle size and distribution is a factor in determining the high-temperature strength. The presence of carbides and their size and distribution also may affect high-temperature strength of weld deposits.

The data presented in Table 5 illustrate the effect of aging treatments on 19 Cr-9 Ni-Cb and 25 Cr-20 Ni weld deposits and may reflect to some extent the influence of carbide precipitation and sigma-phase formation on the stress-rupture strength of these weld metals at 1200 F. For these tests weld-metal samples were used which had been aged for 100 hr at 1250 F, 1350 F, 1450 F, 1550 F, and 1650 F. Other samples were heat-treated at 1600 F for 5 hr, and 1750 F for 1 hr, which were representative of two shop stress-relieving heat-treatments. After these

TABLE 4 WELD METALS LISTED IN ORDER OF DECREASING STRESS-RUPTURE STRENGTH

Temperature, F			
1050	1200	1350	1500
25Cr-20/Cb	18Cr-12Ni-3Mo Cb	18Cr-12Ni-3Mo cb	19Cr-9Ni DW
19Cr-9Ni LC	25Cr-20Ni Cb	18Cr-12Ni-3Mo LC	25Cr-20Ni
19Cr-9Ni	18Cr-8Ni CbTa	18Cr-12Ni-3Mo	18Cr-12Ni-3Mo
25Cr-20Ni	19Cr-9Ni	25Cr-20Ni	
	18Cr-12Ni-3Mo		
	19Cr-9Ni		
	19Cr-9Ni LC		
	18Cr-12Ni-3Mo LC		
	25Cr-20Ni		

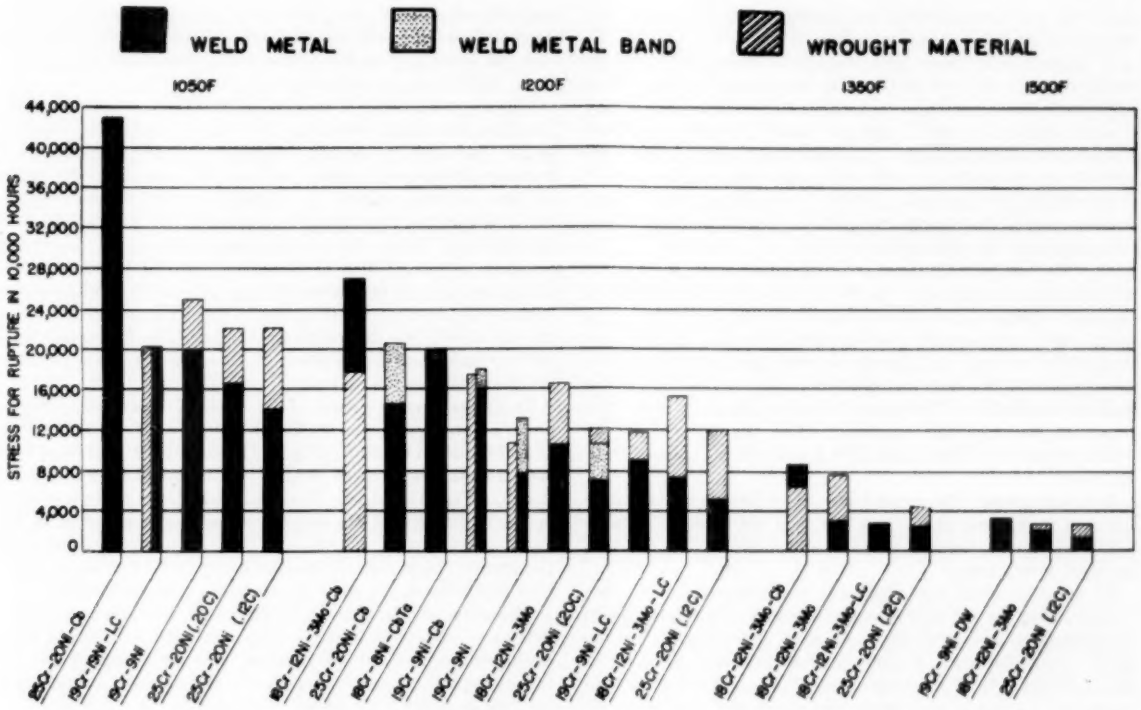

FIG. 13 COMPARISON OF 10,000-HR RUPTURE STRENGTHS OF WELD METALS AND WROUGHT MATERIALS

TABLE 5 EFFECT OF AGING TREATMENT ON THE STRESS-RUPTURE PROPERTIES AT 1200 F ON 19 CR-9 NI-CB AND 25 CR-20 NI WELD DEPOSITS

Aging Treatment	Stress	Fracture Time	% Elong. *
19 Cr-9 Ni Cb			
As Welded	28,000	693	5.0
1750 F-1 hr-AC	28,000	787	18.0
1600 F-5 hr-AC	28,000	477	4.8
1250 F-100 hr	28,000	783	6.0
1350 F-100 hr	28,000	912	5.0
1450 F-100 hr	28,000	884.5	6.0
1550 F-100 hr	28,000	619	7.0
1650 F-100 hr	28,000	231.5	7.0
25 Cr-20 Ni			
As Welded	20,000	237	4.0
1750 F-1 hr-AC	20,000	425.5	0
1600 F-5 hr-AC	20,000	381.5	0
1250 F-100 hr	20,000	341	5.0
1350 F-100 hr	20,000	171.5	9.0
1450 F-100 hr	20,000	123	0
1550 F-100 hr	20,000	356	10.0
1650 F-100 hr	20,000	334.5	15.0

* This value is difficult to measure in these materials due to the type of fracture.

heat-treatments, the samples were tested at 1200 F at a uniform stress level selected for each material.

It appears from these data that the transformations which occurred in the 19 Cr-9 Ni-Cb weld deposits during the 100-hr aging cycle at temperatures up to 1550 F did not produce a drop in stress-rupture strength. Aging at 1650 F, however, produced a sharp decrease in strength. The results obtained on the stress-relieved samples indicated that the original shop heat-treatment is important. For example, a 1750 F stress-relieving heat-treatment increased the rupture time at the same stress level when compared with the as-welded condition.

The 25 Cr-20 Ni weld deposits, on the other hand, reacted in a different manner from that described for the 19 Cr-9 Ni-Cb weld deposits. Aging at 1350 F and 1450 F for 100 hr resulted in a sharp drop in rupture life, indicating that the type of precipitation which occurred as a result of these aging treatments was detrimental to the high-temperature properties. It is believed that the formation of intergranular sigma phase at these temperatures produced this condition. The carbide precipitation which occurred at 1250 F and 1550 F and above appeared to be beneficial.

It would appear that sigma phase when present in isolated islands as in the case of 19 Cr-9 Ni-Cb, is not as detrimental to high-temperature strength as when it is distributed as an intergranular precipitate.

In order to study the significant transformation which occurred during the tests the fractured specimens were subjected to microscopic examination, hardness tests, and magnetic permeability measurements. A group of these fractured specimens is shown in Fig. 14. A common characteristic of all of these weld deposits is the lack of ductility at high temperature even in short-time tests. It will be noted that many of the specimens are broken in more than one location. This resulted from either (*a*) initiation of failure at a secondary location so that the piece broke off during removal from the furnace, or (*b*) severe sigma embrittlement of the specimens during testing, resulting in the specimen breaking after the completion of the test. In the former case the secondary rupture surface was almost completely oxidized, while in the latter case it was entirely bright.

The microstructures of representative alloys which were subjected to the longest stress-rupture time are shown in Figs. 15 to 22. It will be noted that there is a considerable difference between the various austenitic alloys with respect to the effect of time at temperature on microstructural transformations. For example, the structural changes in 19 Cr-9 Ni (Fig. 15) and 19 Cr-9 Ni-LC (Fig. 16) are comparatively simple, involving primarily a precipitation of chromium carbides around the ferrite islands and minor amounts of sigma phase formed from the delta ferrite, in situ. On the other hand, the structure of 18 Cr-12 Ni-3 Mo-Cb (Fig. 20) and 25 Cr-20 Ni-Cb (Fig. 22) contain both alloy carbides and sigma phase which renders separate metallographic identification difficult.

To substantiate the effect of the mode of occurrence of sigma phase on strength, compare the structures of 18 Cr-8 Ni-3 Mo (Fig. 19) and 25 Cr-20 Ni (Fig. 21) both of which had relatively low strength with that of 19 Cr-9 Ni-Cb and 19 Cr-9 Ni-Cb-Ta shown in Figs. 17 and 18. The fine intergranular pattern present in the 18 Cr-12 Ni-3 Mo and the massive sigma formed in the 25 Cr-20 Ni appear to result in a decrease in strength, whereas the smaller, more isolated islands in the 19 Cr-9 Ni-Cb and 19 Cr-9 Ni-Cb-Ta do not affect the high-temperature strength.

Weld deposits by nature do not have a homogeneous microstructure. A typical example of the structure which may exist in different locations in a weld deposit is shown in Figs. 23 and 24. It may be noted that the shape, particle size, and distribution of the carbide phase is considerably different in the two weld beads represented by Fig. 24. Metallographic observations were supplemented with magnetic-permeability measurements and Vickers hardness surveys, which are summarized in Table 6. From these one may make several interesting observations:

MATERIAL	19 CR-9 NI	19 CR-9 NI-CB	18 CR-13 NI-3 MO	25 CR-20 NI	25 CR-20 NI-CB
TEST TEMP. F.	1200	1050	1500	1050	1200
STRESS PSI.	9,000	30,000	2,000	20,000	20,000
RUPTURE TIME-HRS.	5,929.1	6,424.4	14,055.6	4,704.8	12,679.6
ELONG. % IN 2"	*	5.5	1.0	1.0	*

* - ELONGATION WAS NEGLIGIBLE

FIG. 14 REPRESENTATIVE STRESS-RUPTURE SPECIMENS OF FIVE DIFFERENT WELD DEPOSITS

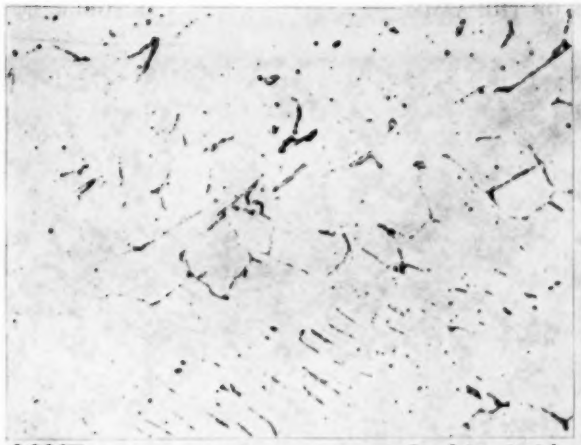

FIG. 15 STRUCTURE 19 CR-9 NI WELD DEPOSIT, 1200 F, 15,000 PSI-3537 HR

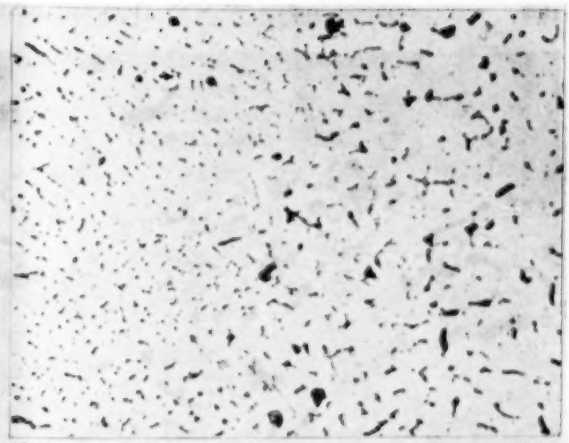

FIG. 16 STRUCTURE OF 19 CR-9 NI-LC WELD DEPOSIT, 1200 F, 10,000 PSI. 6037.2 HR

FIG. 17 STRUCTURE OF 19 CR-9 NI-CB WELD DEPOSIT, 1200 F, 17,000 PSI. 6928 HR

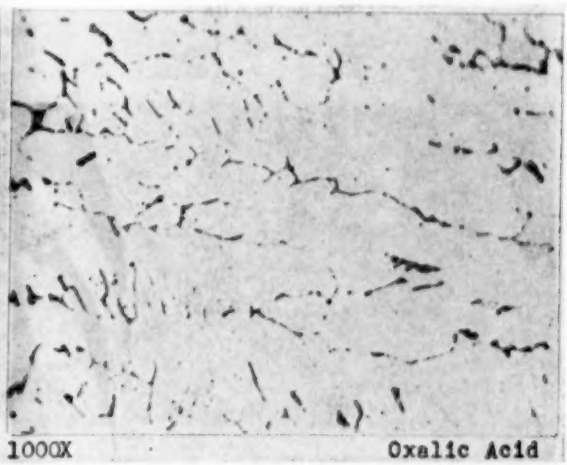

FIG. 18 STRUCTURE OF 19 CR-9 NI-CB-TA WELD DEPOSIT, 1200 F, 22,000 PSI, 3129 HR

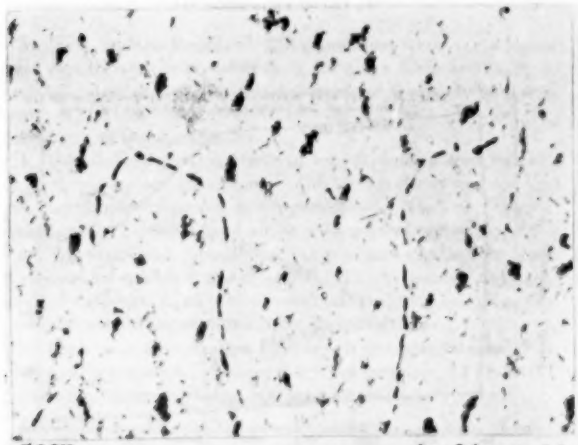

FIG. 19 STRUCTURE OF 18 CR-12 NI-3 MO WELD DEPOSIT, 1350 F, 5000 PSI. 3427.8 HR

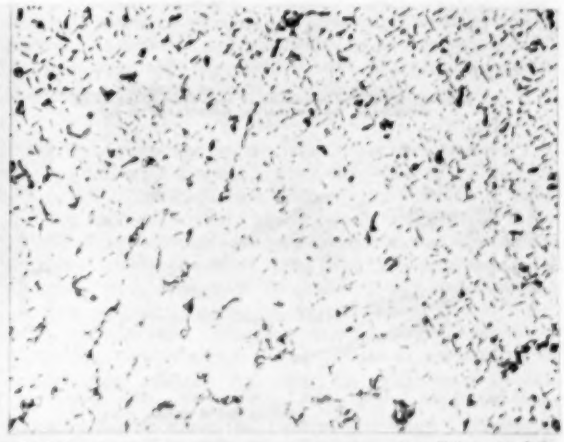

FIG. 20 STRUCTURE OF 18 CR-12 NI-3 MO-CB WELD DEPOSIT, 1350 F, 13,000 PSI. 2020.6 HR

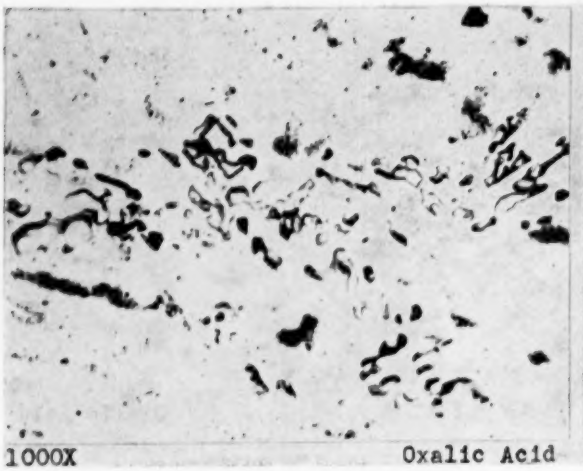

FIG. 21 STRUCTURE OF 25 CR-20 NI WELD DEPOSIT, 1200 F, 8000 PSI, 6270 HR

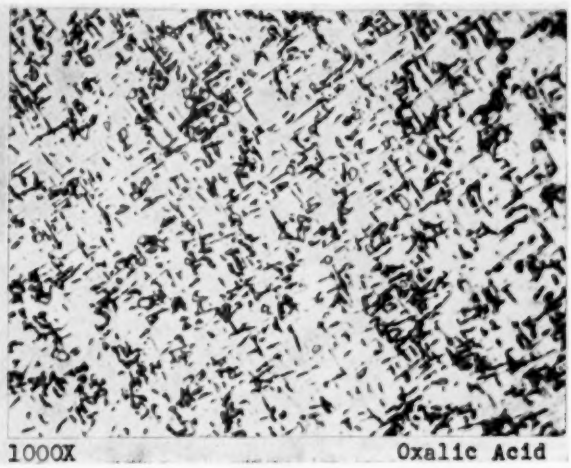

FIG. 22 STRUCTURE OF 25 CR-20 NI-CB WELD DEPOSIT, 1200 F, 15,000 PSI, 9240 HR

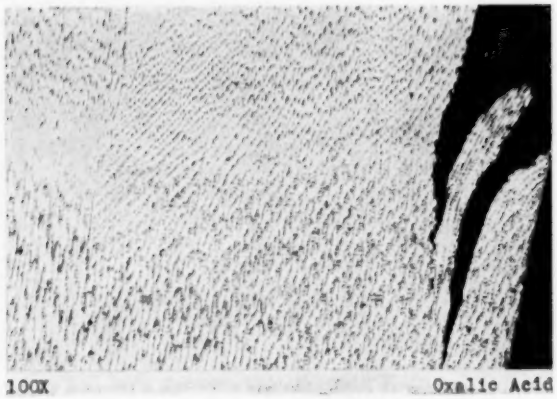

FIG. 23 STRUCTURE OF 18 CR-12 NI-3 MO WELD DEPOSIT, 1200 F, 12,500 PSI, 5707.8 HR

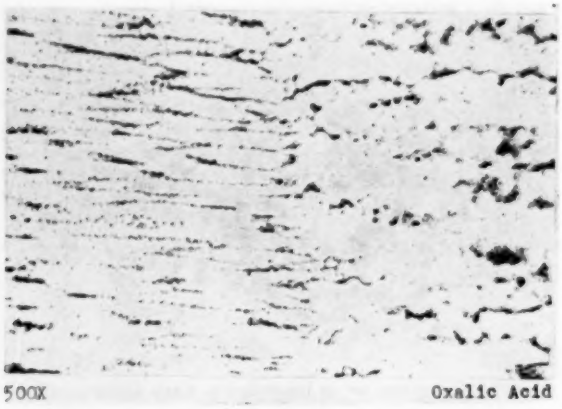

FIG. 24 STRUCTURE OF 18 CR-12 NI-3 MO WELD DEPOSIT, 1200 F, 12,500 PSI, 5707.8 HR

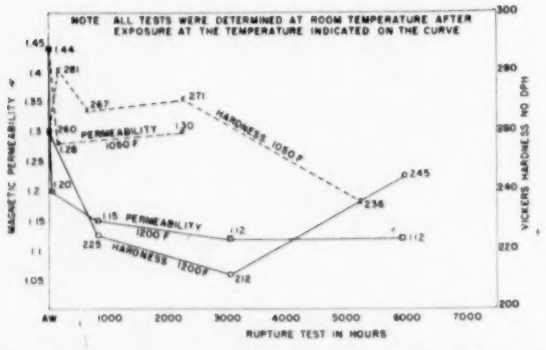

FIG. 25 EFFECT OF TIME AT TEMPERATURE ON VICKERS HARDNESS AND MAGNETIC PERMEABILITY OF 19 CR-9 NI WELD DEPOSITS

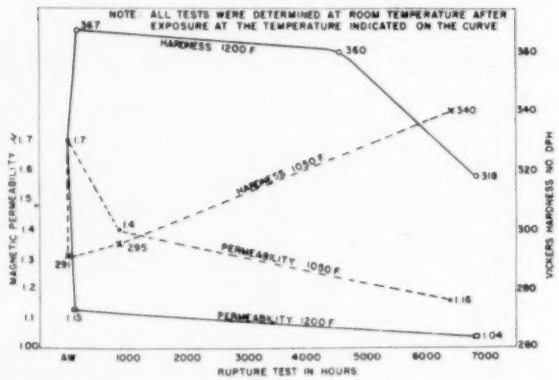

FIG. 26 EFFECT OF TIME AT TEMPERATURE ON VICKERS HARDNESS AND MAGNETIC PERMEABILITY OF 19 CR-9 NI-CB WELD DEPOSITS

TABLE 6 MAGNETIC PERMEABILITY AND VICKERS HARDNESS SURVEY OF STRESS-RUPTURE SPECIMENS

Material	Test Temp. F.	Length of Test	Magnetic Permeability	Vickers Hardness
19Cr-9Ni	AW	None	1.44	260
	1050	2,289.1	1.30	271
	1200	3,087.1	1.12	245
19Cr-9Ni LC	AW	None	1.28	258
	1050	6,934.3	1.15	233
	1200	6,037.2	1.07	232
19Cr-9Ni Cb	AW	None	1.70	291
	1050	6,424	1.16	340
	1200	6,855	1.04	318
19Cr-9Ni DW	AW	None	1.50	376
	1500	16,354.3	1.00	405
18Cr-12Ni-3Mo	AW	None	1.02	239
	1200	2,827.8	1.00	223
	1350	3,427.8	1.00	216
	1500	14,055.6	1.00	228
18Cr-12Ni-3Mo LC	AW	None	-	-
	1200	5,192.2	1.00	238
	1350	5,624.6	1.00	198
18Cr-12Ni-3Mo Cb	AW	None	1.09	263
	1200	5,601.3	1.00	321
	1350	2,020.6	1.00	283
25Cr-20Ni	AW	None	1.00	-
0.12% C	1050	6,512.1	1.00	340
	1200	10,673.9	1.00	288
	1350	6,802.7	1.00	294
	1500	9,866.3	1.00	288
25Cr-20Ni	1050	4,704.8	1.00	339
0.18% C	1200	2,052.2	1.00	386
25Cr-20Ni Cb	AW	-	-	-
	1050	8,494.8	1.00	378
	1200	12,679.6	1.00	467

1 The magnetic-permeability data indicate that the higher the test temperature for the testing periods used in this investigation, the more complete appears to be the transformation of delta ferrite to a nonmagnetic phase; i.e., either sigma or austenite.

2 Weld deposits stabilized with columbium form sigma phase more rapidly and more completely from the delta ferrite than unstabilized deposits. This is reflected in the high hardness values of the stabilized materials as compared with those for the low-carbon or standard grades.

3 Unstabilized weld deposits of low carbon content exhibit no tendency for age hardening at the temperatures and for the test durations employed in this investigation. They also show a lower level of hardness than alloys with normal carbon content.

4 The stabilized deposits exhibit a higher hardness in both the as-welded condition and after test. This is believed to be the result of a strengthening of the matrix solid solution as well as the mode of precipitation of sigma phase and carbides.

5 High room-temperature hardness is not always associated with good stress-rupture properties. For example, 25 Cr-20 Ni shows high hardness values, but poor stress-rupture strength.

In order to illustrate the observed transformations more clearly, two alloys were chosen for more detailed discussion. The charts in Figs. 25 and 26 show the effect of increased rupture time at each of two test temperatures on the magnetic properties and Vickers hardness of 19 Cr-9 Ni-Cb weld deposits. These studies indicate that, in addition to the observations mentioned previously, the magnetic transformations which do occur take place largely within the first 1000 hr of test. Variations in hardness follow the pattern of the aging precipitates. The aging phenomena in these materials are complicated by such factors as welding procedure, alloy composition, test temperature, applied stress, and nonhomogeneity in the weld deposit.

Conclusions

The data presented on the high-temperature properties of stainless-steel weld deposits indicate that weld metals have, in general, lower rupture strength than wrought materials of corresponding chemical analysis, particularly at temperatures above 1200 F. Deposits which were columbium-stabilized showed better stress-rupture properties than those without columbium. Additional work appears to be necessary to develop welding electrodes suitable for use at temperatures above 1200 F.

The test data show that austenitic weld deposits exhibit low rupture ductility at elevated temperatures as compared with corresponding wrought materials. The significance of this with regard to service requirements is not clear at this time. Recent testing has shown that there may be some possibility of improving the rupture ductility particularly in short-time tests by chemical and structural modifications of the austenitic materials.

A testing program for evaluating the high-temperature strength and the residual room-temperature mechanical properties after exposure at elevated temperatures of austenitic welded joints is now being conducted in the company's laboratories. The data presented in this paper represent the first progress report of this program.

It is hoped that the data in this report, together with those presented in subsequent discussion by other organizations, will serve as a guide to the Subcommittee on Stress Allowances for Ferrous Materials of the ASME Boiler Code Committee in the selection of allowable stresses for the chromium-nickel stainless steels.

Acknowledgment

The authors wish to acknowledge the assistance of the many persons in The Babcock & Wilcox Company organization who aided in the testing program, and in the preparation and editing of the manuscript.

BIBLIOGRAPHY

1 "B&W Installs New Equipment for Creep and Stress Rupture Studies," *Industrial Heating*, vol. 17, 1950, pp. 988–994.

2 "The Creep and Stress-Rupture Testing of Steam Boiler Materials," by J. B. Romer and H. D. Newell, Trans. ASME, vol. 74, 1952, pp. 157–172.

3 "Bulletin No. 6E," The Babcock & Wilcox Tube Company, 1948.

4 "Report on the Elevated Temperature Properties of Stainless Steels," by W. F. Simmons and H. C. Cross, ASTM Special Technical Publication No. 124, 1952.

5 "Some Factors Controlling the Ductility of 25 Per Cent Cr-20 Per Cent Ni Weld Deposits," by O. R. Carpenter and N. C. Jessen, *Welding Journal*, December, 1947, pp. 727s–740s.

6 "Effect of Alloying Elements on the Tensile Properties of 25–20 Weld Metal," by H. C. Campbell and R. D. Thomas, Jr., *The Welding Journal*, vol. 25, November, 1946, pp. 760s–768s.

7 "Crack Sensitivity of Chrome Nickel Stainless Weld Metal," by R. D. Thomas, Jr., *Metal Progress*, vol. 50, 1946, pp. 474–478.

8 "Some Considerations in the Joining of Dissimilar Metals for High Temperature, High Pressure Service," by O. R. Carpenter, et al., ASTM Proceedings, vol. 50, 1950, pp. 809–857.

Discussion

W. L. Fleischmann.[9] The authors are to be commended for this excellent paper on the high-temperature strength of austenitic weld deposits which will be referred to by many engineers, for, to the writer's knowledge, this paper is the only comprehensive study in its field.

At the Knolls Atomic Power Laboratory we have obtained data on Type 347 stainless-steel weld deposits which may be of interest as a supplement.

The deposits from which the KAPL all-weld specimens were machined were laid down as butt welds between two $^1/_2$-in-thick plates. These plates were held down by fillet welds on a $2^1/_4$-in-thick stainless-steel plate. Thus the weld deposit was subjected to a greater restraint than the authors' samples machined from weld pads. Other welding conditions—interpass temperature, electrode size ($^5/_{32}$ in. diam) and welding current—were nearly identical.

The composition of the deposit was as follows: 0.066 C, 1.60 Mn, 0.029 S, 0.025 P, 0.40 Si, 9.74 Ni, 20.4 Cr, 0.71 per cent Cb plus Ta.

[9] Metallurgical Engineer, Knolls Atomic Power Laboratory, Schenectady, N. Y. Mem. ASME. The Knolls Atomic Power Laboratory is operated for the United States Atomic Energy Commission by the General Electric Company under Contract No. W-31-109 Eng-52.

The data of the KAPL rupture test[6] are given in Table 7 of this discussion.

The test temperatures and stresses of the KAPL test were selected to allow the construction of the rupture-stress curve as a function of the Larson-Miller parameter.[7] The presentation of the rupture data in this form has the advantage of permitting comparison of rupture results even when the tests were conducted at other temperatures. Since in this paper the rupture strength of the tantalum-free Type 347 weld deposit is given for two temperatures, the data on this deposit were listed in the table for comparison in preference to those of the Cb-Ta type.

TABLE 7 STRESS-RUPTURE DATA FOR TYPE 347 STAINLESS-STEEL WELD DEPOSITS

Temp, deg F	Load, 1000 psi	Hours to rupture	Red. area, per cent	Parameter	Source
1000	45	5508	3	34.7	KAPL
1200	30	222	2	37.1	KAPL
1350	20	62	2	39.4	KAPL
1350	15	122	1	39.9	KAPL
1400	10	221	<1	41.5	KAPL
1050	44	1000		34.7	B&W
1050	27	10000		36.2	B&W
1200	21–25	1000		38.2	B&W
1200	16–18	10000		39.8	B&W

The low ductility exhibited by the weld deposits in the B&W tests is confirmed by our results. Perhaps of greatest interest is the agreement between the KAPL curve and the authors' stress-rupture values for 1000 and 10,000 hr at 1050 and 1200 F, taken from their Table 3, with the exception of the 10,000-hr rupture strength at 1050 F for which the authors claim only a value of 27,000 psi. This is shown graphically in Fig. 27 of this discussion.

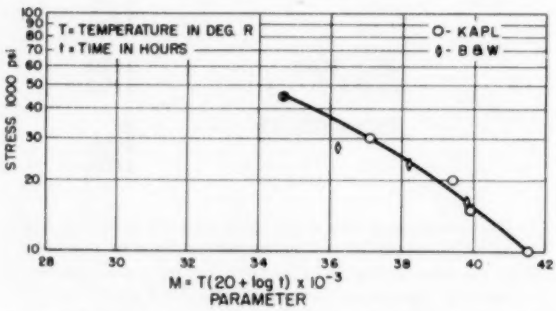

Fig. 27 Rupture Strength of Type 347 Stainless-Steel Weld Deposit

From a designer's point of view it is gratifying to know that a sound weld deposit possesses reproducible high-temperature properties. That the time-saving procedure made possible by the use of the time-temperature parameter gives such good agreement with data extrapolated in the conventional manner, appears to be important, as it adds some more evidence in favor of the accelerated testing procedure. Thus its use should be encouraged to obtain the necessary high-temperature data of the many heat-resistant alloys.

R. D. Thomas, Jr.[8] We are indeed pleased to see this valuable contribution to the knowledge of the properties of weld metals

[6] The rupture test was conducted at the Materials and Processes Laboratory of the Turbine Division, General Electric Company, under the supervision of Mr. R. F. Gill.

[7] "A Time-Temperature Relationship for Rupture and Creep Stresses," by F. R. Larson and James Miller, Trans. ASME, vol. 74, 1952, pp. 765–775.

[8] Arcos Corporation, Philadelphia, Pa.

which are used in high-temperature high-pressure service. We were particularly impressed by the time duration of some of the tests which revealed inflection points in the stress-rupture curves of certain compositions. The revelation of these inflection points may well prevent "underdesign" which easily could result from the extrapolation of curves from short-time tests.

In a joint program with the International Nickel Company, we have made some comparatively short-time stress-rupture tests on four of the weld-metal compositions reported by the authors, namely, 19 Cr-9 Ni-Cb, 19 Cr-9 Ni-Cb-Ta, 18 Cr-12 Ni-Mo, and 19 Cr-12 Ni-Mo-Cb. For simplification in comparing the authors' results with the Inco-Arcos data we have redrawn the stress-rupture curves and/or scatter bands as given in the paper except that the experimental points were omitted and the experimental points from the Inco-Arcos tests were plotted.

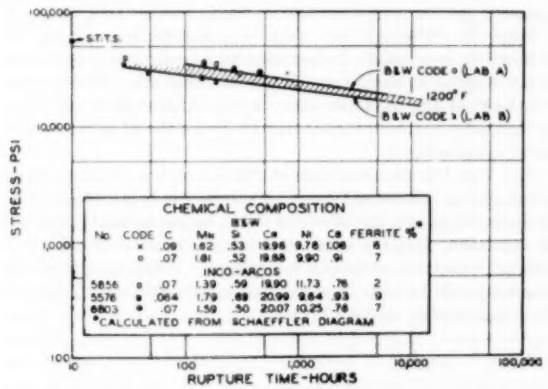

FIG. 28 STRESS-RUPTURE CURVES FOR 19 Cr-9Ni-Cb WELD METAL

Fig. 28, herewith, shows a plot of the experimental points obtained on three lots of 19 Cr-9 Ni-Cb weld deposits together with the scatter band given by the authors at 1200 F. It will be noted from Fig. 28 that some of the Inco-Arcos points fall slightly above and some slightly below the scatter band given by the authors. If, however, the authors had plotted their scatter band to include all of their own points it also would have encompassed the large majority of the Inco-Arcos points.

Collectively, then, we have stress-rupture data at 1200 F on 19 Cr-9 Ni-Cb weld metals deposited from five different lots of electrodes, tested by three different laboratories, and in both the longitudinal and transverse directions. This then establishes, almost without doubt, the scatter that may be expected in the stress-rupture properties of 19 Cr-9 Ni-Cb weld deposits at 1200 F.

Fig. 29 shows a plot of the Inco-Arcos data points and the stress-rupture curve given by the authors for 19 Cr-9 Ni-Cb-Ta weld deposits at 1200 F. It may be noted that the Inco-Arcos data points fall below the curve given by the authors. This indicates that in all probability a scatter band of the same order of magnitude as seen in the case of the 19 Cr-9 Ni-Cb welds exists.

Fig. 30 shows a plot of the Inco-Arcos data points on welds deposited from two lots of electrodes and the stress-rupture curve given by the authors for 18 Cr-12 Ni-Mo weld deposits at 1200 F. The Inco-Arcos points fall slightly below the curve given by the authors and are probably a reflection of the lower carbon contents of the weld deposits tested in the Inco-Arcos program. These combined data would give more information toward the establishment of a scatter band for 18 Cr-12 Ni-Mo weld deposits.

Fig. 31 shows a plot of the Inco-Arcos data points on welds deposited from two different lots of electrodes and the stress-rupture curve given by the authors for 18 Cr-12 Ni-Mo-Cb electrodes at a test temperature of 1200 F. Here again it can be seen that the results agree to within an amount of which reasonably can be attributed to variations in composition and test procedures in conducting a test which in itself is subject to scatter.

In addition to the tests conducted on deposits in the as-welded condition two specimens of each of the foregoing compositions were heat-treated as follows prior to testing:

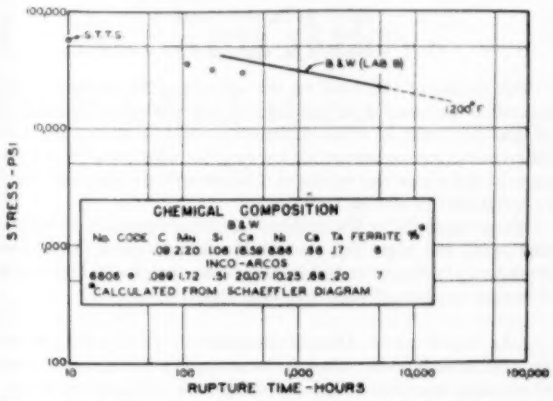

FIG. 29 STRESS-RUPTURE CURVES FOR 19 Cr-9 Ni-Cb-Ta WELD METAL

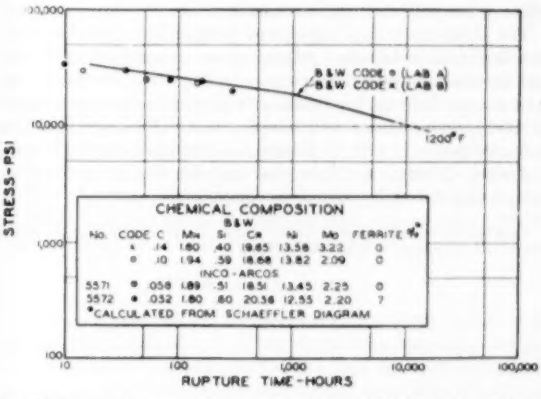

FIG. 30 STRESS-RUPTURE CURVES FOR 18 Cr-12 Ni-Mo WELD METAL

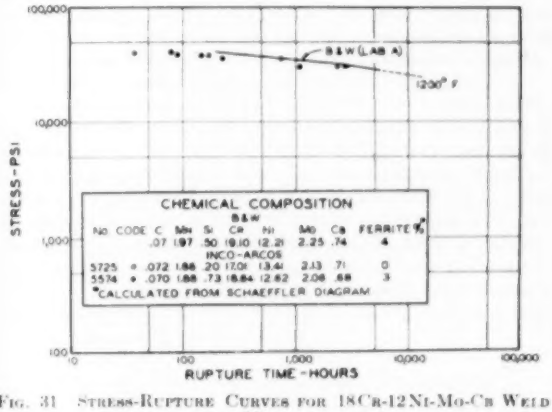

FIG. 31 STRESS-RUPTURE CURVES FOR 18 Cr-12 Ni-Mo-Cb WELD METAL

1950 F, 1/2 hr, water-quench
1200 F, 2 hr, air-cool
1550 F, 2 hr, air-cool

The results of the tests on the specimens which were heat-treated as described were such that no conclusions as to the effect of heat-treatment on stress-rupture life could be drawn since the difference in stress-rupture life between the aged samples and the as-welded samples was within an amount which reasonably could be attributed to scatter.

We are grateful to the authors for the opportunity to review this paper and hope that the substantiating data we have presented may in some way be helpful in achieving the goal for which this vast amount of work has been done.

J. L. Van Ullen.[9] Data of the nature obtained by the authors are always welcomed. They serve as a guide for the application of existing materials and for development of improved alloys. Since this information can be translated into design, it seems worth while to tabulate actual test data or to increase the legibility of the published rupture curves.

The observation that higher test temperatures promote more complete transformation to sigma phase or austenite within the test times employed is documented by the data. However, this does not preclude the formation of larger amounts of sigma phase at lower temperatures and longer times. The sigma-forming potential increases with decreasing temperature, as is well known, and since diffusion reactions slow up with decreasing temperature, a longer time is required to complete the reaction.

[9] Materials and Processes Laboratory, Turbine Division, General Electric Company, Schenectady, N. Y.

Normally, we can place "practical" limitations on temperatures below which little sigma occurs, but some caution should be exercised where equipment with extremely long service life is considered.

Authors' Closure

The authors wish to thank Messrs. Fleischmann, Thomas, and Van Ullen for their discussion of our paper. It is certainly gratifying to investigators when data obtained by other organizations so nicely check with the data which are presented.

They would like to point out to Mr. Fleischmann that in their opinion the 1050 F stress-rupture curve presented in the paper is satisfactory, and that possibly this might be an indication that for certain temperatures and certain materials the parameter, as developed by the General Electric Company, might not satisfactorily predict long-time elevated-temperature properties.

Since Mr. Thomas' test work so parallels the work of the authors, it is especially happy that he was able to present this as a discussion to the paper. It is hoped that other investigators who have similar data may want to publish them at a later time, so that more accurate curves may be drawn for all of these weld-metal compositions.

Mr. Van Ullen's comments on the formation of sigma phase are in order. More and more information is being obtained on these reactions and the effects of sigma on mechanical properties at elevated temperatures and upon the mechanical properties at room temperature after exposure. With this information engineers will be able to more intelligently select materials for operation at high temperatures.

Some 12 Per Cent Chromium Alloys for 1000 F to 1200 F Operation

By D. L. NEWHOUSE,[1] B. R. SEGUIN,[1] and E. M. LAPE[2]

This paper presents a discussion of important engineering properties of some martensitic 12 per cent Cr alloys for use at temperatures up to 1200 F. Detailed high-temperature creep-relaxation and stress-rupture data are given for 12 per cent Cr (Type 403) and for six alloy modifications including 12 per cent Cr-Co-W-V, 12 per cent Cr-W-V, 12 per cent Cr-Mo-V, 12 per cent Cr-Mo-W-V, 12 per cent Cr-Cb, and 12 per cent Cr-Ni-W. Other properties such as thermal expansion, modulus of elasticity, resistance to stress corrosion, and so forth, are discussed. Some of the modified 12 per cent Cr alloys offer a combination of properties which makes them attractive for a number of high-temperature applications.

Introduction

In the manufacture of steam and gas turbines one of the most widely used medium alloys is the class of material commonly referred to as the martensitic 12 per cent chromium steels. The rather unique combination of properties possessed by this class of corrosion-resisting materials makes them particularly well suited for turbine buckets, compressor blading, bolting, valve stems, and so on. Although straight 12 per cent Cr steel (Type 403) has been used in steam-turbine buckets for many years and has proved its qualities in such extended service, there is now considerable interest in the modifications of the 12 per cent Cr steels, not only for steam turbines because of their steadily increasing throttle temperatures, but also for gas turbines and jet engines where strategic alloy factors are forcing the superseding of the more strategic austenitic steels. In consideration of this widespread interest in the 12 per cent Cr steels and their alloys, it is believed to be advantageous to the nation's industry to present a compilation of representative data obtained on this class of material by the various laboratories of the authors' company.

The major specific properties required by the various applications of the 12 per cent Cr family in steam and gas-turbine design can be summarized briefly as follows. In addition to satisfactory strength properties at both room and elevated temperatures, turbine buckets require good internal damping, resistance to corrosion and erosion by condensate in the steam turbine and combustion products in the gas turbine, and sufficient ductility to permit tenon riveting. Compressor blading requires adequate physical strength and resistance to stress corrosion, while materials for gas-turbine wheels must be capable of being forged and heat-treated to desired properties in fairly large sizes. In valve stems, the further ability to be nitrided to provide a satisfactory wear-resisting surface is desirable.

Operating requirements for ferritic turbine bolting are particularly severe since materials for this application not only must combine high room-temperature yield strength and impact strength, but must possess and maintain good creep strength, rupture strength, and ductility for many years of operation at temperatures as high as 1050 F. Resistance to temper embrittlement and in some cases stress corrosion are of importance, and the thermal-expansion characteristics of the bolt should match those of the flange as nearly as possible. A number of these requirements are to some degree contradictory, since high hardness, creep, and rupture strength tend to be accompanied by lower impact strength and rupture ductility.

In the following, data are presented in detail for a number of 12 per cent Cr materials which have been produced and used in commercial quantities for some of the foregoing applications, and which illustrate their desirable qualities as well as some of the problems which should be considered.

The scope of this paper has been confined to the consideration of what might be termed static properties, since time and space do not permit discussion of other important properties such as fatigue strength and internal damping capacity.

Chemical Composition

Both preferred ranges of composition for the several types of 12 per cent chromium alloys and the chemical compositions for the individual items are shown in Table 1, together with a notation as to section size. All items except those so noted were taken from production heats of material. It can be seen that each of the 12 Cr modifications is characterized by additions of one or more carbide-forming elements such as molybdenum, tungsten, and vanadium, and usually by the increase of carbon content and sometimes the addition of nickel or cobalt, which tends to counteract the ferrite-forming tendency of the carbide formers.

The compositions of the 12 Cr-Co-W-V, 12 Cr-W-V, 12 Cr, and 12 Cr-Ni-W alloys are so balanced that little or no ferrite is observed, while the 12 Cr-Mo-W-V, 12 Cr-Mo-V and the 12 Cr-Cb alloys may contain small amounts of ferrite. Such ferrite is not usually detrimental to either low- or high-temperature strength and may contribute to ease of hot-forming and heat-treatment. However, recent work suggests that tensile ductility may be greatly reduced in tests made perpendicular to the direction of ferrite stringers, where they may form a substantially continuous phase, even though strength and ductility are normal in a direction parallel to the stringers.

Heat-Treatment and Mechanical Properties

The heat-treatments applied to the individual items and the resulting mechanical properties are listed in Table 2. The Type 403 steels listed were all air-cooled directly from the hot-rolling operation and were then tempered to produce the desired tensile properties, straightened, and stress-relief-annealed. In contrast to this practice, the modified 12 Cr alloys have all been air or oil-quenched from a relatively high temperature (for the solution of alloy carbides) and then tempered to produce the desired tensile-strength properties. It should be noted that the modified 12 per cent chromium alloys were tempered to very much higher tensile-

[1] Metallurgical Engineer, Materials and Processes Laboratory, General Electric Company, Schenectady, N. Y.

[2] Metallurgical Engineer, Thomson Laboratory, General Electric Company, River Works, West Lynn, Mass.

Contributed by the Joint ASTM-ASME Committee on Effect of Temperature on the Properties of Metals, and presented at a joint session with the Power Division at the Annual Meeting, New York, N. Y., November 29–December 4, 1953, of The American Society of Mechanical Engineers.

Note: Statements and opinions advanced in papers are to be understood as individual expressions of their authors and not those of the Society. Manuscript received at ASME Headquarters, September 1, 1953. Paper No. 53—A-168.

TABLE 1 RANGES OF CHEMICAL COMPOSITION OF 12 PER CENT Cr ALLOYS

Item	Material	Bar Size	Percentage Chemical Composition													
			C	Ni	Co	Cr	Mn	V	W	Mo	Si	P	S	Al	Sn	Cb / Ta
	12Cr (403)	*max	.13	.50		13.0				.80	.50	.03	.03			
		min	.08	---		11.5				.25	---	---	---			
2379	"	1-7/16 x 5-1/16	.10	.41	---	12.67	.32	---	---	.43	.31	.020	.008			
2380	"	1-1/4 x 2-11/16	.10	.41	---	12.67	.32	---	---	.43	.31	.020	.008			
2381	"	1-1/4 x 5	.11	.31	---	12.04	---	---	---	.44	.39	.015	.010			
2382	"	1-5/16 x 1-13/16	.11	.31	---	12.04	---	---	---	.44	.39	.015	.010			
2383	"	3/4 x 1-1/8	.091	.41	---	12.35	.29	---	---	.50	.28	.020	.021			
2597	"	2-1/16 x 8	.13	.18	---	12.36	.45	.03	---	.40	.27	---	---		<.03	
2598	"	1-3/16 x 3-7/16	.13	.36	---	12.31	.19	---	---	.35	.32	---	---			
2599	"	1-1/8" x 4-11/16	.10	.29	---	12.43	---	---	---	.35	.34	---	---	.01	.01	
2600	"	3/4 x 1-1/8	.13	.44	---	12.44	.30	<.03	<.03	.43	.28	---	---	.01		
	12CrCoWV	*max	.22	.50	5.50	13.0	.15	.27	3.50	1.50	.60	.025	.025			
		min	.17	---	4.50	11.5	---	.17	2.50	1.00	.30	---	---			
x 2267	"	7/8 x 7/8	.24	---	5.23	18.19	---	.26	2.98	.78	.36	---	---			
x 2292	"	1 x 1	.2	---	5.0	12	---	.25	3.0	1.0	.4	---	---			
2305	"	3/4 x 3/4	.25	---	5.03	12.08	---	.28	2.78	1.0	.38	.016	.011			
2387	"	1-3/4 x 3-1/8	.20	.43	5.32	12.66	---	.21	2.6	1.23	.56	---	---			
2420	"	1-3/4 x 3-1/8	.20	.43	5.32	12.66	.12	.21	2.68	1.23	.56	---	---			
2489	"	4-1/4 D	.18	.24	5.13	11.61	.07	.27	3.35	1.15	.38	---	---			
2567	"	4" D	.18	.16	4.5	12.34	.12	.25	4.69	.35	.24	.019	---			
2647	"		.19	---	4.9	12.24	---	.25	3.13	1.36	.60	.010	.019			
2648	"	4-9/16" D	.19	.16	4.8	12.18	---	.22	3.05	1.48	.38	.018	.018			
2649	"	4-9/16" D	.19	.16	4.80	12.18	.10	.22	3.05	1.48	.38	.018	.018			
x2663	"	4-11/16" D	.20	1.21	5.08	12.1	---	.27	3.09	-----	.47	---	---			
	12CrWV	*max	.22	.50		13.00		.26	2.75	1.50	.60	.025	.025			
		min	.27	---		11.50		.18	2.25	1.00	.30	-----	-----			
x 2137	"	1/2" D	.20	---	---	13.14	---	.22	3.14	.25	.33	---	---			
2333	"	1" D	.34	---	---	12.47	---	.24	2.93	.46	---	---	---			
2717	"	2-9/16" D	.32	.21	---	12.5	.07	.26	2.44	1.29	.42	.020	.015			
2763	12 CrWV	4-1/16" D	.29	.12	---	11.68	---	.25	2.42	1.00	.26	---	---			
2803-2	"	4-1/16" D	.29	.12	---	11.68	---	.25	2.42	1.00	.26	---	---			
2803-3	"	4-1/16" D	.29	.12	---	11.68	---	.25	2.42	1.00	.26	---	---			
2871		Forged Bucket	.28	.12	---	12.86	---	.23	2.54	1.33	.35	---	---			
2872	"	Forged Bucket	.30	.16	---	12.65	---	.26	2.31	1.26	.40	---	---			
2873	"	Forged Bucket	.30	---	---	12.34	---	.24	2.72	1.24	---	---	---			
2874	"	Forged Bucket	.27	.12	---	12.58	---	.18	2.35	1.18	.33	---	---			
2875	"	Forged Bucket	.28	.12	---	12.74	---	.26	2.37	1.43	.47	---	---			
2876	"	Forged Bucket	.28	.16	---	12.68	---	.23	2.54	1.33	.32	---	---			
	12 CrMoWV	*max	.23	1.00		14.00	1.25	.50	1.25	1.00	1.00	.04	.03			
		min	.18	.50		12.00	.75	.20	.75	-----	-----	---	---			
2746	"	3-1/2" D	.23	.65	---	13.19	1.03	.25	.84	.81	.16	.011	.022			
2757	"	3-1/2" D	.23	.65	---	13.19	1.03	.25	.84	.81	.16	.011	.022			
2870	"	Forged Bucket	.22	.65	---	13.19	1.03	.25	.84	.81	.16	.011	.022			
2911	"	1-5/16" D	.22	.61	---	13.59	1.02	.25	1.02	.80	.30	.022	.015			
3017	"	2-9/16" D	.19	.77	---	12.79	1.03	.24	1.15	.77	.20	.020	.018			
3018	"	4-9/16" D	.20	.77	---	12.85	1.02	.26	1.15	.73	.26	.017	.011			
3020	"	2" x 5"	.19	.77	---	12.79	1.03	.24	1.15	.77	.20	.020	.018			
	12 CrMoV	*max	.15	.50		12.00	1.00	.30		1.25	.50	.030	.030			
		min	.25	---		11.00	2.50	.20		.95	---	-----	-----			
35559	"	4-1/2" rd	.25	.27	---	11.55	2.62	.20	-----	1.09	---	-----	-----			
3706	"	3/8" sq	.27	.21	---	11.75	2.88	.25	-----	1.08	.27	.024	.027			
5119	"	4" rd	.27	.21	---	11.75	2.88	.25	-----	1.08	.27	.024	.027			
5188	"	3-1/2" rd	.32	.18	---	11.58	2.57	.25	-----	1.08	.40	.018	.015			
5219	"	6-1/4" rd	.30	.34	---	12.16	2.80	.28	-----	.90	.30	.020	.023			
5500	"	1" rd	.30	.13	---	11.64	2.60	.28	-----	.98	.31	-----	-----			
5531	"	4" rd	.27	.21	---	11.75	2.88	.25	-----	1.08	.27	.024	.027			
5684	"	1" rd	.26	.11	---	11.10	2.54	.24	-----	1.04	.30	-----	-----			
5757	"	3-3/4" rd	.31	.20	---	11.12	2.84	.23	-----	1.05	.28	.019	.014			
x5787	"	1-1/8" rd	.247	.13	---	11.22	2.78	.26	-----	1.18	.50	.007	.026			
x5788	"	1-3/8" rd	.173	.12	---	11.11	2.81	.26	-----	1.23	.57	.008	.028			
5829	"	1-13/16" x 2-5/16	.26	.15	---	11.06	2.58	.28	-----	.95	.18	-----	-----			
	12 CrNiW	*max	.17	2.20		14.0	.50		3.50	.50	.50	.04	.03	.15	.05	
		min	.12	1.80		12.0	---		2.50	---	---	---	---	---	---	
2079	"		.17	1.78		12.03			2.93	.28	.28					
2366	"		.11	2.05		14.15			2.46	.29	.31					
2429	"		.07	2.05		12.25			2.82	.29	.30					
D14	"		.12	2.1		12.90			3.1	.67	.37					
D6	"		.12	2.08		11.88			2.98	.37	.24	.006	.008			
	12 CrCb	*max	.18	.50		13.00				.60	.50	.040	.030			.45
		min	.13	-----		11.50				.40	---	-----	-----			.35
x2170	"	1" D	.09	.39		12.72				.30	.36					.32
x2236	"		.09	.77		13.42				.42	.42					.32
x2278	"		.06	.70		12.17				.50	.40					.30
x2328	"	1" D	.15			12.28				.53						.26
x2329	"	1" D	.15			12.56				.52						.46
2461	"		.11	.12		12.09				.49	.8					.32
2588	"	Wheel & Shaft Forg.	.12	.27		12.10				.42	.32	.012	.010			.31
x2948	"		.11	.12		12.09				.49	.38	.011	.015			.32
x5256	12 CrTa		.15			12.81				.52	.20	.016	.014			

* Preferred Range

x Induction Melted Laboratory Heat

TABLE 2 HEAT-TREATMENT AND ROOM-TEMPERATURE MECHANICAL PROPERTIES

Item	Material	Heat Treatment	Room Temperature Mechanical Properties: T. S. psi	.02% Y. S. psi	Prop. Limit psi	Elong. in 2" %	Reduc. in area %	Charpy Impact Strength ft. lbs.
2379	12Cr (403)	Finished Rolled at 1450°F, A.C. (on edge) Tempered at 1157°F.	114,900	-------	84,900	23.0	67.5	
2380	"	Same as 2379	117,400	-------	84,900	23.0	67.0	
2381	"	Finish Rolled at 1450°F, A.C. Flat, with Fans, Tempered at 1157°F.	103,900	-------	74,900	24.0	66.3	
2382	"	Finished at 1450F, A.C. Flat (Fans), Tempered at 1157°F.	106,400	-------	78,900	24.0	64.2	
2383	"	Finished at 1450F, A.C. Flat (Fans), Tempered at 1157°F.	112,400	-------	82,400	24.0	67.9	
2597	"	Air Cooled from Rolls.	106,200	79,400	-------	24.5	67.2	
2598	"	Finish Rolled at 1450F, A.C. Flat (Fans), 1175F 15 Hrs, 1100F, 15 Hrs.	114,900	92,900	-------	24.5	66.3	
2599	"	Finish Rolled at 1450,A.C., 1175F, 15 Hrs, 1100F, 15 Hrs.	111,400	-------	88,400	21.5	67.5	
2600	"	A.C. From Rolls	107,900	80,900	70,900	26.5	70.0	
2267	12CrCoWV	2012F - 3 hrs. - Cool at 1800F/hr; 1200F 3 hrs - F. C.	165,900	-------	65,400	12.0	23.0	18
2292	"	2012F - 3 hrs. - Cool at 1800F/hr; 1200F 3 hrs - F. C.	157,400	-------	101,900	16.0	37.9	22
2305	"	2012F - 4 hrs. - Cool at 1900F/hr; 1200F 4 hrs - F. C.	167,400	-------	87,400	13.5	24.4	11
2387	"	2000F - 1½ hrs. - A.C.; 1200F - 3½ hrs - F. C.	166,900	-------	74,900	12.0	22.3	
2420	"	1750F - 1½ hrs. - A.C.; 1200F - 5 hrs - A. C.	163,400	-------	109,900	17.5	48.1	18
2489	"	1742F - 5 hrs. - A.C.; 1200F - 8 hrs. A. C.	147,800	100,000	-------	15.7	39.4	11.5
2567	"	1775F - 6 hrs. - A.C.; 1200F - 12 hrs. - A.C.	155,900	-------	-------	18.0	48.9	14 - 15
2647	"	1750F - 4½ hrs. - A.C.; 1200F - 12½ hrs. - 1150F - 5½ hrs.	161,400	-------	-------	16.0	45.2	12 - 13
2648	12CrCoWV	1750F - 4 hrs. - A.C.; 1200F - 12 Hrs. 1150F - 7 hrs.	161,400	123,900	-------	16.0	45.0	12 - 13
2649	"	1742F - O.Q.; 1200F - A.C.	149,900	115,900	-------	15.5	37.3	10 - 12
2663	"	1742F - A.C.; 1200F Temper						
2137	12CrWV	2012F - 4 hr. A.C.; 1200F - 2 hrs. A.C. 1112F - 2 hrs. - A.C.	146,500	-------	76,000	19.0	43.6	20
2333	"	2050F - O.Q.; 1400F - A.C.	133,000	-------	-------	17.0	38.0	-------
2717	"	1885F - A.C.; 1202F - 12 Hrs. - A.C.	156,300	126,200	102,500	14.5	41.0	10
2763	"	1900F - A.C.; 1200F - 16 Hrs. - A.C. 1150F - 20 Hrs. - A.C.	153,500	103,000	-------	16	41.4	12 - 12
2803-2	"	1900F - A.C.; 1200F - 16 Hrs. - A.C. 1150F - 20 Hrs. - A.C. 1300F - 5 Hrs. A. C.	142,000	93,000	-------	19.5	49.8	14 - 16
2803-3	"	1900F - A.C.; 1200F - 16 Hrs. - A.C. 1150F - 20 Hrs. - A.C. 1400F - 5 Hrs. A. C.	126,250	75,000	-------	23.5	52.5	18 - 18
2871	"	1900F - 4 Hrs. - A.Q.; 1200F - 12 Hrs. A.C.	158,200	117,000	-------	18.5	44.0	16
2872	"	1900F - 4 Hrs. - A.Q.; 1200F - 12 Hrs. A.C.	162,000	111,250	-------	14.5	34.1	8 - 11
2873	"	1900F - 4 Hrs. - A.Q.; 1200F - 12 Hrs. A.C.	159,000	106,250	-------	16.0	37.9	11 - 12
2874	"	1900F - 4 Hrs. - A.Q.; 1200F - 12 Hrs. A.C.	150,000	104,000	-------	17.0	45.2	12 - 14
2875	"	1900F - 4 Hrs. - A.Q.; 1200F - 12 Hrs. A. C.	149,250	105,000	-------	18.0	47.8	14 - 14
2876	"	1900F - 4 Hrs. - A.Q.; 1200F - 12 Hrs. A.C.	151,250	100,000	-------	18.0	47.2	15 - 15
2746	12CrMoWV	1900F - A.C.; 1100F - 4 Hrs. A.C.	164,000	117,800	-------	18.5	46.6	17 - 19

TABLE 2 (*Continued*)

Item	Material	Heat Treatment	Room Temperature Mechanical Properties: T. S. psi	.02% Y. S. psi	Prop. Limit psi	Elong. in 2" %	Reduc. in area %	Charpy Impact Strength ft. lbs.
2757	12CrMoWV	1900F - A.C.; 1100F - 4 Hrs. - A.C. 1200F - 5 Hrs. F.C.	149,000	94,000	88,400	18.5	50.4	20
2870	"	1900F - 4 Hrs. A.Q.; 1200F - 12 Hrs. A.C.	149,200	114,200	-------	24.0	51.7	22
2911	"	1900F - O.Q.; 1150F Temper	152,200	113,000	-------	19.5	50.6	18 - 20
3017	"	1900F - 3 Hrs. - O.Q.; 1150F - 12 Hrs.	143,500	107,300	-------	18.5	49.2	20 - 20
3018	"	1900F - O.Q.; 1150F - 12 Hrs. - F.C.	156,000	116,800	-------	17.0	41.4	13 - 14
3020	"	1900F - O.Q.; 1150F - A.C.	146,000	116,000	-------	17.5	47.5	19 - 21
35559	12CrMoV	2000F - O.Q.; Temper						
3706	"	2000F - 1 Hr. O.Q. - 1300 2 Hrs. A.C.	149,300	101,900	-------	19.0	44.1	
5119	"	2000F - 6 Hr. O.Q. - 1300 6 Hrs, A. C.	136,300	87,000	-------	15.0	31.8	16.5 - 17.0
5188	"	2000F, 6 hr. O.Q. - 1300F 6 Hrs., A. C.	143,500	87,500	-------	17.0	45.4	8.5
5219	"	2000F, 6 hr. O.Q. - 1300F 6 Hrs., A. C.	107,000	71,000	-------	22.5	46.9	10.0
5500	"	2000F - 1 hr. O.Q. - 1325 2 Hrs., A. C.	143,750	95,000	-------	15.0	33.10	14 - 15.5
5684	"	2000F - 1 hr. O.Q. - 1325 2 Hrs., A. C.	140,250	94,000	-------	15.0	36.94	17.5 - 18.5
5757	"	2000F - 1 hr. O.Q. - 1325 2 Hrs., A. C.	129,250	76,000	-------	17.5	34.71	11.5
5787	"	2000F - 1 hr. O.Q. - 1200F 2 Hrs., A. C.	154,500	107,500	-------	16.5	41.0	18
5788	"	2000F - 1 hr. O.Q. 1100F 3 Hrs., A. C.	156,250	104,000	-------	20.0	65.2	31
5829	"	2000F - 1 hr. O.Q. 1100F 3 hrs., A. C.	124,750	78,750	-------	19.5	39.7	14
D6	12CrWiV	½ Hr. 1800°F, A.C. 1½ Hr. 1260F, A.C.	130,000		59,000	21	62	40
D14	"	1800°F, O.Q. - 1000°F, A.C. 1000F, A.C.						
2079	"	2012°F, ½ hr. A.C. - 1202°F, 4 hrs. A.C. 1112°F, 2 hrs. - F.C.	143,400	87,500		16.4	40	30
2366	"	1900°F, 8 hrs. - A.C. - 1200°F, 4 hrs. - A.C. - 1100°F, 2 hrs. - A.C.	134,500	98,500		20	55	36.5
2429	"	2050°F, 1 hr. O.Q. - 1200°F, 2 hrs. A.C.						
2170	12CrCb	2012F, 2 Hrs. A.C. - 1200F, 2 Hr. F.C.	131,900		95,900	18	56	22
2236	"	2012F, 2 Hrs. A.C. - 1200F, 2 Hr. F.C.	137,900		95,900	16	49	
2278	"	2012F, 2 Hrs. A.C. - 1200F, 2 Hr. F.C.	117,000		57,900	21	62	31
2328	"	2000F, O.Q. 1200F, A.C.	138,000	103,000		20	64	40 Izod
2329	"	2050F, O.Q. 1200F, A.C. 1200F, A. C.	135,000	99,000		18	64	35 Izod
2451	"		130,500			19	61	35
2588	"		134,500	98,000		20	59	
2948	"	2125F, ½ Hr. O.Q. - 1200F 2 Hrs. A.C. 1200F 2 Hrs. A.C.	143,500	103,500		18	60	
4256	12CrTa	2000F, 1 Hr. O.Q. - 1200F, 2 Hrs. A.C.	135,750	105,000		17	60	

strength levels than were the Type 403 steels listed. Items 2803-2 and 2803-3 are identical to Item 2763 except that successively greater amounts of tempering were given to them to show its effect on high-temperature strength properties.

It has been found that the application of the high solution temperature (2000 F) to the 12 Cr-Co-W-V material tended to produce low impact strength at room temperature and low rupture ductility at high temperatures. A solution heat-treatment of 1750 F to 1800 F has proved more satisfactory for this alloy. An intermediate temperature, approximately 1900 F, has been satisfactory for the 12 Cr-W-V and 12 Cr-Mo-W-V alloys; while for 12 Cr-Mo-V and 12 Cr-Cb, a 2000 F solution temperature normally is used.

Room-temperature keyhole Charpy impact-strength values, while not high, usually can be maintained above 10 ft-lb; and for the 12 Cr-Mo-W-V, tend to run close to 20 ft-lb.

Thermal-Expansion Characteristics

In designing for elevated-temperature service, it is important to consider the relative thermal expansion of materials, since failure to do so may produce relative movements of parts which may cause difficulty with excessive stress and distortion. In particular, a difference in thermal expansion between bolts and the flanges being bolted may cause either excessive tightening or loosening of the joint on heating to operating temperature. Typical thermal-expansion curves for the three major types of steel are shown in Fig. 1. While these curves are based upon a considerable number of tests (1, 2, 3),[3] agreement was very good and only average curves are included.

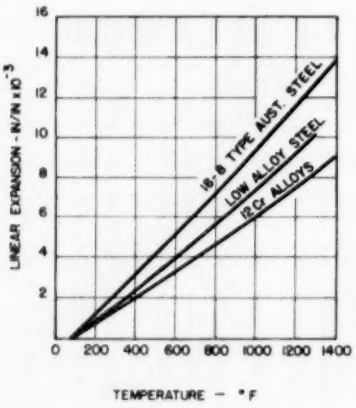

Fig. 1 Thermal Expansion of 12 Per Cent Cr Alloys as Compared to Low-Alloy Steel and 18-8 Type Austenitic Steels

It should be noted that the 12 Cr grades at 1000 F have almost as great a deviation in thermal expansion below low-alloy steel as do the 18-8 steels above that of low-alloy steels. This means that in heating a 12 per cent Cr alloy bolt to 1000 F in a low-alloy flange, the stress at operating temperature for a given tightening practice would be appreciably higher than if bolt and flange had the same expansion characteristics. In a like manner, an austenitic bolt in a low-alloy flange would loosen by 0.002 in./in. on heating to 1000 F. For this reason, it is considered good practice to tighten 12 per cent Cr alloys to a lower initial stress value at room temperature, when bolting low-alloy flanges, so as to avoid overstressing during operation.

[3] Numbers in parentheses refer to the Bibliography at the end of the paper.

Modulus of Elasticity

The decrease in modulus of elasticity, which occurs as service temperatures are raised, also may be important to the proper use of materials at elevated temperatures. Fig. 2, which was plotted from data listed in Table 3, shows tensile modulus-of-elasticity values for Type 403 and the 12 per cent Cr modifications, which were obtained from creep-test-loading curves, plotted along with data from Garofalo, et al. (4). It is interesting to note that the values of E obtained from creep-loading curves appear to deviate from the Garofalo curve at about 800 F for Type 403 and at about 950 F for the modified 12 per cent Cr alloys. This may be due to the occurrence of creep or nonelastic strain at the higher temperatures while applying load at the rate of about 2000 to 4000 psi per min. Such creep was avoided by Garofalo by using unloading data and lower stress values. In any case, the agreement appears reasonable and the tensile modulus of elasticity is some 30 to 35 per cent lower at 1000 F to 1050 F than at room temperature.

TABLE 3 MODULUS OF ELASTICITY (psi × 10^{-6}) VERSUS TEMPERATURE

Temp °F	*12Cr(Type 403)	*12CrCoWV *12CrWV *12CrMoWV	12 Cr (Type 410) (Garofalo) (4)
75	----------	------	29.8 - 29.7
300	----------	------	27.7 - 27.8
500	----------	------	25.8 - 27.2
700	----------	------	24.6 - 26.1
800	25.0 (1)	------	----------
900	23.1 (5)	------	23.3 - 24.4
1000	19.1 (11)	21.5 (16)	----------
1050	20.3 (1)	18.6 (4)	----------
1100	16.2 (1)	17.0 (2)	19.2 - 18.6
1200	----------	15.4 (1)	----------

* Data from creep test loading curves

() Indicates number of test points averaged

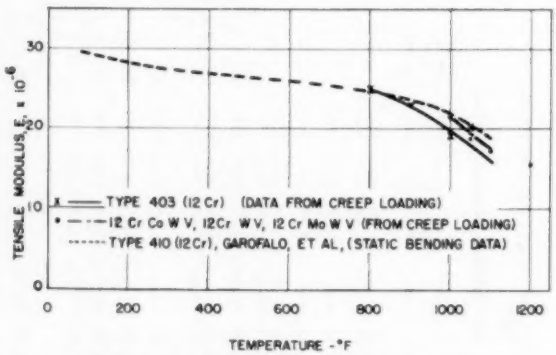

Fig. 2 Static Tensile Modulus of Elasticity Versus Temperature for 12 Per Cent Cr Steels

Rupture Strength and Relaxation Strength

Creep and rupture-strength considerations are most important to the successful use of 12 Cr steels in the temperature range between 900 F and 1200 F. Rupture tests provide a means of evaluating long-time strength for design purposes. They also yield ductility data which, if moderately high, give reasonable expectation that the occurrence of notch embrittlement will be minimized (5).

Relaxation-creep tests simulate service conditions for bolting in that the length of specimen is maintained at or near a constant value as the elastic strain is replaced by creep strain, with a resulting decrease in stress. Unlike many other parts where maximum working stresses are specified, bolting must maintain a

given minimum tension and so actual bolt stress always must exceed the design stress.

The problem of estimating accurately the creep and rupture behavior of materials for the very long life expected of apparatus such as steam turbines has long been important. Some of the stronger 12 per cent Cr steels may show no break in the log-log rupture curves for 900 F and 1000 F, even when tests of long duration, as long as 5000 to 10,000 hr, are run. This leads to excessively high predictions of 100,000-hr strength by extrapolation, since a break in the curve at any later time would lower the predicted strength considerably. Furthermore, a relatively small scattering of test points may affect drastically the estimation of 100,000-hr strength.

The time-temperature relationship for creep and rupture stresses, $T(C + \log t)$, proposed by Larson and Miller (6) has proved a most useful tool in the evaluation of high-temperature strength, since it yields not only more reasonable and consistent predictions of 100,000-hr strength, particularly at temperatures between 900 F and 1100 F, but permits the use of short-time tests for this purpose.

Detailed rupture-test data, and strengths derived therefrom, are given in Table 4. The listing of rupture-test data includes test temperature, stress, rupture time, rupture elongation and reduction of area, and the equivalent value of the time-temperature parameter, $P_{25} = T(C + \log t)$, where T is the absolute temperature in degrees Rankine, t is time in hours, and C equals 25. It has been found that a constant of 25 is more correct for 12 Cr steels, as contrasted to 20 reported by Larson and Miller for most steels.

Rupture-strength values listed in Table 4 were obtained both from conventional log stress versus log time-to-rupture plots and from log rupture stress versus $T(25 + \log t)$ plots. The latter values are designated by a suffix P, while values obtained by extrapolation of log-log curves are enclosed in parentheses.

A comparison between rupture strengths obtained by conventional extrapolation as compared to those from parameter curves in Table 4 shows that in many cases, particularly at 900 F and 1000 F, the parameter data indicate a continuing curvature which may yield much lower strength predictions for 100,000-hr life than do the corresponding log-log extrapolations, and which frequently appear to be much more reasonable.

Relaxation-test data obtained from Robinson step-down flow-rate tests (7), in the form of residual stress at 0.2 per cent total elastic plus plastic strain, are listed in Table 5 for specified times. Enough points are given in each case so that the residual-stress curves may be reconstructed, if desired, and extrapolated values are indicated by enclosing parentheses.

Both the individual rupture-test points and residual-stress data for the several 12 per cent Cr alloys are shown in Figs. 3 through 9 in the form of plots of rupture strength and residual stress at 0.2 per cent total strain versus $T(25 + \log t)$.

Consideration of the summation curves shown in Fig. 10 and of the data for the individual alloys leads to some interesting comparisons. All of the 12-Cr modifications show great improvement in rupture strength and in relaxation strength for a given time and temperature as compared to 12 Cr (403). The 12 Cr-Co-W-V and 12 Cr-Mo-V are highest in rupture strength, while the 12 Cr-Mo-V and 12 Cr-Mo-W-V have the best relaxation strength. The 12 Cr-Ni-W has relatively good rupture strength but poor creep strength as compared with the other 12 per cent Cr modifications. The residual stress of 12 per cent Cr-Cb falls off more rapidly than the other modifications at higher values of $T(25 + \log t)$.

Smooth and Notched-Bar Rupture Ductility

Most of the rupture strength and smooth-bar ductility data listed came from the testing of specimens with 0.253-in. diam and 2-in. or 4-in. gage length, with the exception of the 12 Cr-Mo-V tests and some others noted in Table 4 for which a 0.160-in-diam and 1-in-gage-length specimen was used. The smaller test specimen generally produces higher elongation values.

Rupture ductility for 12 Cr (403) was consistently high; that for the 12 Cr-Co-W-V was quite low when a high solution treatment was used, but was considerably improved by the lower (1750 F) solution heat-treatment. For the other modifications, rupture elongation was reasonably high, falling off somewhat at longer times.

The notched-rupture-test results for 12 Cr-Co-W-V at 1000 F (Table 4, Item 2489) show notch strengthening at 1000 hr, no effect at 10,000 hr, and an apparent notch embrittlement at 100,000 hr as compared to the smooth-bar-parameter strength values. It is felt, however, that either extrapolation of log-log plots or the use of short-time parameter methods [$T(25 + \log t)$] is unwise in so far as notched-bar data are concerned, the data being completely significant only for the time and temperature ranges used in the tests.

The notch-rupture strength for 12 Cr-W-V (Table 4, Item 2717) at 1100 F shows notch strengthening for all the times tested. Brown, Jones, and Newman (5) found no notch weakening for Crucible 422 (12 Cr-Mo-W-V) under any of the conditions which they investigated.

It has been observed that when temperature is raised at a given stress to give a shorter rupture time according to $T(25 + \log t)$, the rupture elongation for a 0.253-in-diam test specimen will approximately double for each 100 deg F rise in temperature for some of the 12 Cr modifications. The implication of this observation, if valid, is that a rough estimation of long-time rupture elongation may be made from short-time tests at higher temperatures and comparable stresses.

Tempering Effects

The high tensile-strength levels typical of the 12 per cent Cr modifications listed tend to produce reduced ductility, impact strength, and machinability, as compared to material tempered to a lower hardness. However, as can be seen in Fig. 11, additional tempering produces a pronounced lowering of rupture strength at the lower values of P_{25}. This effect is much less at higher values, being almost negligible at $P_{25} = 45.0$. The residual-stress curves, however, are roughly parallel, showing a continued advantage for the higher tensile-strength level. Another example is shown in the case of 12 Cr-Mo-V, Fig. 7, where both rupture points and residual-stress curves for items with room-temperature tensile strength under 140,000 psi show the same trend as was shown in the foregoing. For this reason, only the items with tensile strengths above 140,000 psi were used in comparing this alloy with the others in Fig. 10.

Stress Corrosion

In general, these alloys are less susceptible to stress corrosion than the austenitic-type alloys. However, under certain conditions of high hardness and high stress, failure can occur. Fig. 12 presents data on Type 403, 12 Cr-Mo-V, and 12 Cr-Ni-W in an accelerated stress-corrosion test which has been found useful in the evaluation of the relative susceptibility of this type of material to stress-corrosion-cracking in service. In this test the specimens were in the form of strips, stressed in bending, and immersed in a solution of 1-1 HCl with 1 per cent by weight of SeO_2 at room temperature. In this test the various modified 12 per cent Cr alloys resist stress-corrosion cracking by a factor of ten to one in time over Type 403 for equivalent hardness and applied stress.

TABLE 4 RUPTURE-TEST AND RUPTURE-STRENGTH DATA

		RUPTURE TEST DATA						RUPTURE STRENGTH - psi $\times 10^{-3}$											
								900 F			1000 F			1100 F			1200 F		
Item	Material	Test Temp. (°F)	Stress (psi)	Rupture Time (Hours)	% El.	% RA	P_{25}	10^3 hr.	10^4 hr.	10^5 hr.	10^3 hr.	10^4 hr.	10^5 hr.	10^3 hr.	10^4 hr.	10^5 hr.	10^2 hr.	10^3 hr.	10^4 hr.
2379	12 Cr (403)	1000	40000	11	18	85	38.0	40P	34P	28P	28	(22)	(18)						
		"	32000	201	19	82	39.9												
		"	28000	577	16	84	40.5												
		"	26300	1442	17	76	41.7												
		"	24000	4751	18	72	41.9												
2380	12 Cr (403)	1000	40000	14	21	84	38.2	40P	34P	29P	29	(22)	(17)						
		"	32000	268	18	82	40.0												
		"	28000	1174	14	76	41.0												
		"	26000	2293	16	72	41.4												
		"	24000	4561	12	60	41.9												
2381	12 Cr (403)	1000	40000	18	17	85	38.3	42P	32P	25P	25	(18.5)	(14)						
		"	34000	42	21	84	38.8												
		"	30000	198	23	86	39.8												
		"	24000	1390	20	86	41.1												
		"	20000	5946	20	84	42.0												
2382	12 Cr (403)	800	57000	654	17	78	35.0	39P	32P	24P	24P	17P	11P	11P	6.8P	—			
		"	55000	2707	19	77	35.8												
		850	75000	1	8	68	32.7												
		"	66000	2	5	70	33.1												
		"	54000	28	3	74	34.7												
		900	50000	68	19	76	36.5	39	(34)	(29)									
		"	45000	101	22	82	36.7												
		"	42000	189	22	82	37.1												
		"	40000	765	20	83	37.9												
		"	36000	4044	20	84	38.9												
		"	35000	5102	16	84	39.1												
		1000	35000	42	27	84	38.8				24	17	(12)						
		"	26000	611	28	87	40.6												
		"	22000	1748	28	86	41.2												
		"	18000	7438	28	84	42.2												
		1100	20000	46	31	88	41.6							11	6.8	(4)			
		"	15000	263	27	86	42.8												
		"	12000	690	58	90	43.4												
		"	7000	8356	37	91	45.1												
2383	12 Cr (403)	1000	36000	67	24	86	39.1	—	35P	27P	27	(20)	(15.5)						
		"	32000	214	30	85	39.9												
		"	26000	1337	23	85	41.1												
		"	22000	5324	20	84	42.0												
2597	12 Cr (403)	1000	42000	25	16	85	38.5	45P	38P	33P	32	25	(20)						
		"	32000	1229	16	86	41.0												
		"	29000	1864	18	85	41.3												
		"	26000	7182	16	86	42.1												
2598	12 Cr (403)	1000	50000	6	14	80	37.6	48P	40P	34P	34	28	(23)						
		"	42000	57	17	82	39.0												
		"	32000	1811	16	84	41.3												
		"	29000	6624	21	87	42.1												
2599	12 Cr (403)	1000	42000	12	15	82	38.1	42P	35P	29P	28	(21)	(16)						
		"	32000	410	16	86	40.3												
		"	28000	683	17	83	40.6												
		"	26000	1743	16	81	41.2												
		"	22000	6762	17	66	42.1												
3600	12 Cr (403)	1000	42000	15	18	85	38.2	43P	38P	32P	31	(25)	(20)						
		"	36000	222	18	85	39.9												
		"	32000	815	18	82	40.8												
		"	30000	920	18	87	40.8												
		"	27000	4409	17	88	41.8												
3267	12CrCoWV	1000	76000	23	9	51	38.5	—	74P	69P	68P	59P	43P	44P	26P	12P	31P	15P	—
		"	74000	1748	4	12	41.3				66	(60)	(56)						
		"	69000	668	9	29	40.4												
		"	64000	3510	5	14	41.7												
		1100	64000	57	9	61	41.7							46	(29)	(18)			
		"	50000	424	4	16	43.1												
		"	40000	1992	4	9	44.1												
		"	35000	3667	4	4	44.5												
		1200	37300	51	7	36	44.3										30	15	(7.1)
		"	30000	92	7	32	44.7												
		"	20000	330	9	32	45.7												
		"	13000	1822	14	36	46.9												
2292	12CrCoWV	1100	60000	62	9	54	41.8	—	—	—	—	57P	44P	45P	27P	15P	31P	17P	—
		"	50000	497	4	12	43.2							48	23	(11)			
		"	41000	1655	2.5	7	44.0												
		"	20000	16413	3	8	45.6												
		1200	66000	1.5	13	80	41.8										32	18	(8.7)
		"	30000	175	5	48	45.2												
		"	20000	709	10	48	46.2												
		"	12000	2590	18	25	47.2												
		"	10000	6406	8	15	47.8												
2305	12CrCoWV	1000	80000	4	12	52	37.4	79P	75P	68P	67P	55P	41P	42P	27P	15P	31P	17P	—
		"	75000	109	10	36	39.5				48	(60)	(54)						
		"	68000	832	5	12	40.8												
		"	62000	5013	4	9	41.9												
		1200	40000	16	10	71	43.5										33	17	(9)
		"	30000	158	10	32	45.1												
		"	20000	585	12	18	46.1												
		"	14000	2010	10	23	47.0												

TABLE 4 (*Continued*)

		RUPTURE TEST DATA						RUPTURE STRENGTH – psi x10^{-3}											
								900 F			1000 F			1100 F			1200 F		
Item	Material	Test Temp. (°F)	Stress (psi)	Rupture Time (Hours)	% El.	% RA	P_{25}	10^3 hr.	10^4 hr.	10^5 hr.	10^3 hr.	10^4 hr.	10^5 hr.	10^3 hr.	10^4 hr.	10^5 hr.	10^2 hr.	10^3 hr.	10^4 hr.
2387	12CrCoWV	900	90000	164	8	41	37.0	83F	73F	64F	64F	50F	36F	37F	24F	14F	27F	15.5F	—
		"	85000	3982	7	16	38.9	87	(83)	--									
		1000	70000	64	12	48	39.1				63	48	(36)						
		"	64000	727	7	20	40.7												
		"	60000	1635	4	14	41.2												
		"	56000	2840	2	4	41.6												
		"	50000	7192	3	10	42.2												
		1100	52000	105	7	45	42.1							36	—	—			
		"	48000	151	7	45	42.4												
		"	38000	828	5	24	43.6												
		"	32000	2368	6	18	44.3												
		"	28000	3383	4	11	44.5												
		"	25000	3772	6	20	44.6												
		1200	35000	30	12	71	43.9										27	15	8
		"	28000	104	11	64	44.8												
		"	25000	138	11	65	45.0												
		"	18000	585	10	36	46.1												
		"	12000	2161	10	25	47.0												
		"	9000	6686	10	18	47.8												
2420	12CrCoWV	850	120000	0.5	5(d)	45	32.4			70F	66F								
		"	100000	1498	7(d)	51	36.9												
		1000	74000	32	11	66	38.7				66	(53)	(40)						
		"	70000	171	10	60	39.8												
		"	64000	1787	6	21	41.3												
		"	61000	2918	5	15	41.6												
		"	58000	4170	4	10	41.8												
2420	12CrCoWV	1000	54000	2.5	Double shear	pin (a)					39	30	(24)						
		"	45000	44															
		"	40000	804	---	---													
		"	38000	821	---	---													
		"	35000	2873	---	---													
		"	30000	9361	---	---													
2489	12CrCoWV	1000	70000	29	12	65	38.6			67F	60F	59F	43F	30F	31F	22F	—		
		"	66000	478	14	66	40.4					63	(54)	(47)					
		"	64000	559	12	63	40.5												
		"	62000	1421	10	60	41.1												
		"	59000	2704	9	54	41.5												
		1100	52000	15	12	76	40.8							31	(19)	(12)			
		"	46000	139	11	69	42.3												
		"	42000	171	11	72	42.5												
		"	38000	383	11	72	43.0												
		"	32000	804	5	11	43.5												
		"	24000	3410	12	54	44.5												
		"	21000	2591	13	46	44.3												
		1200	35000	8	15	84	43.0										25	(15)	—
		"	32000	27	14	81	43.9												
		"	28000	68	14	80	44.5												
		"	24000	110	17	79	44.8												
		"	22000	211	17	80	45.3												
		1000	76000	474	Notched	(b)					70	(42)	(24)						
		"	74000	751	"	—													
		"	70000	1088	"	—													
		"	60000	2022	"	—													
		"	50000	4190	"	2													
2567	12CrCoWV	1000	65000	33	10	68	38.7	---	58F	49F	49F	39F	28F	28F	---	---			
		"	60000	79	7	67	39.2												
		"	58000	1087	12	63	41.0												
		1100	42000	68	14	74	41.8							28	(18)	(11)			
		"	35000	298	12	72	42.8												
		"	28000	1042	13	68	43.7												
		"	22000	3411	9	29	44.5												
2137	12CrWV	1000	69000	13	15	65	38.1	69F	65F	61F	60	55	(51)						
		"	60000	1817	12	60	41.3												
		"	55000	11913	8	35	42.5												
2333	12CrWV	1000	60000	17	21	65	38.3	55F	53F	49F	48	(41)	(35)						
		"	56000	11	19	72	38.0												
		"	52000	83	15	66	39.3												
		"	50000	594	16	71	40.5												
		"	40000	13000+	Removed		42.5+												
2717	12CrWV	1000	60000	82	14	66	39.3	---	59F	54F	53F	44F	28F	29F	17F	9.4F	19F	10F	—
		"	54000	1118	11	64	41.0				53	(44)							
		"	50000	4195	9	62	41.8												
		1050	58000	17	18	69	39.6												
		"	50000	407	11	69	41.7												
		"	45000	762	11	71	42.1												
		"	32000	4422	7	28	43.3												
		1100	35000	427	11	74	43.1												
		1200	35000	2	20	78	42.0												
		"	25000	15	18	85	43.5												
		"	20000	88	17	84	44.7												
		1300	10000	32	36	92	46.6												
	12CrWV	1100	56000	96	Notched (b)		3.2	---						35	(20)	(11)			
		"	46000	336	"	1.6	---												
		"	34000	1197	"	.8	---												
		"	24000	4920	"	< 1	---												

TABLE 4 (*Continued*)

		RUPTURE TEST DATA						RUPTURE STRENGTH - psi $\times 10^{-3}$											
								900 F			1000 F			1100 F			1200 F		
Item	Material	Test Temp. (°F)	Stress (psi)	Rupture Time (Hours)	% El.	% RA	P_{25}	10^3 hr.	10^4 hr.	10^5 hr.	10^3 hr.	10^4 hr.	10^5 hr.	10^3 hr.	10^4 hr.	10^5 hr.	10^2 hr.	10^3 hr.	10^4 hr.
2763	12CrWV	1000	60000	393	13	70	40.3	---	---	57P	56P	44P	32P	33P	21P	---	24P	---	---
		1050	55000	192	12	73	41.2												
		1100	45000	167	12	77	42.5												
		1200	35000	7	17	85	42.9												
		"	30000	44	14	85	44.2												
		"	20000	227	16	83	45.4												
		1350	13000	4	30	93	46.3												
2803-2	12CrWV	1100	45000	9	10	81	40.5	---	---	44P	43P	35P	28P	28P	20P	---	23P	---	---
		1200	35000	3	21	85	42.3												
		"	30000	19	18	83	43.6												
		"	20000	192	8	80	45.2												
2803-3	12CrWV	1150	40000	1	21	81	40.2	---	---	37P	36P	31P	26P	26P	20P	---	22P	---	---
		1200	35000	1	23	85	41.5												
		"	20000	171	16	84	45.2												
2871	12CrWV	1050	56000	16	14	(a)	39.6	---	57P	50P	50P	40P	29P	30P	18P	---	21P	---	---
		1100	48000	24	17	"	41.2												
		1150	35500	73	13	"	43.2												
		1100	34900	512	19	"	43.2												
		1100	33000	709	22	"	43.4												
		1050	33000	6467	11	37	43.6												
		1200	28000	29	19	(a)	43.9												
		1250	20000	20	20	"	45.0												
		1300	16000	5	29	"	45.2												
		1200	14200	465	29	"	45.9												
		1300	12000	12	42	"	45.9												
		1150	10000	4516+	Discontinued		46.1												
2872	12CrWV	1050	55000	7	22	(a)	39.0	---	51P	41P	41P	31P	22P	23P	15P	---	17P	---	---
		1150	40000	3.5	19	"	41.1												
		1100	26000	712	24	"	43.4												
		1250	20000	7	27	"	44.2												
		1300	12000	9	38	"	45.7												
		1200	11000	433	29	"	45.9												
2873	12CrWV	1050	55000	154	14	(a)	41.1	---	---	58P	58P	44P	31P	32P	20P	11P	23P	12.5P	---
		1150	40000	140	11	"	43.7												
		1100	37000	501	15	"	43.2												
		1050	33000	8293	7	24	43.7												
		1250	20000	28	21	(a)	45.2												
		1200	16000	233	---	"	45.4												
		1300	11800	30	44	"	46.6												
2874	12CrWV	1050	56000	8	16	(a)	39.1	---	55P	52P	51P	44P	35P	36P	22P	11P	26P	12P	---
		1150	40000	168	13	"	43.8												
		1050	38000	5151	6	21	43.4												
		1100	37000	396	18	(a)	43.1												
		1250	20000	38	19	"	45.4												
		1200	15800	461	---	"	45.9												
		1300	12000	32	38	"	46.6												
2875	12CrWV	1050	55000	94	12	(a)	40.8	---	---	55P	54P	43P	29P	30P	17P	---	20P	---	---
		1150	40000	39	11	"	42.8												
		1100	35400	473	19	"	43.2												
		1250	20000	16	21	"	44.8												
		1300	11800	11	34	"	45.8												
		1200	11000	592	---	(a)	46.1												
		1150	10000	4517	Discontinued		46.1												
2876	12CrWV	1050	56000	4	9	(a)	38.7	---	51P	42P	42P	32P	23P	24P	15P	---	17P	---	---
		1150	40000	4	16	"	41.2												
		1100	26000	701	---	"	43.4												
		1050	26000	10787	9	47	43.9												
		1250	20000	7	27	(a)	44.2												
		1300	11800	10	37	"	45.7												
		1200	11000	298	34	"	45.6												
2746	12CrMoWV	1100	50000	28	14	74	41.3	---	---	---	52P	40P	28P	29P	18P	9.6P	20P	11P	---
		"	35000	595	10	62	43.4												
		1200	35000	4	20	85	42.5												
		"	25000	43	16	85	44.2												
		"	20000	133	16	79	45.0												
		"	15000	257	19	85	45.5												
		1300	10000	29	30	94	46.7												
2757	12CrMoWV	1100	50000	19	16	71	41.0	---	---	52P	51P	38P	27P	28P	18P	---	20P	---	---
		1200	25000	34	17	85	44.0												
		1200	15000	415	19	89	45.8												
2870	12CrMoWV	1050	56000	21	13	(a)	39.8	---	58P	50P	50P	39P	27P	28P	17P	---	20P	10P	---
		1100	47300	13	16	"	40.7												
		1150	35000	24	19	"	42.5												
		1100	32300	676	21	"	43.4												
		1100	30000	591	19	"	43.3												
		1200	28000	31	17	"	43.9												
		1250	20000	19	20	"	44.9												
		1200	15800	241	30	"	45.4												
		1300	15800	7	---	"	46.5												
		1200	13500	554	27	"	46.0												
		1300	11800	17	39	"	46.2												
		1150	12000	4517	Discontinued		46.1+												

TABLE 4 *(Continued)*

Item	Material	RUPTURE TEST DATA: Test Temp. (°F)	Stress (psi)	Rupture Time (Hours)	% El.	% RA	P_{25}	RUPTURE STRENGTH - psi $x10^{-3}$: 900 F 10^3 hr.	900 F 10^4 hr.	900 F 10^5 hr.	1000 F 10^3 hr.	1000 F 10^4 hr.	1000 F 10^5 hr.	1100 F 10^3 hr.	1100 F 10^4 hr.	1100 F 10^5 hr.	1200 F 10^2 hr.	1200 F 10^3 hr.	1200 F 10^4 hr.
2911	12CrMoVV	1050	60000	40	14	70	40.2	—	—	54F	54F	42F	32F	32F	23F	13F	25F	15F	—
		1150	50000	3	16	78	41.0												
		1150	40000	29	18	78	42.6												
		1150	30000	170	17	82	43.8												
		1200	25000	109	22	83	44.8												
		1200	20000	359	18	84	45.7												
		1300	15000	15	27	91	46.1												
		1300	10000	73	41	93	47.3												
3017	12CrMoVV	1050	50000	327	24	75	41.6	—	—	—	—	44F	33F	33F	22F	13F	25F	14.5F	—
		1050	49000	548	23	72	41.9												
		1100	38000	1293	23	72	43.9												
		1200	30000	36	27	86	44.1												
		1200	20000	300	37	88	45.6												
		1300	15000	22	40	83	46.3												
		1300	10000	103	52	92	47.5												
3018	12CrMoVV	1200	25000	82	24	83	44.6	—	—	—	—	—	—	—	21F	—	24F	—	—
		1250	18000	46	20	89	45.6												
		1250	13000	107	26	91	46.2												
3020	12CrMoVV	1100	45000	117	19	76	42.2												
		1200	30000	65	81	21	44.5												
		1200	22000	246	18	79	45.4												
		1250	15000	52	29	88	45.7												
3706	12CrMoV	1000	100000	.074	21	(a)	34.9	82F	72F	60F	60F	47F	35F	35F	24F	14F	26F	16F	—
		"	80000	21.0	24	"	38.4				64	(48)	—						
		"	90000	1.3	22	"	35.2												
		"	70000	82.0	24	"	39.3												
		"	60000	3121	17	"	41.7												
		"	50000	>7800	>3	"	42.2												
		900	100000	318	10	"	37.4												
		1100	60000	10	32	"	40.7							41	—	—			
		"	100000	.0014	18	"	34.6												
		"	90000	.017	17	"	36.2												
		"	80000	.15	25	"	37.7												
		"	70000	2.7	22	"	39.7												
		"	50000	163.6	21	"	42.4												
		"	40000	1922	14	"	44.1												
		"	30000	3819	17	"	44.6												
		1200	60000	.067	38	"	39.6										24	15.7	—
		"	50000	.50	54	"	41.0												
		"	40000	4.4	33	"	42.6												
		"	30000	73.0	28	"	44.7												
		"	25000	90.0	19	"	44.8												
		"	20000	280.0	20	"	45.6												
		"	15000	1203	26	"	46.7												
		1350	50000	.001	30	"	39.9												
		"	40000	.016	34	"	42.0												
		"	30000	.14	21	"	43.7												
		"	20000	0.8	65	"	45.2												
		"	15000	2.7	60	"	46.1												
		"	10000	25.2	50	"	47.8												
5119	12CrMoV	1100	60000	.7	34	"	38.8	—	56F	48F	47F	39F	28F	29F	—	—	20F	—	—
		"	50000	9.0	34	"	40.6												
		1200	40000	1.8	30	"	42.0												
		"	30000	18.6	46	"	43.7												
		"	20000	100.0	26	"	44.9												
5188	12CrMoV	1200	30000	30.0	39	(a)	44.0					38F	30F	31F	23F		25	20	—
		"	25000	113.7	22	"	44.9												
		"	20000	1061.8	22	"	46.6												
5219	12CrMoV	1200	30000	0.9	57	"	41.6					27F	22F	23F			19F		
		"	25000	4.4	49	"	42.6												
		"	20000	57.2	34	"	44.5												
5376	12CrMoV	1200	30000	99.4	29	"	44.8								24F				
		"	25000	147.3	32	"	45.1												
		"	20000	410.4	31	"	45.7												
5500	12CrMoV	1100	60000	4.4	13	"	40.0		62F	57F	57F	49F	38F	38F	24F		29F		
		"	50000	127.7	13	"	42.3												
		1200	30000	52.3	19	"	44.4												
		"	20000	384.0	18	"	45.8												
5531	12CrMoV	1100	50000	5.6	23	"	40.2		53F	47F	46F	35F	31F	31F	23F		26F		
		1200	30000	38.3	29	"	44.2												
		"	20000	438.3	28	"	45.9												
5684	12CrMoV	1100	60000	3.1	34	"	39.8		61F	54F	54F	44F	33F	33F	21F		25F		
		"	40000	434.1	26	"	43.1												
		1200	30000	24.2	36	"	43.9												
		"	20000	207.8	45	"	45.4												
5757	12CrMoV	1100	60000	1.7	32	"	39.4		55F	44F	44F	35F	27F	27F	20F		22F		
		"	50000	6.9	44	"	40.3												
		1200	40000	0.4	40	"	40.9												
		"	30000	9.3	33	"	43.2												
		"	20000	377.9	26	"	45.8												
5787	12CrMoV	1100	60000	11.5	19	(a)	40.7			60F	59F	50F	37F	37F	24F		29F		
		"	50000	293.2	11	"	42.9												
		1200	40000	14.5	21	"	43.5												
		"	30000	59.8	20	"	44.4												
		"	20000	300.5	21	"	45.7												

TABLE 4 *(Continued)*

		RUPTURE TEST DATA						RUPTURE STRENGTH - psi x10⁻³											
								900 F			1000 F			1100 F			1200 F		
Item	Material	Test Temp. (°F)	Stress (psi)	Rupture Time (Hours)	% El.	% RA	P_{25}	10^3 hr.	10^4 hr.	10^5 hr.	10^3 hr.	10^4 hr.	10^5 hr.	10^3 hr.	10^4 hr.	10^5 hr.	10^2 hr.	10^3 hr.	10^4 hr.
5788	12CrMoV	1100	60000	11.7	29	*	40.7			60P	60P	53P	43P	43P	28P		25P		
		*	50000	208.7	24	*	42.6												
		1200	40000	30.3	23	*	44.0												
		*	30000	111.9	27	*	45.0												
		*	20000	270.0	30	*	45.6												
5829	12CrMoV	1100	50000	3.3	40	*	39.8			43P	43P	32P	25P	25P	19P		21P		
		1200	40000	0.2	34	*	40.4												
		*	30000	1.6	37	*	43.9												
		*	20000	160.9	30	*	45.2												
D6	12CrWV	900	70000	5	—	—	35.0	50P	43P	37P	37P	30P	24P	24P	18P	10P	19P	12P	
		*	65000	11	—	—	35.4	47	(40)	(34)									
		*	60000	34	—	—	36.1												
		*	55000	110	—	—	36.8												
		*	45000	2850	—	—	38.7												
		1000	45000	51	—	—	39.0				36	—	—						
		*	35000	1630	—	—	41.2												
		1100	35500	17	—	—	40.9							24	(14.3)	—			
		*	33000	65	—	—	41.8												
		*	30000	165	—	—	42.5												
		*	28000	345	—	—	43.0												
		*	24000	890	—	—	43.6												
		*	20000	2250	—	—	44.3												
		1200	25000	28	—	—	43.9										19	11.9	(5.9)
		*	20000	63	—	—	44.5												
		*	17300	295	—	—	45.6												
		*	15000	450	—	—	45.9												
		*	12500	710	—	—	46.2												
		*	10000	1850	—	—	46.9												
D14	12CrWV	1000	65000	138	10.0		39.6			65P	50P								
		*	55000	700	8.0		40.7												
		*	45000	1550	8.0		41.2				53	(29)	(16)						
		*	40000	3450	5.0		41.7												
		*	35000	4500	4.0		42.0												
2079	12CrWV	1000	60000	8.0			37.9	60P	54P	47P	47P	37P	28P	28P					
		*	50000	295.0			40.2												
		*	40000	5500			42.0												
		1100	40000	58			41.8							30	19	(12)			
		*	30000	1000			43.8												
		*	25000	2650			44.4												
		*	20000	7300			45.0												
2429	12CrWV	1000	66000	1	13.4	73	36.5	60P	53P	46P	46P	37P	28P	28P					
		*	60000	8	13.9	76	37.8				46	37	(29)						
		*	50000	283	13.9	76.5	40.0												
		*	45800	1167	13.4	76	41.1												
		*	42800	3278	10.6	72.5	41.5												
		*	38000	7695	10.4	61	42.3												
		1100	50000	1	14.6	81	39.1							29	19	(12.5)			
		*	44000	17	14.6	81	40.9												
		*	37000	179	10.5	75.5	42.6												
		*	32000	552	9.8	75	43.4												
		*	26000	1772	14.6	83	44.1												
2170	12 CrCb	900	82000	17	6		35.6	72P	65P	57P	57P	48P	—						
		*	70000	2500	7		38.6	73	68	(64)									
		*	67000	19100	1.9	(Removed)	39.8												
		1000	66000	33	6		38.8				58	(49)	(41)						
		*	58000	790	7		40.7												
		*	52000	4000	4		41.8												
2236	12 CrCb	900	78000	11	7.5		35.5	65P	58P	52P	52P	40P	24P	24P					
		*	72000	430	7.5		37.6												
		*	66000	3000	7.5		38.8	64	(58)	(51)									
		*	63000	1100	7.0		38.2												
		*	60000	4000	5.5		39.0												
		1000	70000	1.5	8.2		36.7				52	(39)	(33)						
		*	64000	178	6.0		39.8												
		*	58000	580	9.0		40.5												
		*	52000	870	6.0		40.8												
		*	47000	1700	8.0		41.2												
		*	40000	3700	9.0		41.7												
		1100	46000	150	4		42.4												
		*	26000	540	9		43.3												
		*	14000	2600	17		44.6												
		1200	20000	46	12.5	78	44.3												
2278	12 CrCb	1000	66000	2.5	12	57	37.1	64P	56P	45P	45P								
		*	58000	72	6	54	39.2												
		*	56000	247	2	11	40.1												
		*	52000	114	8	71	39.6												
		*	48000	325	6	69	40.2												
		1100	46000	22	7	50	41.2												
		1000	42000	1640	9	77	41.2												
		*	38000	2468	6	73	41.5												
2328	12 CrCb	1000	64000	15.0	16.0	72.0	38.2	64P	60P	—									
		*	60000	239.0	9.0	69.0	40.1				(51)								
		*	56000	461.0	9.0	72.0	40.4												
2329	12 CrCb	1000	70000	13.0	8.0	69.0	38.2	90P	65P	56P	56P								
		*	60000	520.0	9.0	69.0	40.5				56	(46)							
		*	52000	2566	8.0	68.0	41.5												
2466	12 CrCb	1000	65000	414	7	62	40.4	—		61P	60P								
		*	60000	1196	6	52	43.1				60								
		*	55000	2994	5	45	43.5												
2588	12 CrCb	1000	66000	132	6.8	67.5	39.6	—	67P	59P	58P								
		*	60000	1134	7.4	68.0	41.0				60	(43)	(33)						
		*	56000	2071	6.8	60.0	41.4												
		*	52000	2311	7.4	59.0	41.5												
		*	48000	5282	7	55.0	42.0												

TABLE 4 (Continued)

Item	Material	Test Temp. (°F)	Stress (psi)	Rupture Time (hours)	% El.	% RA	P_{25}	200 F 10^3 hr.	200 F 10^4 hr.	200 F 10^5 hr.	1000 F 10^3 hr.	1000 F 10^4 hr.	1000 F 10^5 hr.	1100 F 10^3 hr.	1100 F 10^4 hr.	1100 F 10^5 hr.	1200 F 10^2 hr.	1200 F 10^3 hr.	1200 F 10^4 hr.
	RUPTURE TEST DATA							RUPTURE STRENGTH - psi $\times 10^{-3}$											
2948	12 CrCb	1000	65000	414	7	62.0	40.4	80F	71F	62F	62F	50F	39F	39F	—	—			
		"	60000	1196	6	52.0	41.1												
		"	55000	2394	5	45.0	41.5												
		1200	45000	12.0	4	21.0	43.4												
		"	40500	19.9	9	25	43.7												
		"	35250	41.5	7	14	44.3												
5256	12 CrTa	1200	40000	9.9	21	(c)	43.2						29F	29F					
		"	30000	24.2	13	(c)	43.8												
		"	25000	24.2	20	(c)	43.8												
		"	20000	58.1	30	(c)	44.5												

(a) 0.187" dia. pin loaded in double shear with a clevis-type fixture.
(b) Notched bar with 0.253" root diameter, 0.357" major diameter, 60 degree notch, and 0.011" notch radius.
(c) Test specimen with 1" gage length and 0.160" diam.
(d) Test specimen with reduced test section 0.160" dia. and ¼" gage length.
P Indicates strength value obtained by use of Larson-Miller parameter $T(25/\log t)$.
( ) Indicates strength value obtained by extrapolation of log time-log rupture stress curve.

Rupture strength values identified with "P," appearing opposite the item number, have been determined by the use of all test data at all temperatures for the item in question. Other strengths listed were obtained from log stress-log rupture time plots and were determined by the use of all the tests at the particular temperature in question.

TABLE 5 CREEP RELAXATION STRENGTH

Item	Material	Temp °F	Test Duration	Residual Stress at .2% Total Strain 1	10	100	500	1000	5000	10000 Hours
2379	12 Cr	900	4065	-----	28.5	22.5	20.5	19.2	17.5	(16)
"	(405)	1000	5880	-----	17.0	13.5	12.2	10.4	9.0	----
"	"	1050	2982	-----	15.9	11.9	9.7	7.7	6.1	(4.5)
2380	"	800	2548	-----	-----	45	43	41	39	(37)
"	"	1000	3530	-----	21	18	14.3	12.5	10.3	(7)
2381	"	1000	5831	18	13.9	10.7	9.4	8.0	6.8	(5.8)
2382	"	800	2548	-----	-----	27	24	21	19.5	(16)
"	"	1000	5831	18	12.5	9.0	7.7	6.4	5.2	(3.8)
2385	"	900	3018	32	24	20	17.8	15.8	(14.0)	(12.2)
"	"	1000	3311	-----	18.7	12.0	10.3	8.7	(7.2)	(6)
2386	"	1000	3540	-----	17.8	13.9	12.2	10.7	9.5	(8.0)
2389	"	1000	2540	-----	19.2	14.4	12.7	11.1	(9.8)	(8.6)
2387	12CrCbMV	1000	2389	-----	36.0	30.0	27.0	23.7	19.7	(18.0)
2306	"	1000	3210	-----	36.0	31.0	28.0	25.8	20.0	(18.0)
2387	"	1000	2913	38.0	31.0	26.5	24.0	21.0	18.0	(15.0)
2389	"	1000	1815	----	35.0	29.0	26.0	22.0	19.0	(16.0)
"	"	1100	3085	27.0	22.0	16.3	13.1	8.9	8.4	(5.0)
2387	"	1000	1675	32.0	29.0	24.0	21.7	19.0	16.5	(14.0)
"	"	1100	2582	-----	19.5	16.3	11.6	7.8	6.8	(2.5)
2347	"	1000	725	-----	27.5	23.6	21.0	19.8	(17.0)	------
2348	"	1000	2696	-----	24.0	20.0	18.0	16.7	(13.5)	(11.9)
2349	"	1000	3480	-----	32.0	28.0	24.0	20.0	17.0	(13.8)
2345	"	1000	2484	-----	-----	18.0	16.7	13.4	(11.9)	(10.0)
2137	12CrMV	1000	3384	-----	36.0	30.0	27.5	23.5	17.5	(13.3)
2353	"	1000	3480	-----	27.0	23.0	21.0	18.0	15.0	(12.0)
2717	"	1000	3700	-----	28	23	21.3	19	14.5	(11.7)
"	"	1050	2180	-----	25	18.2	15.4	12.5	10	(7.8)
2721	"	1050	3230	-----	26	21.2	18.8	15.5	12.5	(9.8)
2808-2	"	1050	3478	-----	21	16.5	14.4	12.0	10.0	(7.9)
2808-3	"	1050	3478	-----	20.5	16.1	13.8	11.3	9.7	(8.0)
2757	12 CrMoV	1100	2660	-----	18.5	13.9	11.8	8.3	6.9	(5.9)
"	"	1200	980	16	11.0	8 .0	2.4	.98	-----	-----
2911	"	1000	In test	-----	32.0	28.5	25.5	22.0	19.3	-----
"	"	1050	2880	-----	21.0	24.5	20.5	16.4	13.5	(10.5)
"	"	1100	In test	-----	23.0	16.5	13.2	10.6	-----	-----
3017	"	1000	" "	-----	29.0	25.0	22.7	19.0	16.0	-----
3018	"	1000		-----	34.0	29.0	26.0	22.0	17.5	-----
26859	12 CrMoV	1000	1960	36.5	31.2	25.0	21.5	17.7	(14)	
"	"	1050	4056	27.6	23.5	17.5	15.5	12.5	9.5	
"	"	1150	573	21.0	15.9	10.7	7.0	(5.0)	-----	
5189	"	1000	1960	37.2	31.9	27.6	24.5	20.5	16.7	
"	"	1050	4206	29.0	24.7	20.0	16.6	13.0	10.1	
"	"	1150	1050	21.7	16.9	11.4	8.3	4.9	-----	
5219	"	1000	705	31.9	26.5	19.5	15.5	8.8	-----	
"	"	1050	5024	30.0	14.4	9.8	7.2	5.5	3.5	
"	"	1150	265	10.4	8.0	6.7	4.6	----	-----	
5831	"	1000	5804	32.5	27.3	21.0	17.5	14.7	12.0	
"	"	1050	1775	23.7	19.2	12.5	9.0	6.2	4.8	
"	"	1150	816	17.9	13.2	7.5	5.9	4.6	-----	
2079	12 CrMoV	1000	5384	-----	25	19	15.5	11.5	8.8	(6.2)
"	"	1100	2890	-----	16	11	8.6	6.5	-----	-----
2346	"	1000	5344	25	21	17	14.2	9.4	6.1	(3.8)
2179	12 CrCb	900	3480	45	41	39	36	34	(31)	(28.5)
"	"	1000	2873	-----	-----	31.5	28	25	(22)	(19.5)
2334	"	1000	2153	36	31	28.0	24.1	21.2	(18.4)	
2276	"	1000	4188	-----	-----	26.5	23.0	18.8	14.5	(10.4)
2328	"	1000	5178	-----	30	25	22	18.5	13	(13.3)
2329	"	1000	5179	-----	-----	30	26	22	19.2	(14.2)
2461	"	1000	2704	-----	34	29.5	27	23.5	20.2	(17.1)
"	"	1100	2721	-----	22	15.5	10.5	6.0	3.1	(.9)

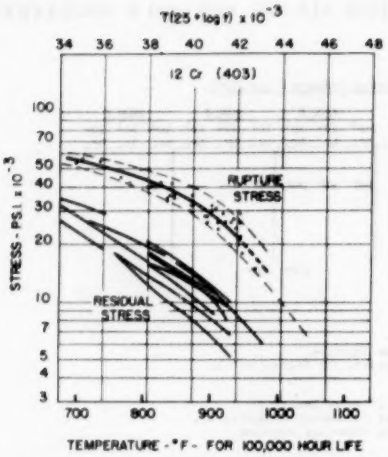

FIG. 3 RUPTURE STRENGTH AND RESIDUAL STRESS AT 0.2 PER CENT TOTAL STRAIN VERSUS $T(25 + \log t)$ FOR 12 PER CENT CR (TYPE 403)

(T = absolute temperature in degrees R; t = time in hours. A temperature scale is given for 100,000-hr life. For other periods, scales may be computed from the parameter $T[25 + \log t]$.)

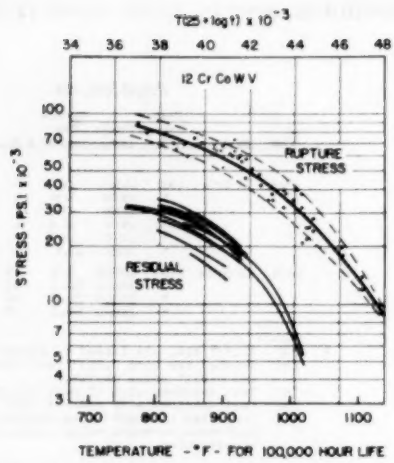

FIG. 4 RUPTURE STRENGTH AND RESIDUAL STRESS AT 0.2 PER CENT TOTAL STRAIN VERSUS $T(25 + \log t)$ FOR 12 CR-CO-W-V

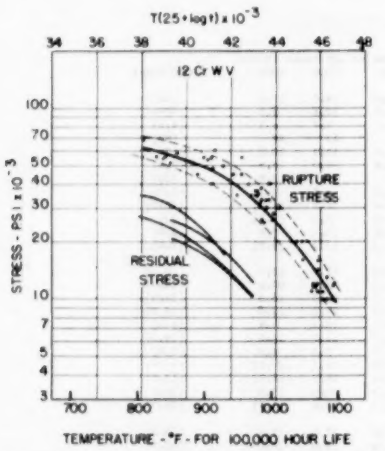

FIG 5 RUPTURE STRENGTH AND RESIDUAL STRESS AT 0.2 PER CENT TOTAL STRAIN VERSUS $T(25 + \log t)$ FOR 12 CR-W-V

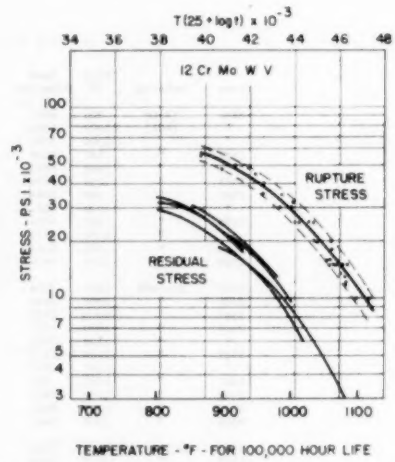

FIG. 6 RUPTURE STRENGTH AND RESIDUAL STRESS AT 0.2 PER CENT TOTAL STRAIN VERSUS $T(25 + \log t)$ FOR 12 CR-MO-W-V

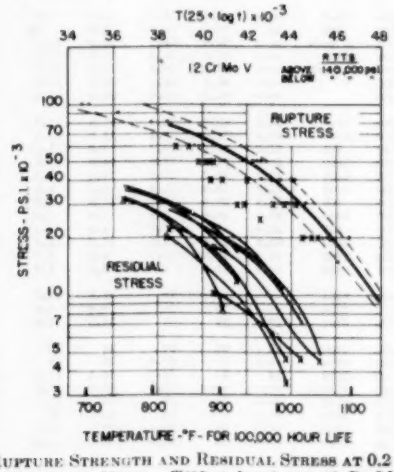

FIG. 7 RUPTURE STRENGTH AND RESIDUAL STRESS AT 0.2 PER CENT TOTAL STRAIN VERSUS $T(25 + \log t)$ FOR 12 CR-MO-V

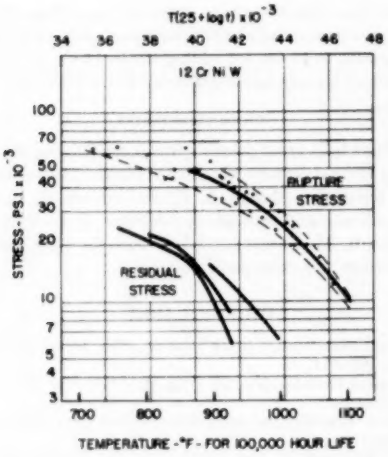

FIG. 8 RUPTURE STRENGTH AND RESIDUAL STRESS AT 0.2 PER CENT TOTAL STRAIN VERSUS $T(25 + \log t)$ FOR 12 CR-NI-W

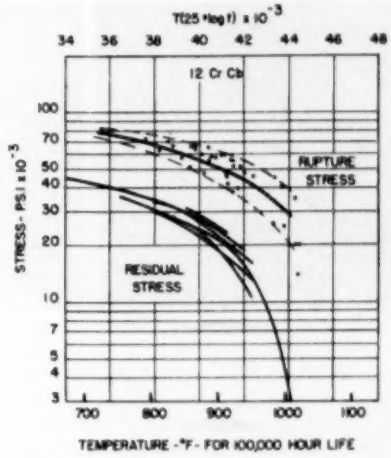

FIG. 9 RUPTURE STRENGTH AND RESIDUAL STRESS AT 0.2 PER CENT TOTAL STRAIN VERSUS $T(25 + \log t)$ FOR 12 CR-CB

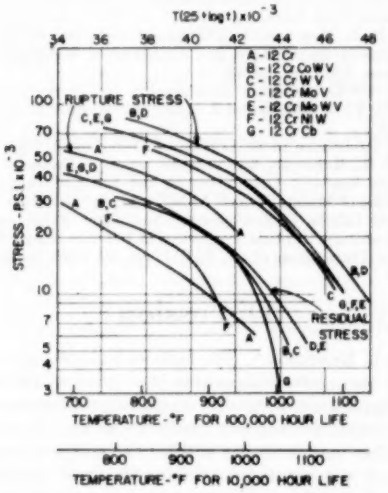

FIG. 10 SUMMARY PLOT SHOWING RUPTURE STRENGTH AND RESIDUAL STRESS AT 0.2 PER CENT TOTAL STRAIN VERSUS $T(25 + \log t)$ FOR THE SEVERAL 12 CR ALLOYS

(Temperature scales are given for 10,000-hr life and for 100,000-hr life; for other periods, scales may be computed from the parameter $T[25 + \log t]$.)

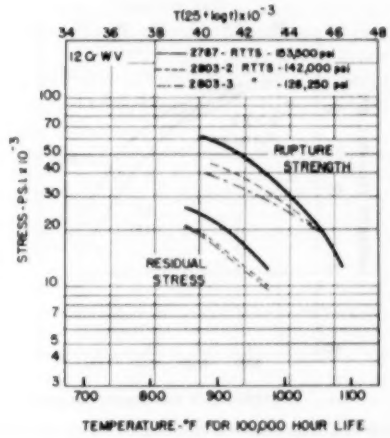

FIG. 11 EFFECT OF LOWER ROOM-TEMPERATURE TENSILE STRENGTH PRODUCED BY ADDITIONAL TEMPERING ON RUPTURE AND RELAXATION STRENGTH OF 12 CR-W-V

NITRIDING OF 12 PER CENT CR ALLOYS

The surface-hardening of these 12 per cent Cr types of alloys for use as valve stems and bushings can best be accomplished by using an ammonia-gas method of nitriding. This method produces a case with satisfactory depth, hardness, and corrosion resistance to steam. The usual procedure for preparing Nitralloy parts for nitriding also must be used for preparing the 12 per cent Cr types of alloys. In addition, the 12 per cent Cr alloys must be nitrided immediately after grit-blasting or pickling. This nitriding process readily produces a case thickness of 0.006 to 0.008 in. with a minimum hardness of 91 Rockwell 15 N (62 Rockwell C). Fig. 13 is a photomicrograph at ×100 of a 12 Cr-W-V part nitrided, using the foregoing process. The diamond-shaped impressions are Knoop hardness readings.

An important question can be raised concerning the persistence of hardness in parts exposed to high service temperature for long

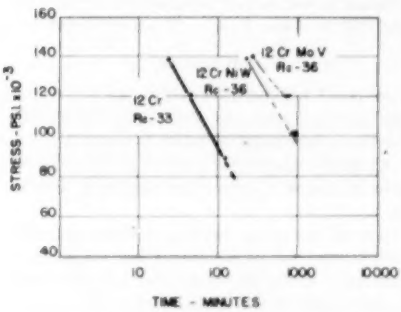

FIG. 12 ACCELERATED STRESS-CORROSION TESTS USING STRIP SAMPLES STRESSED BY BENDING, IMMERSED IN SOLUTION OF 1:1 HCl WITH 1 PER CENT SeO_2

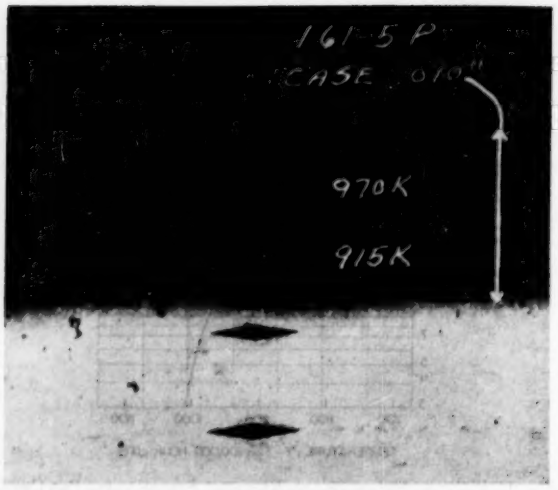

FIG. 13 PHOTOMICROGRAPH AT × 100 SHOWING NITRIDED CASE ON A 12 CR-W-V PART

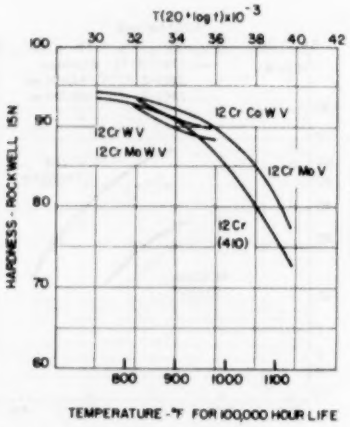

FIG. 14 SURFACE HARDNESS OF NITRIDED 12 PER CENT CR ALLOYS AS AFFECTED BY TEMPERING

times. Fig. 14 shows the results of tempering tests in a plot of Rockwell 15 N hardness at room temperature versus the tempering parameter $T(20 + \log t)$ which indicates that the surface hardness should indeed fall off to some extent, but that the hardness should still be above $R_{15N} = 85$ after 100,000 hr at 1050 F.

WELDING

The 12 per cent Cr alloys discussed in this paper are either fully or partially hardened when air-cooled from the welding temperature, and extreme care must be taken to prevent cracking during welding. Carefully controlled preheat and postheat treatments are required to insure a crack-free weldment with satisfactory properties.

In the authors' company, welding of these alloys has been applied in the fabrication of steam-turbine diaphragms for high-temperature use. From an economical and production point of view, a modification of the chemistries of these martensitic alloys to make a duplex martensite-plus-ferrite alloy is more satisfactory than trying to maintain the rigid welding control necessary for the fully martensitic alloys. Such duplex ferrite-plus-martensite structures have been obtained in welding grades of 12 Cr steel by the increasing of chromium and addition of aluminum or molybdenum to 12 Cr, by adding Cb to 12 Cr, or by lowering the carbon and increasing tungsten for 12 Cr-W-V (8).

ACKNOWLEDGMENT

The authors take great pleasure in acknowledging the contributions of the several persons who assisted in the preparation of this paper; in particular, Messrs. A. W. Rankin and E. L. Robinson for their guidance and counsel, and Messrs. F. L. Behrmann, P. E. Sherman, R. M. Curran, and J. E. Erb for their assistance in the preparation and analysis of data.

BIBLIOGRAPHY

1 "Metals Handbook" (1948 edition), The American Society for Metals, pp. 309–311.

2 Technical Bulletin No. 20, August, 1946, The Timken Roller Bearing Company.

3 General Electric Company unpublished data (available from the authors).

4 "The Influence of Temperature on the Elastic Constants of Some Commercial Steels," by F. Garofalo, P. R. Malenock, and G. V. Smith, ASTM Special Technical Publication No. 129, Symposium on Determination of Elastic Constants, 1952, pp. 10–30.

5 "Influence of Sharp Notches on the Stress-Rupture Characteristics of Several Heat-Resisting Alloys," by W. F. Brown, Jr., M. H. Jones, and D. P. Newman, ASTM Special Technical Publication No. 128, Symposium on Strength and Ductility of Metals at Elevated Temperatures, 1953, pp. 25–48.

6 "A Time-Temperature Relationship for Rupture and Creep Stresses," by F. R. Larson and J. Miller, Trans. ASME, vol. 74, 1952, pp. 765–775.

7 "The Resistance to Relaxation of Materials at High Temperature," by E. L. Robinson, first progress report of Project 16, ASTM-ASME Joint Research Committee on the Effect of Temperature on the Properties of Metals, Trans. ASME, vol. 61, 1939, pp. 543–554.

8 "Some Effects of Composition and Heat Treatment on the High Temperature Rupture Properties of Ferrous Alloys," by R. H. Thielemann, Proceedings of the ASTM, vol. 40, 1940, pp. 788–804.

Discussion

ERNEST L. ROBINSON.[4] The authors include a great number of detailed test results in support of the curves which summarize them for application purposes. Both long-time rupture-test results and long-time creep-test results are given. The use of the Larson-Miller parameter has enabled the compact presentation of the many test results in a remarkably small number of diagrams which readily present to the eye the maximum possible spread between tests. Fig. 10 of the paper gives the authors' interpretation of their average test results on the several alloys. This is a very useful diagram. Two specific temperature scales are given at the bottom for the benefit of those who are not using the Larson-Miller formula habitually.

The creep-test results are presented in terms of residual stresses after stated times of relaxation. For the benefit of readers who may want to get ordinary creep rates, the writer suggests that another scale be added to Fig. 10 to show the residual stress at the end of 1000 hr. On the average, this stress is the stress which is accompanied by a creep rate of 1/100 per cent per 1000 hr. In other words, in a relaxation test as the load drops, the rate of creep slows down and at just about 1000 hr passes through the 10^{-7} rate referred to.

This convenient relationship was presented in the Second Progress Report of Project 16 ASTM-ASME Joint Committee on the Effect of Temperature on the Properties of Metals,[5] where the ratio of the 10^{-7} creep strength to the 1000-hr residual stress aver-

[4] General Electric Company, Schenectady, N. Y. Fellow ASME.

[5] Proceedings of the ASTM, vol. 48, 1948, p. 234

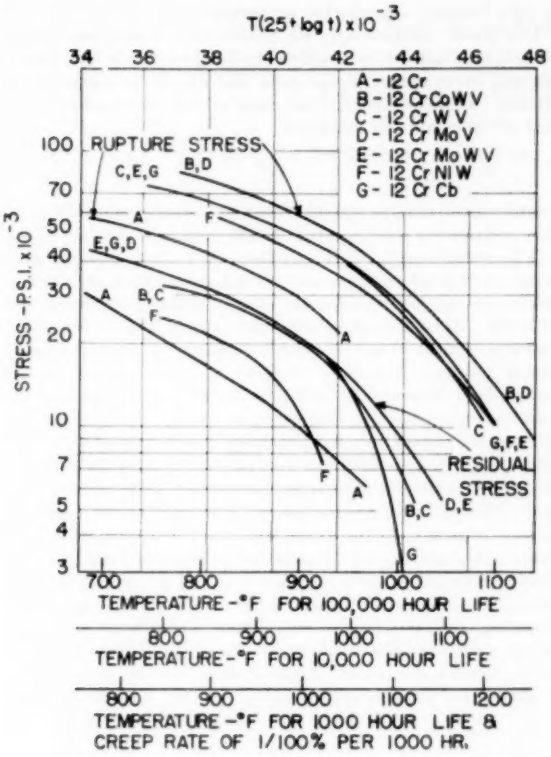

FIG. 15 DUPLICATE OF FIG. 10 OF PAPER, EXCEPT FOR ADDITION OF BOTTOM SCALE OF TEMPERATURE FOR 1000-HR LIFE

(Readings of residual-stress curves on this scale give, on the average, stress for creep rate of 1/100 per cent per 1000 hr. At the end of 1000 hr in a relaxation test, specimen is creeping at nominal rate noted.)

aged 1.00 for 87 tests. Of course, in individual cases, this standard rate may occur somewhat earlier or later than the thousandth hour but for the engineer who desires to form a judgment on the basis of the average of a good many tests, it is a useful relationship to keep in mind. Fig. 15, herewith, presents the curves in Fig. 10 of the paper with the suggested additional scale at the bottom for the benefit of those who care to use it.

E. A. STICHA.[6] The tremendous volume of high-temperature data for the modified 12 per cent chromium-alloy steels studied by the authors will be appreciated greatly by engineers concerned with elevated-temperature materials problems. The AISI Type 403 and 410 steels have served admirably in many applications at temperature levels somewhat below those contemplated for the latest central-station designs and attempted extension of their utility by suitable alloying is a worthy project.

The authors suggest high-temperature bolting as one possible application of these steels and cite properties of interest for this service. One characteristic which should be included in any such evaluation is impact strength after elevated-temperature exposure. In our experience, failures of bolts, at least in diameters under 2 in., have occurred at room temperature on remaking joints much more frequently than in actual operation at elevated temperatures. Almost invariably these failures have been associated with materials deficient in impact resistance.

Many of the modified 12 per cent chromium steels of this investigation exhibit precipitation-hardening characteristics upon prolonged exposure at elevated temperatures, especially after austenitizing at relatively high temperatures. Hence it would be of interest to know what order of impact resistance remains in these steels after exposure at contemplated service temperatures so their usefulness as bolting materials might better be assessed. Any data the authors make available on this point would be appreciated.

In their presentation the authors anticipate for nitrided modifications of 12 per cent chromium steel a hardness above R_{15N} = 85 after 100,000 hr at 1050 F. Although we have no data for these specific analyses, long-time aging results for nitrided Type 410 steel as given in Table 6 herewith, indicate that this view may be overly optimistic.

These results are in fair agreement with the low parameter end of the curve for 12 per cent chromium steel shown in Fig. 14 of the paper, but at the other end, which in our case represents the long exposures at 1025 F, there is marked divergence. While the alloying additions undoubtedly assist in retaining hardness, there well may be some question about maintaining the hardness level indicated.

A condition known as "blue-blush" has caused some difficulty on valve stems, particularly the nitrided 12 per cent chromium-steel type. Do any of the modified analyses offer hope of alleviating this condition?

AUTHORS' CLOSURE

The authors appreciate Mr. Robinson's comments concerning the approximate relation between the residual stress at the end of 1000 hr and the stress corresponding to a creep rate of 1/100 per cent per 1000 hr. Mr. Robinson's Fig. 15 is of assistance in expanding the applicability of the data presented in the paper.

With respect to Mr. Sticha's questions concerning precipitation hardening and reduction in impact strength of the alloyed 12 per cent chromium steels after prolonged exposure to service temperatures, we have been using such steels for bolting service since about 1947. During the past few months we have had a few service failures of the cobalt-containing alloy, and these failures have included both room-temperature and high-temperature cracking. Extensive laboratory investigations, including x-ray diffraction studies, aging tests, creep, and rupture on material returned from service, scale-model bolting, notch tests, and so on have not yet progressed sufficiently to reveal the mechanism of these service failures.

Concerning the hardness of nitrided surfaces after service exposure, long-time aging tests at 1100 and 1200 F are in progress, with the samples protected from oxidation, to verify the hard-

[6] Crane Company, Chicago, Ill.

TABLE 6 LONG-TIME AGING RESULTS FOR TYPE 410 STEEL

Time, hr	900 F		1025 F		1250 F		1300 F	
	VPN/5kg	R_{15N}	VPN/5kg	R_{15N}	VPN/5kg	R_{15N}	VPN/5kg	R_{15N}
1	1000	94.1	1185	94.7	752	91.2	473	84.0
100	960	93.2	855	92.5	...	...	...	...
300	890	93.0	750	91.2	...	...	...	...
1000	820	92.0	630	89.0	...	...	...	...
3000	760	91.5	490	84.7	...	...	...	...
6720	720	90.5	290	74.3	...	...	...	...

NOTE: Superficial Rockwell readings were converted from the Vickers values.

ness data presented in the paper. The particular tests for 12 Cr-Co-W-V, 12 Cr-W-V, and 12 Cr-Mo-W-V on which Fig. 14 is based had accumulated less than 100-hr exposure time. Further exposure shows that after 256 hours at 1200 F, the hardnesses for all the materials were approximately 82 to 83 R_{15N}, falling on the curve shown for Type 410 in Fig. 14.

The authors' company has also experienced the difficulty with "blue blush" mentioned by Mr. Sticha, and adequate information is not yet available to establish firmly whether this blue blush is caused by oxidation of the stem material or to carry-over by steam. In either case, it is not expected that the modified analyses will alleviate this condition.

Effect of Certain Elements on the Graphitization of Steel

By R. J. FIORENTINO,[1] A. M. HALL,[2] AND J. H. JACKSON,[3] COLUMBUS, OHIO

An investigation was undertaken to obtain information on (*a*) the relationship, if any, between the aluminum and nitrogen contents of a steel and the susceptibility of the steel to graphitization, (*b*) the manner in which chromium influences the process, and (*c*) the effect of normal amounts of Mn, Si, S, and P in the graphitization of steel. Toward these objectives, twelve laboratory heats of iron-carbon alloy were made from specially prepared melting stock. Various amounts of Al, N, Cr, Mn, Si, S, and P were added to these heats. They were forged to ⅝-in-square bars, variously heat-treated, bead-welded, and tested for graphitization at 1025 F for periods of time extending to 8000 hr. Information on the progress of graphitization in the specimens was obtained by metallographic examination. The data obtained included the number of graphite nodules per unit area (as a measure of nucleation), the average nodule diameter, and the per cent conversion of carbide to graphite—all as functions of time. The evidence generally indicated that the graphitization process, whether occurring in the weld-heat-affected zone or in unaffected parent metal, took place by means of a nucleation and growth mechanism, which envisages a time rate of nucleation.

Introduction

THE following is the final report on the investigation of graphite formation in steel, carried out at Battelle Memorial Institute under the sponsorship of Project No. 29 of the Joint ASTM-ASME Research Committee on the Effect of Temperature on the Properties of Metals. This report summarizes the work done on the project from its initiation, November 1, 1950, to its completion, October 31, 1952.

The objective of the investigation was to obtain information on the following specific points:

1 The relationship, if any, between the aluminum and the nitrogen content of a plain-carbon steel and its susceptibility toward graphitization. In particular, attention was directed toward determining whether aluminum influences susceptibility to graphitization by fixing the nitrogen as aluminum nitride, or whether it is aluminum in solid solution in the ferrite matrix that influences susceptibility.

2 The manner in which chromium acts to increase resistance to graphitization.

3 The effect of normal amounts of manganese and silicon in the steam-pipe steels on the susceptibility of these steels toward graphite formation.

Test Materials

Twelve iron-carbon alloys were prepared in the laboratory from specially purified iron, to which different amounts of aluminum, nitrogen, manganese, silicon, chromium, sulphur, and phosphorus were added in various combinations. The intended composition of the alloy is shown in Table 1.

The iron used for the melting stock was purified by heating 30 hr at 2300 F in carefully dehydrated and deoxidized hydrogen, followed by cooling under similarly treated argon. The treated iron contained 0.003% C, < 0.002% N, < 0.01% Mn, 0.003% P, 0.003% Si, <0.03% Ni, <0.03% Cu, <0.015% Cr, and <0.015% Mo. The other ingredients included: fused chromium, 99.15% pure; electrolytic manganese, 99.96% pure, annealed 16 hr at 1200 F to remove hydrogen; aluminum wire, 99.75% pure; and silicon metal containing 98% Si.

TABLE 1 INTENDED COMPOSITION OF TEST MATERIALS

Alloy	Composition, per cent							
	C	N	Al	Mn	Si	Cr	S	P
1	0.15	..	..	..	..	..	..	..
2	0.15	0.01	..	..	..	..	..	..
3	0.15	..	0.02	..	..	..	..	..
4	0.15	0.01	0.02	..	..	..	..	..
5	0.15	..	..	..	..	0.25	..	..
6	0.15	0.01	..	..	..	0.25	..	..
7	0.15	..	0.02	..	..	0.25	..	..
8	0.15	0.01	0.02	..	..	0.25	..	..
9	0.15	..	..	0.60	0.20	..	0.03	0.02
10	0.15	0.01	..	0.60	0.20	..	0.03	0.02
11	0.15	0.01	0.02	0.60	0.20	..	0.03	0.02
12	0.15	..	0.02	0.60	0.20	..	0.03	0.02

One heat of each alloy was melted and poured into a single ingot weighing 2¾ lb, having a diameter of about 1⅛ in. and a length of 4 in. plus a sinkhead. The ingots were slightly tapered.

The melting furnace used was a small high-frequency induction unit enclosed in a gastight, dome-shaped, copper cover. The ingot mold, made of copper, was attached at an angle to the side of the cover with a gastight seal and connected with the crucible by means of a spout. The entire assembly was suitably pivoted about a horizontal axis. The purpose of the arrangement was to provide means of melting metal under a controlled gas atmosphere and pouring it into an ingot mold under the same atmosphere and, at the same time, prevent access of air to the metal until it had solidified in the form of an ingot. This was ac-

[1] Research Engineer, Battelle Memorial Institute.
[2] Division Chief, Battelle Memorial Institute.
[3] Department Manager, Battelle Memorial Institute, Mem. ASME.

Contributed by the ASTM-ASME Committee on the Effect of Temperature on the Properties of Metals and presented at a joint session of the ASTM-ASME Committee on the Effect of Temperature on the Properties of Metals and the Power Division at the Annual Meeting, New York, N. Y., November 29–December 4, 1953, of THE AMERICAN SOCIETY OF MECHANICAL ENGINEERS.

NOTE: Statements and opinions advanced in papers are to be understood as individual expressions of their authors and not those of the Society. Manuscript received at ASME Headquarters, October 9, 1953. Paper No. 53—A-153.

complished by melting in the crucible and then, when the melting campaign was complete, tipping the assembly on its horizontal pivot to make the metal run along the spout into the mold.

Melting was done in a beryllium-oxide crucible. The hot top for the ingot mold was made of zirconia.

The melting practice used initially involved flushing the melting-furnace assembly with carefully dehydrated and deoxidized argon for 2 hr before making the heat, melting under the same atmosphere, and then flushing again with argon for about 2 hr after casting. Nitrogen was added as calcium cyanamide to those melts requiring it.

The first few ingots made were gassy and, therefore, were discarded. This condition was corrected by preheating the assembly and flushing out the system with argon for an extended period before melting. Shortly thereafter, the casing which attached the mold to the cover was burned through by metal which leaked between the mold and the hot top, when the ingot was poured. This was overcome by fastening the hot top to the mold with core paste.

Chemical analysis of those heats which were supposed to contain considerable nitrogen gave nitrogen contents ranging from 0.002 to 0.004 per cent for all but one. These heats were remelted in an effort to obtain higher nitrogen contents. This time the metal was melted under dry nitrogen instead of argon. No calcium-cyanamide addition was made. Instead, it was intended that the nitrogen be introduced into the melt by absorption from the overlying nitrogen atmosphere. This melting technique was more successful.

The compositions of the heats finally used in this investigation are given in Table 2. It is seen from comparison of Tables 1 and 2 that the actual aluminum and nitrogen contents frequently failed to approximate the intended percentages. These elements were found to be extremely difficult to control. It was disappointing that an extra low-nitrogen low-aluminum heat could not be made. However, the series of heats gave numerous combinations of Al, N, Cr, Mn, Si, S, and P contents which could be expected to permit deductions to be made on the influence of most of these elements on the graphitization process.

Each ingot was hot-forged to a $^{5}/_{8}$-in-square bar. Two $5^{1}/_{2}$-in. lengths were then cut from each bar. One of these lengths was normalized at 1700 F, while the other length was water-quenched from 1360 F, a temperature estimated to be just above the lower critical point of the steels. In this way, each composition would be tested for susceptibility to graphitization in two conditions of heat-treatment. The first condition duplicated a heat-treatment considered, from the results of other laboratory investigations as well as from field tests (1, 2, 3, 4)[4] to retard or inhibit graphite formation—in particular, the formation of concentrations of graphite near the low-temperature edge of the heat-affected zones of welds. The second heat-treatment was designed to simulate the thermal conditions experienced by metal at the low-temperature edge of a weld-heat-affected zone, a region often observed to be especially susceptible to graphitization (5, 6). Thus it was thought that these two heat-treatments might be especially effective in influencing the graphitization process.

TABLE 2 COMPOSITION OF TEST MATERIALS

Heat	Composition, per cent							
	C	N	Al[a]	Mn	Si	Cr	S	P
1	0.23	0.033	0.010	..	..	..	..	..
2	0.19	0.032	0.009	..	..	..	..	..
3	0.19	0.001	0.030	..	..	..	..	..
4	0.18	0.003	0.060	..	..	0.02	..	..
5	0.24	0.002	0.005	..	..	0.24	..	..
6	0.20	0.024	0.011	..	..	0.25[b]	..	..
7	0.18	0.026	0.008	..	..	0.20	..	..
8	0.19	0.002	0.034	..	..	0.23	..	..
9	0.17	0.002	0.020	0.68	0.24	..	0.046	0.023
10	0.19	0.002	0.011	0.69	0.25	..	0.042	0.023
11	0.20	0.031	0.010	0.67	0.24	..	0.040	0.022
12	0.19	0.002	0.050	0.62	0.20	..	0.042	0.023

[a] Total residual aluminum obtained by spectrographic analysis.
[b] Intended composition.

Experimental Procedure

The heat-treated bars of each composition were forwarded to the Crane Company where a bead weld was run along one side of each. The bars were then heated at 1025 F to induce graphitization. Sections of each bar were removed after 100, 500, 1500, 3000, and 8000 hr on test.

These sections were prepared for metallographic examination and an effort was made by means of the microscope to obtain quantitative information on the progress of graphitization in each. Specifically, data were obtained on the degree of conversion of carbon from carbide to graphite, not only in the unaffected parent metal of each specimen, but also in that part of the weld-heat-affected zone of each which lay between the A_{c1} isotherm and the A_{c3} isotherm. The results of other studies of graphitization in welded steels indicate that, if localized concentrations of graphite occur in weld-heat-affected metal, they will usually be found within this region. Graphite formation also occurred in the zone between the A_{c3} isotherm and the weld line, but its occurrence was too haphazard to permit reduction to quantitative terms.

The information on conversion was obtained by comparison of the microstructures of the specimens with a specially prepared comparison chart.

In addition, the number of graphite nodules per unit of area was determined both for the unaffected parent metal and for the heat-affected zone lying between the A_{c1} and A_{c3} isotherms. The unit area used was 0.00028 sq in. It was considered, from the form assumed by the graphite, that the number of graphite nodules observed would very likely be equivalent to the number of graphite nuclei formed. In other words, it was considered that little, if any, coalescence of graphite nodules had occurred during the course of graphitization. However, it was recognized that a type of coalescence could and probably did, in some cases, take place. This type would involve the disappearance of some of the smaller nodules, the carbon therefrom depositing on the larger ones.

Finally, the average diameter of the graphite nodules found in the parent metal and in the region of the heat-affected zone between the A_{c1} and A_{c3} isotherms was measured with the microscope.

Results and Discussion

The results of the graphitization tests of the twelve experimental steels are summarized in Table 3 and shown graphically in Figs. 1 through 10.

[4] Numbers in parentheses refer to the Bibliography at the end of the paper.

TABLE 3 RESULTS OF EXAMINATION OF THE TEST MATERIALS

Heat	Weld-Heat-Affected Parent Metal		Unaffected Parent Metal		Nitrogen, %	Aluminum, %	Chromium, %
	Maximum Conversion of Carbide to Graphite	Incubation Period, hours	Maximum Conversion of Carbide to Graphite	Incubation Period, hours			
1A(1)	0%	–	0%	–	0.033	0.010	–
1B(2)	0%	–	0%	–	0.033	0.010	–
2A	0%	–	0%	–	0.032	0.009	–
2B	0%	–	0%	–	0.032	0.009	–
3A	100% at 1500 hours	None*	92% at 8000 hours	None*	0.001	0.030	–
3B	100% at 1500 hours	None*	90% at 8000 hours	None*	0.001	0.030	–
4A	100% at 8000 hours	None*	90% at 8000 hours	None*	0.003	0.060	0.02
4B	100% at 8000 hours	None*	90% at 8000 hours	None*	0.003	0.060	0.02
5A	78% at 8000 hours	100	60% at 8000 hours	500	0.002	0.005	0.24
5B	40% at 8000 hours	1500	60% at 8000 hours	500	0.002	0.005	0.24
6A	70% at 8000 hours	1500	40% at 8000 hours	1500	0.024	0.011	0.25
6B	80% at 8000 hours	1500	80% at 8000 hours	500	0.024	0.011	0.25
7A	90% at 8000 hours	500	60% at 8000 hours	1500	0.026	0.008	0.20
7B	90% at 8000 hours	500	79% at 8000 hours	500	0.026	0.008	0.20
8A	60% at 8000 hours	100	65% at 8000 hours	100(3)	0.002	0.034	0.23
8B	50% at 8000 hours	100	60% at 8000 hours	100	0.002	0.034	0.23
9A(4)	43% at 8000 hours	500	30% at 8000 hours	1500	0.002	0.020	–
9B(4)	68% at 8000 hours	500	66% at 8000 hours	100	0.002	0.020	–
10A(4)	70% at 8000 hours	500	72% at 8000 hours	500	0.002	0.011	–
10B(4)	50% at 8000 hours	500	83% at 8000 hours	100	0.002	0.011	–
11A(4)	0% at 8000 hours	–	30% at 8000 hours	(5)	0.031	0.010	–
11B(4)	20% at 8000 hours	3000	71% at 8000 hours	500	0.031	0.010	–
12A(4)	80% at 8000 hours	100	82% at 8000 hours	100	0.002	0.050	–
12B(4)	70% at 8000 hours	100	70% at 8000 hours	100	0.002	0.050	–

(1) A – Normalized at 1700 F.
(2) B – Water quenched from 1360 F.
(3) 1% conversion.
(4) These heats also contained Mn, Si, S and P.
(5) The data suggest that it is more than 500 hours, but less than 1500 hours.

* i.e., less than 100 hours.

Examination of Figs. 1 through 10 shows a few cases where the data on nodule number and nodule size for an individual heat seem obviously inconsistent among themselves. For example, nodule size for heat 3, both in the unaffected parent metal and in the A_{c1}–A_{c3} region, decreased when the time at temperature became very long; nodule number in the A_{c1}–A_{c3} region of heat 3 decreased considerably as exposure time became prolonged, even though the spacing of the nodules made it difficult to visualize their coalescence. Growth of the larger nodules, however, may have taken place at the expense of some of the smaller ones. Likewise, for heat 4 as water-quenched from 1360 F, nodule number in the unaffected parent metal decreased with increase in time at temperature. This occurred in spite of the fact that nodule size appeared to be practically constant regardless of exposure time. Again, in the A_{c1}–A_{c3} region of the normalized specimens of heat 4, the data on nodule number and nodule size were extremely erratic from specimen to specimen. In fact, no attempt was made to draw a curve through the nodule-number data. For heat 8 in the normalized condition, nodule number in the unaffected parent metal tended to decrease after long exposure times, even though nodule size remained virtually constant.

These inconsistencies may be indicative of deficiencies inherent in attempts to obtain data of this type on a quantitative basis by metallographic methods. They may reflect a certain degree of probability that the polished section examined is not truly representative of the entire specimen. In general, the determinations were made on one polished section per specimen, except where inconsistencies were observed. In these cases, the specimen was reground and polished and the determinations repeated. However, the inconsistencies tended to persist, which opens the possibility of inconsistent or unexplainable behavior by the entire specimen.

Several of the curves of graphite-nodule size versus time at temperature showed this factor to be constant or to tend to become constant with time. It is not believed that such indications can be taken to mean that growth of the nodules had stopped. The nodules cannot be thought of as dense spheres expanding in size equally in all directions as carbon atoms are uniformly deposited on the surface. Rather, the nodules are actually extremely irregular in contour and encompass a large proportion of space not filled with carbon as they grow. It is probable that in reality this space is being filled in during periods when it seems, from over-all diameter measurements, that the nodules are not growing.

Unaffected Parent Metal. For convenience, the results obtained for the unaffected parent metal of the various test materials will be discussed separately from those obtained for the A_{c1}–A_{c3} region of the weld-heat-affected zone.

Heats 1 and 2 did not graphitize even after 8000 hr on test. They were similar in composition; both contained substantially more nitrogen than aluminum.

Heats 3 and 4 differed in composition from heats 1 and 2 principally in that both contained minimum amounts of nitrogen and comparatively large amounts of aluminum. These two heats graphitized the most readily of the entire group of test materials. Both showed about 90 per cent conversion after 8000 hr on test. In neither heat did the graphitization process appear to have an incubation period nor could effects of prior heat-treatment be discerned. If nodule number can be considered equivalent to the number of nuclei present, then both heats showed a nucleation process proceeding with time at temperature, as a component of

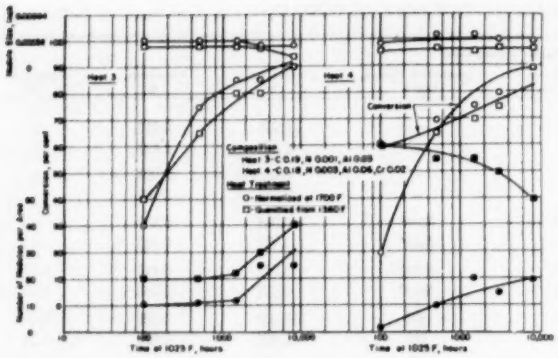

FIG. 1 GRAPHITIZATION OF THE UNAFFECTED PARENT METAL OF HEATS 3 AND 4

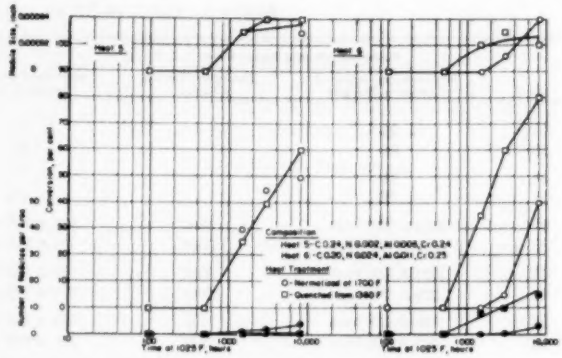

FIG. 2 GRAPHITIZATION OF THE UNAFFECTED PARENT METAL OF HEATS 5 AND 6

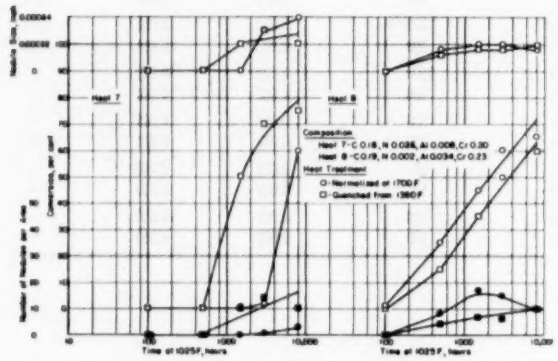

FIG. 3 GRAPHITIZATION OF THE UNAFFECTED PARENT METAL OF HEATS 7 AND 8

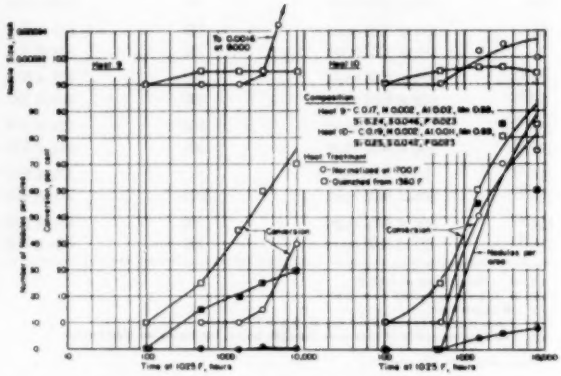

FIG. 4 GRAPHITIZATION OF THE UNAFFECTED PARENT METAL OF HEATS 9 AND 10

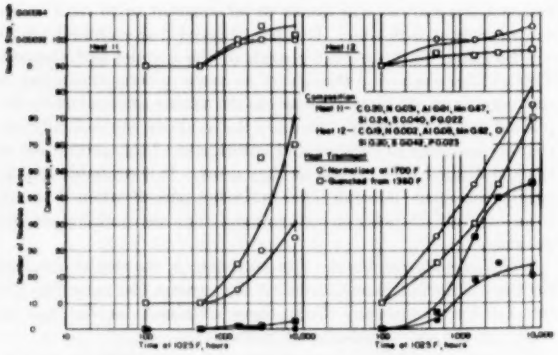

FIG. 5 GRAPHITIZATION OF THE UNAFFECTED PARENT METAL OF HEATS 11 AND 12

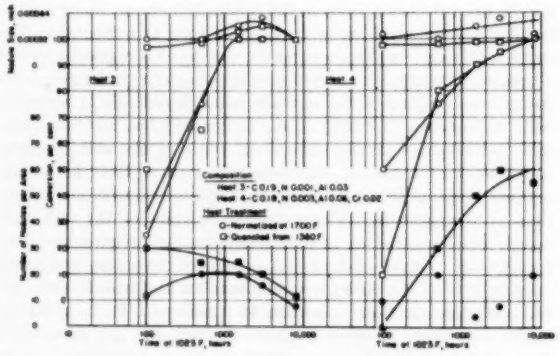

FIG. 6 GRAPHITIZATION IN THE A_{c1}–A_{c3} REGION OF HEATS 3 AND 4

the graphitization process. (As previously mentioned, the nodule-number curve for the specimens of heat 4 quenched from 1360 F seemed anomalous.)

Comparison of the behavior of heats 1 and 2 with heats 3 and 4 suggests that when nitrogen content substantially exceeds aluminum content the steel resists graphitization, but when aluminum content is far in excess of nitrogen content the steel is susceptible to graphitization.

Some confirmation of this observation was found in a graphitization study reported by Wilder and Tyson (7). Among a group of 14 variously melted and deoxidized plain-carbon steels, which had been tested by these authors for periods up to 10,000 hr at 900 F, 1050 F, and 1200 F, only one did not graphitize at least to some extent. This steel was the only one which contained substantial quantities of nitrogen considerably in excess of its aluminum content.

Heat 5 was the first of the series to which $^1/_4$ per cent chromium had been added. In addition, it contained minimum amounts of aluminum and nitrogen. The heat graphitized, attaining a con-

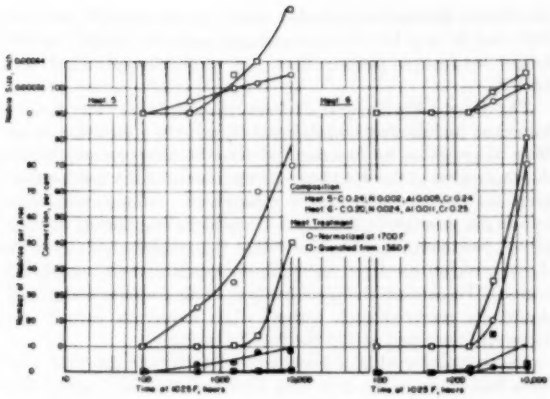

FIG. 7 GRAPHITIZATION IN THE A_{c1}–A_{c3} REGION OF HEATS 5 AND 6

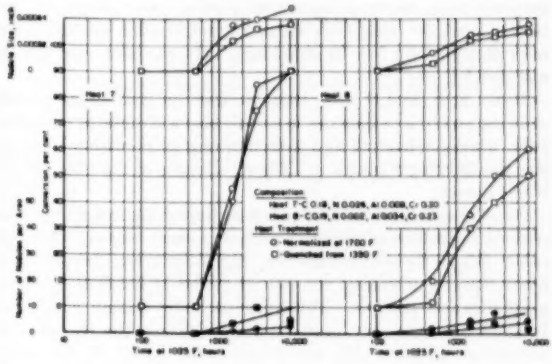

FIG. 8 GRAPHITIZATION IN THE A_{c1}–A_{c3} REGION OF HEATS 7 AND 8

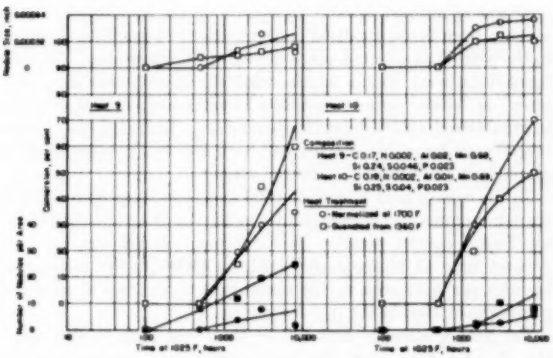

FIG. 9 GRAPHITIZATION IN THE A_{c1}–A_{c3} REGION OF HEATS 9 AND 10

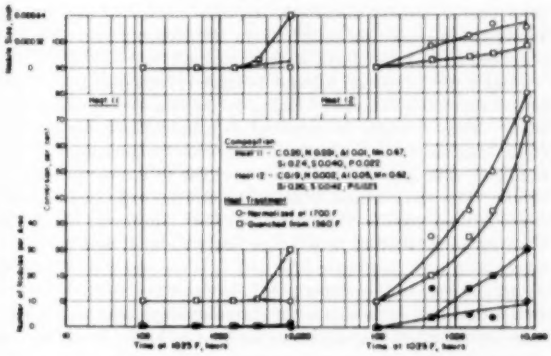

FIG. 10 GRAPHITIZATION IN THE A_{c1}–A_{c3} REGION OF HEATS 11 AND 12

version of about 60 per cent in 8000 hr. The 1/4 per cent chromium addition was definitely insufficient to inhibit graphitization. In this test material the graphitization process had an incubation period of about 500 hr. Graphitization seems to have been accomplished chiefly by nodule growth, the rate of nucleation being low for the normalized specimens and nearly zero for the specimens quenched from 1360 F. The prior heat-treatments, however, seemed to have little influence on the over-all progress of graphitization.

Heats 6 and 7 were similar in composition. Both contained nitrogen substantially in excess of their aluminum content. Like heat 5, they graphitized. The normalized samples of each had an incubation period of about 1500 hr; the specimens of each that were quenched from 1360 F had an incubation period of about 500 hr. Each heat, in both conditions of prior heat-treatment, showed time rates of nucleation and growth.

Heat 8, the last of the series to which chromium had been added, contained a minimum of nitrogen but was high in aluminum content. It graphitized readily, showing an incubation period of about 100 hr. Little difference was observed between the set of specimens normalized before test and the set quenched from 1360 F before test, except for the seemingly anomalous downward turn of the nodule number versus time curves for the normalized specimens.

It is of interest to compare the results obtained for heats 1 through 8. The major difference in composition between heats 1 and 2, on the one hand, and heats 6 and 7, on the other, seems to be the chromium addition to the latter. Yet heats 6 and 7 graphitized, while heats 1 and 2 did not. This raises the possibility that small additions of chromium actually may promote graphitization, even though chromium is usually thought of as an inhibitor of graphitization. In this connection it may be noted that, in other investigations of the influence of chromium, it has been found that more than 1/2 per cent of this element must be present to insure the graphitization resistance of the steel (8). Graphitization frequently has been observed in steels containing 1/4 per cent chromium (9, 10).

It may be speculated that an element which can control the graphitization process is nitrogen and that when this element is present in sufficient amounts it inhibits graphite formation. However, when it is removed, i.e., by the formation of aluminum nitride when sufficient quantities of aluminum are present, graphitization can occur. Chromium is also a nitride former, and it may be that it is in this capacity that small amounts of chromium may promote graphitization. On the other hand, larger amounts of chromium may inhibit graphite formation by increasing the stability of the carbide phase, since chromium is also a powerful carbide former.

Support for the supposition that nitrogen, when present in more than minimum quantities, can inhibit graphite formation is to be found in an investigation reported by Smith, MacMillan, and Dulis (11). These authors found a rim where the carbides were stable around those samples which had been graphitization-tested in air or in a nitrogen atmosphere. Careful studies of the effect of heating atmospheres showed that penetration of nitrogen from the atmosphere had inhibited graphitization.

The supposition that small additions of chromium promote

graphitization also may explain, at least in part, the graphitization of heat 5. This heat showed graphitization susceptibility even though very low in aluminum. (It was also very low in nitrogen.)

Heats 5, 6, and 7 were characterized by nodule-size curves showing an obvious increase in nodule size with time at temperature, while for heats 3 and 4 (containing no chromium) nodule size was seemingly constant. The significance of this observation is not known.

All of the chromium-bearing heats showed distinct incubation periods regardless of nitrogen and aluminum content. On the other hand, the chromium-free, high-aluminum, low-nitrogen heats thus far discussed showed no period of incubation in the graphitization process. This suggests that, though chromium in small amounts may promote graphitization, the 1/4 per cent chromium addition did not produce the effect of the high-aluminum additions.

It was also of interest to note that in only the high-nitrogen heats, among the chromium-bearing series, was an effect due to prior heat-treatment discerned. In these heats, the normalizing treatment increased the length of the incubation period over that observed for the specimens water-quenched from 1360 F.

Heat 8 was of special interest because it combined the 1/4 per cent chromium addition with high-aluminum and low-nitrogen content. Thus it might be expected to behave like heats 3 and 4 (high aluminum, low nitrogen), but with modifications in accordance with any characteristics peculiar to the chromium addition. The observations, in fact, bore out this expectation. Heat 8 graphitized readily like heats 3 and 4. However, instead of showing no incubation period, like heats 3 and 4, or a comparatively long one, like heats 5, 6, and 7, it showed a short one of about 100 hr. In this respect, its behavior was a compromise between that of a high-aluminum chromium-free heat and a low-aluminum, high-nitrogen, chromium-bearing heat. As in the case of heats 3 and 4, prior heat-treatment seemed not to influence the length of the incubation period. Also, like heats 3 and 4, nodule size seemed to become constant with time at temperature.

Heats 9, 10, 11, and 12 are distinguished from the others in that each contained additions of Mn, Si, S, and P, in addition to Al and N. The trends found in the case of the preceding eight heats are not so clearly evident in these four heats, though they are, nevertheless, discernible. For example, heat 11 graphitized even though it contained about the same percentages of aluminum and nitrogen as heats 1 and 2, which did not graphitize. It may be speculated that one of the additional elements, like sulphur, may have promoted graphitization. Sulphides and graphite frequently have been observed in contact with each other in a manner suggesting nucleation of the graphite nodule by the sulphide inclusion. On the other hand, heat 12, which was high in aluminum and low in nitrogen, graphitized readily but, unlike heats 3 and 4, showed a short incubation period. Again, it might be speculated that one of the other additional elements, perhaps manganese, had a retarding influence on the graphitization process.

The normalized specimens of heat 9 showed a condition not observed to the same degree in other heats. Nodule number per unit area was very low, but nodule size became exceptionally large at the end of 8000 hr.

In the case of heats 9, 10, and even 11, the normalized specimens showed incubation periods longer than those observed for the specimens quenched from 1360 F. On the other hand, the results for heat 12 indicated little effect due to prior heat-treatment.

In examining the results for all 12 heats, a tendency was observed for the high-N low-Al heats to have the longer incubation periods generally, while the low-N high-Al heats tended to have the shorter incubation periods. Also, except when Al was very high and N very low, the normalized specimens tended to show longer incubation periods than the specimens quenched from 1360 F.

The A_{c1}–A_{c3} Region of Weld-Heat-Affected Zone. The data obtained on nodule size, nodule number, and the conversion of carbide to graphite, as functions of time at temperature, for the A_{c1}–A_{c3} region of the weld-heat-affected zones of the test heats are given by the curves in Figs. 6 through 10. Though conversion curves are presented, they are not considered significant in themselves, because of the likelihood that the graphite nodules in the A_{c1}–A_{c3} region received carbon from localities well outside this region. To confuse the issue further, these graphite nodules undoubtedly received such carbon while numerous carbide particles still remained within the A_{c1}–A_{c3} region.

Another factor which beclouds the data is that the weld beads were laid down on the test bars after they had been given their pretest heat-treatments. This circumstance arose from the fact that it had not been part of the original plan to study the influence of welding.

It was of interest to note, in examining the specimens, that in no case were dense localized concentrations of graphite observed in the weld-heat-affected zones of any of the specimens. No configurations were found which remotely approached the "eyebrow" or "chain" types of graphite formation sometimes observed in graphitized welded joints in steam lines. In fact, in most cases it could not be said that there had been any real concentration of graphite in the weld-heat-affected zone.

In the case of heat 3, only the 500 and 1500-hr samples showed more numerous and larger nodules in the A_{c1}–A_{c3} zone than in the unaffected parent metal. This difference faded out with increased time at temperature until, at 8000 hr, the number of nodules per unit area in the unaffected parent metal exceeded considerably that in the A_{c1}–A_{c3} region.

For heat 4, after the first 500 hr, there was little to distinguish the A_{c1}–A_{c3} zone over the unaffected parent metal regarding graphitization.

The behavior of heat 5 in the weld-heat-affected zone seemed inconsistent. The specimens quenched from 1360 F showed an incubation period of 1500 hr, while the normalized samples showed an incubation period of 100 hr. Some of this inconsistency may be attributed to difficulty encountered in locating the A_{c1} and A_{c3} isotherms in the metallographic sections of this series of specimens.

In the case of heats 6 and 7, there was little to distinguish the graphitization in the A_{c1}–A_{c3} region from that in the unaffected parent metal. Any effects that might have been attributed to the heat-treatments prior to welding seemed obliterated by the welding operation. In the case of heat 6, the incubation period was the same length as that of the normalized unaffected parent metal. For heat 7, the incubation period was the same as that of the specimens of unaffected parent metal that had been quenched from 1360 F.

The graphitization of heat 8 in the A_{c1}–A_{c3} region was quite similar to that in the unaffected parent metal. The incubation periods for both regions were about 100 hr.

There was little to distinguish the graphitization in the A_{c1}–A_{c3} region of those specimens of heat 9 that had been quenched from 1360 F over that in the unaffected parent metal of the same specimens. However, in the normalized specimens, some apparent concentration of graphite in the A_{c1}–A_{c3} zone occurred. This arose from the extremely low nodule-number count in the unaffected parent metal for this material.

For heat 10, nodule number tended to be less while nodule size tended to be somewhat greater in the A_{c1}–A_{c3} region than in the unaffected parent metal.

In heat 11, graphitization in the A_{c1}–A_{c3} region lagged that in the unaffected parent metal.

In heat 12, graphite in the A_{c1}–A_{c3} region was quite similar to that in the unaffected parent metal.

It appears that generalizations cannot be made regarding most aspects of the graphitization process in the A_{c1}–A_{c3} regions of the test materials. However, one observation can be made. Just as in the unaffected parent metal, there was a tendency for those heats high in N and low in Al to have the longer incubation periods while the low-N high-Al heats tended to have the shorter incubation periods. Also, the preponderance of evidence supported the thesis that the graphitization process in the A_{c1}–A_{c3} region takes place by a nucleation and growth mechanism.

Conclusions

It is believed that the following tentative conclusions are justified:

1 High total aluminum content, in the presence of minimum amounts of nitrogen, promoted susceptibility toward graphitization.

2 Nitrogen content, substantially in excess of the total aluminum content, promoted resistance toward graphitization. This was brought about by extension of the incubation period in the graphitization process. In two cases, no graphitization occurred even after 8000 hr on test. Perhaps it could be said that, in these instances, the incubation period exceeded 8000 hr.

3 Additions of 1/4 per cent chromium appeared to promote graphitization, even though chromium in amounts exceeding 1/2 per cent renders steel very resistant to graphitization. The effect of the 1/4 per cent chromium addition, however, was not equivalent to that produced by the high-aluminum additions, and the process had an incubation period when chromium was present.

4 Normalizing at 1700 F prior to the graphitization test tended to increase the incubation period in the graphitization process, except when Al was very high and N was very low. Under the latter conditions, the normalizing treatment was ineffective.

The effect of heat-treatment was not discernible in the weld-heat-affected zones of the test materials, probably because the weld bead had been laid after the heat-treating operation.

5 From the behavior of heats 9, 10, 11, and 12, it was speculated that some of the other elements besides Al, N, and Cr might influence the graphitization process. For example, sulphur might promote it, while manganese might tend to retard it.

6 The graphitization process generally took place by means of a nucleation and growth mechanism both in the A_{c1}–A_{c3} region of the weld-heat-affected zone of the test materials and in the unaffected parent metal. This mechanism usually seemed to involve a time rate of nucleation.

BIBLIOGRAPHY

1 "The Effect of Normalizing on the Properties of Welds in Carbon-Molybdenum Steel Pipe," by I. A. Rohrig, D. H. Corey, and Sabin Crocker, *Welding Journal*, vol. 22, Welding Research Supplement, October, 1943, pp. 521S–527S.

2 "Investigation of Graphitization at Detroit," by R. M. Van Duzer, Jr., I. A. Rohrig, and A. McCutchan, Trans. ASME, vol. 67, 1945; special pamphlet, "Graphitization of Steel Piping" in back of volume, pp. 57–63.

3 "Influence of Postweld Heat-Treatment on Graphitization," by I. A. Rohrig and A. McCutchan, Trans. ASME, vol. 69, 1947; special pamphlet, "Graphitization of Steel Piping," in back of volume, pp. 47–51.

4 "Report on Graphitization Studies on High-Temperature Welded Piping of the Philadelphia Electric Company," by J. B. Abele and A. E. White, Trans. ASME, vol. 72, 1950, pp. 37–52.

5 "Progress Report No. 1 on Survey of Graphitization of Piping," Edison Electric Institute Bulletin 11, 1943, pp. 307-308, 318.

6 "Carbide Instability of Carbon-Molybdenum Steel Piping," by R. W. Emerson, Trans. ASME, vol. 66, 1944 (special pamphlet, "Graphitization of Steel Piping," in back of volume, pp. 5–15.

7 "Graphitization of Steel at Elevated Temperatures," by A. B Wilder and J. D. Tyson, Trans. ASM, vol. 40, 1948, pp. 233–262.

8 "Studies on Susceptibility of Casting Steels to Graphitization," by J. J. Kanter and E. A. Sticha, Trans. ASME, vol. 69, 1947; (special pamphlet at back of volume), pp. 1–5.

9 "Comparative Graphitization of Some Low-Carbon Steels With and Without Molybdenum and Chromium," by G. V. Smith, S. H. Brambir, and W. G. Bens, Trans. ASME, vol. 68, 1946, pp. 589–595.

10 "Continuation of Joint EEI-AEIC Investigation on Graphitization of Piping," by S. L. Hoyt and A. M. Hall, Trans. ASME, vol. 69, 1947 (special pamphlet), pp. 39–46.

11 "Some Aspects of Graphitization in Steel," by G. V. Smith, J. A. MacMillan, and E. J. Dulis, Trans. ASM, vol. 43, 1951, pp. 692–717.

Discussion

Floyd Brown.[8] The effects of third elements on the graphitization of carbide is of particular importance in the manufacture of the various cast irons. It is always interesting to compare the results of investigations on graphitization in steel, which has been actively studied for less than two decades, with the voluminous literature on graphitization in cast iron reaching back to the turn of the century. A study of this literature suggests that only a very few elements are inherent graphitizers, such as copper and nickel (and perhaps a few of the noble metals), and that most elements act as if they are graphitizers because they are, in fact, scavengers of other elements which are strong carbide stabilizers. The following are observations on cast irons related to the subject paper:

1 Wüst observed that in small quantities aluminum in cast iron increased the tendency for carbon to exist as graphite rather than as carbide, although in larger quantities the effect reversed and aluminum appeared to behave as an intrinsic stabilizer of carbide.[6]

2 Nitrogen has been shown to stabilize graphitization in various cast-iron types, an effect which is counteracted by the addition of aluminum.[7]

3 The behavior which the authors found in steels with chromium contents of about 1/4 per cent is reflected in somewhat similar behavior in cast iron.[8]

4 Both manganese and sulphur are known to be strong carbide stabilizers, and a large segment of the malleable-iron industry hinges in fact upon the tendency of high manganese to stabilize the eutectoid carbide to yield a pearlitic malleable iron, while the remainder of the industry carefully balances the sulphur against the manganese to promote the graphitization of this eutectoid carbide. (The optimum manganese/sulphur ratios for these two purposes were determined with care in the laboratory by Rehder.[9])

5 The coalescence of graphite nodules, which as the authors recognized may have occurred in some instances in steels, has been rather convincingly documented in malleable cast irons.[10]

---

[8] Research Associate Professor of Metallurgy, North Carolina State College, Raleigh, N. C.

[6] "Hochwertiges Gusseisen," data summarized by E. Piwowarsky, J. Springer, Berlin, Germany, 1942, p. 105.

[7] "Some Effects of Nitrogen in Cast Iron," by J. V. Davison, L. W. L. Smith, and B. B. Bach, *Journal of Research and Dev.*, BCIRA, vol. 4, June, 1953, p. 540.

[8] J. W. Donaldson, *Foundry Trade Journal* (quoted by Piwowarsky), Op. cit., p. 738; vol. 40, 1929, p. 489.

[9] "The Effect of Mn/S Ratio on the Rate of Anneal of Blackheart Malleable Iron," by J. E. Rehder, Trans. AFS, vol. 56, 1948, p. 138.

[10] "Kinetics of Graphitization in Cast Iron," by B. F. Brown and M. F. Hawkes, Trans. AFS, vol. 59, 1951, p. 181.

A. B. Wilder.[11] The authors have presented information of a fundamental nature on the graphitization of steel. They have referred to our work on the influence of nitrogen in carbon steel and on graphitization after the steel had been exposed for 10,000 hr at elevated temperatures. We have observed recently that carbon steels not killed with aluminum and containing about 0.015 per cent nitrogen did not graphitize after 34,000 hr exposure at 900 F and 1050 F. Similar steels with 0.005 per cent nitrogen graphitized.

The authors observed that 1/4 per cent chromium appeared to promote graphitization. We believe steel should contain about 1 per cent chromium and then graphitization will be avoided. Although some electric-furnace steels contain about 0.015 per cent nitrogen, which inhibits graphitization, there have been indications that chromium may combine with nitrogen and therefore remove the effectiveness of nitrogen. Under these conditions the effectiveness of chromium as an inhibitor of graphitization would be retarded, and this may explain why small amounts of chromium appear to promote graphitization.

AISI C-1118 steel with 0.16% C, 1.65% Mn, 0.121% S, and 0.047% Al, and AISI C-1137 steel with 0.37% C, 1.51% Mn, 0.129% S, and 0.023% Al were exposed for 34,000 hr at 900 F and 1050 F. Graphitization was only observed in C-1137 steel. The presence of sulphur and possibly manganese were responsible for the absence of graphitization in the C-1118 steel. Both steels contained an appreciable amount of aluminum.

[11] Chief Metallurgist, National Tube Division, U. S. Steel Corporation, Pittsburgh, Pa.

Authors' Closure

The authors wish to express their appreciation to Professor Brown and Dr. Wilder for their interesting and valuable discussions. The authors are particularly gratified that additional information was bought out which tends to support their observations regarding the influence of small amounts of chromium.

Dynamic Characteristics of Silicone Rubber

By G. W. PAINTER,[1] ERIE, PA.

The unusual high and low-temperature properties of silicone rubber have made it a desirable materiel for vibration isolators designed for service at temperature extremes. In general, silicone cannot be substituted directly for such elastomers as natural rubber and neoprene in established designs. This lack of interchangeability results principally from the lower tensile strength and the unusual load-deflection characteristics of the material. A program to investigate the dynamic properties of silicone rubber was undertaken to provide the design engineer with information which would allow the material to be utilized properly. This paper deals with the viscoelastic properties of silicone rubber under various conditions of strain, frequency, and temperature. Where possible, comparisons are made with natural rubber.

Viscoelasticity

THE application of sinusoidal deformation to a viscoelastic material results in the generation of a resisting force. If the force-deflection relation is linear, the resisting force is also sinusoidal. The presence of internal friction causes a phase difference between the force and the deformation. The total force can be represented as a vector which can be resolved into two components, one in phase with the strain and one 90 deg out of phase. We shall refer to these forces as elastic and viscous components. The relationship between the total force and its components is shown in Fig. 1 where F_T, F_E, and F_V represent the total force and its elastic and viscous components, respectively.

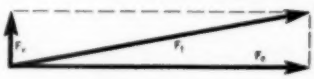

Fig. 1 Relationship Between Total Force and Its Components

The magnitude of the components of force depends upon the amplitude of deflection, the shape and size of the test specimen, and the dynamic modulus of the material. The dynamic modulus can best be represented by complex notation. If the complex dynamic shear modulus is represented by G^* and its real and imaginary components by G' and G'', then

$$G^* = G' + iG''$$

where $G' = \frac{F_E q}{X}$, $G'' = \frac{F_V q}{X}$

X = amplitude of deflection, in.

q = shape factor dependent on size and shape of test specimen, 1 per in.

Letting $|G^*|$ represent the absolute value of dynamic shear modulus, we have

$$|G^*| = \sqrt{(G')^2 + (G'')^2}$$

It will be shown that the apparatus used in this work allows $|G^*|$ and G'' to be measured directly. G' is then calculated.

Test Equipment

The dynamic modulus of elastomers has been measured by a wide variety of methods (1–7).[2] The investigators naturally have designed their apparatus to explore the variation of modulus over a specific range of test conditions in which they had particular interest. As a result, some machines are well-suited to cover a very wide frequency at very low amplitude, and others cover a limited frequency range but allow considerable amplitude variation. The equipment employed in the present case was designed to measure the modulus of elastomers under conditions of strain, temperature, and frequency which are of particular interest to the designer of vibration isolators. Particular emphasis has been placed on the precision of measurement, simplicity and speed of operation, and flexibility to allow measurements to be made throughout a variety of test conditions. A description of an early version of the testing machine has been given by the author (8) in an earlier paper to which the reader is referred for details of the testing method not reported here.

The test apparatus consists of three functional divisions:

1 A flexometer which deflects the test specimen through the desired amplitude.

2 Two strain-gage pickups and a steel-beam spring for producing electrical signals proportional to $|G^*|$ and G''.

3 An amplifier-voltmeter circuit which amplifies and measures the signal produced by the pickups.

The force-sensing part of the apparatus is shown in Fig. 2. Each of the pickups consists of a thin-walled steel tube with two strain gages cemented on longitudinally and opposite to each other. The four gages make up four arms of a Wheatstone bridge excited by a 2000-cycle carrier current. When force is applied to the end of either pickup, one gage will be placed in tension and the opposite one in compression. Bridge connections are so made that the electrical signals produced by the two gages on a given pickup will be added.

The machine is calibrated by placing a steel ball between the lower pickup and a previously calibrated steel-beam spring which passes above it. The steel spring is attached to the oscillating platen, and the signal which the spring generates in the lower pickup is proportional to the amplitude of motion and the stiffness of the spring. The electric circuit is then calibrated by adjusting an amplifier-gain control until the voltmeter reading is equal to $Kq \times 10^{-3}$, where K = spring rate of beam spring, lb per in., and q = shape factor applicable to test specimen to be used, 1 per in.

This method of calibration allows the operator to read $|G^*|$ directly when the ball is removed and the test specimen is attached to the lower pickup and deflected through the same amplitude. During calibration and during the measurement of $|G^*|$, the upper pickup is not subjected to any force and its strain gages serve as dummy resistors. In measuring G'', the steel ball is placed between the spring and the upper pickup. The upper pickup can be rotated about its longitudinal axis and, since the steel spring has negligible hysteresis, the force

[1] Research Engineer, Lord Manufacturing Company.

Contributed by the Rubber and Plastics Division and presented at the Annual Meeting, New York, N. Y., November 29–December 4, 1953, of The American Society of Mechanical Engineers.

Note: Statements and opinions advanced in papers are to be understood as individual expressions of their authors and not those of the Society. Manuscript received at ASME Headquarters, August 6, 1953. Paper No. 53—A-88.

[2] Numbers in parentheses refer to the Bibliography at the end of the paper.

which it applies to the upper pickup is in phase with the platen motion. The electrical signal produced by the gages in the upper pickup will be either in phase or 180 deg out of phase with the signal produced in the lower pickup by the elastic-force component F_E, depending upon the bridge connections. When the upper pickup is rotated, the amplitude of the signal produced by its gages is changed since the position of the gages relative to the neutral strain axis is altered. G' is measured by rotating the upper pickup slowly until a minimum voltmeter reading occurs. This minimum will appear when the signal produced by the upper pickup is exactly equal and opposite to that produced by the F_E-component acting on the lower pickup. Thus the voltmeter reading is proportional to F_V and equals G'.

Range and Precision of Test Equipment

The double amplitude of dynamic deflection is variable from 0 to 0.250 in., although 0.004 in. ordinarily represents the lowest amplitude at which G' can be measured accurately. Except for the results given in Fig. 10, in which dynamic strain was varied, a dynamic double amplitude of 0.01 in. (0.02 in. per in. dynamic strain) has been employed throughout this work.

Tests can be conducted on both shear and compression specimens either bonded or unbonded. When running tests on unbonded specimens it is necessary to supply sufficient precompression to avoid slipping.

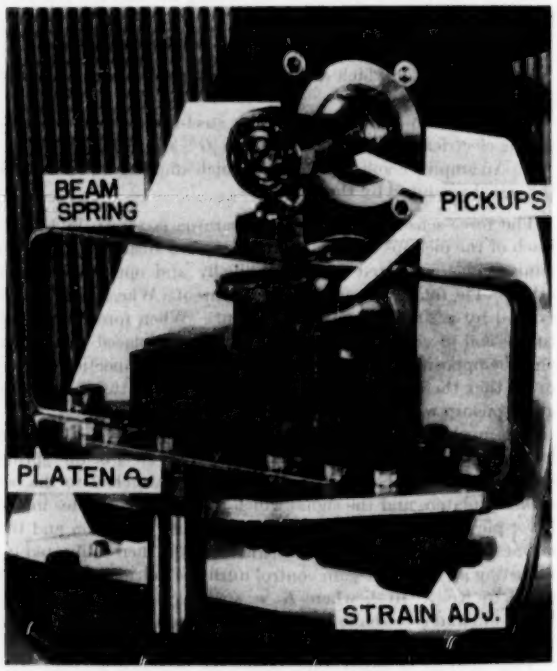

Fig. 2 Force-Sensing Apparatus

Although all of the dynamic shear-modulus results reported here were obtained on the ASTM shear specimen (designed originally for use with the Yerzley oscillograph), it is possible to conduct tests on double or single shear specimens having a shear wall as high as 1 in. or as low as desired. When the ASTM specimen is used, the static deflection across the specimen perpendicular to the direction of shear strain is variable from 0 to 0.5 in. in tension and from 0 to 0.3 in. in compression. The static shear deflection can be varied from 0 to 0.5 in. All of the static-strain adjustments are continuously variable within the given limits and can be made with or without the flexometer in operation by turning a strain-control screw, Fig. 2.

Variable temperature tests employing air as the cooling medium are made by placing a small insulated enclosure over the upper section of the flexometer. Heated or cooled air is supplied to this chamber from an external temperature-control unit. The data reported on the dynamic properties of silicone compounds SE450 and SE550 at very low temperatures were obtained with the test specimen immersed in a bath of isopropyl alcohol and dry ice.

The frequency is ordinarily variable from 15 to 60 cycles per second (cps) although the lower limit could be reduced readily to 3 cps by employing a low-frequency vacuum-tube voltmeter. In this work a Brush Development Company recorder was used to extend the lower frequency limit to 1.6 cps. Except for certain results, given in Fig. 9, all tests were run at 24 cps.

The precision of the machine at room temperature has been checked by allowing two operators to conduct tests independently on 100 test specimens. A statistical analysis of the results indicated no significant difference in the means of the measurements obtained by the two operators and a testing-error coefficient of variation (standard deviation divided by the mean) of less than 1 per cent.

Test Results

The elastomers investigated include silicone-rubber compounds SE450 and SE550 produced by the General Electric Company and a soft natural-rubber compound. The composition of the natural-rubber compound is given in Table 1.

TABLE 1 NATURAL-RUBBER COMPOUND A

Smoked sheet	100
ARP	1.5
Pine tar	2
P-33	10
ZNO	5
Altax	1
Ethyl zimate	0.2
Sulphur	2.5

The curing cycle employed in making the silicone specimens is as follows:

2 hours at 300 F.
2 hours going from 300 F to 400 F.
2 hours at 400 F.
2 hours going from 400 F to 480 F.
24 hours at 480 F.

The natural-rubber compound was cured at 274 F for 45 min.

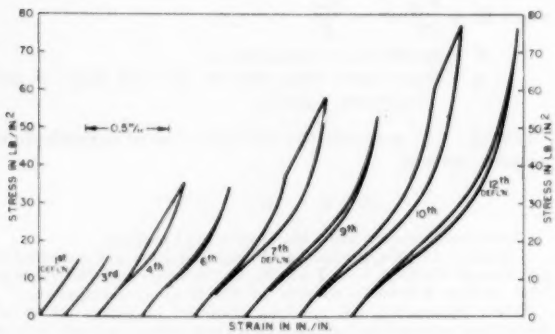

Fig. 3 Effect of Repeated Shear Deformations on Load-Deflection Characteristics

Strain Effects

All elastomers are known to be changed permanently when they are subjected to strain. Quite often the effect of strain upon the viscoelastic properties is so slight that it is of no "practical" importance. The modulus of silicone rubber is markedly changed by strain, however. This phenomenon is shown in Fig. 3 which consists of a series of load-deflection curves obtained by subjecting a specimen made in SE450 to a number of cyclic shear deformations. The testing apparatus employed was a Tate-Emery machine which plots force versus deflection directly. After the completion of each cycle, the curve-tracing pen was shifted along the deflection axis and another force-deflection cycle was traced.

At strains which do not exceed 0.30 in. per in. the material undergoes virtually no change in stiffness. As the degree of

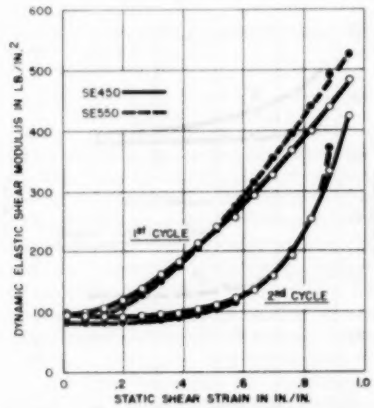

Fig. 4 Variation of Dynamic Elastic Shear Modulus G' With Static Shear Strain

strain is increased further, the load-deflection curve exhibits an abrupt reduction in slope when the strain exceeds the maximum reached in a previous cycle. This behavior probably results from the rupture of various structural bonds either between the polymer and the filler or between the polymer molecules. Nearly all of the bonds can withstand a macro strain of 0.30 in. per in. but more and more of them break as the strain is increased beyond this value. A reduction in stiffness brought about by strain has been noted in natural rubber and neoprene, particularly in compounds employing a high carbon-black content. The structural breakdown in these elastomers is considerably less pronounced than in silicone, however, and the structure tends to rebuild partially if the material is allowed to "rest" for a few days. No recovery of the silicone was noted when the tests were repeated after 10 days. It is possible that a longer period of time might bring about some degree of structural recovery.

Fig. 4, which shows the variation of dynamic elastic shear modulus (G') with static shear strain, indicates that the structural breakdown also is reflected in the dynamic stiffness. The first cycle curves were run on previously undeflected test specimens by subjecting them to an increasing static strain while applying an alternating double-amplitude strain of 0.020 in. per in. After reaching a static strain of approximately 0.95 in per in. the strain was reduced to zero, and the entire cycle was then repeated. The second cycles are seen to exhibit a considerably lower dynamic stiffness. Additional cycles (not shown) gave curves which are practically identical to those obtained during the second cycle.

The variation of modulus with static strain is considerably more pronounced in silicone rubber than in natural rubber.

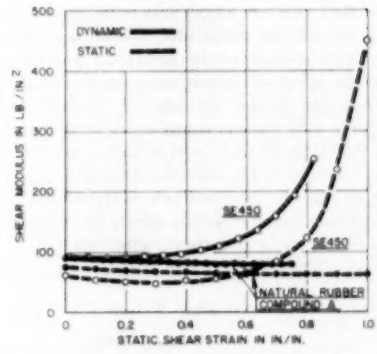

Fig. 5 Variation of Dynamic and Static Shear Modulus With Static Shear Strain

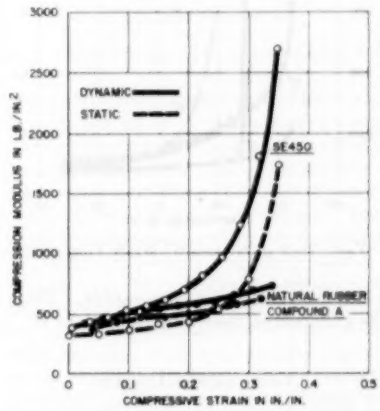

Fig. 6 Variation of Dynamic and Static Compression Modulus With Compressive Strain

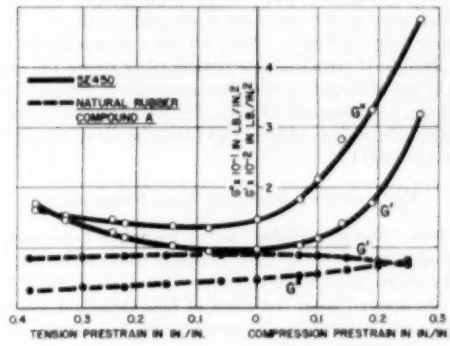

Fig. 7 Effect of Static Compression and Tension Prestrain Applied Perpendicular to Direction of Dynamic Shear Strain

This is shown in Figs. 5, 6, and 7. Fig. 5 demonstrates the effect of shear strain upon both the static and dynamic elastic-shear modulus of compound SE450. Both the static and dynamic moduli experience a sharp rise with increasing strain above 0.50. The static-modulus values were obtained by taking the slope of the static load-deflection curve at various strains. Natural rubber exhibits very little change even at 1 in. per in. strain.

Static and dynamic compression modulus versus static compression-strain curves are given in Fig. 6. The bonded com-

pression specimen used had a load area to bulge area ratio of 0.32. As in Fig. 5, the silicone compound exhibits a greater degree of nonlinearity in its modulus-strain curve than does natural rubber. Fig. 7 shows the effect of tension and compression prestrain, applied perpendicular to the direction of dynamic shear strain, upon the elastic and viscous components of dynamic modulus. Here again, the static strain is seen to have a marked effect upon the dynamic modulus of the silicone compound.

As shown in Fig. 10, the amplitude of dynamic strain (within the dynamic-strain range covered) affects the dynamic-modulus components of silicone and natural rubber similarly. The principal difference shown is the much higher value of the viscous

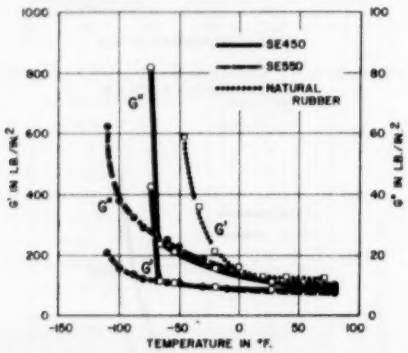

FIG. 8 VARIATION OF G' AND G'' WITH TEMPERATURE

component G'', exhibited by silicone rubber. The curves representing the variation of the elastic component G', are seen to coincide.

TEMPERATURE EFFECTS

The most desirable property which silicone possesses is its maintenance of room-temperature properties over an extended temperature range. A comparison between a 45 durometer natural-rubber compound and silicone compounds SE450 and SE550 in regard to the variation of dynamic modulus with temperature is given in Fig. 8. Both silicone compounds are seen to remain flexible at temperatures considerably below the point at which the natural-rubber modulus-temperature curve exhibits a steep slope. Compound SE550, designed especially for low-temperature flexibility, showed but little change in elastic modulus even at —100 F.

VARIATION OF MODULUS WITH FREQUENCY

The term "static modulus" is, of course, a misnomer since static-modulus tests are actually dynamic tests carried out at low velocities of strain. Static-modulus values given here, Figs. 5 and 6, are derived from the slope of load-deflection curves obtained at a strain velocity of approximately 1 in. per in. per minute.

It is interesting to compare the static and dynamic-modulus values of natural-rubber and silicone-rubber compound SE450 given in Fig. 5. The natural-rubber compound is seen to have a higher static modulus but a slightly lower dynamic modulus than compound SE450. This behavior is somewhat clarified by Fig. 9 which shows the variation of the total shear modulus over a frequency range from 96 cpm to 3600 cpm. Throughout most of the frequency range the silicone compound has the higher modulus. At the lower frequency limit the modulus of SE450 falls below that of natural rubber. The relatively flat modulus versus frequency curve shown here should not be interpreted as applying

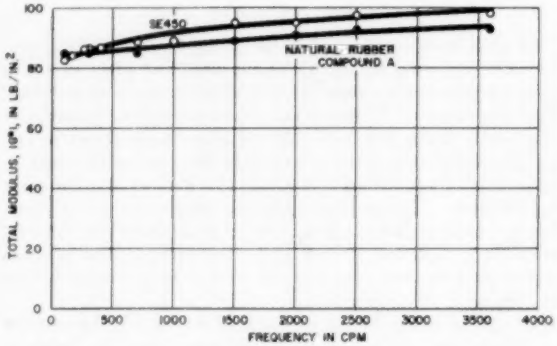

FIG. 9 VARIATION OF TOTAL MODULUS $|G^*|$ WITH FREQUENCY

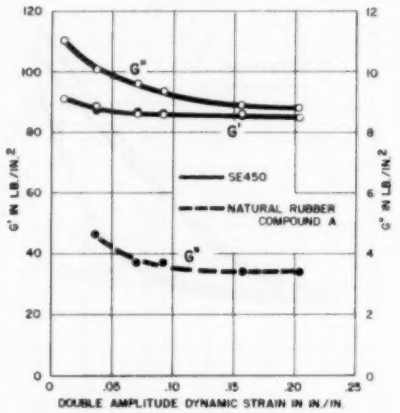

FIG. 10 VARIATION OF G' AND G'' WITH DOUBLE AMPLITUDE OF DYNAMIC STRAIN

to natural-rubber compounds in general. For example, Philippoff, who performed dynamic modulus measurements on both gum and tread natural-rubber compounds, found that the G' of gum rubber was constant from 0.0001 cps to 100 cps. He found a very considerable increase in G' with increasing frequency in tread stocks, however. Natural-rubber compound A contains a carbon loading which is representative of that normally employed in vibration isolators. The effect of frequency shown here is considered to be typical for most isolators made in natural rubber.

SUMMARY

A dynamic modulus-testing machine having considerable flexibility and high efficiency of operation has been described. Comparisons between the viscoelastic properties of silicone rubber and natural rubber have been made at various conditions of strain, temperature, and frequency.

The excellent low-temperature properties of silicone rubber provide the vibration-isolator designer with a material which will allow the isolator to function properly at —100 F. Although the modulus of the material is affected considerably more by static strain than is natural rubber, provision for this characteristic can be made in design.

BIBLIOGRAPHY

1 "Dynamic Evaluation of Damping and Durability of Rubber Compounds," by H. Roelig, Rubber Technology Conference, London.

England, 1938, pp. 821–829; *Rubber, Chemistry and Technology*, vol. 12, 1939, pp. 394–400.

2 "Dynamic Properties of Rubber; Dependence on Pigment Loading," by S. D. Gehman, D. E. Woodford, and R. B. Stambaugh, *Industrial and Engineering Chemistry*, vol. 33, 1941, pp. 1032–1038.

3 "Hysteretic and Elastic Properties of Rubber-Like Materials Under Dynamic Shear Stresses," by J. H. Dillon, I. B. Prettyman, and G. L. Hall, *Journal of Applied Physics*, vol. 15, 1944, pp. 309–323.

4 "Methods for Measuring Dynamic Mechanical Properties of Rubber-Like Materials," by A. W. Nolle, *Journal of Applied Physics*, vol. 19, 1948, pp. 753–774.

5 "Measurement of the Dynamic Properties of Rubber," by W. P. Fletcher and A. N. Gent, Trans. Institution of the Rubber Industry, vol. 26, 1950, pp. 45–63.

6 "Measurements of Mechanical Properties of Polyisobutylene at Audiofrequencies by a Twin Transducer," by R. S. Marvin, E. R. Fitzgerald, and J. D. Ferry, *Journal of Applied Physics*, vol. 21, 1950, pp. 197–203.

7 "Mechanical Investigations of Elastomers in a Wide Range of Frequencies," by W. Philippoff, *Journal of Applied Physics*, vol. 24, 1953, pp. 685–689.

8 "The Measurement of the Dynamic Modulus of Elastomers by a Vector Subtraction Method," by G. W. Painter, ASTM Bulletin No. 177, October, 1951, pp. 45–47.

Discussion

S. D. Gehman.[3] As stated in the introduction it is quite true that a linear viscoelastic system will respond to a sinusoidal strain with a sinusoidal resisting force. But the system under study is not strictly linear. Since the calculations assume a sinusoidal response, the question may be raised as to whether this invalidates any of the work. Apparently it does not. Rubber compounds which show a very pronounced nonlinearity when the dynamic properties are measured as a function of amplitude, still give a response at any one amplitude which is practically free of harmonic content. In fact, a train of free oscillations of a rubber-mass system also does not betray the nonlinearity of the system. It appears as if rubber assumes a different temporary equilibrium molecular structure corresponding to each amplitude of vibration. This structure responds in a sinusoidal way. But if the amplitude is changed, the system can be shown to be nonlinear. For the train of free vibrations, the "structural memory" from the first vibration appears to be sufficient to obscure the nonlinearity even though the amplitude changes.

The calibration procedure assumes that the steel spring and ball move in phase with the platen. This requirement is met only if the natural frequency of the system is large compared to the driving frequency. Although this condition is no doubt realized, it would be reassuring if the frequency of the spring-and-ball combination were given.

The relatively high stiffening temperature shown for natural rubber in Fig. 8 of the paper is noteworthy. A "static" test undoubtedly would give a much lower stiffening point. Thus, as the temperature is lowered, the dynamic properties are impaired first. Rubber loses the ability to respond to rapid forces in a rubber-like way long before there is any serious stiffening apparent in a conventional modulus test. The curve for G'' for natural rubber is not included on the graph, but, as with the silicone rubbers, G'' for natural rubber is more sensitive to temperature than is G'.

It is unfortunate that studies such as this must be made with silicone rubbers having unspecified filler contents. Undoubtedly the filler is largely responsible for many features of the results. The statement in the summary that the viscoelastic properties of silicone rubber have been compared with those of natural rubber must be construed to take this situation into account.

[3] The Goodyear Tire & Rubber Company, Akron, Ohio.

Author's Closure

The author wishes to thank Dr. Gehman for his excellent discussion.

The accuracy of the test method would be adversely affected by the presence of nonlinearities. This was discussed at some length by the author in an earlier paper. The effect of nonlinearity has been investigated by employing a wave analyzer to measure the magnitude of higher harmonics of force. These harmonics have been found to be negligibly small except in cases where the modulus was measured under conditions where the stress-strain curve exhibited a rapidly changing slope. For example, it would not be advisable to attempt to measure the internal-friction component under the conditions described in Fig. 6 except at very low amplitudes of dynamic strain.

The natural frequency of the steel spring is approximately 400 cps. Since the maximum frequency of the machine is 60 cps, there is no possibility that the spring and platen will be out of phase.

The author does not mean to imply that this paper provides a general comparison between the dynamic properties of natural rubber and silicone. Dr. Gehman (2) and others (3 to 5) have shown that the type and amount of filler used in natural rubber has a marked effect upon the dynamic characteristics. The natural-rubber compound investigated in the present work was chosen as a typical stock having about the same stiffness as the silicone compounds. The information obtained is considered to be representative of soft natural rubber and silicone compounds.

Synthesis of the Four-Bar Mechanism When the Position of Two Members Is Prescribed

By B. W. SHAFFER[1] and I. COCHIN,[2] NEW YORK, N. Y.

The four-bar mechanism is analyzed, and a differential equation is derived which tells whether or not it is possible to find a particular design in which the position of the driver and follower are related by a prescribed function during the entire range of operation. If there is such a mechanism, the length required for each of the links may be found by substituting into the appropriate equations, also derived in this paper.

Introduction

THE problem to be considered in this paper is the design of a four-bar mechanism shown in Fig. 1, in which the position of the follower arm *ut* is to be related to the position of the driving arm *rs*, in a prescribed manner during the entire range of operation. If φ is the angle the driver makes with the fixed link, and γ is the angle the follower makes with the fixed link, then the relationship between the two, prescribed in advance, is some function

$$\gamma = f(\varphi) \quad [1]$$

Problems of this type have been considered by some recent investigators[3,4] but they were not primarily concerned, as we are in this paper, with finding an exact analytical solution to the problem.

Not all relationships such as Equation [1] can be reproduced exactly by the four-bar mechanism, for if they could, there would be no need for any of the other configurations now being used for similar purposes. It seems reasonable, therefore, to devise a test which would indicate whether or not a prescribed function can be reproduced by some four-bar mechanism. If it passes this test, we know there is such a mechanism and can proceed to find the required design proportions.

We will assume, as is customary with the design of such mechanisms, that the links are rigid. Even though there will be some elastic strain in an actual mechanism, the order of magnitude of the resulting deformations will be very much smaller than the order of magnitude of the actual movement of the links themselves, and, therefore, rigidity of the members is a reasonable assumption.

No restriction will be made, in the development to follow, on the range of the input angle φ. As a result, the method will be equally applicable to a problem in which the driving link is to oscillate through a finite angle, and to the problem in which the driving link is to rotate continually a full revolution.

Development of Required Equations

If one is interested in the relationship between the angles φ and γ, as we are in this problem, it is obvious that once the required design is found it is easy to find an entire family of four-bar mechanisms that will do the same job, by simply enlarging or reducing the original solution. For any one design within this family, there are four unknowns *a*, *b*, *c*, and *d*, corresponding to the length of each of the links shown in Fig. 1.

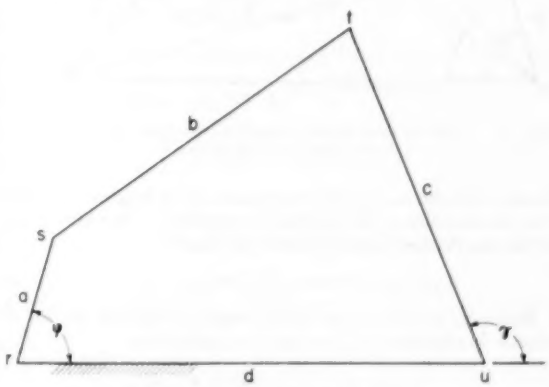

Fig. 1 The Four-Bar Mechanism

This family of designs can be avoided, and at the same time the number of unknowns in the problem can be reduced to three by choosing a scale for which the length of the fixed link is unity, and the lengths of the remaining links are *A*, *B*, and *C*. In terms of the dimensions *a*, *b*, *c*, and *d*, the numerical values *A*, *B*, and *C* also may be thought of as dimensionless ratios *a*/*d*, *b*/*d*, and *c*/*d*, respectively.

Let us examine the geometry of the four-bar mechanism shown in Fig. 2, where the links are shown to be equal to *A*, *B*, *C*, and 1, in order to find an equation relating the position of the output link to the position of the input link. The original mechanism is shown by the solid lines joining the points *r*, *s*, *t*, and *u*, and the construction lines are shown by the dashed lines. Essentially, there are two groups of construction lines which are of interest. The first group was obtained by drawing *tv* parallel and equal to *sr*, and *rv* parallel and equal to *st*. The second group was obtained by drawing lines from *u* to *v*, from *r* to *t*, and from *u* to *s*. These lines are of length *E*, *F*, and *G*, respectively, when the fixed link is equal to unity.

Some of the included angles are also of interest in the analysis, and they have been labeled φ, γ, η, and λ. They will be considered positive when measured in the counterclockwise direction. The input angle, which is, in fact, the independent variable of the mechanism once it is designed, is designated by the letter φ. The output angle is called γ. As stated in the first section, these two angles are to be related by the prescribed function. η is the angle

---

[1] Associate Professor, Mechanical Engineering Department, New York University. Assoc. Mem. ASME.

[2] Research Associate, Mechanical Engineering Department, New York University.

[3] "Analysis of the Four-Bar Mechanism: Its Application to the Synthesis of Mechanisms," by J. A. Hrones and G. L. Nelson, John Wiley & Sons, Inc., New York, N. Y., 1951.

[4] "Computing Mechanisms and Linkages," by V. Svoboda, McGraw-Hill Book Company, Inc., New York, N. Y., 1948.

Contributed by the Machine Design Division and presented at the Annual Meeting, New York, N. Y., November 29–December 4, 1953, of The American Society of Mechanical Engineers.

Note: Statements and opinions advanced in papers are to be understood as individual expressions of their authors and not those of the Society. Manuscript received by Machine Design Division, February 4, 1953, and at ASME Headquarters, September 1, 1953. Paper No. 53—A-144.

vru, equal to the angle link *st* makes with the fixed link, and λ is the angle *utv*, numerically equal to $(\gamma - \varphi)$.

The various lengths and angles shown in Fig. 2 are related to each other by the fact that *rstur* forms a closed loop. This fact

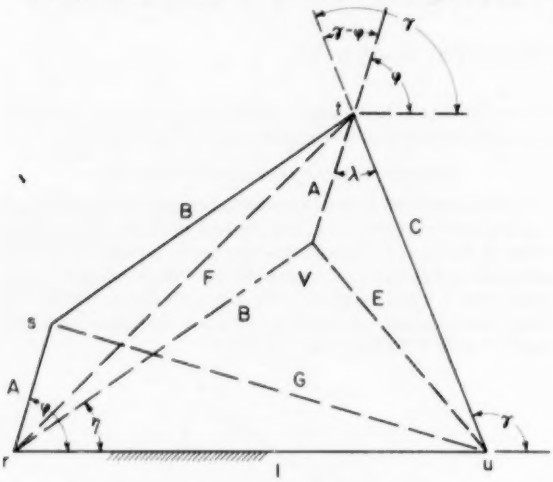

FIG. 2 CONSTRUCTION LINES NEEDED FOR THE DERIVATION OF THE EQUATION OF STATE

implies that the sum of the components of the lengths A, B, and C in the direction of the fixed link is equal to 1. Stated in terms of the lengths and angles described previously

$$A \cos \varphi + B \cos \eta + C \cos (\pi - \gamma) = 1 \quad [2]$$

However, in view of the results found in applying the law of cosines to triangles, *rsu*, *rvu*, and *rtu*, respectively

$$A \cos \varphi = \frac{A^2 + 1 - G^2}{2} \quad [3a]$$

$$B \cos \eta = \frac{B^2 + 1 - E^2}{2} \quad [3b]$$

$$C \cos (\pi - \gamma) = \frac{C^2 + 1 - F^2}{2} \quad [3c]$$

Equation [2] can be written

$$A^2 + B^2 + C^2 + 1 = E^2 + F^2 + G^2 \quad [4]$$

Written in this form, the equation states that the sum of the squares of the sides of the four-bar mechanism is equal to the sum of the squares of the three lines constructed previously.

Should we now apply the law of cosines to triangle *u*, *t*, *v*, we find that

$$E^2 = A^2 + C^2 - 2AC \cos \lambda \quad [5]$$

and in view of Equations [3*c*] and [3*a*], which can be rewritten

$$F^2 = C^2 + 1 - 2C \cos (\pi - \gamma)$$

and

$$G^2 = A^2 + 1 - 2A \cos \varphi$$

Equation [4] can be rewritten

$$B^2 = 1 + A^2 + C^2 - 2A \cos \varphi - 2AC \cos \lambda + 2C \cos \gamma \quad [6]$$

Only the cosine of the angle, not the angle itself, appears in Equation [6]. We find it convenient, therefore, to introduce the identities

$$x = \cos \varphi \quad [7a]$$

$$y = \cos \gamma \quad [7b]$$

$$z = \cos \lambda \quad [7c]$$

into Equation [6], so that it reads

$$B^2 = 1 + A^2 + C^2 - 2Ax - 2ACz + 2Cy \quad [8a]$$

where

$$z = \cos (\gamma - \varphi) = yx + \sqrt{(1 - y^2)(1 - x^2)} \quad [8b]$$

Equation [8] is an equation of state, relating the output angle γ, the input angle φ, and the length of each of the links. This expression is, in fact, the general solution of all functions that will satisfy the requirements of the problem.

It is possible to rewrite this equation of state in many different forms. One of these forms, an explicit equation for y, is found in the Appendix. In general, a given expression may not look exactly like either one of these equations and yet belong to the family of solutions described by the equation of state. One can recognize all such equations by reducing them to one of the recognizable forms, or by noting that all forms of the equation of state must satisfy the same differential equation. The first method may prove cumbersome and time-consuming because in practice it may not represent a straightforward procedure. The latter method, involving the use of a differential equation, is to be preferred.

This differential equation, to be called the compatibility equation, can be found by differentiating Equation [8] three times with respect to the independent variable x. In performing this differentiation, it should be remembered that A, B, and C are constants. The first differentiation, it is found, yields

$$C = \frac{A}{y' - Az'} \quad [9]$$

The second yields

$$A = \frac{y''}{z''} \quad [10]$$

and the third

$$O = \frac{y''z''' - z''y'''}{(y'')^2} \quad [11]$$

Equation [11] is the compatibility equation for the four-bar mechanism. The prime shown with y and z indicates the first derivative with respect to x. Double prime indicates the second derivative, while triple prime indicates the third derivative. The derivatives of y will depend on the prescribed function, written

$$y = g(x) \quad [12]$$

which, in view of Equation [7], corresponds to Equation [1]. The derivatives of z have been evaluated in the Appendix.

DISCUSSION OF RESULTS

It is possible to determine whether or not a four-bar mechanism can be designed in which the position of the driver and follower arm are related by a prescribed function, merely by substituting the given expression into Equation [11]. If this compatibility equation is satisfied, there is a four-bar mechanism that will do the job.

Actually, if one wishes, it is possible to determine whether or not the compatibility equation will be satisfied without having to evaluate the third derivatives, as required in Equation [11], for if a function satisfies Equation [11], it would yield a constant value for A, evaluated in Equation [10], for all numerical values of the independent variable. In some cases it may be easier to check this fact numerically, instead of proceeding with another differentiation.

Once it has been established that the required design exists, the length of the driving link A can be found by substituting the second derivative of the function into Equation [10]. A subsequent substitution into Equation [9] will yield the length C, and then, Equation [8] will yield the length B. Knowing the length of each of these members completes the design of the required mechanism.

It may be found that the compatibility equation is not satisfied for all possible values of x, but only for a finite range of real values, say, $x_1 \leq x \leq x_2$. Should a situation of this type arise, it merely implies that the resulting design will be one in which the input angle will be restricted by the physical design of the mechanism to lie between the corresponding angular limits. A similar situation might arise whenever the numerical approach is used. It also will mean that the mechanism will lock whenever an attempt is made to exceed the bounds on the input angle. Nevertheless, the length of each of the members will still be given by Equations [10], [9], and [8], whenever the appropriate substitution is made.

There are relatively few relationships that can be reproduced exactly by the four-bar mechanism. In fact, the general solution of all the expressions that do is given by Equation [8], or the explicit form Equations [17] of the Appendix.

There are numerous relationships which can only be approximated by the four-bar mechanism. These functions will not satisfy the compatibility equation over an entire range, but will do so at a finite number of points. A physical design may be found corresponding to each of these points, and the resulting approximation may be checked by analysis.

For example, if we set Equation [31] (Appendix) equal to zero, the roots $x_1, x_2, x_3, \ldots$, are points for which the compatibility equation is satisfied. These roots, when introduced into Equations [29], will furnish values for the derivatives $y'(x_1)$, $y'(x_2)$, $y'(x_3)\ldots$, $y''(x_1)$, $y''(x_2)$, $y''(x_3)\ldots$, $y'''(x_1)$, $y'''(x_2)$, $y'''(x_3)\ldots$. For each of these roots we may find a solution for A by making the appropriate substitution into Equation [10]; we may find a solution for C by substituting into Equation [9], and a solution for B by substituting into Equation [8]. The resulting designs should then be checked to see the range for which we get a reasonable approximation to the prescribed function.

This procedure will result in a good but not necessarily the best approximation. Problems of this type are beyond the scope of this paper, but will be considered in a future publication.

Conclusions

Not only is it possible to tell whether a four-bar mechanism can be designed in which the position of the driver and follower are related by a prescribed function, but if it can, then it is possible to find, by analytical means, the required design proportions.

Appendix

The Explicit Equation of State

Recall that in Equation [8a] $B^2 = 1 + A^2 + C^2 - 2Ax - 2ACz + 2Cy$ and that in Equation [8b], $z = yx + \sqrt{(1-y^2)(1-x^2)}$. Solving Equation [8a] for z

$$z = \frac{y}{A} - \frac{x}{C} + \frac{K}{2AC} \quad [13a]$$

where

$$K = A^2 - B^2 + C^2 + 1 \quad [13b]$$

Then, equate Equation [8b] and Equation [13a], rearrange terms, and square, to find

$$\left[\frac{y}{A} - \frac{x}{C} + \frac{K}{2AC} - yx\right]^2 = (1-x^2)(1-y^2) \quad [14]$$

If we define

$$\left.\begin{aligned} H &= 2C(1 - Ax) \\ I &= 4A^2C^2 \\ J &= K - 2Ax \end{aligned}\right\} \quad [15a]$$

Equation [14] can be rewritten

$$(Hy + J)^2 = (1-x^2)(1-y^2)(I) \quad [15b]$$

Expand and collect equal powers of y

$$(H^2 + I - Ix^2)y^2 + (2HJ)y + (J^2 - I + Ix^2) = 0 \quad [16]$$

so that we can solve, and find

$$y = \frac{-2A^2x^2 + A(K+2)x - K + AL}{-4ACx + 2C(A^2+1)} \quad [17a]$$

where

$$L^2 = (1-x^2)[-4A^2x^2 + 4A(K - 2C^2)x + 4C^2(A^2+1) - K^2] \quad [17b]$$

$$K = A^2 - B^2 + C^2 + 1 \quad [13b]$$

Derivatives of z

Recall from Equation [8b] that

$$z = yx + \sqrt{(1-y^2)(1-x^2)}$$

and let

$$a = \left[\frac{1-y^2}{1-x^2}\right]^{1/2} \quad [18]$$

so that Equation [8b] will read

$$z = yx + a(1-x^2) \quad [19]$$

The first derivative is found to be

$$z' = y + y'x + a'(1-x^2) - 2ax \quad [20]$$

where, in view of Equation [18]

$$a' = \frac{ax}{1-x^2} - \frac{yy'}{a(1-x^2)} \quad [21]$$

This equation can be put in the simpler form

$$z' = y + y'x - ax - \frac{yy'}{a} \quad [22]$$

by combining Equations [20] and [21]. Another differentiation yields

$$z'' = 2y' + xy'' - a - xa' - \frac{yy''}{a} - \frac{y'^2}{a} + \frac{yy'a'}{a^2} \quad [23]$$

and a third yields

$$z''' = -2a' - za'' + 3y'' + xy''' - \frac{3y'y''}{a} - \frac{yy'''}{a} + \frac{yy'a''}{a^2} + \frac{2y'^2a'}{a^2} + \frac{2yy''a'}{a^2} - \frac{2yy'a'^2}{a^3} \quad [24]$$

where, in view of Equation [21]

$$a'' = \frac{a + a'x + ax^2 - a'x^2}{(1 - x^2)^2} - \frac{yy'' + y'^2}{a(1 - x^2)} + \frac{yy'(a' - 2ax - a'x^2)}{a^2(1 - x^2)} \quad [25]$$

Illustrative Examples

(*a*) Consider the design of a four-bar mechanism where

$$\gamma = \pi - 2\varphi \quad [26]$$

For such a relationship

$$\cos \gamma = \cos (\pi - 2\varphi) \quad [27]$$

and, in view of the notation indicated in Equation [7]

$$y = 1 - 2x^2 \quad [28]$$

The derivatives of this equation are simply

$$y' = -4x \quad [29a]$$

$$y'' = -4 \quad [29b]$$

$$y''' = 0 \quad [29c]$$

and, in view of Equation [24]

$$z''' = 26 - \frac{2}{x^2} - \frac{4x^2}{(1 - x^2)^2} \quad [30]$$

The right-hand side of the compatibility equation, Equation [11], becomes

$$-\frac{13}{2} + \frac{1}{2x^2} + \frac{x^2}{(1 - x^2)^2} \quad [31]$$

which is not equal to zero for a finite range of x.

(*b*) Consider the design of a mechanism where

$$\gamma = \cos^{-1}\left[\frac{\cos \varphi}{2} + \frac{1}{2}\sqrt{\frac{2 - 3\cos^2 \varphi - \cos^3 \varphi}{1 - \cos \varphi}}\right] \quad [32]$$

In view of the notation introduced in Equation [7], this expression can be rewritten

$$y = \frac{x}{2} + \frac{1}{2}\sqrt{\frac{2 - 3x^2 - x^3}{1 - x}} \quad [33]$$

By differentiating this function, we find that the first and second derivatives are

$$y' = \frac{1}{2} + \frac{2y^2 - 2xy - x^2 - 3x}{2(1 - x)(2y - x)} \quad [34a]$$

$$y'' = \frac{(2y' - 1)^2(1 - x) - 3(1 + x) + 4y - 2x}{2(2y - x)(1 - x)} \quad [34b]$$

When $x = 0$, it is found that

$$y = \frac{\sqrt{2}}{2} \quad [35a]$$

$$y' = \frac{1}{2} + \frac{\sqrt{2}}{4} \quad [35b]$$

$$y'' = -\frac{3\sqrt{2}}{8} \quad [35c]$$

$$z'' = -\frac{3\sqrt{2}}{8} \quad [35d]$$

and Equation [10] shows that $A = 1$. It has also been found by a similar process that $A = 1$ whenever

$$-\frac{\sqrt{2}}{2} \leq x \leq \frac{\sqrt{2}}{2}$$

but not beyond these values.

Since A is constant, within a prescribed range of input angle, the compatibility equation obviously will be satisfied. Subsequent substitution into Equations [9] and [8] shows that $C = 1$, and $B = \sqrt{3}$.

For a design in which d is to be, say, 3.500 in., the dimensions for a, b, and c are 3.500 times the value just computed, or $a = 3.500$, $b = 6.062$, and $c = 3.500$.

Discussion

A. E. Richard de Jonge.[1] Invited by the authors to discuss their paper, the writer's remarks shall deal with the terminology and mathematics of the paper.

Although the authors have made changes in the final printing, based on the writer's criticisms, the remarks made during the verbal discussion of the original paper are, nevertheless, appropriate generally as they emphasize the writer's deep concern for the correct use of technical and particularly kinematic terms, to which he had drawn special attention at the 1953 Fall Meeting of the Society.[2]

The original title of the paper was "Synthesis of the Quadric Chain When the Position of Two Members Is Prescribed." (This has now been changed to the title at the head of the paper.)

First of all, the title is incomplete, for it should have been extended by the phrase, "by a Functional Relationship," as the construction of a four-link mechanism when the directions of any two links are prescribed and the length of one of them and any other geometrical relation between two links are given also would fall into the field of kinematic synthesis, but would not be the type of problem the authors wish to investigate. Also, there is in the title a term to which the writer takes exception. Unfortunately, this term is quite generally used in the wrong sense not only by the authors, but throughout the American technical literature dealing with kinematics and mechanisms. This is the term "chain" instead of "mechanism." The present paper deals with mechanisms, but not with chains.

"Chain," or better "kinematic chain," is the higher concept of the configuration of all the links without preference for any one of them, "mechanism" is a specific aspect of a chain, namely, that in which one link receives special consideration by being fixed to the surrounding space, and the motions of all other links being referred to this fixed link. The loose use of the term "chain" instead of "mechanism" frequently leads to misunderstandings and should be avoided. Consequently, the reference by the authors in the original paper to ". . . a four-bar mechanism, or quadric chain as it is sometimes called" should have been omitted as incorrect and it has now been omitted in the final printing of the paper.

---

[1] Mechanical Engineer and Consultant, Reeves Instrument Company, New York, N. Y. Mem. ASME.

[2] See the paper "An Analytical Approach to the Design of Four-Link Mechanisms," by F. Freudenstein, ASME Trans., vol. 76, 1954, pp. 483–492, particularly the final sentence of the author's closure, p. 492.

The authors, further, spoke of three diagonals *uv*, *rt*, and *us* with respect to their Fig. 2. Strictly speaking only *rt* and *us* are diagonals of the four-link mechanism, but *uv* is not. If, however, one considers the supplementary mechanism *rvtur*, in which *tv* is parallel to *sr* and *st* parallel to *rv*, then *uv* would be a diagonal of this supplementary mechanism. In accordance with the writer's criticism, the term "diagonal" has now been replaced by "construction lines," which does not help clarification.

Next, the writer dislikes very much the term "equation of state." In the paper, there is no state involved at all. Thus, why call it so? The whole idea, apparently, comes from the introduction by the authors of stress-analysis terminology into kinematics. In the case of stress analysis, there is, naturally, a "state" of stress involved. In the present paper, however, only configurations are dealt with. Thus, it would be far more appropriate to call Equation [8] the "characteristic equation," for it is characteristic of the configuration.

There is another term to which the writer takes exception, likewise adopted by the authors from the theory of stresses. This is the term "compatibility equation," for what the paper is concerned with is only a "criterion," that is, whether or not a certain equation fulfills this criterion. Thus, "applicabillty criterion" seems more appropriate to the writer. When these terms are adopted, there would be no confusion possible with the terminology of the stress theory.

Regarding the mathematical part of the paper, the writer finds that the formulas developed are correct. Equation [6] is one which was derived independently in a paper submitted to the Society in March, 1953, by a junior member, Mr. Freudenstein, who presented a very excellent paper on four-bar mechanisms at the 1953 Fall Meeting at Rochester, N. Y.[6]

While the applicability criterion, as the writer has called it, may prove of value in a number of cases, it can be seen from the Appendix that it may not always be simple to apply, because generally very cumbersome equations result.

There is also an important point that must be definitely kept in mind. Since a four-link mechanism can but have a cyclic recurring motion it can only be used to represent accurately equations or functions that are also cyclic. This eliminates the entire field of functions which are noncyclic. However, for limited intervals of such functions approximate solutions by means of four-link mechanisms may still be feasible provided the allowable tolerances are sufficiently wide, as was shown by V. Svoboda[7] and will be shown also in the paper by Freudenstein when it will be presented.

The introduction by the authors of concepts from the theory of stress analysis into the theory of kinematic synthesis is intriguing and actually may prove to be very useful. The terminology for the equations should be changed to those suggested in order to prevent confusion with the terminology of the stress theory. It is the writer's purpose to call attention to this fact and to congratulate the authors for having taken this interesting and useful step.

FERDINAND FREUDENSTEIN.[8] The authors have applied concepts successful in the field of applied mechanics to the analysis of four-bar linkages. These concepts are the concepts of the equation of state and of compatibility. For introducing these concepts, the authors merit commendation. The four-bar linkage is elusive when it comes to analysis and the large amount of work required to develop a presentable analysis deserves to be appreciated.

The Equation of State (*Equation* [6]). This equation has been derived independently in a paper entitled "Approximate Synthesis of Four-Bar Linkages,"[9] in the following more concise manner:

Referring to Fig. 1 of the paper under discussion, let the links a, b, c, d be represented by vectors $\vec{a}, \vec{b}, \vec{c}, \vec{d}$, respectively, such that

$$\vec{a} + \vec{b} + \vec{c} + \vec{d} = 0$$

Hence $$\vec{b}^2 = b^2 = (\vec{a} + \vec{c} + \vec{a})\cdot(\vec{d} + \vec{c} + \vec{d})$$

where the dot ($\cdot$) refers to the scalar product of two vectors

$$= a^2 + c^2 + d^2 + \vec{2a}\cdot\vec{c} + \vec{2a}\cdot\vec{d} + \vec{2c}\cdot\vec{d}$$

$$= a^2 + c^2 + d^2 - 2ac\cos(\gamma - \varphi) - 2ad\cos\varphi + 2cd\cos\gamma$$

which is the equation of state. It is evident from this derivation that the equation of state is an expression of the physical fact that the four links of the linkage form a closed chain.

The compatibility equation. The idea of a compatibility equation is good. It seems, however, that the practical evaluation of the derivatives (as per the Appendix) is often lengthy and that a numerical method is to be preferred, as demonstrated in example (*b*) of the Appendix.

In the design of computing linkages, it is often desired to generate functions which are given in the form of a numerical table, listing corresponding values of the independent and dependent variables. The functional form of such a relationship may be complicated and is frequently not known. In such cases, a differential form of the compatibility equation, as given in this paper, cannot be used.

However, a difference equation can be used as a compatibility equation under all circumstances and can be derived in the following manner:

Let x_0, y_0, z_0, denote a set of values of x, y, z, belonging to the function which is to be tested for compatibility. Writing Equation [8*a*] for the values of x_0, y_0, z_0 and subtracting it from Equation [8*a*] as given in the paper, one obtains

$$-\frac{X}{C} + \frac{Y}{A} = 1$$

where $$X = \frac{x - x_0}{z - z_0} \qquad Y = \frac{y - y_0}{z - z_0}$$

This suggests the following compatibility criterion: Plot a graph of X versus Y on ordinary graph paper. If the function is "exact," the curve should be a straight line. The intercept with the X-axis would occur at $X = -C$ and the intercept with the Y-axis would occur at $Y = A$, thus providing a simple means of determination of the side ratios. For exact values, the foregoing (straight-line) equation can be solved analytically. The value of B can be found by using Equation [8*a*] of the paper.

The procedure just given can be used for functions defined either analytically or numerically and may be faster than the application of the differential form of the compatibility equation, depending upon the nature of the function in question.

A good many functions can be eliminated without any analytical tests whatsoever by noting their lack of "periodicity" and it is only those functions which cannot be so eliminated which merit a formal compatibility test.

Application of Authors' Methods to Design of Computing Linkages. The portion of synthesis of interest to the designer of computing linkages is known as approximate synthesis. In this type of synthesis a linkage is designed to generate a function ap-

[7] Reference 4 of the paper.

[8] Department of Mechanical Engineering, Columbia University, New York, N. Y.

[9] Submitted by the writer to the Society, March 30, 1953, and referred to the Machine Design Division, May 15, 1953. Scheduled for presentation as Paper No. 54—F-14 at the ASME Fall Meeting, Milwaukee, Wis., September 8–10, 1954.

proximately. The linkage is considered satisfactory if the error in the mechanization does not exceed the limit specified by design considerations. The majority of functions encountered in practice are not "exact" and are synthesized in an approximate manner.

The given quantity in an approximate synthesis is usually not the relationship between the crank angles, but the function $y = f(x)$ which is to be synthesized and the range of x, within which the synthesis is desired. A relationship of the form $y = f(x)$ must then be converted into a relationship between the crank angles. This requires the determination of scale factors and zero points on these scales, which can be imagined attached to the four-bar linkage. These additional four adjustable parameters will have to be considered if a practical design procedure is to be developed.

If, for example, the function given in example (*a*) of the Appendix were to be used as a computing linkage, one would consider changing the sign of the scale factor of γ. The function would then become $\gamma = 2\phi - \pi$. This function can be represented exactly by a four-bar linkage in which the fixed link and the driven crank are of equal length and the other links are infinite. The practical form of this linkage would be a rotating slider-crank (or turning-block) linkage with the crank equal in length to the fixed link.

The authors deserve credit for the introduction of promising new concepts to linkage design. Further investigation is required, however, as the authors realize, in order to develop the analysis to the stage at which it can be applied to the approximate synthesis of computing linkages; i.e., to the practical design of computing mechanisms.

A. S. Hall.[10] The authors have performed a valuable service in calling attention to the possibility of testing a function to determine whether or not it can be generated by a bar mechanism. Their result for the four-bar mechanism is important in itself but a greater contribution is the fresh thinking displayed in their approach to the problem.

It would be interesting to learn whether similar thinking might lead to a test to determine whether or not a bar linkage could generate a prescribed function approximately; i.e., not exactly, but within specified limits for a specified range. The authors indicate that they have given some thought to this problem. It is hoped that they will be encouraged to continue along this line.

J. A. Hrones.[11] This paper is another welcome sign of a gathering interest and enthusiasm directed toward the development of a solid understanding of the fundamental properties of linkages so essential to the solution of the problem of the synthesis of mechanism. In setting up a condition of compatibility for a quadric chain and applying it to the solution of two specific problems, certain limitations of the four-bar linkage are implied which do not exist. A much greater versatility exists and becomes evident if one does not restrict consideration to:

1 The ratio of the angular motions of the two cranks.
2 The "exact" duplication of a desired motion.

The great storehouse of motions available in any linkage is associated with the motions of points on the connecting rod or connecting rod extended (see Fig. 3, herewith). Reference to Hrones' and Nelson's "Analysis of the Four-Bar Linkage," indicates the possibilities. To define the motion of any point on the connecting rod of a four-bar linkage, five nondimensional ratios must be specified; the three nondimensional link-ratio terms used by the

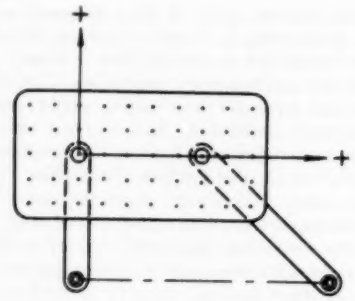

Fig. 3

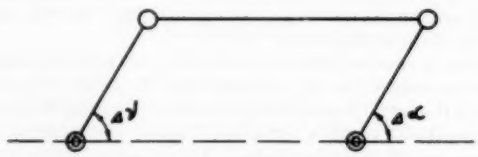

Fig. 4

authors and two additional ratios required to locate the point on the connecting rod. The methods used by the authors can be extended to this case to determine if a linkage exists which will give a desired motion. However, the equations will be more complicated and involve the fifth derivative. In addition, the demand that an exact solution exist again places serious limitations on the value of the method.

There are few engineering problems where an exact solution as required by this method is essential. In practically all cases a band of tolerance is defined. An answer within this band is satisfactory. The compatibility equations as developed by the authors involve high derivatives of the variables, the presence of which will make it difficult to use the compatibility relationships to design linkages to provide a motion which lies within a permissible tolerance band.

One hopes that the authors of this paper will extend their work to the much more important and much more versatile area which admits solutions which are not exact.

The first example given by the authors in the Appendix raises some very interesting questions. The conclusion is reached that there is no four-bar mechanism which will reproduce the function $\nu = \pi - 2\varphi$. From the viewpoint of pure mathematics, this may be true but it is certainly not true from the engineering viewpoint of doing the job. The constant π can be handled by simply establishing a fixed reference point. The mechanism must merely produce changes about this reference point to conform with

$$\nu = \pi - 2\varphi \quad [36]$$

$$\Delta\nu = -2(\Delta\varphi) \quad [37]$$

If a substitution of $\Delta\alpha$ for $-2(\Delta\varphi)$ is made the following relationship results

$$\Delta\nu = \Delta\alpha \quad [38]$$

Equation [38] is solved exactly by the parallel crank mechanism shown in Fig. 4 of this discussion. The reversal of sign and the factor of 2 can be simply handled in a number of ways depending upon the system in which the linkage is to be an element.

Max Luming.[12] Equation [8] represents a family of functions

[10] Professor of Mechanical Engineering, Purdue University, West Lafayette, Ind.

[11] Professor of Mechanical Engineering, Massachusetts Institute of Technology, Cambridge, Mass. Mem. ASME.

[12] Research Assistant, Massachusetts Institute of Technology, Cambridge, Mass.

relating x and y with the parameters A, B, and C. The authors differentiate this equation three times and arrive at the differential Equation [11]. It is logical to conclude that any function which belongs in the family described by Equation [8] must satisfy Equation [11], since [11] is derived from [8]. However this is no guarantee that any function which satisfies Equation [11] must belong in the family of Equation [8], unless it can be proved that Equation [8] represents the most general solution of the nonlinear differential Equation [11].

The results of this paper are still useful as they now stand, in that Equation [11] provides a necessary condition for a function to be generated exactly by a four-bar linkage. When a function is given, if it does not satisfy Equation [11] one is sure that it can never be generated exactly by a four-bar linkage, but if it does satisfy Equation [11] one can only say that it may or may not be generated exactly by a four-bar linkage, for we are not sure that the members of the family described by Equation [8] and only these members can satisfy Equation [11].

In order for Equation [11] to be a necessary and sufficient condition for a function to be an exact four-bar-linkage function, it must be verified that only members of the family of functions, Equation [8], can satisfy Equation [11].

EDWARD MILLER.[13] Engineering colleges in this country as evidenced by typical course contents dealing with the science of kinematics show a preponderant emphasis on problems involving the determination of displacement, velocity, and acceleration of mechanisms whose configuration and dimensions have been prespecified. In addition, the majority of technical articles published on this subject, also, deal largely with the motion of linkages whose proportions already are known.

A great number of practical problems faced by the design engineer, however, involve the necessity of obtaining a definite prescribed output motion from a given input motion. The design of a linkage to accomplish this task, commonly referred to as "kinematic synthesis," is ofttimes a problem of great complexity; and it is in this phase of kinematics that we have fallen behind our European colleagues.

This contribution of the authors represents another step forward in an area where much further work must be done. The analysis presented stands out in the generality of its application, since any functional relationship between the angular displacement of the driver and follower links may be investigated. Although the authors have exemplified only the case of a given relationship of driver-follower link displacement, this approach can easily be extended to problems dealing with velocity and acceleration considerations.

The limitations discussed in this paper regarding the relatively few mathematical relationships which may be reproduced exactly by the quadric chain are no great drawback. This unique method forms the basis of an approximate solution which can take into cognizance the permissible tolerances of a practical design.

The synthesis presented has value beyond pure academic importance. In the automatic-machinery and the computing-mechanism field, linkages enjoy a number of positive advantages over cams. Friction forces are usually lower, particularly when a drive free of backlash is required, and it is usually easier to obtain high accelerations in the driven member. Wear can be reduced because of greater surface contact. In addition, a linkage has only a small number of dimensions compared to the multitude of dimensions necessary to describe a cam profile accurately. Compared to cam manufacture, simpler standard machines can be utilized to fabricate a four-bar linkage.

[13] Mechanical Engineering Department, Newark College of Engineering, Newark, N. J. Mem. ASME.

From a practical standpoint, therefore, the utilization of quadric chains based on the method of kinematic synthesis presented in this paper can be reflected in reduced costs and maintenance.

MELVIN ZAID.[14] The authors have presented a useful method for rapidly determining whether or not a four-bar mechanism can exactly satisfy input-output requirements. As such it has great practical application. Before embarking on any approximate analysis, the possibility of an exact solution should first be investigated through the compatibility Equation [11] of the paper.

This exact solution also might be used in obtaining a "good" four-bar mechanism by numerical methods. This could be obtained as follows:

Good mechanism. To obtain a good four-bar mechanism the method of collocation can be used. Knowing the desired $y = f(x)$, three points (x_1, y_1), (x_2, y_2) and (x_3, y_3) are selected. These are substituted into Equations [8a] and [8b] yielding three equations that are solved simultaneously to give

$$C = \frac{(x_1 - x_2)(y_1 - y_2) - (y_1 - y_2)(x_1 - x_3)}{(y_1 - y_2)(x_1 - x_3) - (x_1 - x_2)(y_1 - y_3)} \quad [39]$$

$$A = \frac{C(y_1 - y_2)}{(x_1 - x_2) + C(x_1 - z_2)} \quad [40]$$

$$B^2 = 1 + A^2 + C^2 - 2Ax_1 - 2ACz_1 + 2Cy_1 \quad [41]$$

It is interesting to note that Equation [39], herewith, may be written in vector form as follows

Let

$$U = i + j + k$$

$$X = x_1 i + x_2 j + x_3 k$$

$$Y = y_1 i + y_2 j + y_3 k$$

$$Z = z_1 i + z_2 j + z_3 k$$

Then

$$C = \frac{U \cdot X \times Y}{U \cdot Y \times Z} \quad [42]$$

With a little experience it should not be difficult to select values of x_1, x_2, x_3 which will give a good four-bar mechanism.

AUTHORS' CLOSURE

The authors wish to thank the discussers for their valuable suggestions and criticisms. Several of the discussers expressed interest in the extension of the present analysis to include a wider range of functions. This is certainly a natural and timely comment.

Synthesis of a greater number of functions than is permitted by the method described in the present paper may be accomplished by increasing the versatility of the mechanism, by permitting a tolerable variation between the prescribed and generated functions, or both. Versatility may be gained by introducing the following four additional parameters: the input scale factor k the output scale factor m, the initial set of the input angle φ_0, and the initial set of the output angle γ_0. A design procedure could be formulated to generate a function containing these additional parameters by generalizing the concepts proposed in the present paper.

If we chose to permit a tolerable variation between the pre-

[14] Bulova Research and Development Laboratories, Inc., Flushing, N. Y. Assoc. Mem. ASME.

scribed and generated functions, then the following suggestion is made. Find a solution for each of the points which satisfy the compatibility equation by following the procedure outlined at the end of the original paper and then compare the function actually being generated with the original function. One of the resulting designs may be satisfactory.

The greatest number of functions may be generated by combining both of these methods.

The apparent paradox which arose in connection with the function

$$\gamma = \pi - 2\varphi \quad [43]$$

does not arise when the additional four parameters k, m, φ_0, and γ_0 are introduced to the problem. For the case under discussion, the input scale factor is two, the output scale factor is unity, the initial set of the input angle is π, while the initial set of the output angle is zero. Equation [43] may be shown to satisfy the compatibility equation if the existence of these parameters is accounted for in advance. The illustrative problem was restricted to the case in which the parameters did not enter the picture, and the compatibility equation, therefore, was not satisfied. The parameters were of course included in the solution offered by the discussers.

The authors are grateful to Mr. Freudenstein for presenting in his discussion of our paper his derivation of Equation [6] which he developed independently and has reported in his paper No. 54—F-14. The vector approach does shorten the number of steps needed to derive Equation [6]. The derivation of Equation [6] may also be shortened from an entirely algebraic point of view. If this were done, however, the interesting geometric relationship described in Equation [4] would have been overlooked. May we take this opportunity to emphasize the difference between Equation [6] and Equation [8], the equation of state. The introduction of Equations [7], as we can see, enabled the authors to differentiate with respect to $\cos \varphi$ rather than φ itself. As a result, the subsequent work was greatly simplified.

The point (x_1, y_1) for which the compatibility equation yields zero may also be used in the collocation method to accelerate the process of obtaining good results. It should be emphasized, however, that care should be taken in using the collocation method to see that the resulting design is well behaved within the entire range being studied.

The authors wish to commend Mr. de Jonge for his consistent vigilence in seeing to it that exact kinematic terminology is rigidly adhered to. We are in sympathy with this viewpoint and we wish to thank him for his assistance in this direction. It is felt, however, that the concept described in Equation [8] is in fact an "equation of state" and Equation [11] is a "compatibility equation." Equation [8] describes the manner in which the links must be combined so that the mechanism always forms a closed loop. The suggested title "characteristic equation" has a mathematical significance not intended in the present analysis. Equation [11] assures us of the fact that the motion required to generate a prescribed function is compatible with the restraints imposed by the physical restrictions of the mechanism, thus the term "compatibility equation." We feel that no confusion will arise with stress theory as a result of the terminology assigned to the afore-mentioned equations.

AN ASME PAPER

Its Preparation, Submission and Publication, and Presentation

To a large degree the papers prepared and presented under the ASME sponsorship are evidence by which its professional standing and leadership are judged. It follows, therefore, that to qualify for ASME sponsorship, a paper must not only present suitable subject matter, but it must be well written and conform to recognized standards of good English and literary style.

The pamphlet on "AN ASME PAPER" is designed to aid authors in meeting these requirements and to acquaint them with rules of the Society relating to the preparation and submission of manuscripts and accompanying illustrations. It also includes suggestions for the presentation of papers before Society meetings.

CONTENTS

Price 50¢. 20% Discount to ASME Members.

THE AMERICAN SOCIETY OF MECHANICAL ENGINEERS

29 West 39th Street, New York 18, N. Y.

ASME —BOOKS—

VISCOSITY OF LUBRICANTS UNDER PRESSURE

This new publication reviews and co-ordinates twelve experimental investigations made in England, Germany, Japan, Russia, and the United States over a period of thirty-five years. The tests were made on 148 lubricants comprising 25 fatty oils, 94 petroleum oils, 17 compounded oils, and 12 other lubricants. Data are co-ordinated by means of sixty tables in which the results originally appearing in diversified units are compared. The methods proposed for correlating viscosity-pressure characteristics of oils with properties determined at atmospheric pressures are reviewed and illustrated. Pertinent aspects such as experimental work on heavily loaded bearings, lubrication calculations, and additional techniques for viscosity are covered. Conclusions and recommendations are presented. Other chapters give the required computation of the temperature coefficients of viscosity, method of computing pressure coefficients, a bibliography of 189 items, and symbols used.

$5.00

METALS ENGINEERING—DESIGN

This first of the four-volume ASME Handbook is the design engineer's own guidebook of vital data on the properties, testing, inspection, and selection of metals. Comprising 48 sections and written by 43 well-known authorities, it provides: Criteria for facing the over-all problems of selection of materials; facts on potential weaknesses of various metals and ways of making the metals strong; details of the specific problems of corrosion and the mechanical factors which influence corrosion; present knowledge of testing by nondestructive methods; special requirements of design and surface finish set up by mass production; modern basic information on the design theory, design practice, experimental design; and the special requirements of aluminum and magnesium. Here, too, are important design data—equations for determining such factors as stress, creep, impact strength; results of such methods as the use of residual stresses to improve fatigue resistance; the use of flame hardening to increase resistance to fatigue failure; methods for making your structure or machine part stronger, such as shot peening, cold working, and case carburizing.

400 pages **$10.00**

METALS PROPERTIES

This second of the four-volume ASME Handbook provides in convenient charts and tables data on a broad range of metals in common industrial use—AISI steels, ASTM steels, cast copper alloys, aluminum alloys, tin, magnesium, etc. Tabulated under each of the more than 500 metals listed is such information as the chemical composition of the metal; its brittleness, heat-treatment, and other characteristics; its industrial uses; treatment temperatures for forging, annealing, quenching, etc.; such technological properties as recrystallization temperature and hot working temperature, and a great deal of other pertinent information to help the designer choose the proper metal for each part or product.

445 pages **$11.00**

GENERAL DISCUSSION ON HEAT TRANSFER

The complete proceedings of the 1951 Heat Transfer Conference, arranged by the IME and ASME, it mirrors a decade's development in heat transfer and in the design of the apparatus relating thereto, offering first-hand information on significant investigations, new discoveries in the field, actual performance of fundamental data, and on new practical applications of known principles. Over 200 specialists have collaborated to present the 93 timely papers in its pages, of which sixteen deal with problems associated with heat transfer with change of state; twenty-three are concerned with problems associated with heat transfer between fluids and surfaces; sixteen treat problems connected with conduction in solids and fluids; eighteen cover convection, radiation, instrumentation, and measurement techniques; and twenty discuss special problems, such as, heat transfer in turbine-blade cooling, in liquid metals, in gas engines, in piston engines, mercury boiler, etc. Additionally, there are seventy-five pages of discussions, critical summaries of the papers, and hundreds of bibliographical references.

500 pages **$10.00**

MANUAL ON CUTTING OF METALS

Look to this book for shop-tested data on metals which are machined commercially...the best cutting practices...the tool shapes which experimental work has shown to be most efficient...and a hundred other helps for cutting costs, stepping up production, and standardizing practice. Specifically it shows how to machine a variety of metals including high-nickel alloys, stainless steels, copper and its alloys, magnesium, cast irons, and plastics; discusses the mechanical characteristics and structures of the materials being worked and the relations of their behavior and properties to microscopic structure; gives detailed consideration to types and sizes of tools, tips, inserts, and holders; to tool materials, grinding and evaluating tool performance. Cutting fluids and their influence on cutting speeds, etc., are covered; also cutting forces for machining a variety of metals. Cutting, idle and loading time, as well as tool changing and grinding costs are analyzed, and the cost per piece formula presented along with an example showing how costs are calculated.

546 pages **600 illustrations** **$10.00**

THE AMERICAN SOCIETY OF MECHANICAL ENGINEERS 29 W. 39th St., New York 18, N. Y.

20% Discount to ASME Members